

Aus dem Bereich Klinische Bioinformatik
Klinische Medizin
der Medizinischen Fakultät
der Universität des Saarlandes, Homburg/Saar

Identification of miRNAs as master regulators of aging signatures

Dissertation

zur Erlangung des Grades
eines Doktors der Naturwissenschaften
der Medizinischen Fakultät
der Universität des Saarlandes
(2023)

vorgelegt von

Viktoria Philine Wagner
geb. am 10.09.1995 in Homburg (Saar)

Dekan: Prof. Dr. Michael D. Menger

Berichterstatter 1: Prof. Dr. Andreas Keller

Berichterstatter 2: Prof. Dr. Eckart Meese

Berichterstatter 3: Prof. Dr. Tony Wyss-Coray

Publications

Partial results of this work have been published previously. Publications are referenced when applicable.

Peer-reviewed articles:

Wagner V, Kern F, Hahn O, Schaum N, Ludwig N, Fehlmann T, Engel A, Henn D, Rishik S, Isakova A, Tan M, Sit R, Neff N, Hart M, Meese E, Quake S, Wyss-Coray T, Keller A. Characterizing expression changes in noncoding RNAs during aging and heterochronic parabiosis across mouse tissues. *Nat Biotechnol.* 2023 Apr 27. doi: 10.1038/s41587-023-01751-6. Epub ahead of print. PMID: 37106037.

Kern F, Kuhn T, Ludwig N, Simon M, Gröger L, Fabis N, Aparicio-Puerta E, Salhab A, Fehlmann T, Hahn O, Engel A, **Wagner V**, Koch M, Winek K, Soreq H, Nazarenko I, Fuhrmann G, Wyss-Coray T, Meese E, Keller V, Laschke MW, Keller A. Ageing-associated small RNA cargo of extracellular vesicles. *RNA Biol.* 2023 Jan;20(1):482-494. doi: 10.1080/15476286.2023.2234713. PMID: 37498213; PMCID: PMC10376918.

Planned articles:

Engel A*, **Wagner V***, Hahn O, Ludwig N, Foltz A, Atkins M, Mazid H, Beganovic A, Guldner I, Lu N, Saksena A, Fischer U, Meese E, Wyss-Coray T, Keller A. MiRNA expression atlas of the aging mouse brain.

* These authors contributed equally to this study.

Table of contents

I	SUMMARY	1
II	ZUSAMMENFASSUNG	2
III	TABLE OF FIGURES	4
IV	ABBREVIATIONS	7
1	MOTIVATION	10
2	THEORETICAL BACKGROUND	11
2.1	Aging	11
2.1.1	Hallmarks of aging	11
2.1.2	Aging as a risk factor for disease	14
2.2	Aging interventions	16
2.2.1	Exercise	16
2.2.2	Caloric restriction	17
2.2.3	Partial reprogramming	17
2.2.4	Drugs: Rapamycin, Metformin & Senolytics	17
2.2.5	Heterochronic parabiosis	18
2.3	Small non-coding RNAs	19
2.3.1	MicroRNAs	20
2.3.2	Bioinformatic tools for miRNA analysis	21
2.3.3	microRNAs in aging	22
3	GOAL OF THE PHD THESIS	24
4	METHODS	26
4.1	Samples	27
4.1.1	Aging cohort (TMS)	27

4.1.2	Heterochronic parabiosis cohort	27
4.1.3	Circulatory cohort	28
4.1.4	Region-specific brain aging cohort	28
4.1.5	RNA isolation	29
4.2	Library preparation	29
4.3	Sequencing and data analysis	30
4.4	Cell lines	33
4.5	Plasmids	33
4.6	High-throughput miRNA interaction reporter assay (HiTmIR)	33
4.7	Data availability	34
5	RESULTS	36
5.1	ncRNA expression across mouse organs during aging	36
5.2	miRNA correlation with age	40
5.3	Non-linear expression changes during aging	41
5.4	Whole organism trajectory clustering	43
5.5	miRNA-mRNA interactions of global aging miRNA	45
5.5.1	miRNA-mRNA interactions of miRNAs positively correlated with age	45
5.5.2	miRNA-mRNA interactions of miRNAs negatively correlated with age	48
5.6	Tissue-specific rejuvenation response of global aging miRNAs... ..	50
5.7	Circulating miRNAs	54
5.8	miR-29 family target validation.....	55
5.9	Region-specific brain aging.....	57
5.9.1	Region-specific miRNA expression patterns in brain	58
5.9.2	Brain miRNA miR-9	59

5.9.3	Sex-specific signatures of miRNA expression in brain regions	59
5.9.4	Linear miRNA aging signatures	60
6	DISCUSSION	62
7	CONCLUSION	72
8	REFERENCES	74
9	APPENDIX	86
9.1	Appendix A	86
9.2	Appendix B	96
	ACKNOWLEDGEMENT	152
	LEBENS LAUF	154

I Summary

Molecular mechanisms of organismal and cellular aging are only partially elucidated to this date. Previous studies have focused on understanding the changes in the coding transcriptome over the lifespan. We analyzed 771 samples from 16 different organs over ten time points to construct a comprehensive body-wide expression map of non-coding RNA to fill the existing knowledge gap for this layer of RNA diversity. Within individual tissues, local aging microRNAs (miRNAs) were identified, exhibiting specific alterations in their expression patterns as part of an organ-specific signature in aging. Additionally, eight global aging miRNAs were identified, five of them displayed a continuous increase in expression across all organs over time (miR-29a-3p, miR-29c-3p, miR-155-5p, miR-184-3p, and miR-1895), while the remaining three (miR-300-3p, miR-487b-3p, and miR-541-5p) showed a continuous decrease in expression.

MiRNAs interact with coding mRNAs through complementary base pairing, thereby regulating gene expression. The previously published dataset of coding RNAs was utilized to identify novel target mRNAs of the global aging miRNAs, along with their overarching pathway structures. These analyses revealed that aging miRNAs regulate well-known aging pathways, such as extracellular matrix organization.

The identified alterations in the expression of global aging miRNAs were reversed organ-specifically in the context of the aging intervention known as heterochronic parabiosis. In this intervention a young and an old mouse share a circulatory system. Systemic factors influencing aging processes can be investigated, as positive rejuvenation effects have been observed in old animals subjected to this treatment. Furthermore, global aging miRNAs are more abundantly expressed in the blood compared to local aging miRNAs. These results suggest that changes in the expression of global aging miRNAs have a causal impact on aging processes. Moreover, similar trends in region-specific miRNA alterations during aging were observed in a regionally segmented brain atlas.

II Zusammenfassung

Um die Expressionsmuster der nicht-kodierenden RNAs, speziell der microRNAs während des Alterungsprozesses, zu entschlüsseln wurden Daten über die gesamte Lebensspanne der Maus aus 16 verschiedenen Organen gesammelt und analysiert. In den einzelnen Geweben konnten lokale Alterungs-miRNAs identifiziert werden, deren Expressionsmuster sich spezifisch in einer organ-eigenen Signatur im Alter verändern. Es wurden außerdem acht globale Alterungs-miRNAs identifiziert, wobei fünf davon einen kontinuierlichen Anstieg ihrer Expression über die Zeit in allen Organen zeigen (miR-29a-3p, miR-29c-3p, miR-155-5p, miR-184-3p und miR-1895) und die anderen drei (miR-300-3p, miR-487b-3p und miR-541-5p) einen kontinuierlichen Abfall ihrer Expression zeigen.

Bekanntermaßen interagieren miRNAs mit den kodierenden mRNAs durch komplementäre Basenbindung und regulieren dadurch die Genexpression. Der bereits publizierte Datensatz der kodierenden RNAs wurde genutzt, um neue Target-mRNAs der globalen Alterungs-miRNAs sowie deren übergeordnete *Pathway*-Strukturen zu identifizieren. Diese Analysen zeigen, dass die Alterungs-miRNAs bekannte Alterungs-*Pathways*, wie zum Beispiel die extrazelluläre Matrixorganisation regulieren.

Es konnte nachgewiesen werden, dass die identifizierten Veränderungen der Expression von Alterungs-miRNAs organspezifisch umkehrbar sind in der Alterungsinterventionsmethode der „heterochronischen Parabiose“. Diese Intervention, in der eine junge und eine alte Maus einen Blutkreislauf teilen, wird genutzt, um systemische Faktoren zu erforschen, die Alterungsprozesse beeinflussen, da positive Auswirkungen der Verjüngung bei alten Tieren mit dieser Behandlung festgestellt werden konnten. Außerdem sind die globalen Alterungs-miRNAs im Blut stärker exprimiert als die lokalen Alterungs-miRNAs. Diese Ergebnisse deuten darauf hin, dass die Veränderungen in der Expression der globalen Alterungs-miRNAs einen kausalen Einfluss auf Alterungsprozesse haben. Außerdem konnte in einem regionsspezifisch aufgeschlüsselten Gehirn Atlas ähnliche Trends zu regionsspezifischen miRNA Veränderungen im Alter festgestellt werden.

III Table of figures

Figure 1: Aging as a risk factor in disease.....	14
Figure 2: Non-coding RNA types and their main functions.	20
Figure 3: Revealing miRNA expression changes during aging.	25
Figure 4: Simplified workflow for processing of cohorts.	26
Figure 5: TMS Study set-up.	36
Figure 6: t-SNE clustering of all tissues.	37
Figure 7: Count percentage per tissue after local filtering.	38
Figure 8: Count distribution of ncRNAs during aging per tissue.	39
Figure 9: Spearman correlation of ncRNAs with age.....	39
Figure 10: miRNA correlation with age.	40
Figure 11: Heatmap of deregulated miRNA count.....	41
Figure 12: Volcano plot foldchange miRNA expression of all later timepoints versus three months versus respective <i>P</i> -values. ¹	42
Figure 13: Heatmap of mean count isoforms per miRNA per tissue per time point....	42
Figure 14: Tissue-specific miRNA trajectory clusters.	43
Figure 15: Continuously increasing expression aging cluster.	44
Figure 16: Positively correlated global aging miRNA-mRNA interactions.....	46
Figure 17: Heatmap of enriched pathways in predicted mRNA targets of positively correlated local aging miRNAs per tissue. ¹	47
Figure 18: Negatively correlated global aging miRNA-mRNA interactions.	48
Figure 19: Heatmap of enriched pathways in predicted mRNA targets of negatively correlated local aging miRNAs per tissue ¹	49
Figure 20: Schema drawing of heterochronic parabiosis as an aging intervention. ...	50
Figure 21: t-SNE clustering of parabiosis samples.	51
Figure 22: Count of deregulated miRNAs per tissue per condition.	52
Figure 23: Boxplot of z-scored miR-29c-3p expression in liver in aging and parabiosis cohort ¹	53
Figure 24: Overlap local and global aging miRNAs with circulating miRNAs.....	54

Figure 25: Luciferase assay results.....	55
Figure 26: Scheme drawing of validated miR-29 targets downregulated in aging (newly validated targets in red).....	56
Figure 27: Study set up brain aging cohort.....	57
Figure 28: UMAP of all samples of the brain aging cohort overall expressed miRNAs.	58
Figure 29: Binarized heatmap of most variable region-specific miRNAs overall brain regions.	58
Figure 30: Median miR-9-5p expression in reads per million mapped for each brain region over all ages.....	59
Figure 31: Percentage of variation introduced by age and sex in each region.	60
Figure 32: Heatmap of spearman rank correlation with age for each miRNA	61
Appendix A	
Supplemental Figure 1: Share of read distribution per tissue of detected ncRNAs per RNA class, color coded by RNA class.	86
Supplemental Figure 2: Mapped read length analysis.....	86
Supplemental Figure 3: Biological and technical parameters as drivers of variance.	87
Supplemental Figure 4: Share counts per ncRNA class for each individual tissue after abundance filtering.....	88
Supplemental Figure 5: Mean variance of ncRNA count shares per RNA class for each tissue.	89
Supplemental Figure 6: Volcano plots of FC versus <i>P</i> -values for all tissues.....	90
Supplemental Figure 7: Mean expression of all miRNA features after local filtering per time point per tissue versus foldchange calculated versus three months of age.	91
Supplemental Figure 8: Mean expression of all non-coding RNA features after local filtering per time point per tissue versus foldchange calculated versus three months of age.	91
Supplemental Figure 9: Fuzzy c-means clustering in 20 clusters of all z-scored miRNA trajectories for all miRNAs expressed in each tissue.	92
Supplemental Figure 10: Z-scored increasing expression patterns of miR-184-3p in liver for aging cohort and parabiosis cohort.	93

Supplemental Figure 11: Z-scored decreasing expression patterns of miR-300-5p in GAT for aging cohort and parabiosis cohort.....	93
Supplemental Figure 12: Positive control Luciferase assay.....	94
Supplemental Figure 13: Boxplot of expression of miR-9-5p over time in reads per mapped million versus age in month.....	95
Supplemental Figure 14: PVCA brain aging cohort over all samples with both genders.	95

IV Abbreviations

ACC	accelerated aging effect
AD	Alzheimer's disease
AGO	Argonaute protein
ASO	antisense oligonucleotides
BAT	brown adipose tissue
cDNA	complementary DNA
CNS	central nervous system
CR	caloric restriction
CSF	cerebrospinal fluid
DNA	deoxyribonucleic acid
DNMT	DNA methyltransferase
ECM	extracellular matrix
EtOH	ethanol
FACS	fluorescence activated cell sorting
FC	fold change
FDA	Food and Drug Administration
GAT	gonadal adipose tissue
HA	heterochronic aged mice
HITmiR	high-throughput miRNA interaction reporter assay
HY	heterochronic young mice
IA	isochronic aged mice
IGF1	Insulin-like growth factor 1
IY	isochronic young mice
lncRNA	long non-coding RNA
LOX	lysyl oxidase
MAT	mesenteric adipose tissue
mRNA	messenger RNA
miEAA	miRNA enrichment analysis and annotation tool
miRNA	microRNA
mTOR	mammalian target of rapamycin
MuSC	muscle stem cells

NCD	non-communicable chronic diseases
ncRNA	non-coding RNA
NGS	next generation sequencing
nt	nucleotide
ORA	over-representation analysis
OSKM	<i>Oct4, Sox2, Klf4</i> and <i>c-Myc</i>
PCR	polymerase chain reaction
PD	Parkinson's disease
PVCA	principal variance component analysis
REJ	rejuvenation effect
piRNA	PIWI-interacting RNA
pre-miRNA	precursor miRNA
RIN	RNA integrity number
RNA	ribonucleic acid
RNAi	RNA interference
RT	reverse transcription
ROS	reactive oxygen species
rpmm	reads per million mapped
rpmmm	reads per million mapped to miRNA
rRNA	ribosomal RNA
SASP	senescence associated secretory phenotype
scaRNA	small Cajal body-specific RNA
SCAT	subcutaneous adipose tissue
sc-miRNA	single cell miRNA
siRNA	small interfering RNA
snoRNA	small nucleolar RNA
snRNA	small nuclear RNA
SVZ	neurogenic subventricular zone
TET	ten-eleven translocation protein
TMS	<i>Tabula muris senis</i>
t-SNE	t-distributed stochastic neighbor embedding
tRF	t-RNA derived small fragment

tRNA	transfer RNA
UMAP	uniform manifold approximation and projection
UTR	untranslated region
WHO	World Health Organization

1 Motivation

People aged 60 years and over outnumber children younger than 5 years since 2020². Until 2050 the proportion of the world's population aged 60 years and older is predicted to be equal to the proportion of people under age 15 with each 2 billion (21% of the world's population). Sustaining public spending on pensions and health care are major challenges resulting from this process called global population aging³. Falling mortality rates are driving this process. Healthy living, regenerative medicine, disease prevention and cure as well as age retardation or senescence prevention are responsible for life extension. With increased life expectancy not only the healthy lifespan (health span) is extended but also the time lived with disease, disabilities, and frailties. With advancing age, the risk of diseases like cancer, cardiovascular disorders, immune system, musculoskeletal, metabolic, and neurodegenerative diseases increases^{4,5}.

Understanding molecular processes of aging in detail will hopefully lead to the discovery of therapeutics to decrease the risk of disease in elderly people and increase the length of the healthy life span. The objectives within the realm of aging biology research are extensive and ambitious. They involve comprehending the interplay of numerous genes, pathways, and mechanisms across various levels, which collectively contribute to the deterioration of functionality, health, and lifespan. Many studies aimed to identifying important individual genes, pathways, and molecules, along with elucidating their interconnections within mechanisms that regulate the aging process. Nonetheless, our grasp of how these elements synergize to create a comprehensive array of aging phenomena remains somewhat limited⁶.

In this work, we add another tier of information, namely the non-coding RNA expression patterns, to the already available proteomic and single-cell and bulk transcriptomic data. Data of all measurable information will provide insight into the complex processes responsible for the aging process and reveal underlying mechanisms.

2 Theoretical background

2.1 Aging

Whether or not aging itself is a disease has been discussed previously^{7,8}. Undoubtedly, old age is a risk factor for various disease, and this is caused by molecular changes in the entire organism. Hallmarks of aging have been defined to better grasp the phenotype.

2.1.1 Hallmarks of aging

Every organ and every tissue is affected by the functional decline caused by the multifaceted process of aging. A characteristic has (1) to associate with chronological aging, (2) to accelerate aging when increased intentionally in an experimental setting and (3) must be targetable by therapeutic interventions, which slow, stop or reverse the aging phenotype, to be considered a hallmark of aging⁹. Hallmarks of aging have been first defined in 2013⁵ and extended in 2023⁹, namely: Genomic instability, telomere attrition, epigenetic alterations, loss of proteostasis, deregulated nutrient sensing, mitochondrial dysfunction, cellular senescence, stem cell exhaustion, disabled macroautophagy, chronic inflammation, dysbiosis, and altered intercellular communication.

Genomic instability in aging occurs due to the accumulating DNA damage throughout life, caused by exogeneous reagents, like chemicals and radiation and endogenous damage like replication errors, reactive oxygen species (ROS) and spontaneous reactions^{5,10}. Especially the DNA damage at the telomers, caused by incomplete copying of these regions leads to their shortening and eventually either apoptosis or cell senescence⁹.

Telomere attrition itself though, as a hallmark of aging, can act against cancer formation as it limits lifespan of malignant cells and is therefore mentioned separately from genomic instability that tends to act in an oncogenic manner. Cellular senescence, organismal aging and even lifespan alterations have been directly linked to telomere length in model organisms¹¹. Telomerase, the ribonucleoprotein, acting as a reverse-transcriptase, can elongate telomeres to preserve their optimal length. Hence, it represents a therapeutic target, the impacts of which have undergone comprehensive investigation¹².

Dysbiosis, refers to the disruption of bacteria-host bidirectional communication in the gut microbiome, which plays an important role in several physiological processes such as nutrient adsorption and digestion, production of essential metabolites and protection against pathogens. This disruption can contribute or worsen multiple

diseases such as cancer, neurological disorders, cardiovascular diseases, and type 2 diabetes⁹. In humans, age-related alterations in gut microbiota composition are associated with inflammation, depression, and frailty¹³. By employing fecal microbiota transplantation in model organisms, it was demonstrated that gut dysbiosis plays a causative role in the age-related deterioration of adaptive immunity and the onset of persistent systemic inflammation¹⁴.

Chronic inflammation occurs as a systemic manifestation as well as regionally confined pathologies in later life stages. Circulating inflammatory cytokines are used as predictors of mortality. Even though most hallmarks of aging (genomic instability and loss of proteostasis) contribute to inflammation, it is a hallmark in its own, as it can be targeted in aging interventions with anti-inflammatory drugs and result in slowing the aging process across organs⁹.

Another hallmark of aging is the loss of proteostasis, impaired protein homeostasis often leads to aggregation of proteins, that accumulate in intracellular inclusion bodies or extracellular plaques. These aggregates, consisting mostly of misfolded proteins, are associated with neurodegenerative diseases such as Alzheimer's, Parkinson's and amyotrophic lateral sclerosis (ALS), all known for having age as one of their major risk factors⁹. The two main protein quality control mechanisms, the ubiquitin-proteasome system and the autophagy lysosomal system, decline during aging. These two systems are responsible for the removal of misfolded proteins. The mechanism of stabilizing correctly folded proteins, mediated via chaperones is significantly impaired as well^{5,15}. Lifespan extensions were observed by specifically targeting this aging hallmark, e.g. via administering human chaperones to mice¹⁶.

Disabled macroautophagy is a hallmark of aging as well, now separately mentioned but related to loss of proteostasis. During this process cytoplasmic components are encapsulated within double-membrane vesicles (autophagosomes) that ultimately fuse with lysosome for content degradation. The encapsulated components include proteins, but also any macromolecule or even entire organelles¹⁷. As this mechanism is impaired in aging, organelle turnover is reduced, which leads to the accumulation of dysfunctional organelles. The stimulation of autophagic flux in model organism has been linked to lifespan extensions¹⁸.

Dysfunctional organelles, like mitochondria contribute to aging by affecting apoptotic signaling, triggering inflammatory reactions and reducing biogenesis⁹. Mitochondrial microproteins, like humanin, whose levels decline in plasma during aging, have been linked to lifespan extension in model organisms⁹.

Another well-known characteristic of aging is the reduction of regenerative potential of tissues, this includes the declining renewal during a steady state as well as

the flawed tissue regeneration after injury. Stem cell exhaustion can be observed in all adult stem cell compartments, for instance a decline in production of adaptive immune cells is caused by reduced hematopoiesis⁵. Reprogramming of cells resulting in reversing stem cell exhaustion has been shown to extend lifespans in model organisms¹⁹.

Cellular senescence is defined as an irreversible arrest of the cell cycle, which is accompanied by phenotypic changes as well. One of these changes observed in senescent cells is called the senescent associated secretory phenotype (SASP), which refers to the drastically altered secretome that mainly consists of proinflammatory cytokines and matrix metalloproteinases. This proinflammatory signaling links cellular senescence also to another hallmark of aging, namely altered intercellular communication. Cells enter this state to limit excessive or aberrant proliferation and thereby evade formation of cancer. The transition can be caused by multiple mechanisms, best known are the “Hayflick Factors”, which include telomere shortening, extensive DNA damage and derepression of the INK4a/ARF locus²⁰. Senescent cells accumulate during aging and may induce inflammation and reduce tissue function and contribute to stem cell exhaustion.

As the nutrient sensing network is highly conserved in evolution, its deregulation during aging has various functional consequences, like unrestrained inflammation, inhibition of autophagy and resistance to diverse stressors. One of the most conserved aging-controlling pathways within intracellular signaling is the pathway of insulin and *IGF1*. Multiple genetic mutations or polymorphisms that reduce function therein or its downstream targets have been associated with longevity⁵.

Another hallmark of aging are epigenetic alterations, which consist of DNA methylation changes, histone modifications, chromatin remodeling, altered non-coding RNA expression, derepression of retrotransposons and gene expression changes. Unlike other changes, e.g. DNA damage, are these alterations reversible. These changes result in formation and advancing of human pathologies through regulating gene expression and other cellular processes. DNA methylation changes are associated with aging but a causal link from DNA methylation, like e.g. defective DNA methylation maintenance resulting in accelerated aging is yet to be found. During aging a global loss of histones occurs and tissue-dependent changes of post-translational modifications were observed. Chromatin remodeling, like global heterochromatin loss and redistribution are common occurrences in aged cells. Chromatin remodeling factors are involved in genomic stability DNA repair and proposed to modulate aging⁹.

Altered cellular communication, as another aging hallmark is the connection between the cell intrinsic changes and the overall occurring organismal changes like

chronic inflammation. Especially interesting in this regard are systemic factors located in the blood, as they are also promising therapeutic targets. Pro-aging factors in blood, like CCL11/eotaxin, IL-6 and TGF-beta, as well as anti-aging factors, like CCL3/MIP-1alpha, TIMO2 and IL-37 have been identified. The extracellular matrix (ECM) and its long-lasting protein constituents are also affected in detrimental ways by aging. Elastin is fragmented and crosslinking of collagen is impaired, which causes tissue fibrosis. Factors like TGF- β , other growth and transcription factors, cause activation of profibrotic genes like transglutaminase-2, lysyl oxidase (LOX) and LOX-like enzymes. Notably, the stiffness of the ECM also impacts the behavior of senescent cells. These cells secrete matrix metalloproteases that exacerbate ECM damage. These patterns, termed damage-associated molecular patterns, activate pathways that promote cellular senescence, fibrosis, and inflammation. Numerous research investigations have presented causal proof regarding the role of ECM stiffness in the aging process. Abnormal ECM in the brain has been shown to result in early memory loss and accelerated brain aging in mice^{5,9}.

2.1.2 Aging as a risk factor for disease

Aging is the major risk factor for diseases like cancer, cardiovascular disease, metabolic disorders, and neurodegenerative diseases (Figure 1). Non-communicable chronic diseases (NCDs) are chronic medical conditions with extended durations and gradual advancement.

Three of the top four NCDs, that in total are responsible for 71% of deaths worldwide share age as their common risk factor. These three diseases are diabetes (with 1.6 million deaths a year), cancer (9 million) and cardiovascular disease (17.9 million)²¹.

Furthermore, NCDs are the cause of most years spent with morbidities and disabilities.

Understanding the molecular changes responsible for aging phenotypes is essential to research therapeutic interventions to improve the number of healthy years spent at old age²².

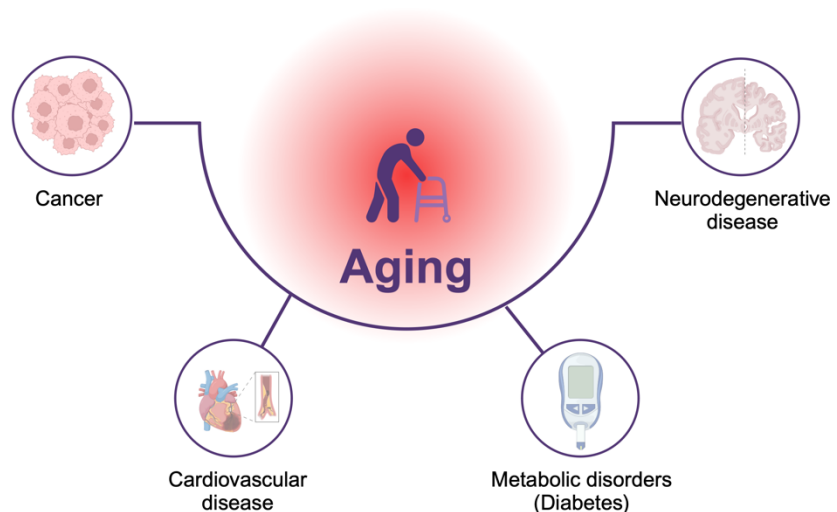


Figure 1: Aging as a risk factor in disease.

Aging represents the major risk factor for neurodegenerative disease, metabolic disorders, cardiovascular disease and cancer, created with BioRender.

Cardiovascular diseases (CVD) that are responsible for almost 18 million death a year are mainly myocardial infarction, atherosclerosis, stroke, and hypertension²³. Telomere shortening and DNA damage are linked the CVD, but the causality remains unclear.

In the final decades of life, the occurrence of cancer increases exponentially, driven largely by epithelial carcinomas²⁴. Cancer is a neoplastic disease with very complex and diverse causes, general hallmarks of cancer have been defined previously to give a framework to better understand the disease. Maintaining growth signaling, bypassing growth inhibitory mechanisms, avoiding cell death, continuous replication, angiogenesis, initiating metastasis, and invasion are the six hallmarks of cancer. Underlying these hallmarks of cancer is a hallmark of aging, namely genomic instability²⁵. During aging tissue microenvironments are not maintained effectively, which leads to a decline of the overall fitness of the tissue which results in a relative inability to clear altered cells and aging-associated clonal proliferation increases. Some of these cells can be oncogenic and therefore the risk of cancer increases with older age²⁶. Hallmarks of aging like dysfunctional mitochondria can be responsible for cancer development as well, mtDNA mutations are oncogenic. Mitochondria mediated ROS production can drive malignancy progression. Mutations driving cancerous development can accumulate due to defects in the DNA damage response⁴.

Other hallmarks of aging, like telomere shortening have been linked to metabolic disorders such as diabetes, insulin resistance and obesity²⁷. Age-standardized prevalence of diabetes increased significantly over the last 30 years, population growth and aging are responsible for 40% of this increase²². Impaired insulin secretion and insulin resistance are the two main characteristics of type 2 diabetes mellitus²⁸. Furthermore, diabetes is also a known cause of accelerated aging, thereby speeding up the ongoing deterioration process²⁷ and increase the risk for cognitive impairment and dementia²².

Not included in the WHO defined NCDs, but another important group of diseases are neurological NCDs, such as Alzheimer's and Parkinson's. Alzheimer's disease (AD), as the most common neurodegenerative disease can occur due to genetic factors, called familial AD or as sporadic AD, thought to be caused by interactions of environmental and genetic factors. AD is characterized clinically by memory and learning impairments, disorientation and mood fluctuations²⁹. The initial causes for AD are still not completely understood, but likely include A β plaques (abnormal proteolytic fragment aggregates), cholinergic dysfunction, tau aggregation and known hallmarks of aging like inflammation, DNA damage and mitochondrial dysfunction³⁰.

Parkinson's disease (PD) is defined by intracellular inclusions of α -synuclein aggregates and loss of neurons in the substantia nigra, which leads to striatal dopamine deficiency. PD is diagnosed based on movement speed and amplitude which is an indicator for neuromuscular dysfunction and tremors. On a molecular level, multiple mechanisms and pathways are involved, including the aging related neuroinflammation, mitochondrial function and oxidative stress³⁰.

The element contributing most to the risk of suffering from neurological NCDs such as Alzheimer's or Parkinson's is growing old. Every tenth individual above the age of 65 experiences AD and this number continuously increases with progressing age³⁰. Nine of the twelve hallmarks of aging are especially correlated with vulnerability to neurodegenerative disease. For example, epigenetic alterations are implicated in neurodegenerative disease and disorders. One epigenetic mechanism of gene regulation is histone acetylation, which is tightly linked to memory formation. Deregulation of histone acetylation is associated with memory impairments and ultimately with neurodegenerative disease. Regulation of DNA methylation of memory-linked genes via DNA methyltransferases (DNMT) and ten-eleven translocation proteins (TET) is also crucial for synaptic plasticity and memory storage as well as acquisition³¹. Loss of proteostasis is another hallmark of aging playing an important role in development of neurodegenerative disorders, as the disease pathology is usually a result of defective autophagy processes which allow toxic protein aggregates to accumulate⁴.

2.2 Aging interventions

The above discussed hallmarks of aging are potential targets to analyze the effects of novel therapeutics and broad preventatives to slow or even prevent aging and age-related diseases³². A way to reveal mechanisms of aging is to study so called lifespan-extending interventions and their effects and mode of action on hallmarks of aging.

2.2.1 Exercise

Regular physical activity is proven to increase life expectancy in humans and mice^{33,34}. Moderate exercise in mice is shown to decrease oxidative stress, a hallmark of aging³⁴. Cognitive aging and neurodegeneration are slowed down in this intervention due to a reduction of inflammation and increased plasticity in the hippocampus. Recent studies identified anti-inflammatory exercise factors in the plasma, like clusterin, that benefit the brain by targeting the brain vasculature³⁵. Different hallmarks of aging, like telomerase deficiency, lead to reduced tissue repair capacities in aging, especially in skeletal muscles. Muscle stem cells (MuSC) contribute to the regenerative capacities.

Through voluntary wheel running in mouse experiments MuSCs can be activated via restoration of Cyclin D1 and improve tissue regeneration³⁶.

2.2.2 Caloric restriction

Caloric restriction (CR) is defined as the chronic reduction of total calorie intake without malnutrition. A particular form of CR is intermittent fasting, which alternates between ad libitum feeding and episodes of no caloric uptake. CR strategies are the only known intervention to robustly improve health- and lifespan in most living organisms³⁷. Though the impact on lifespan is strain and sex specific, studies in rodents, non-human primates and humans showed a decrease in cancer incidence, type 2 diabetes and obesity after this intervention³⁸. The anti-aging effects observed in CR are mainly mediated by inhibition of inflammatory pathways and the reduction of ROS³⁹.

2.2.3 Partial reprogramming

The ideal goal of partial reprogramming as an aging intervention is to reshape the epigenetic landscape in one cell-type to its initial state. This initial state is defined as the moment right after differentiation is completed and functionality of all specialized cellular functions is achieved. Aging hallmarks, like telomere shortening, oxidative stress and chromatin remodeling, have been shown to be reversed or improved by (partial) reprogramming in vitro and in vivo⁴⁰. Expression of the Yamanaka factors leads to reprogramming differentiated cells back into pluripotency⁴¹. By expressing these factors, namely OSKM, in a transient manner, dedifferentiation to progenitor-like states can be achieved. Lifespan extension and improvement of age-associated phenotypes have been reported while cyclic in vivo induction of OSKM in a progeria mouse model. Furthermore, short-term expression of OSKM in aged mice can improve wound healing after injury, which indicates that tissue regeneration capacities can be improved via partial reprogramming⁴⁰. Long-term partial reprogramming has been proven to be most effective in skin and kidney and results in a reversion of age-associated transcriptional and epigenetic changes, even in later life stages in mice aged 22-25 months⁴². But before age reprogramming can become a therapy in regenerative medicine, adverse effects like the risk of cancer must be eliminated or minimized⁴³.

2.2.4 Drugs: Rapamycin, Metformin & Senolytics

Administration of drugs that have been shown to increase life span as well. Rapamycin is an FDA-approved drug that inhibits the mTOR signaling pathway, therefore age-related diseases are delayed, and life span is extended in various model organisms⁴⁴. The positive effects persist even if treatment is started later in life

compared to earlier treatment and even after treatment end⁴⁵. The effects range from suppression of cell senescence over reduction of cardiac hypertrophy to improvement in cognition and neuroprotective effects on neurovascular disease and brain injury. But in humans serious metabolic and immunological side effects were observed⁴⁴, therefore this drug is more interesting to be studied in the clinic as a treatment for Alzheimer's disease rather than aging itself⁴⁵.

Metformin, usually prescribed to treat type 2 diabetes has been shown to extend health and life span in male mice⁴⁶. Mechanistically, the drug works by attenuating hallmarks of aging. Nutrient sensing is improved, and autophagy and intercellular communication are enhanced⁴⁷.

Senolytic drugs, like navitoclax, kill senescent cells in a targeted approach, hence imitating physiological tissue clearance. Senescent cells contribute to the aging phenotype mainly via their secreted proteins⁴⁸. Navitoclax, for example, specifically targets proteins that mediate resistance against apoptosis and survival in senescent cells. Senolytics have been shown to extend life spans in model organisms and are entering clinical trials for different indications⁹. Repression of the SASP during Rapamycin treatment is mediated by mTOR inhibition. Metformin is also able to inhibit SASP, both drugs mediate the positive effect without eliminating senescent cells⁴⁸.

2.2.5 Heterochronic parabiosis

Another aging intervention is heterochronic parabiosis. During a surgical procedure a young and an old mouse are joined together resulting in a shared circulatory system for the two living animals⁴⁹. This method has been used for over 150 years to test the effects of systemic or circulatory factors from one animal influencing the other animal. In the aging context several circulatory factors have been identified with pro-/anti-aging effects, e.g. effectors of the Wnt and TGF- β signaling pathway⁵⁰ and cytokines acting on stem cell populations⁵¹. In heterochronic parabiosis, the aged mice exhibit functional improvement of the central nervous system (CNS) as well as various other organs⁵¹. In the CNS, exposure to young blood can rejuvenate synaptic plasticity and lead to an improvement of cognitive function⁵². Furthermore, the neuronal stem cell population in the subventricular zone exhibit a higher self-renewal and differentiation⁵³.

In contrast to reprogramming during induced pluripotent stem cell formation the reprogramming occurring on a molecular level induced by parabiosis does not involve loss of differentiation characteristics. It is composed of an epigenetic memory as a response to systemic influences. It is only the rejuvenation of cells rather than

dedifferentiation⁴⁹. Therefore, using this intervention to identify circulating factors is a powerful experimental tool to find new therapeutic targets.

2.3 Small non-coding RNAs

Apart from coding RNAs, the messenger RNAs (mRNAs), eight main classes of non-coding RNAs (ncRNAs) exist: microRNA (miRNA), PIWI-associated RNA (piRNA), long ncRNA (lncRNA), small nucleolar RNA (snoRNA), small nuclear RNA (snRNA), transfer RNA (tRNA), ribosomal RNA (rRNA) and small Cajal body-specific RNA (scaRNA) (Figure 2). tRNA and rRNA are well known for their integral role in translation. In addition to the mature tRNAs themselves, functional tRNA derived fragments (tRFs) have been recently identified. tRFs are now explored as disease-associated biomarkers, because of their crucial role in regulation of different pathological conditions⁵⁴.

PiRNAs repress transcription through directing chromatin modifications and are best studied in the male germline. lncRNAs are transcribed autonomously and have a length over 200 nt. They can regulate assembly and function of nuclear bodies, modulate chromatin function, influence the translation and stability of mRNAs and regulate signaling pathways. These capacities are mediated in a location dependent manner via specific interactions with DNA, RNA and proteins. Expression of these non-coding RNAs is tissue- and condition-specific⁵⁵. SnoRNAs serve as guide RNAs in pre-rRNA processing and modification, but also modify mRNAs and tRNAs. In cancer, these RNAs can either act as tumor-suppressors or in a tumor-promoting manner and their expression is linked to clinical prognosis⁵⁶. Another RNA class with similar function are scaRNAs, but these are located in the Cajal body, not in the nucleolus, and are longer with 200-300 nt length compared to snoRNAs (70 nt). ScaRNAs are guide RNAs for modifications mediated via splicosomal snRNAs⁵⁷. SnRNAs have a length of 100-300 nt and are in the cell nucleus⁵⁸. They are crucial components of the spliceosome, improving splicing of pre-mRNA via complementary base pair binding within a small nuclear ribonucleoprotein complex⁵⁹.

Types of non coding RNA

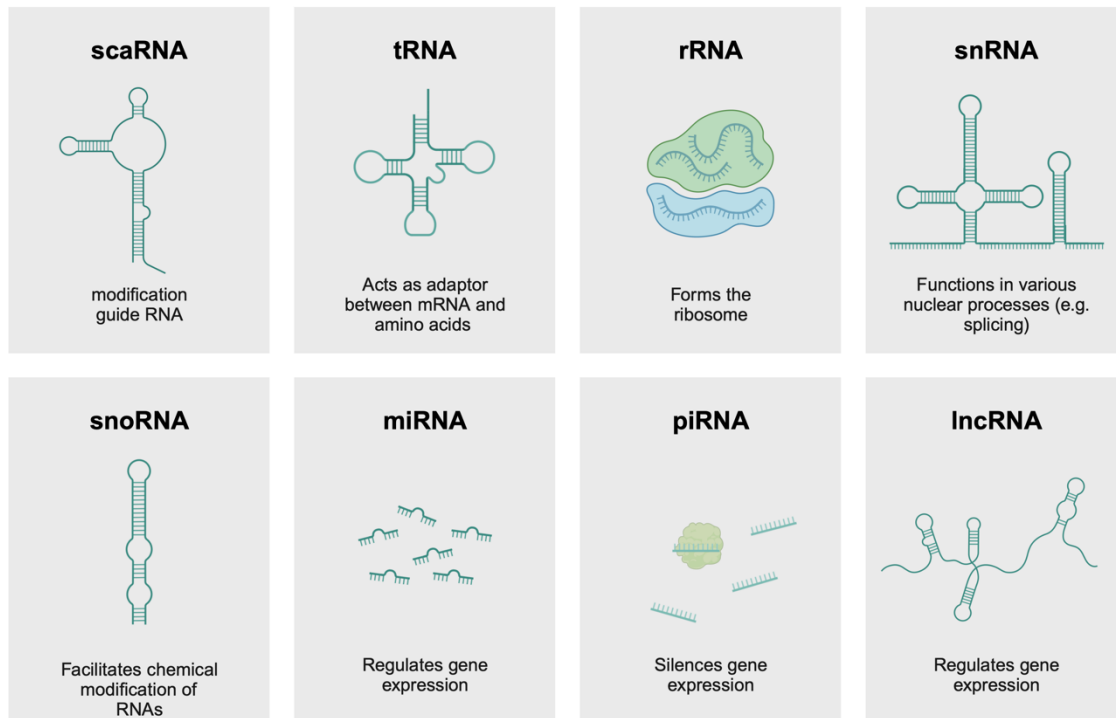


Figure 2: Non-coding RNA types and their main functions.

All types of ncRNAs including scaRNA, a guide RNA responsible for modifications; tRNAs acting as adaptors between amino acids and mRNAs; rRNAs, forming the ribosome; snRNAs, involved in splicing; snoRNAs, facilitating chemical modifications of RNAs; miRNAs, piRNAs and lncRNAs regulating gene expression; modified from BioRender.

2.3.1 MicroRNAs

MicroRNAs (miRNAs) are RNAs with a length of ~ 22 nt. Pri-miRNAs are transcribed via RNA polymerase II from genes encoding miRNAs as long primary transcripts. These transcripts are processed into precursor miRNAs (pre-miRNAs) through interaction with DROSHA (RNase III enzyme), while in the nucleus. Export from the nucleus into the cytoplasm is mediated by Exportin 5. Another RNase III enzyme, namely DICER together with TRBP cleaves the pre-miRNA into a duplex. This duplex consists of a guide strand miRNA, which will become the mature miRNA and its complementary sequence, the passenger star strand⁶⁰.

In complex with AGO protein, miRNAs use seed sequences near their 5' end to pair with the complementary bases of a target mRNA in their 3' untranslated region (UTR). This pairing induces deadenylation and decay or translational regulation⁵⁸, this mechanism lets them act as post-transcriptional regulators of gene expression.

Estimations claim that more than half of all mRNAs are targeted by miRNAs, thereby regulating various processes such as apoptosis, differentiation and proliferation⁶⁰. MiRNAs make an important contribution to gene regulatory networks, as one miRNA targets multiple mRNAs and collaborative effects of multiple miRNAs targeting one mRNA are even increasing their effects⁶¹.

MiRNAs do not only mediate gene silencing, but they can also activate translation of mRNAs by binding different target sites and in specific sub-cellular locations and under certain cellular circumstances⁶². For example, let-7, which inhibits translation in proliferating cells of certain genes, activates it during cell cycle arrest. During amino acid starvation miRNAs can bind to the 5'UTR of mRNAs and thereby mediate activation⁶³. In addition to this control mechanism, miRNA can also mediate transcriptional and post-transcriptional gene regulation.

MiRNAs do not exclusively act in their cell of origin but can also be used in intercellular communication. MiRNAs can be sorted into extracellular vesicles, secreted, transported in e.g. blood and regulate gene expression in their recipient cells. Various functions are mediated by these miRNAs in the recipient cells like immunosuppression, promote neurogenesis, fibrosis and angiogenesis⁶⁴. Because of their prevalence in easily accessible bodily fluids, mirroring changes in their origin tissue, miRNAs have been heavily studied as biomarkers in various diseases^{65,66}.

2.3.2 Bioinformatic tools for miRNA analysis

Numerous bioinformatic tools have been developed since the discovery of the first miRNA in 1993⁶⁷ to facilitate analysis of multiple aspects of miRNA studies, like miRNA prediction and discovery, analysis, structure and target prediction. Well over 100 miRNA tool papers are published per year since 2012⁶⁸. This number has risen quite rapidly for miRNA related tools, compared to all other ncRNA related tools, which have less than 50 publications a year⁶⁹. Especially the technological advances, namely NGS (next generation sequencing) simplified prediction of novel miRNAs, which was previously laborious and expensive, involving e.g. cloning. Furthermore, data was noisy and therefore only highly abundant miRNAs could be identified⁶⁸. The other hot spot in the field apart from miRNA identification in the past decade is target prediction⁶⁹.

A variety of tools for miRNA target site prediction exists. These can be grouped into five categories: energy-based tools, like PicTar⁷⁰; sequence-based tools, like TargetScan⁷¹; machine learning-based tools, like MBSTAR⁷²; database-based tools, like STarmirDB⁷³; statistics-based tools, like RNA22⁷⁴. These miRNA target prediction tools are extremely valuable assets in miRNA research, as they enable researchers to narrow down likely miRNA-mRNA interactions and lead to targeted validation

experiments reducing not only cost of experimental consumables but also time and increasing validation rates. The current tools are ever evolving, like e.g. integrating different approaches of miRNA target site prediction into one tool considering multiple factors of prediction like binding energy, sequence properties and structure at once⁷⁵. But even though numerous new tools exist, classic tools like TargetScan⁷¹ and miRDB⁷⁶ and their updates are amongst the highest cited papers in the field, indicating that not only these tools are well maintained but also still relevant and highly used⁶⁹. These mostly webserver-based tools enable miRNA researchers to streamline different tools during their research without the need of developing additional software while analyzing new data sets with different questions.

2.3.3 microRNAs in aging

Recent studies identified age-related miRNAs in whole blood in humans and sets of age-related miRNAs as disease biomarkers for multiple diseases such as Parkinson's, non-tumor lung disease and lung cancer. The cell intrinsic expression changes of miRNAs are likely responsible for the observed changes rather than changes in the cell type abundance. This data can be used to develop age-specific disease biomarkers and serve as a starting point to understand miRNA expression changes and their potential effects on disease and healthy aging⁷⁷.

Studying RNA expression in human tissue always faces the challenge of heterogeneous RNA quality due to varying post-mortem intervals which can affect the results of small RNA sequencing. Hence, to study tissue expression patterns of RNA mostly model organisms like mice are used^{78,79}.

There is only one miRNA, namely miR-17 known to date that extends lifespan in the mammalian model, mouse and inhibit cellular senescence⁸⁰. Even though formally known to be an oncogenic miRNA, whose overexpression results in development of liver tumors, transgenic miR-17 mice also exhibit significantly extended life spans. This miRNA silences *ADCY5* and *IRS1*. Generally, miRNAs have been studied in the aging context in multiple studies in different tissues such as brain, heart, bone and muscle, as well as age-related disease but a comprehensive study of all major organs from multiple biological replicates over the entire lifespan is missing⁸¹. The issue with multiple studies is that contradictory results are challenging to interpret, and comparing data is difficult due to variations in the data handling and technical biases.

3 Goal of the PhD thesis

MiRNAs are well known for their capacity as biomarkers in disease but as they can interact with a broad spectrum of target genes, they are also emerging as interesting therapeutic tools. To reinstate homeostasis, ideally, regulatory functions of miRNAs on mRNAs could be used to restore cell functions disrupted in the disease context⁶¹. As most aging studies focus on deciphering the changes in coding RNA and protein expression, understanding the underlying changes in the layer of regulating small non-coding RNAs will add additional information to further complete the picture of the complex process of aging.

Samples for the *Tabula muris senis* (TMS) project were collected from all major mouse organs over the lifespan, namely ten different time points ranging from 1-27 months from 16 different tissues. Bulk sequencing data was generated, and the changes of the coding transcriptome were analyzed⁸². By reisolating the RNA from these tissue samples for small RNA sequencing, we were able to reuse these samples to generate our aging cohort dataset (Figure 3). We studied non-coding RNA expression changes during aging within this dataset and their potential interactions with the coding transcriptome. To investigate if the observed expression changes of miRNAs during aging were reversible, samples from a heterochronic parabiosis experiment were collected, generating the parabiosis cohort¹. Heterochronic Parabiosis is an aging intervention in which a young and an old mouse share their circulatory system, as they are surgically sutured together forming a continuous peritoneal cavity. In addition, we investigated miRNA expression patterns in samples of the circulatory system, the plasma and extracellular vesicles (circulatory cohort)^{1,83}.

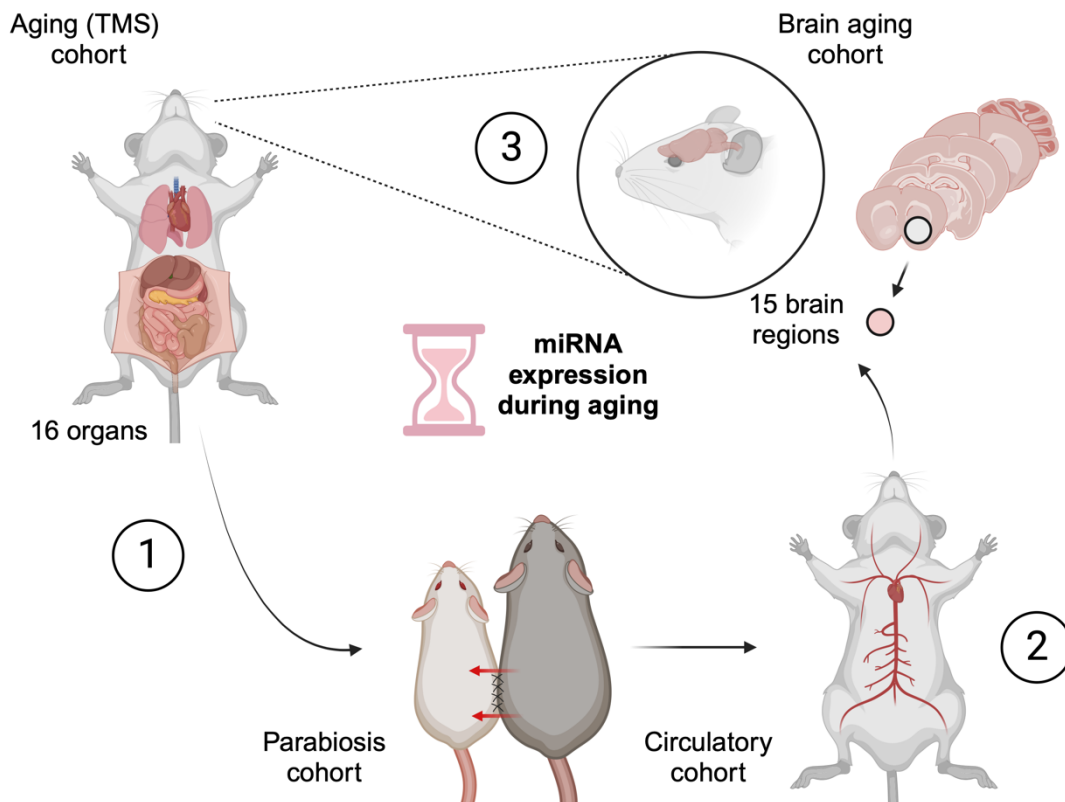


Figure 3: Revealing miRNA expression changes during aging.

Overview of datasets in this work: Aging cohort and parabiosis cohort (1)¹, circulatory cohort (2)^{1,83} and brain aging cohort (3, manuscript under preparation); created with BioRender.

Finally, since bulk tissue sequencing only provides a broad picture of the averaged expression in one organ in this study and as the brain is one of the most complex organs in the body, an additional set of samples from different brain regions was collected, the brain aging cohort (Figure 3). These samples were initially used to decipher the changes in the coding transcriptome⁸⁴. We selected 15 different brain regions and collected samples from these regions at seven different time points. The data adding insight into the changes in the non-coding transcriptome was generated in our group via small RNA sequencing. These four datasets combined, present new insights into the miRNA expression patterns during aging and potential regulation mechanisms of miRNAs in aging.

4 Methods

All cohorts housed and aged their mice in US facilities, except the circulatory cohort. Organ dissection and first RNA isolation was performed by the Stanford collaborates as well. Re-isolation of RNA was performed in Homburg for the TMS cohort. We optimized the library preparation protocol used in this study for automatized handling on the MGI-SP960 before processing all study samples. The in-house optimized protocol is now the standard protocol for Small RNA Library Preparation on the MGI-SP960. After library preparation, samples were sent to BGI Hong Kong for Sequencing. Data was aligned using miRMaster⁸⁵ and read counts were analyzed using R software and respective packages (Figure 4).

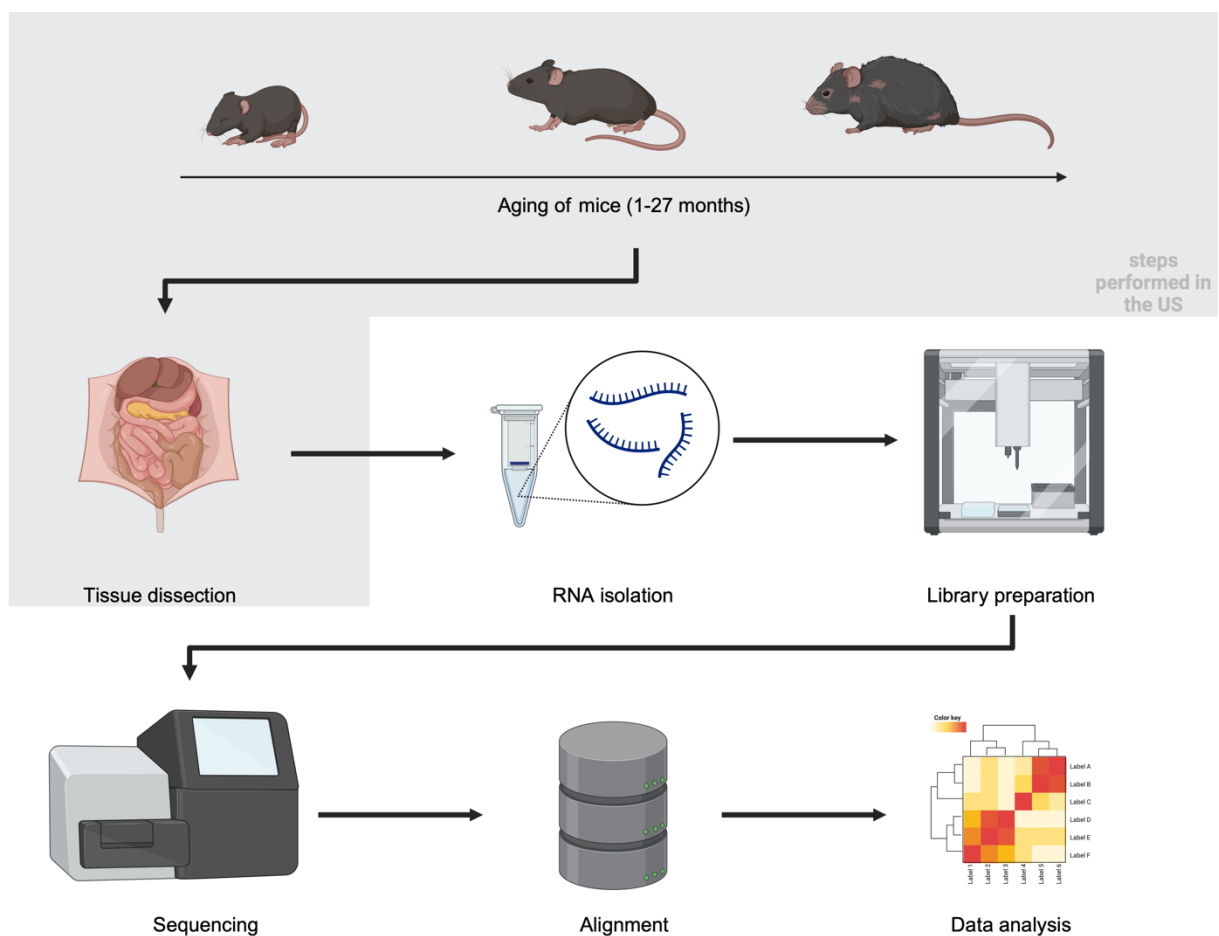


Figure 4: Simplified workflow for processing of cohorts.

Housing of animals and tissue dissection were performed in the US, (re)isolation of RNA, small RNA library preparation, sequencing, alignment and data analysis was performed in this work, created with BioRender.

4.1 Samples

Different mouse specimens were collected over the mouse lifespan in multiple cohorts. All animal samples and procedures were collected/ conducted in compliance with the respective guidelines (directive 2010/63/EU and NIH Publication #85-23 Rev.1985).

4.1.1 Aging cohort (TMS)

Mice for the aging cohort of this study were obtained as previously described⁸² from the National Institute of Ageing colony (Charles River) and shipped to the Veterinary Medical unit at the VA in Palo Alto. The cohort consists of male and virgin female C57BL/6JN mice, that were housed at 20-24°C with water and food provided *ad libitum* (Table 1). A 12 h light/dark cycle was applied, and the measured humidity was between 23-55%. 2.5% v/v avertin was used to anesthetize mice, after which mice were shaved and weighed. Via cardiac puncture blood was drawn and then mice were perfused with 20 mL PBS. Organs were dissected and instantly frozen on dry ice. Dissection occurred in this order: pancreas, spleen, brain, heart, lung, kidney, mesenteric adipose tissue, intestine (duodenum), gonadal adipose tissue, muscle (tibialis anterior), skin (dorsal), subcutaneous adipose tissue (inguinal pad), brown adipose tissue (interscapular pad), bone and bone marrow (femurs and tibiae).

4.1.2 Heterochronic parabiosis cohort

From the heterochronic parabiosis cohort bulk RNA samples were collected, comprising male C57BL/6JN, C57BL/6J, and C57BL/6-Tg(UBC-GFP)30Scha/J mice, following the methodology described earlier⁸⁶ (Table 1). The mice, aged between 3 to 4.5 months and 19 months, were kept in the same conditions as the aging cohort mice. During the parabiosis procedure the peritoneum of two mice is sutured together at the adjacent flanks to create a continuous peritoneal cavity. To facilitate coordinated movement post-surgery, adjacent knee and elbow joints of the mice were connected using nylon monofilament sutures, along with surgical autoclips to close the skin. All surgical steps were carried out in sterile conditions on heated pads, while the mice were under continuous isoflurane anesthesia. To prevent infection, alleviate pain, and maintain hydration, mice were administered Baytril (5 µg g⁻¹), buprenorphine, and 0.9% (wt/vol) sodium chloride, as previously detailed⁸⁶. The paired mice shared their circulation system for a period of 5 weeks after surgery, at the end of this period organs were collected. The sequence of collection was as follows: heart, liver, kidney, followed by MAT and GAT, and finally, limb muscle. All of these steps were completed within a time frame of 30 to 40 minutes. The ethical treatment of animals and all procedures

were conducted in compliance with institutional guidelines approved by the VA Palo Alto Committee on Animal Research (Protocol, LUO1736).

4.1.3 Circulatory cohort

Samples for the circulatory cohort were collected from 14 female C57BL/6N mice. These animals were housed in the animal facility of the Institute of Clinical & Experimental Surgery (Saarland University, Homburg/Saar, Germany). Free access to water and standard pellet food was guaranteed and a controlled 12 h day/night cycle was implemented. The study was approved by the local State Office for Health and Consumer Protection and conducted in accordance with Directive 2010/63/EU. Blood sampling and EV isolation was performed according to previously published protocols⁸³. In brief, after anesthesia mice were fixed and blood was drawn from the vena cava. Samples were centrifuged at 20°C, 10,000 x *g* for 5 mins, resulting in plasma samples. For EVs, 200 microliters of the plasma samples were diluted in 800 microliters of phosphate-buffer saline and centrifuged at 4°C, 100,000 x *g*. Pellets containing the EVs fraction were resuspended in 20 microliters buffer.

4.1.4 Region-specific brain aging cohort

As previously described male and female C57BL/6JN mice from the National Institute of Aging colony (Charles River) were shipped to the Stanford ChEM-H animal facility (Palo Alto), where they were housed at least one month before euthanasia. For each age group of 3, 12, 15, 18 and 21 months 5 female mice and 5-6 male mice were used; age groups 26 and 28 months consisted only of 5 and 3 male mice respectively (Table 2). Animals were housed in cages of 2-3 mice, with a 12/12 light/dark cycle, at 19.4 – 22.8 °C and provided with food and water ad libitum. Over the course of four consecutive days the sample collection was performed between 10 am and 12 pm. Mice were anaesthetized with 2.5% v/v Avertin, 700 µl of blood was drawn via cardiac puncture and followed by transcatheterial perfusion with 20 ml cold PBS. After immediate removal of the brains, the organs were snap-frozen by immersion in liquid nitrogen-cooled isopentane (60 seconds) and ultimately stored at -80°C before further processing. The respective regions were dissected via slicing and atlas-guided tissue punching while frozen. Using a metal brain matrix coronal sections of 1 mm thickness were sliced with .22 razor blades (Ted Pella, 15045; VWR, 55411-050). Regions of interest (1.5mm and 2mm diameter) were dissected quickly from the right hemisphere of these sections using disposable biopsy punches (Alimed, 98PUN6-2, 98PUN6-3). The following 15 regions were collected: three cortical regions (motor cortex, visual cortex and entorhinal cortex), anterior (dorsal) and posterior (ventral) hippocampus, hypo- thalamus, thalamus, caudate putamen (part of the striatum), pons, medulla,

cerebellum and the olfactory bulb, corpus callosum, choroid plexus and the subventricular zone. Four regions were collected in the following order, as the collection required overlapping punches: (1) motor cortex, (2) caudate putamen, (3) subventricular zone, (4) corpus callosum.

4.1.5 RNA isolation

RNA isolation was carried out according to the manufacturer's protocol using the miRNeasy Kit (Qiagen, 217084). For the brain aging cohort, the RNeasy 96 kit (Qiagen, 74181) was used. The extracted RNA samples were sent to the Institute of Human Genetics. In the case of the TMS cohort samples, additional purification steps were performed due to salt contamination. 150 ng of RNA was mixed with 3M NAAC (pH 7.0) and 100% EtOH, and left to incubate overnight at -20°C. This mixture was then centrifuged at 20,817g at 4°C for 60 minutes. After discarding the supernatant, the pellet was washed with 80% EtOH and subjected to another centrifugation for 30 minutes (20,817g, 4°C). The supernatant was once again discarded, the pellet was dried on ice, and finally, it was resuspended in 50 µl of 1x TE buffer. The concentration of RNA was determined using the NanoDrop 2000 spectrophotometer (Thermo Fisher Scientific), and RNA integrity was assessed using the Agilent RNA 6000 Nano Kit (Agilent Technologies, 5067-1512) for randomly selected samples from the cohorts.

4.2 Library preparation

The MGIEasy Small RNA Library Prep Kit (Item 940-000196-00) was used for library preparation on the high-throughput MGI SP-960 sample prep system according to the manufacturer's protocol. In principle this library preparation method works by ligating 3'- and 5'-adapters to all RNAs in each sample. During reverse transcription (RT), specific RT primers that bind to the adapters are used to generate cDNA and also introduce sample specific barcodes. Amplification of this cDNA is performed via a 21-cycled PCR. Size-selection of this PCR product is performed via magnetic beads (AMPure Beads XP, Beckman Coulter). To focus on the small RNAs a size of around 110 bp was selected, this was checked using an Agilent DNA 1000 Kit (Agilent Technologies). The concentration of each sample was measured by a QuBit 1x dsDNA High Sensitivity Assay (Thermo Fisher Scientific). Each library in this study consisted of 16 samples, barcoded with the following barcodes: 1–4, 13–16 and 25–32. All samples of one library were pooled after concentration measurement in an equimolar fashion to reach a concentration of 4.56 ng µl⁻¹ for each sample in each pooled library. After circularization the pooled libraries were sent for sequencing.

4.3 Sequencing and data analysis

All libraries were sequenced via single-end sequencing on BGISEQ500RS using High-throughput Sequencing Sets (SE50) (Small RNA) in a BGI core facility. MiRMaster 2.0 was used in standard settings to process the sequencing data⁸⁵ to generate count matrices and mapped read percentages. Additionally the following RStudio Software packages and Rstudio v4.0.3 were used to perform data analysis: viper v1.26.0, data.table v1.14.2, ggrepel v0.9.1, ggvenn v0.1.9, M3C v1.14.0, ggridges v0.5.3, forcats v0.5.1, purrr v0.3.4, tidyr v1.2.0, tibble v3.1.6, ggplot2 v3.3.5, tidyverse v1.3.1, viridisLite v0.4.0, ColorBrewer v1.1-2, reshape2 v1.4.4, pheatmap v1.0.12, Mfuzz v2.52.0, DynDoc v1.70.0, widgetTools v1.70.0, e1071 v1.7-9, stringr v1.4.0, dplyr v1.0.8, readr v2.1.2 and Biobase v2.52.0.

Only samples were considered for further analysis if more than 2 million aligned reads were detected, allowing one mismatch per read. All reads were mapped using Bowtie (v1.2.3) against RNA sequences derived from the respective databases for each RNA class, namely: miRNAs: miRBase 22, tRNAs: GtRNAdb 18.1, piRNA: RNACentral 15, all other ncRNAs: Ensembl 100. In Table 3 (Appendix B) are all additional paralogs listed, as only the first paralog was kept for analysis. Detailed statistics for the covered sequence length were calculated, since only two RNA classes namely, miRNAs and piRNA optimally matched the sequence length favored with this protocol in their mature forms⁸⁷. Through these analyses the risk that only random RNA fragments of the other RNA classes were sequenced was excluded. RNA fragments can either be the product of post-mortem degradation processes and therefore occur at random or they are generated in physiological processes through e.g. enzymatic cleavage like tRNA fragments and exert biological functions (e.g. regulation in aging⁸⁸). RNA quality is the main driver of variance in the distribution and amount of degradation fragments⁷⁹. All statistics were calculated, namely: reference read, length covered percentage reference length, covered read length, longest covered region, longest mapping read, average covered read length and total reads mapping for all detected ncRNAs. The highest counting precursor was selected to present all mature ncRNAs.

Mean percentages per timepoint and tissue of aligned reads were calculated based on the percentage of aligned reads per sample from miRMaster analysis.

For global analysis, two filtering steps were implemented. First, detected piRNAs were reduced to only piRNAs encoded in the prepachytene genomic piRNA cluster to ensure only true somatic piRNAs were considered in the analysis^{89,90}. Second, only RNA features were retained in each cohort, that were detected with minimal 1 rpmm in at least one sample. A t-SNE and a principal variance component analysis (PVCA) were

performed as global analyses. To comprehensively visualize high-dimensional data, dimensionality reduction is the method of choice, for which t-SNE is an optimized method. Settings for the t-SNE clustering using the M3C package were a seed of 40 and unweighted clustering of all samples. An estimation of the variability introduced by biological and technical parameters was done by performing a PVCA, in which data reduction is performed via principal component analysis.

For local analyses, in which the focus was on tissue-specific rather than overall patterns, a tissue-specific filtering of ncRNAs was performed. Exclusively, RNAs with a minimal expression of 1 rpmm in 10% of all samples in each individual tissue were retained for calculations. Proportions of RNA class counts in relation to tissue were computed by dividing the total count for each RNA class within a tissue by the corresponding mean count of all RNA classes. Proportions of tissue and time point counts were determined by calculating the percentage of counts for each sample after applying local filtering using the overall RNA class counts. Mean percentages for time points were derived from the respective samples across each time point and tissue. In each tissue for each locally abundant ncRNA the correlation of expression with age was calculated via Spearman rank correlation. These correlation values were illustrated in a density plot, categorized and colored by RNA class. Correlation of miRNAs with age were grouped into positively ($r > 0.5$) and negatively ($r < -0.5$) correlated RNAs and P values were calculated. The count of tissues in which each miRNA was (anti-) correlated with age was calculated relying on this grouping. Foldchanges (FC) of miRNAs in later life were calculated using 3 months as a control reference. With the mean expression of all later timepoints and the mean expression at 3 months in each tissue FC was determined. MiRNAs with a mean expression of zero at 3 months old in a specific tissue were excluded from this analysis. A FC value was categorized as deregulated if the value exceeded the interval of $2/3$ and $3/2$. For these comparisons t -tests were calculated, only for comparisons with a minimum of 3 replicates per timepoint P values were determined. These were adjusted for each tissue and timepoint separately using the Benjamini and Hochberg method. All FC equal to 0 were discarded for $\log_2(\text{FC})$ calculations. These calculations were used for generation of volcano plots together with $-\log_{10}(P \text{ values})$, dots were colored by timepoint. For the non-linear age correlation analysis, the package Mfuzz was used to cluster the organism-wide miRNA trajectories with fuzzy c-means clustering. Each miRNA trajectory in each tissue in this clustering was based on the z-scored miRNA expression. The optimal number of clusters c between 2 and 20 was determined using the minimum centroid distance measure, for this clustering 20 clusters were determined as optimal. Clusters with at least 30% miRNAs originating from one tissue were deemed tissue-specific.

In a previous study the coding transcriptome data of the identical samples was generated⁸². This data was used to predict miRNA-mRNA interactions via correlation of expression. mRNAs were identified as miRNA targets expression of the interacting pair was significantly negatively correlated ($r < -0.4$, $P < 0.05$). For local aging miRNAs, defined as miRNA with a correlation above 0.5 or below -0.5 with age, miRNA-mRNA interactions were predicted per tissue. A higher cutoff for local miRNAs was implemented to ensure the identification of true age-related interactions within the millions of potential miRNA-mRNA interactions. Cross-organ interaction analyses were performed based on the newly identified global aging miRNAs. The five positively correlated miRNAs (miR-29a-3p, miR-29c-3p, miR-155-5p, miR-184-3p and miR-1895) and the three negatively correlated ones (miR-300-3p, miR-487b-3p and miR-541-5p) were tested for significantly inverse correlations with mRNAs in all tissues. Exclusively, miRNA-mRNA interactions were retained in the filtered target set, that were predicted in at least two tissues for one miRNA. The known connections between the proteins encoded by these target genes were illustrated using a protein-protein association network database⁹¹ (STRING).

For the local and global aging miRNAs, positive and negative respectively, a pathway enrichment analysis was performed. An over-representation analysis (ORA) was chosen to identify the pathways related to the predicted target mRNAs. The analysis was performed using GeneTrail 3.2 with its standard parameters, FDR adjustment and a significance level of 0.001⁹². For mRNA targets of the locally positively correlated miRNAs in each tissue, a heatmap was plotted for the top 20 non-disease-related pathways with the lowest P value regulated in most tissues. Respectively, for the targets of the locally negatively correlated miRNAs the top 25 non-disease-related pathways were plotted.

Filtering criteria used for analyzing the TMS data set were also implemented for the parabiosis data set. 50,776 ncRNAs were detected in total within the raw reads and 5,248 ncRNAs remained as abundant after filtering for the global analysis (t-SNE). Foldchanges between HA and IA, as a control were determined, to quantify the rejuvenation effect (REJ) of parabiosis treatment. For accelerated aging (ACC) the foldchange between HY and IY (control) was also calculated. As control comparison for physiological data from the TMS dataset was used to define AGE (Foldchange 3 months versus 21 months). This comparison reflects the ages of the parabiosis cohort at takedown best. Deregulated FC thresholds were used as before ($FC < 2/3$ or $FC > 3/2$, $P < 0.05$).

For the circulating miRNA dataset, filtering was performed as implement for TMS (10% per group with at least 1 rpmm). The intersection of expressed miRNA in EVs and

plasma was used to determine the share of local and global miRNAs in the circulatory system and displayed in a Venn diagram.

4.4 Cell lines

HEK293T (ACC635) cells (Deutsche Sammlung von Mikroorganismen und Zellkulturen, DSMZ) were used were cultured with DMEM (Life Technologies) supplemented with Penicillin (100 U ml⁻¹), Streptomycin (100 µg mL⁻¹) and 10% (vol/vol) FCS. Cells were passaged twice a week and experimental culture times did not extend 3 months.

4.5 Plasmids

The pSG5-miR-29a expression plasmid was cloned as previously described⁹³. Predicted targets from miRNA-mRNA interaction analysis in Figure 16A were used to generate reporter plasmids. Predicted gene targets for miR-29a-3p and miR-29c-3p were filtered for targets with at least a 7mer binding site and the minimal possible hamming distance between human and mouse in the entire 3'UTR and specifically the binding site. Binding sites were identified using TargetScan⁷¹. Target validation was performed for simultaneously for miR-29a-3p and miR-29c-3p as they share the same seed sequence. The reporter constructs were synthesized and integrated into the respective plasmid pMIR-RNL-TK, utilizing SpeI and SacI as restriction sites through a service of GeneArt (Life Technologies GmbH). For assay performance assessment, the previously identified pMIR-COL1A2 reporter plasmid⁹⁴ was used as a positive control (Supplemental Figure 12). In Table 4 all tested 3'UTR sequences are listed with the respective NM accession numbers.

4.6 High-throughput miRNA interaction reporter assay (HiTmiR)

The HiTmiR technique was used to validate mRNA targets of miRNAs, as previously described⁹⁵. Concisely, the epMotion 5,075 (liquid handling system, Eppendorf) was used to distribute HEK 293T cells (3.2×10^4 cells per well) in a 96 well plate. Transfection of cells was performed 24h after seeding. 50 ng per well of either the reporter plasmid pMIR-RNL-TK, without or with insert, were used together with 200 ng of miRNA expressing plasmid pSG5-miR-29a or pSG5 (empty expression vector). HEK T293 cells were lysed 48h after transfection and lysates were measured in a GloMax Navigator microplate luminometer (Promega) with the Luciferase substrate of

the Dual-Luciferase Reporter Assay System (Promega). This assay was conducted for each miRNA-mRNA target interaction prediction with four technical replicates.

4.7 Data availability

All published sequencing data is freely available from Gene Expression Omnibus (GSE217458, GSE222857).

5 Results

5.1 ncRNA expression across mouse organs during aging

In order to study changing ncRNA expression patterns during aging, we collected samples from 16 different tissues over ten different time points and isolated the RNA (Figure 5A). The tissue samples were collected from bone (femurs and tibiae), brain (hemibrain), brown adipose tissue (BAT, interscapular depot), gonadal adipose tissue (GAT, inguinal depot), heart, kidney, limb muscle (tibialis anterior), liver, lung, bone marrow, mesenteric adipose tissue (MAT), pancreas, skin, small intestine (duodenum), spleen and subcutaneous adipose tissue (SCAT, posterior depot)⁸². RNA extracted from these tissue samples was prepared in libraries to perform sequencing of small RNA fragments. The sequencing results were analyzed for expression of the eight non-coding RNA classes (piRNA, lncRNA, miRNA, snoRNA, snRNA, tRNA, rRNA and scaRNA). All samples with sufficient quality control measures were sequenced, resulting in 771 samples sequenced and mapped to 58,422

features as detected once in any sample in the data set (Appendix B, Table 1). We mapped the features to the standard databases for each ncRNA class (cf. Methods), which summed up to a total of 87,590 reference features. MiRNAs were the most abundant class of all non-coding RNA classes with an average of 36.2% of reads mapped over all tissues (Figure 5B). SnoRNAs were responsible for the second largest share of reads on average with 22.6%. This average distribution did not reflect a stable state over all tissues, the distribution of reads per class varied significantly between the different tissues ($P < 0.05$, Kruskal-Wallis test). By plotting the detected read shares of

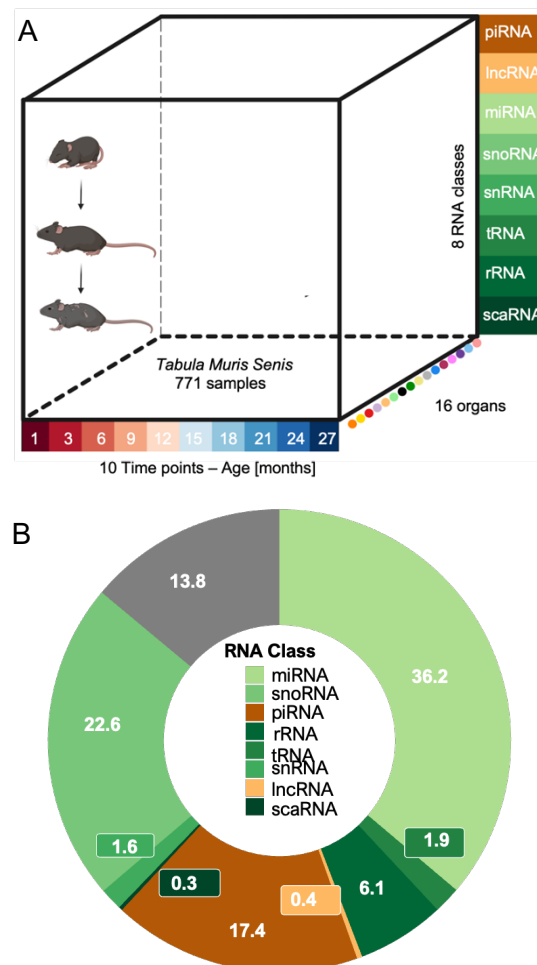


Figure 5: TMS Study set-up.

(A) Study set-up, samples from ten time points taken for 16 different organs measured for 8 different RNA classes, created with BioRender (B) Averaged read distribution of all samples in the dataset for the 8 RNA classes, before abundance filtering.¹

all tissues, the distribution differences became visible (Appendix A, Supplemental Figure 1). Limb muscle, brain, lung and heart exhibited the highest share with over 50% of all detected reads being miRNA reads. For bone and pancreas on the other hand less than 25% of all reads mapped to miRNA sequences.

We investigated the relation of the varying read distribution to the length of representative sequences by generating aligned sequence profiles to determine the extent of sequences covered entirely by mapped reads. Partial large fractions or the complete sequence were recovered even for long sequences consisting of over 10,000 bases (Appendix A, Supplemental Figure 2A). Additionally, the longest continuous mapping read was calculated for each sequence in relation to the reference sequence length. For larger RNAs this so-called maximal assembly decreased (Spearman's $\rho = -0.43$), but throughout all RNA classes a reproduction of a subset of sequences exhibiting up to 100% of full-length references was possible (Appendix A, Supplemental Figure 2B). This data has been published as a reference data set¹. For the following analysis, filtering steps were conducted to enhance reliability. For example, the detected number of somatic piRNAs was higher than expected. This was likely driven by artifacts in piRNA annotation databases⁹⁶, therefore an additional quality control filtering step was implemented for this RNA class. Exclusively piRNAs encoded in prepachytene piRNA genomic clusters were considered as true positives^{89,90}. Overall non-coding RNA classes lowly abundant features were removed. Exclusively, ncRNAs with a minimum of one read per million mapped (rpmm) in at least one sample were retained, composing a dataset of 7,883 features. This filtering especially excluded many piRNAs, reducing their number from 43,799 detected features to 43 abundant features. This reduction is likely caused by false annotations⁹⁶.

By clustering all samples over all abundant features in a t-SNE a clear separation over all tissues was observed (Figure 6). Samples originating from skin, GAT and SCAT appeared in one cluster. This can be explained by their

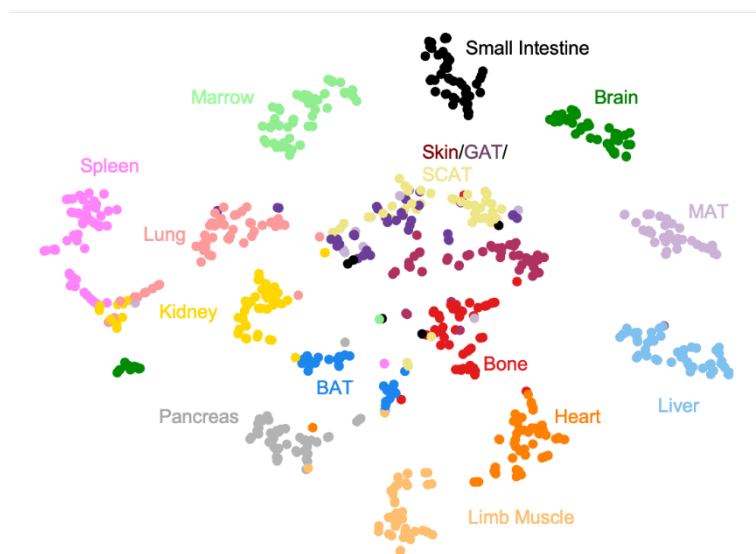


Figure 6: t-SNE clustering of all tissues. Clustering of all samples, colored by tissue over all abundant ncRNA features in the dataset.¹

close functional relationship and the shared cell types within the tissues potentially driving the tissue signature. A PVCA confirmed that the major driver of variance in the data set was the tissue identity (Appendix A, Supplemental Figure 3A). Sex did not contribute to variance in a notable way (below 0.5%) and could neither be identified in the t-SNE-clustering as major driver of the cluster formation (Appendix A, Supplemental Figure 3B).

A local filtering was implemented after this global feature analysis was performed to better account for differences in expression per tissue during aging. In each tissue only ncRNAs were considered for further analysis if the feature was detected with at least 1 rpmm in a minimum of 10% of all samples within the tissue in question. First,

we checked for differences during aging in each tissue in read distribution. Read count percentages were calculated for all ncRNA classes within the locally filtered data. Like the distribution of the detected reads the distribution of the locally filtered reads varied greatly between tissues (Figure 7).

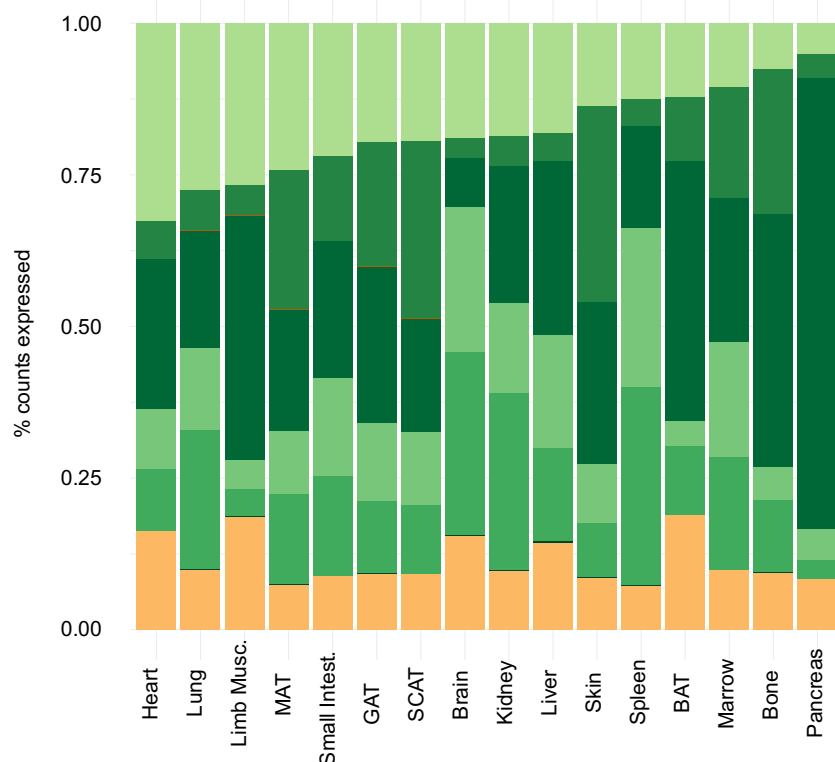


Figure 7: Count percentage per tissue after local filtering.

Percentage of all 8 ncRNA classes for each individual tissue after local filtering, ordered from highest to lowest miRNA share, color coded for RNA classes as indicated in Figure 5A.¹

We plotted the count distribution of

ncRNAs in percent resolved for every measured timepoint in each tissue individually (Appendix A, Supplemental Figure 4). Looking into the local count distribution in each tissue over the lifespan, tissues exhibited either a stable count distribution over time or high variation. The tissues were separated into the stable and high variation group based on a histogram visualizing the mean variance over all time points and non-coding RNA classes (Appendix A, Supplemental Figure 5). The high variation group is composed of brain, BAT and limb muscle exhibiting a mean variance higher than 4.5%. All other tissues were included in the stable group, identified through a variance lower

than 4.5% variance. As an example, for the tissues with high variation brain and BAT were displayed (Figure 8A, B). The miRNA share increased from 9.1% to 28.5% in brain meanwhile the share of snRNA reads dropped from 77.9% to 10.0%. In BAT, the miRNA share increased as well from 4.1% to 26.4%, accompanied by a decrease of rRNAs from 62.7% to 27.8%. The read count distribution of marrow and liver were examples for stable tissues with low variance during aging (Figure 8C, D).

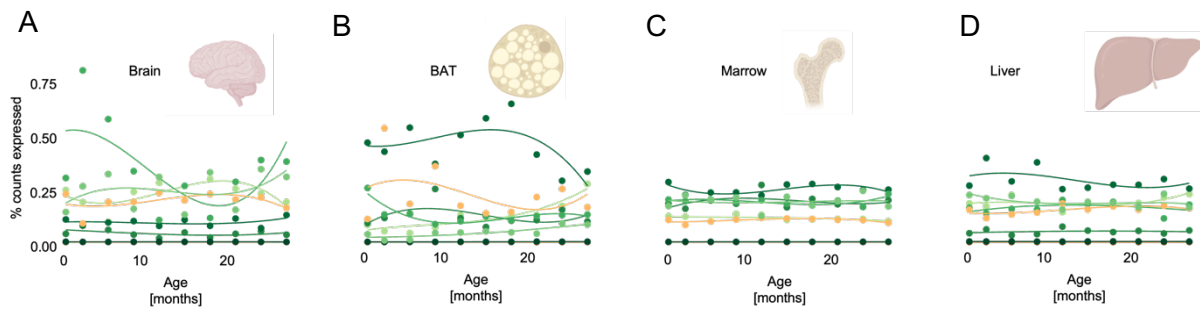


Figure 8: Count distribution of ncRNAs during aging per tissue.

Distribution of ncRNA counts after local filtering per tissue over the measured lifespan (1-27 months) for brain (A), BAT (B), marrow (C) and liver (D), created with BioRender.¹

Investigating the relation of each ncRNA in each tissue with age, the correlation was calculated for each RNA of each class in each tissues separately. These correlation values were grouped by RNA class and displayed as a density plot in Figure 9. 23 tRNA fragments exhibited decreasing expression with age (in bone, limb muscle, skin and GAT) opposed to eight tRNA fragments whose expression increased with age (in brain and lung). The higher amount of decreasing tRNA fragments is likely linked to the general tRNA expression decrease during aging. Modification, transcription and derivatives of tRNAs and their metabolism play vital roles in aging and longevity of organisms⁹⁷.

MiRNAs showed the most extreme correlation values, exceeding the interval of -0.5 and 0.5. This indicates that multiple miRNAs in different tissues became strongly

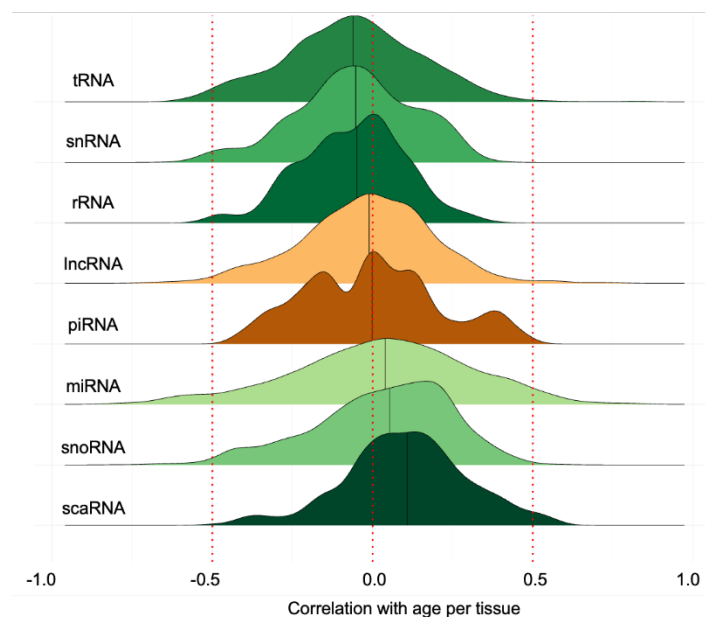


Figure 9: Spearman correlation of ncRNAs with age.

Spearman rank correlation for each ncRNA in each tissue after local filtering grouped and colored by ncRNA class.¹

deregulated during aging. Therefore, and due to the restrictions of the library preparation protocol, all further analysis was only focused on miRNAs.

5.2 miRNA correlation with age

Closer investigation of these miRNAs exceeding the interval between -0.5 and 0.5 with their correlation values and with a shared minimal expression in all tissues revealed exclusive tissue signatures. Positively and negatively correlated miRNAs per tissue were depicted in a heatmap for the union of miRNAs expressed in all tissues (Figure 10A). Certain miRNAs, like e.g. miR-107 was only correlated with age in one tissue, namely BAT. Including miR-107, a total of 37 miRNAs were uniquely correlated in BAT. In limb muscle, on the other hand six miRNAs were anti-correlated with age.

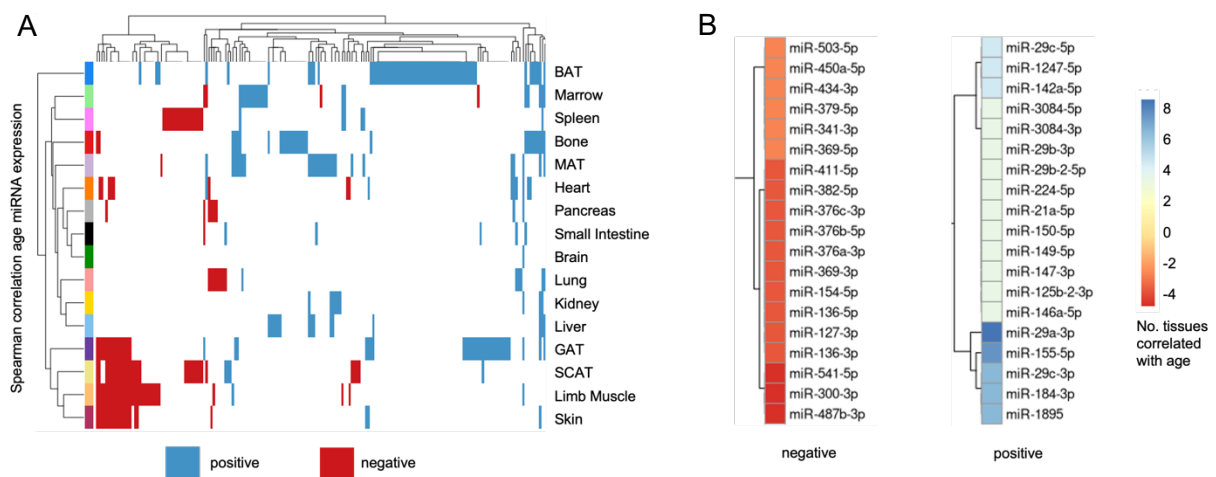


Figure 10: miRNA correlation with age.

(A) Heatmap of spearman rank correlation with age of miRNAs expressed in all 16 tissues after local filtering, color coded in blue for correlation ($r > 0.5$) and red for anticorrelation ($r < -0.5$); (B) Heatmap of tissue count for miRNAs (anti-) correlated with age in at least two tissues, separated for positive and negative correlation.¹

In contrast to these tissue-specific correlations, few miRNAs were (anti-) correlated in multiple tissues. All miRNAs (anti-) correlated in more than two tissues were listed in separate heatmaps for positive and negative correlation (Figure 10B). Filtering for miRNAs correlated with age in more than five tissues resulted in five miRNAs positively correlated and three miRNAs negatively correlated with age fulfilling this criterion. Namely, miR-29a-3p, miR-29c-3p, miR-155-5p, miR-184-3p and miR-1895 are correlated and miR-300-3p, miR-487b-3p and miR-541-5p are anti-correlated with age. These miRNAs were identified as global aging miRNAs, as they exhibit an aging signature over multiple tissues. MiRNAs exhibiting a (anti-) correlation

with age in exclusively one tissue were identified as local aging miRNAs and miRNAs not showing age-correlation in any tissue, were considered non-aging-related miRNAs.

5.3 Non-linear expression changes during aging

This grouping was based solely on linear correlation, to gain a more complete picture of all changes occurring during aging non-linear expression changes were explored as well. Fold changes (FC) between all later time points and three months as a grown adult reference were calculated to quantify the deregulation in each time point. Quantification was achieved by counting all miRNAs deregulated in each time point. A miRNA was considered deregulated if the FC exceeded the interval of $2/3$ and $3/2$. Prominently, an increasing number of deregulated miRNAs in BAT was observed, as expected because of the high number of age-correlated miRNA in this tissue (Figure 11). A peak deregulation of miRNAs in the brain was observed at 12 and 18 months of age. During linear correlation analysis only one local aging miRNA was identified in the brain. In contrast, during FC analysis 412 (at 12 months) and 427 (at 18 months) miRNAs were found to be deregulated. Volcano plots for each tissue were plotted to check if the deregulation identified via foldchange was also significant (Appendix A, Supplemental Figure 6). For brain, we observed that the majority of all significantly deregulated miRNAs with 77.6% originated from the comparisons of 12 and 18 months versus three months, visualized in a volcano plot (Figure 12). These findings were in line with our expectation of changing

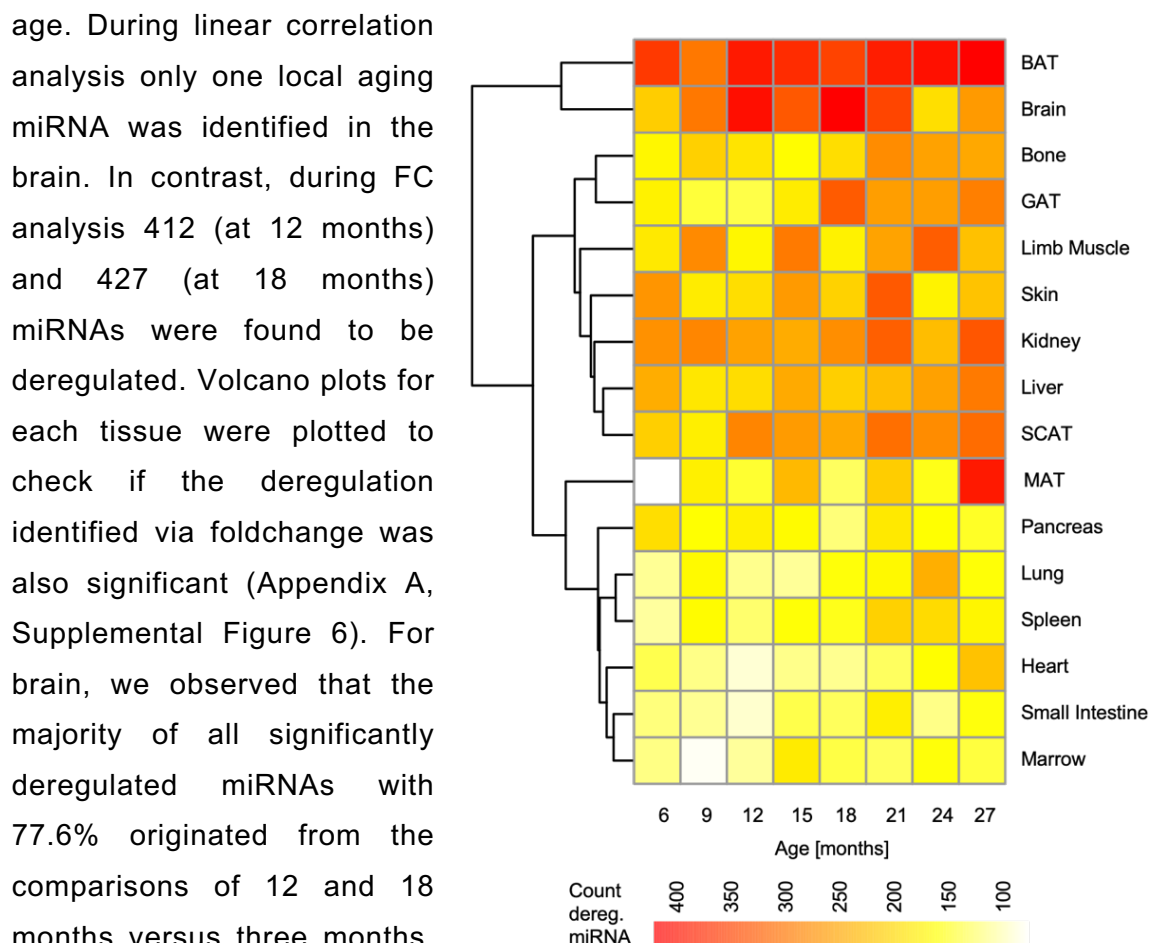


Figure 11: Heatmap of deregulated miRNA count.
Count of deregulated miRNA (exceeding FC range of $2/3$ to $3/2$) in the comparison of each consecutive time point to three months of age as a grown adult reference per tissue.¹

miRNA expressions in the brain during aging, since major transcriptome changes were observed previously⁸². These could be partially caused by miRNA expression alterations. Calculation of FC can lead to extreme high values for rather minor changes at low expression levels. Therefore, we checked that the significantly deregulated FC in all tissues were not due to only lowly expressed features by plotting FC versus expression for all miRNAs (Appendix A, Supplemental Figure 7) and all ncRNAs (Appendix A, Supplemental Figure 8).

Additionally, we

investigated isoform distribution at each timepoint. The average number of isoforms per

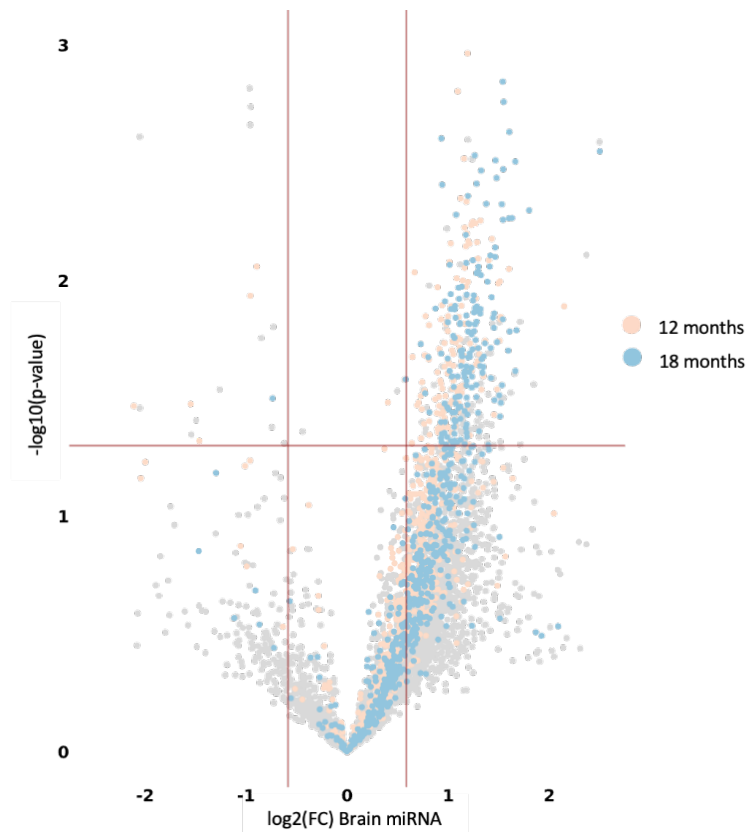


Figure 12: Volcano plot foldchange miRNA expression of all later timepoints versus three months versus respective *P*-values.¹

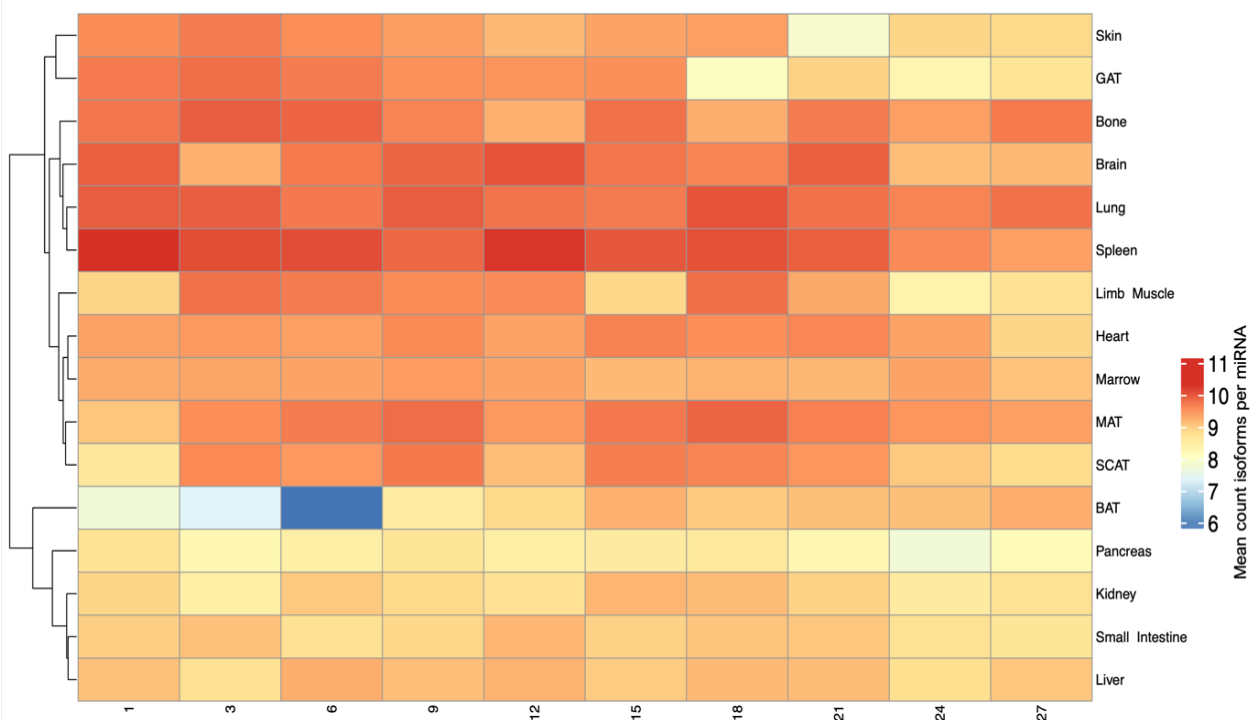


Figure 13: Heatmap of mean count isoforms per miRNA per tissue per time point.

miRNA overall miRNAs expressed in each tissue was calculated for each measured time point. The distribution of mean isoforms per miRNA per tissue was mostly stable within each tissue except for BAT (Figure 13). In BAT the mean count of isoforms per miRNA was very low for three and six months of age. The reason for this variation was likely because at these two time points there were less than three biological replicates analyzed because samples were excluded due to low quality.

5.4 Whole organism trajectory clustering

For each miRNA in each tissue a z-scored tissue-specific miRNA aging trajectory was calculated. These trajectories were clustered by fuzzy c-means clustering over all organs to identify common patterns like local and global aging miRNAs also for non-linear changes. The optimal number of clusters was identified as 20 clusters via minimal centroid distance as cluster validity index. All 20 clusters were displayed as an overview (Appendix A, Supplemental Figure 9). A detailed analysis of these clusters revealed that ten of these 20 clusters were composed mainly of miRNA aging trajectories originating from only one tissue. For these ten clusters, more than 30% of all trajectories grouped in the cluster were from only one tissue. This number is far higher than a random distribution which would be expected with 6.25% of trajectories originating from each tissue. These strong cluster identities proposed the existence of organ-specific miRNA time course signatures.

The signature trajectories for skin were displayed in cluster 2, as an example. The main cluster trajectory exhibited a peak at three months and an additional

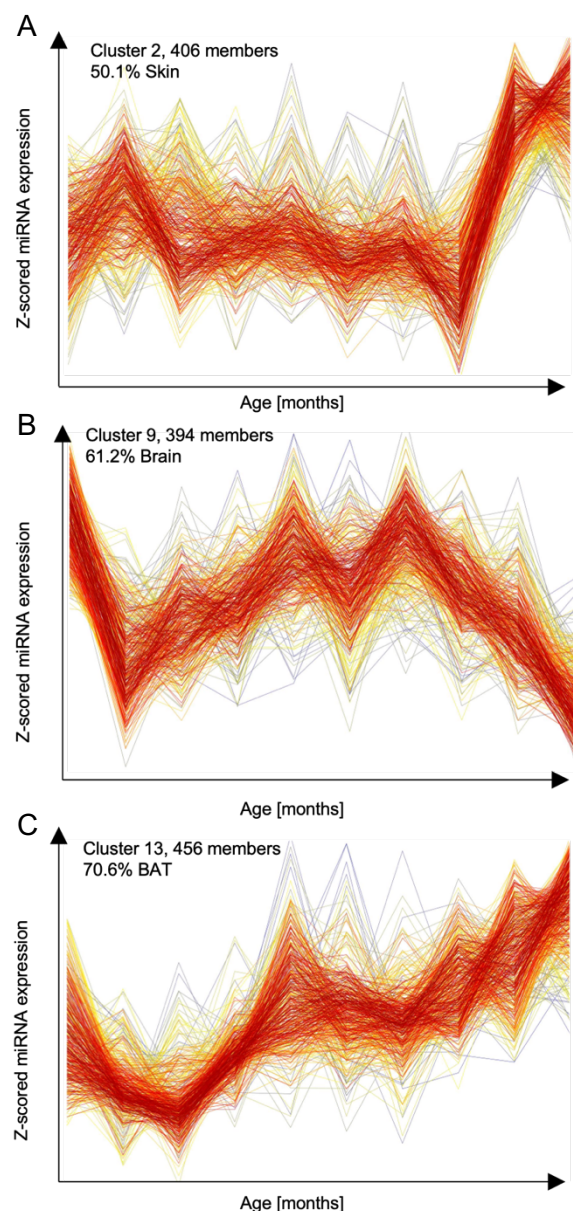


Figure 14: Tissue-specific miRNA trajectory clusters.

z-scored miRNA trajectory cluster for fuzzy c-means clustering of miRNA trajectories of each miRNA expressed in each tissue, examples for tissue specific clusters for (A) skin, (B) brain and (C) BAT.¹

increase at 21 months up to 24 months (Figure 14A). A total of 50.1% of all trajectories were miRNA trajectories from skin. Another example of organ-specific miRNA time course signatures is visible in the brain specific cluster 9 (Figure 14B). This cluster exhibited the previously discussed peaks of expression at 12 and 18 months of age and was composed of 61.2% brain miRNA trajectories. As a last example, the BAT signature cluster 13 showed that most miRNAs were linearly correlated with age in this tissue. The expression increased continuously from six months of age. This cluster exhibited the strongest tissue signature with 70.6% of all miRNA trajectories originating from BAT (Figure 14C).

MiRNAs originating from one tissue in such tissue-specific clusters were analyzed in an over-representation analysis with miEAA⁹⁸. Among the top five most significant pathways in BAT, GAT and MAT was 'insulin resistance' and in GAT and SCAT the 'AGE-RAGE signaling pathway in diabetic complication'. These tissue-specific miRNA expression changes in adipose tissues are interesting targets for further investigation as potential therapeutic targets, because insulin resistance plays a role in deregulated nutrient-sensing, one of the hallmarks of aging⁵. In addition to the adipose tissue-specific clusters, 'insulin resistance', 'type II diabetes mellitus' and the 'insulin signaling pathway' were enriched in the brain specific cluster. In one of the kidney specific clusters 'cellular senescence' lead the enriched pathways.

Contrary to the organ-specific signatures, global aging signatures were also observed in the clustering. In cluster 20 expression increased from one month of age until the end of the measurement and in this cluster miRNA trajectories from one miRNA originating from different organs were found. For example, miR-29a-3p and miR-29c-3p, which were previously identified as global aging miRNA via linear correlation analysis, were found in cluster 20 from 10 and 8 different organs, respectively (Figure 15). Even though we found these strong organ-specific miRNA time course signatures, the global aging identity of the previously identified global aging miRNAs was still present in the

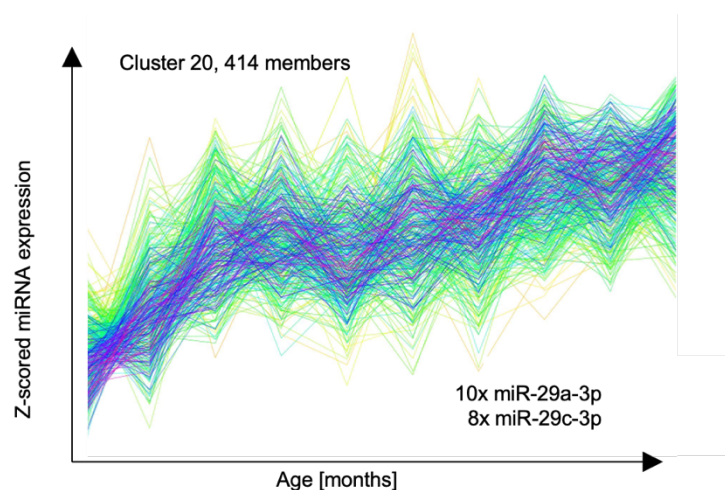


Figure 15: Continuously increasing expression aging cluster.

Cluster with global aging miRNAs: miR-29a-3p and miR-29c-3p, exhibiting continuous increase in expression over time with trajectories originating from ten and respectively eight different tissues.¹

trajectory clustering. As for seven out of the eight global miRNAs, more than five trajectories of the respective miRNA were found from different organs clustering together in one cluster instead of clustering in an organ-specific manner. This strong trend of expression de-/increase for very specific miRNAs indicates that these candidates regulate crucial pathways related to aging in all major organs.

5.5 miRNA-mRNA interactions of global aging miRNA

As miRNAs mediate gene silencing by binding to the 3'UTR of their target mRNAs, a decrease in mRNA expression is expected for a target of a miRNA with increasing expression. We chose an unbiased target identification approach to reveal new mRNA targets of the global aging miRNAs. We correlated miRNA expression patterns with all mRNA expression patterns in each tissue and labeled mRNAs as miRNA targets if Spearman's r of correlation was below -0.4 and this correlation was significant with a P -value below 0.05. The validity of this approach was tested by checking the amount of conserved binding sites within the predicted target mRNAs of the positive global aging miRNAs against a control. miRNA-mRNA interactions predicted by positive correlation of miRNA and mRNA expression were used as a control. At least one conserved binding site was found in 7.3% (9 of 122) of the via inverse correlation predicted miRNA-mRNA interactions. In the control only 2.1% (120 of 54,992) of mRNAs had one conserved binding site for the respective miRNA. The share of conserved binding sites in the predicted miRNA-mRNA interaction was significantly higher than in the control (Fisher's exact test, $P = 0.0018$).

As one gene can contain multiple binding sites across multiple 3'UTRs and binding sites differ in strength, the analysis was conducted separately for each binding site type as well. A 6.3-times enrichment of 8mer binding sites was observed in the predictions over the control (4.91% inverse correlation, 0.78% control, $P = 0.0006$). For conserved 7mer-8m binding sites the amount was 3.8 times higher than the control (4.92% inv. correlation, 1.30% control; $P = 0.0062$) and for conserved 7mer-1a binding sites the difference was an enrichment of 9-fold (2.45% inv. correlation, 0.27% control; $P = 0.0064$). These enrichments of conserved binding sites and especially the high enrichment of strong binding sites prove the validity of this naïve target identification approach. Selected targets were validated via luciferase assay experiments (see 5.8).

5.5.1 miRNA-mRNA interactions of miRNAs positively correlated with age

Five global aging miRNAs showed increasing expression over the lifespan in multiple organs, namely miR-29a-3p, miR-29c-3p, miR-155-5p, miR-184-3p and miR-1895. As miRNA abundance clearly correlates with its impact on gene

expression⁵⁸, we calculated the inverse correlations between mRNAs and miRNAs during aging to identify potential miRNA-mRNA interactions as described above. Predicted targets for the global aging miRNAs were filtered to be at least predicted for one miRNA in two organs to be included in pathway analysis. We identified multiple overlapping targets, as seen the Venn diagram (Figure 16A). Six targets were shared between all miRNAs: *Ptn*, *Pdgfrl*, *Meg3*, *Eln*, *Col1a1* and *Col3a1*. The latter three all play a role in protein digestion and adsorption and were validated targets for miR-29b-1/miR-29a⁹⁹.

A STRING-network was composed of proteins encoded by these predicted mRNA targets of the global aging miRNAs (Figure 16B). The main signature of this network were ECM related processes, for instance ECM organization, ECM-

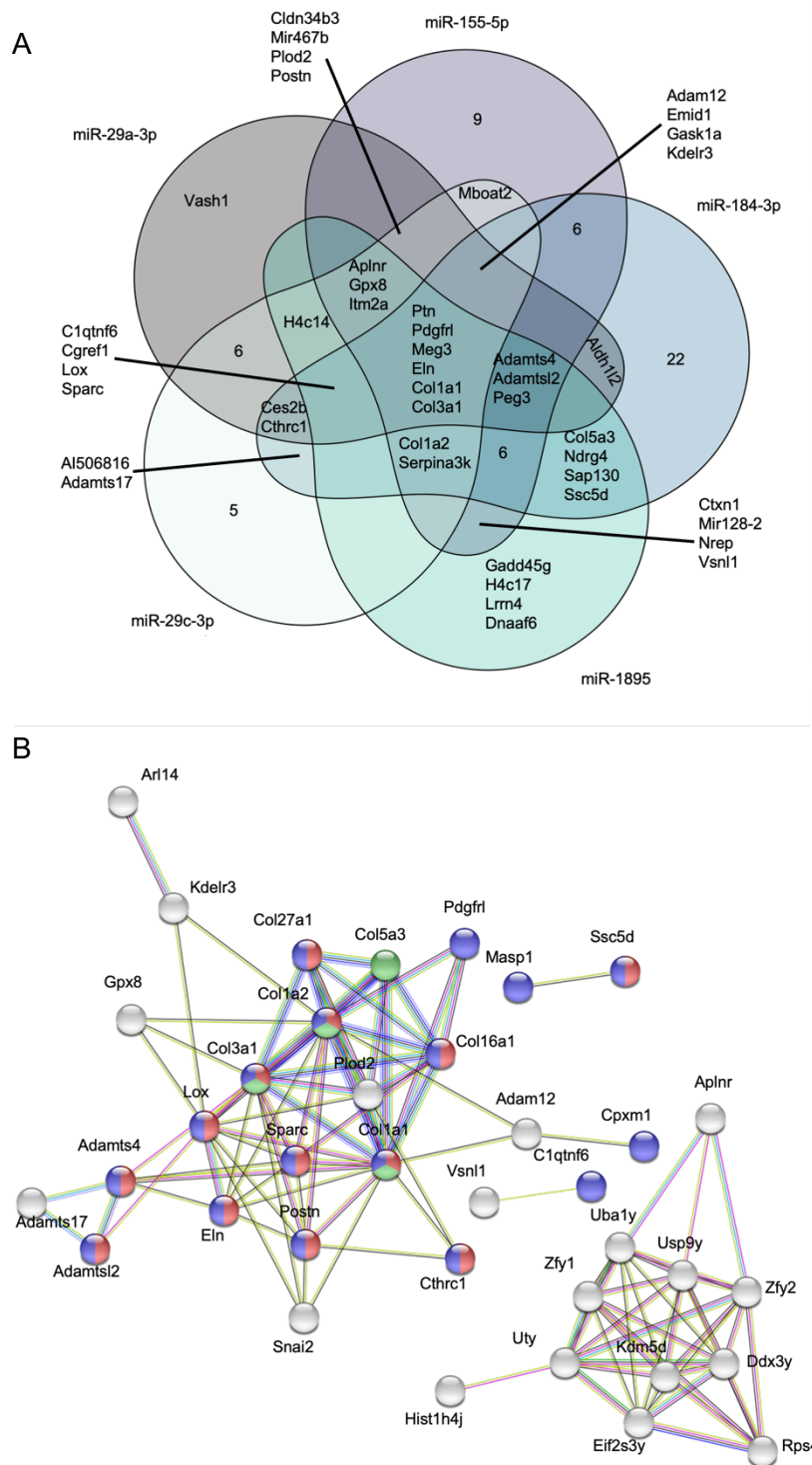


Figure 16: Positively correlated global aging miRNA-mRNA interactions.

(A) Venn diagram of predicted miRNA-mRNA interactions for the five positive global aging miRNAs, (B) STRING network of all validated interacting proteins encoded by predicted mRNA targets of positive global aging miRNAs, enriched pathways colored: 'secreted' (purple), 'ECM' (red) and 'dysregulated miRNA targeting in insulin PI3K-AKT signaling' (green).¹

receptor interaction and collagen fibril organization⁹¹. The ‘senescence-associated secretory phenotype’ is an identification marker for senescent cells and characterized by ECM alterations and an altered secretome^{9,100}. Given the strong correlations, this phenotype could be mediated by expression changes of global aging miRNAs. Another subset of this network is composed mainly of Y-chromosome encoded proteins, for instance histone modification introducing proteins (*Kdm5d*), probable transcriptional activators (*Zfy1*, *Zfy2*) and ubiquitin-proteasome dependent proteolysis’ (*Usp9y*). These were all factors playing a role in gene expression regulation as well, therefore we propose that other layers of gene regulation were likely influenced by global aging miRNA changes as well. Furthermore, two pathways associated with deregulated nutrient sensing, namely ‘dysregulated miRNA targeting in insulin/PI3K-AKT signaling’ and the ‘AGE-RAGE signaling pathway in diabetic complications’ were enriched in this network.

In addition to the targets of the global aging miRNAs increasing with age, the mRNA targets for local aging miRNAs of each tissue were predicted as well and pathways analysis of these targets was conducted. The enriched pathways of local aging miRNAs exhibit similar signatures to the global aging miRNAs (Figure 17). Among the top 20 locally enriched pathways were ‘Protein digestion and adsorption’ as a pathway related to ECM organization and pathways related to deregulated nutrient sensing (‘adipocytokine signaling pathway’, ‘PI3K-AKT signaling pathway’, ‘metabolic pathways’, and ‘insulin resistance’). These findings associated the

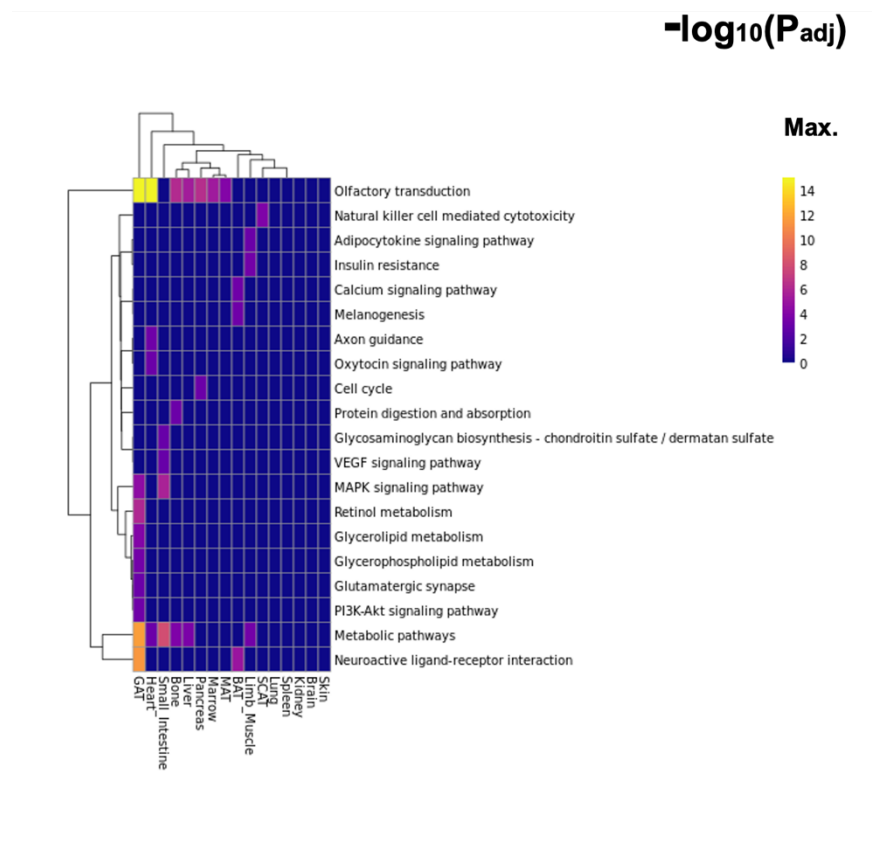


Figure 17: Heatmap of enriched pathways in predicted mRNA targets of positively correlated local aging miRNAs per tissue.¹

findings associated the

increase of global and local aging miRNA expression during aging with the deregulation of nutrient sensing and ECM organization.

5.5.2 miRNA-mRNA interactions of miRNAs negatively correlated with age

Three global aging miRNAs showed decreasing expression during aging over multiple tissues (miR-300-3p, miR-487b-3p and miR-541-5p). As a result, the targets regulated by these miRNAs should show an increase in mRNA expression. The target identification strategy applied before was implement as well for the global aging miRNAs negatively correlated with age. Targets of miRNA-mRNA interactions were predicted via inverse correlation ($r < -0.4$, $P < 0.05$) and filtered for interactions predicted in at least two tissues for one miRNA. A total of 138 out of 327 targets overlapped between the three miRNAs (Figure 18A).

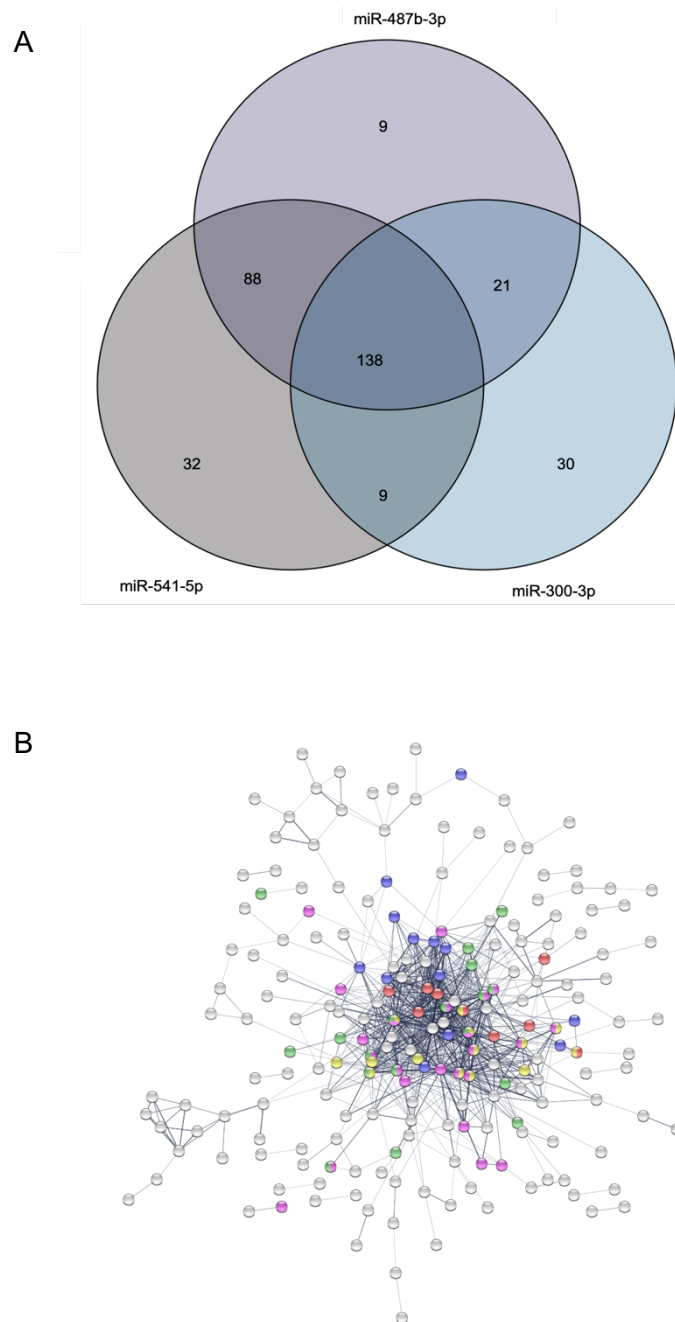


Figure 18: Negatively correlated global aging miRNA-mRNA interactions.

(A) Predicted miRNA-mRNA interactions for the three negative global aging miRNAs, (B) STRING network of all validated interacting proteins encoded by predicted mRNA targets of negative global aging miRNAs, enriched pathways colored: 'cytokine activity' (purple), 'immune receptor activity' (red), 'hematopoietic cell lineage' (yellow), 'immunoglobulin' (green) and 'adaptive immunity' (pink)¹.

A functional enrichment of pathways associated with processes related to the immune system was observed for these targets ('Th17 cell differentiation', cytokine–cytokine receptor interaction', 'NF-kappa B signaling pathway' 'Th1 and Th2 cell differentiation' and 'chemokine signaling pathway'), when visualizing the targets as a STRING network (Figure 18B). The center of the network was composed of the proteins encoded by the predicted targets and exhibited an especially dense center with features associated to 'hematopoietic lineage', 'adaptive immunity', 'immunoglobulin' 'cytokine activity' and 'immune receptor activity'. These findings were in line with previous studies which showed that miR-487b was able to inhibit cell inflammation and apoptosis¹⁰¹. Furthermore, miR-487 has been reported in humans as tumor repressor¹⁰².

Respectively, the pathways regulated by the local aging miRNAs were predicted and analyzed. Immune-related processes were enriched as well in this

analysis, namely 'Chemokine signaling pathway', 'B cell receptor signaling pathway', 'Natural killer cell mediated cytotoxicity', 'Cytokine-cytokine receptor interaction', multiple T-cell differentiation pathways, and the 'Hematopoietic cell lineage'(Figure 19). Chronic inflammation and immune senescence are known hallmarks of aging⁵. With this data, we can associate the decrease of global and local aging miRNAs expression with the deregulation of the immune system.

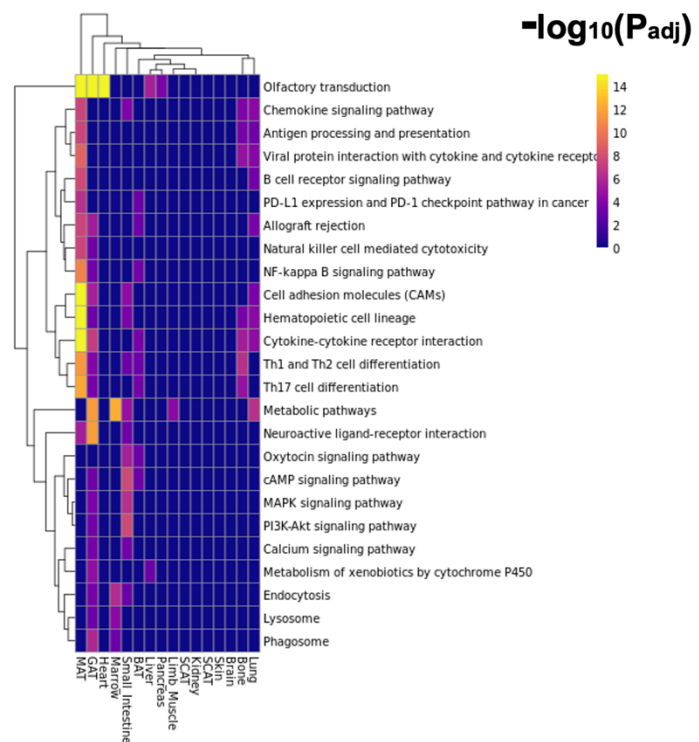


Figure 19: Heatmap of enriched pathways in predicted mRNA targets of negatively correlated local aging miRNAs per tissue¹.

5.6 Tissue-specific rejuvenation response of global aging miRNAs

Are the expression changes of global aging miRNAs and their potential effects in aging reversible via heterochronic parabiosis? Heterochronic parabiosis as an aging intervention has been shown to provide beneficial effects on health (cognition, muscle strength and bone repair) of the aged counterpart. Heterochronic parabiosis was defined by a shared common circulation as in this study or systemic infusions of young blood⁸⁶. The molecular mechanisms that change gene regulation and expression via this intervention remain unclear.

This intervention is especially useful to identify systemic factors from the young environment that activate molecular signaling in the old and lead to improved function. MiRNAs are a promising target for investigation, because they are part of epigenetic regulation and because of their capability to be transported via extracellular vesicles and their thereby mediated regulation of gene expression¹⁰³. To illuminate if changes in non-coding RNA expression could be the cause of these effects, we sequenced tissue samples from parabiosis mice.

The parabiosis cohort consisted of 176 samples taken from six different organs, involving both isochronic young (IY) and aged (IA), as well as heterochronic young (HY) and aged (HA) mice (as outlined in Table 1, Appendix B). The goal of the intervention was to achieve rejuvenation, which refers to the reversal of aging-related features. However, it's worth noting that this process comes with the drawback of accelerated aging, which is the adverse consequence of introducing old blood into younger individuals. Our study measured the rejuvenation effect by comparing the expression levels in IA mice to those in HA mice. On the other hand, the accelerated aging effect was determined by the contrast between IY and HY mice (Figure 20).

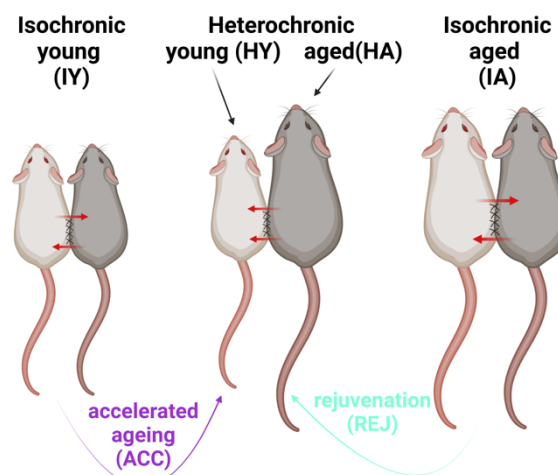


Figure 20: Schema drawing of heterochronic parabiosis as an aging intervention.

Created with BioRender¹.

We also established a benchmark for healthy aging by comparing mice from the TMS cohort aged 3 and 21 months (referred to as AGE), which closely matched the age distribution of the parabiosis cohort at the time of assessment. Using t-SNE clustering, our analysis showed that the primary source of variation across all samples was the identity of the tissue and not the signature of the experimental groups (Figure 21A,B).

MiRNAs detected and analyzed were assigned into three major groups of interest. First, miRNAs that were uniquely deregulated in parabiosis and not in aging were assigned to a group. Herein we differentiated into two subgroups, uniquely

deregulated in rejuvenation (REJ unique) and uniquely deregulated in accelerated aging (ACC unique). Second, miRNAs that were deregulated in rejuvenation and aging in opposite directions, divided into two subgroups as well, namely: rejuvenation upregulated and aging downregulated (REJ up and AGE down) and rejuvenation downregulated and aging upregulated (REJ down and AGE up). Third, miRNAs deregulated in physiological and accelerated aging in the same direction were grouped together in two subgroups of up- (AGE/ACC up) and downregulated (AGE/ACC down) miRNAs. Deregulation was defined as a fold change exceeding the interval of $2/3$ and $3/2$ while exhibiting a *P*-value below 0.05 in a t-test.

In none of the analyzed tissues any miRNAs were deregulated in the same direction in physiological and accelerated aging, as visible in the heatmap (Figure 22). Most miRNAs were deregulated uniquely in rejuvenation (233) and accelerated aging

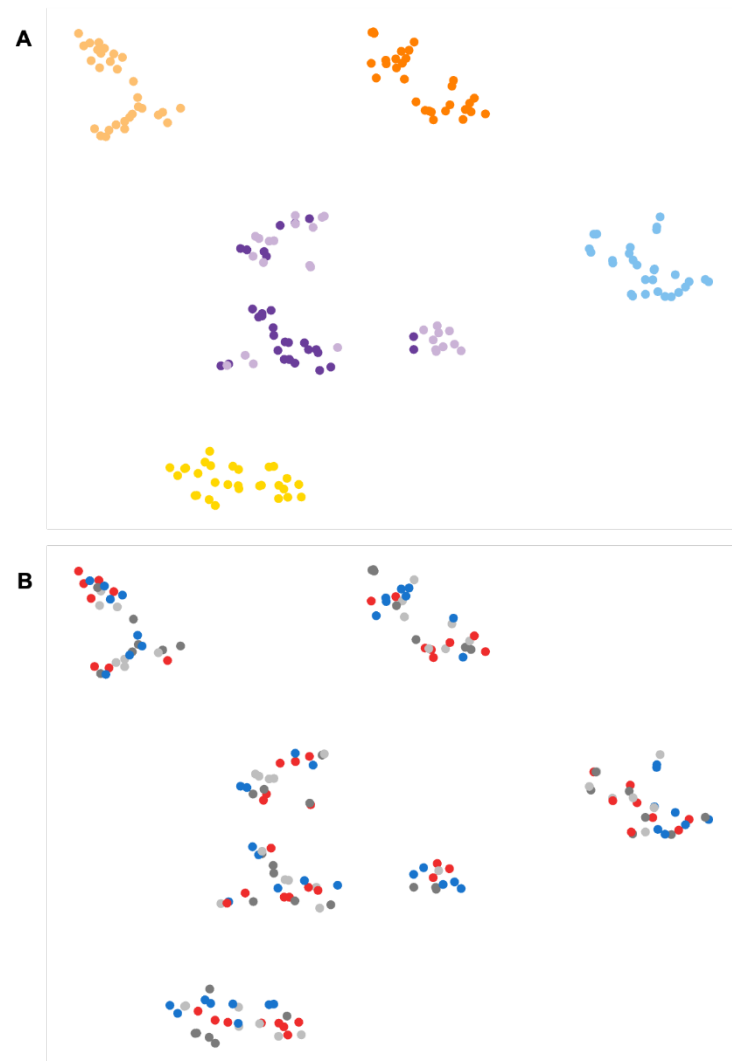


Figure 21: t-SNE clustering of parabiosis samples. Clustering of all parabiosis samples overall abundant ncRNAs colored by tissue (A) and by treatment group (B)¹

(43) over all measured tissues. This indicated that the rejuvenation effect is at least partially regulated by different mechanisms than physiological aging. The initiation of novel pathways during rejuvenation, which mediate the positive effects was reported previously during single-cell transcriptome analysis⁸⁶.

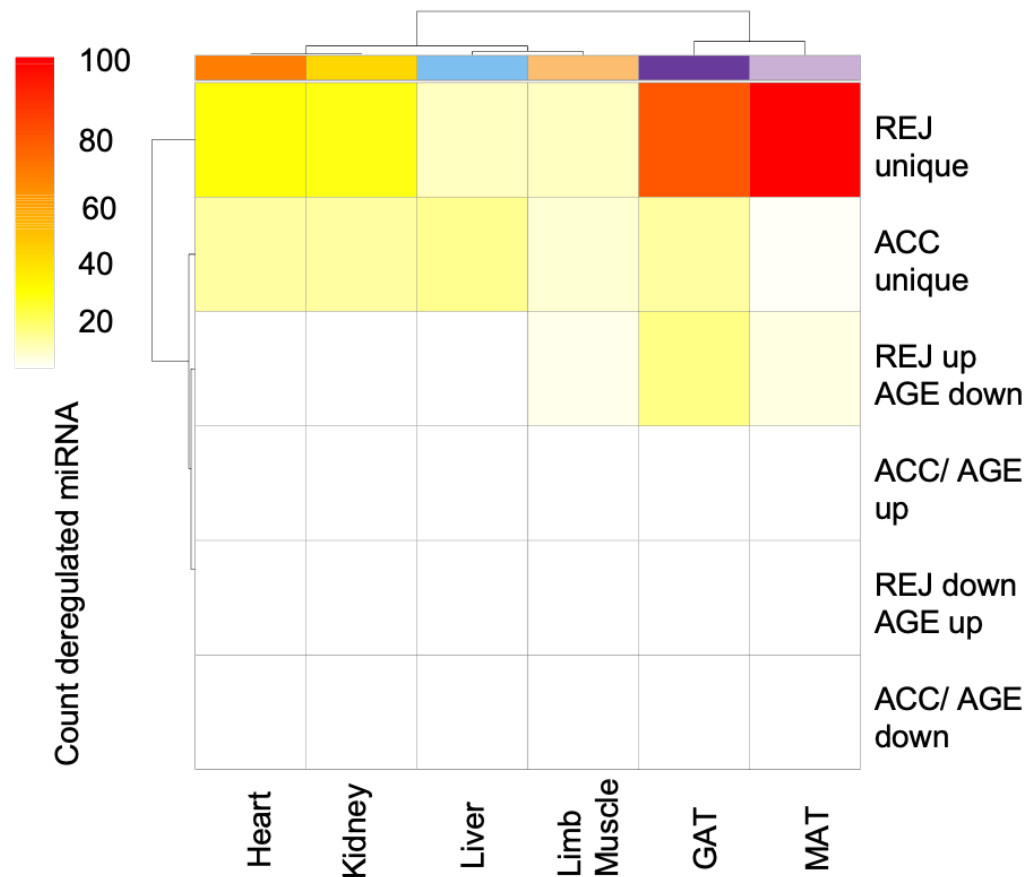


Figure 22: Count of deregulated miRNAs per tissue per condition.

Heatmap of count of deregulated miRNAs (FC exceeding interval 2/3 and 3/2, P -value < 0.05) in each tissue for all six comparisons¹.

This activation of novel pathways could be mediated by these miRNAs uniquely deregulated in rejuvenation. In MAT, uniquely deregulated miRNAs in rejuvenation were enriched in pathways associated with the aging hallmark deregulated nutrient sensing. These pathways were ‘insulin resistance’, ‘type 2 diabetes mellitus’ and ‘adipocytokine pathway’. But on the other hand, there were 17 miRNAs, that were regulated in the opposite direction in rejuvenation as in aging, indicating that the changes occurring in later life can potentially be reversed.

A partial reversion of the observed deregulation of global aging miRNAs was detected for three of the global aging miRNAs in specific tissues during parabiosis experiments. Most prominently, the increase of miR-29c-3p expression during aging

was reversed in liver (Figure 23). The effect measured for rejuvenation was a four-fold higher than the effect of accelerated aging.

In liver miR-184-3p (Appendix A, Supplemental Figure 10) and miR-300-5p in GAT (Appendix A, Supplemental Figure 11) exhibited similar rejuvenation reversion effects, but at a lower degree. These results of local rejuvenation patterns of the global aging miRNAs, especially miR-29c-3p, prompted investigation of these miRNAs as systemic effectors.

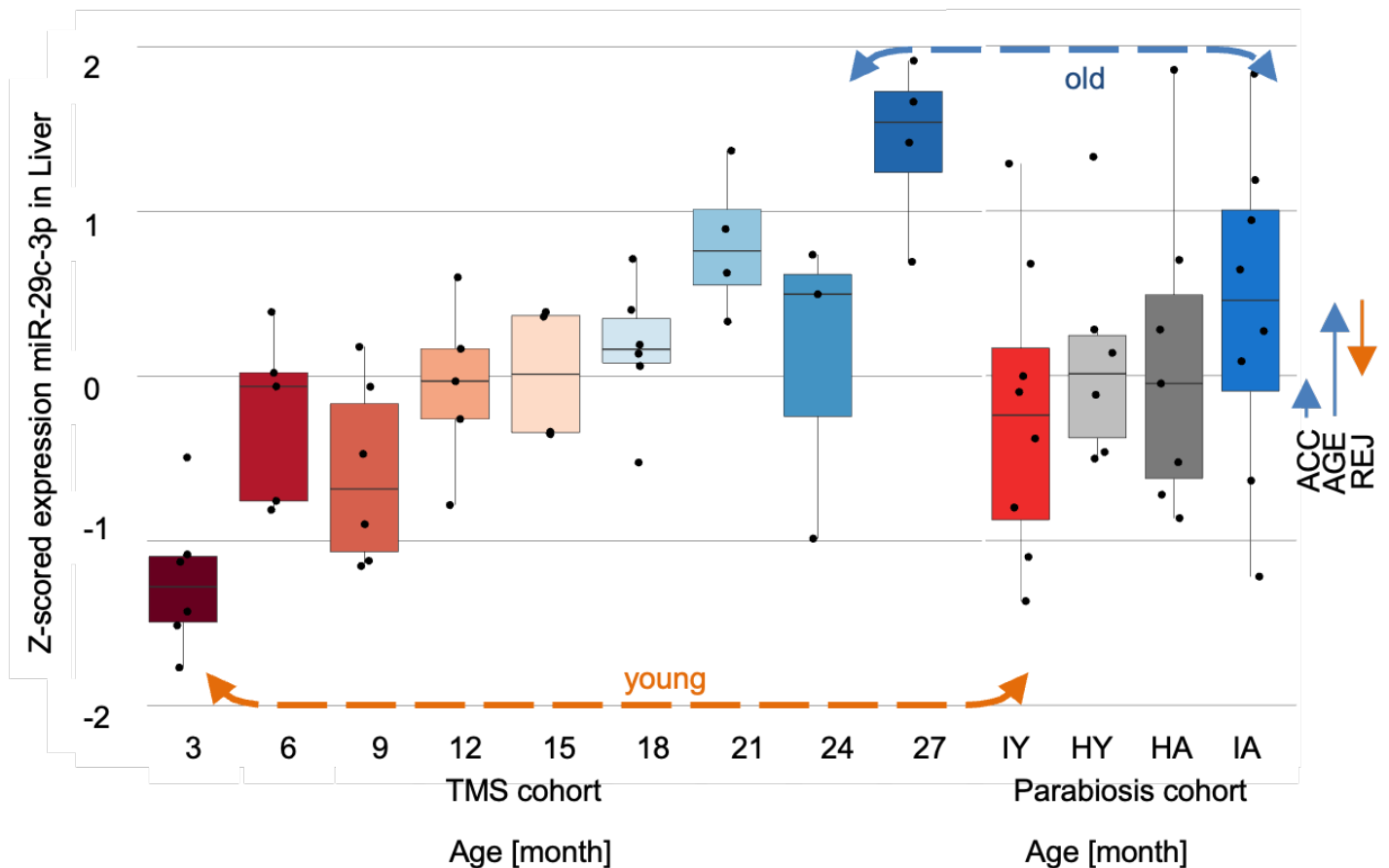


Figure 23: Boxplot of z-scored miR-29c-3p expression in liver in aging and parabiosis cohort¹.

5.7 Circulating miRNAs

As miRNAs are known to circulate in the plasma and extracellular vesicles (EVs) throughout the entire organism, they could act as systemic factors during aging. In order to determine whether it is more likely that the observed miRNA expression changes in heterochronic parabiosis are causal for the positive effects or a consequence of other factors additional data had been collected. If the miRNAs themselves partially mediate the effects of this intervention, elevated levels of the global aging miRNAs should be present in older age. RNA samples from plasma and EVs were collected from an independent cohort at the ages 2, 6, 8, 12 and 18 months^{1,83}.

Compared to local aging miRNAs the share of global aging miRNAs detected as circulating was higher, with four out of five age-increasing miRNAs compared to 38.3% of all local aging miRNAs (Figure 24). Global aging miRNAs likely act therefore as systemic regulators travelling via plasma and EVs to recipient cells in different organs. Assessment of the miRNA expression in these two circulating fractions for miR-29c-3p, the most prominent global aging miRNA showed a correlation with age in both fractions (plasma $r = 0.56$ and EVs $r = 0.65$).

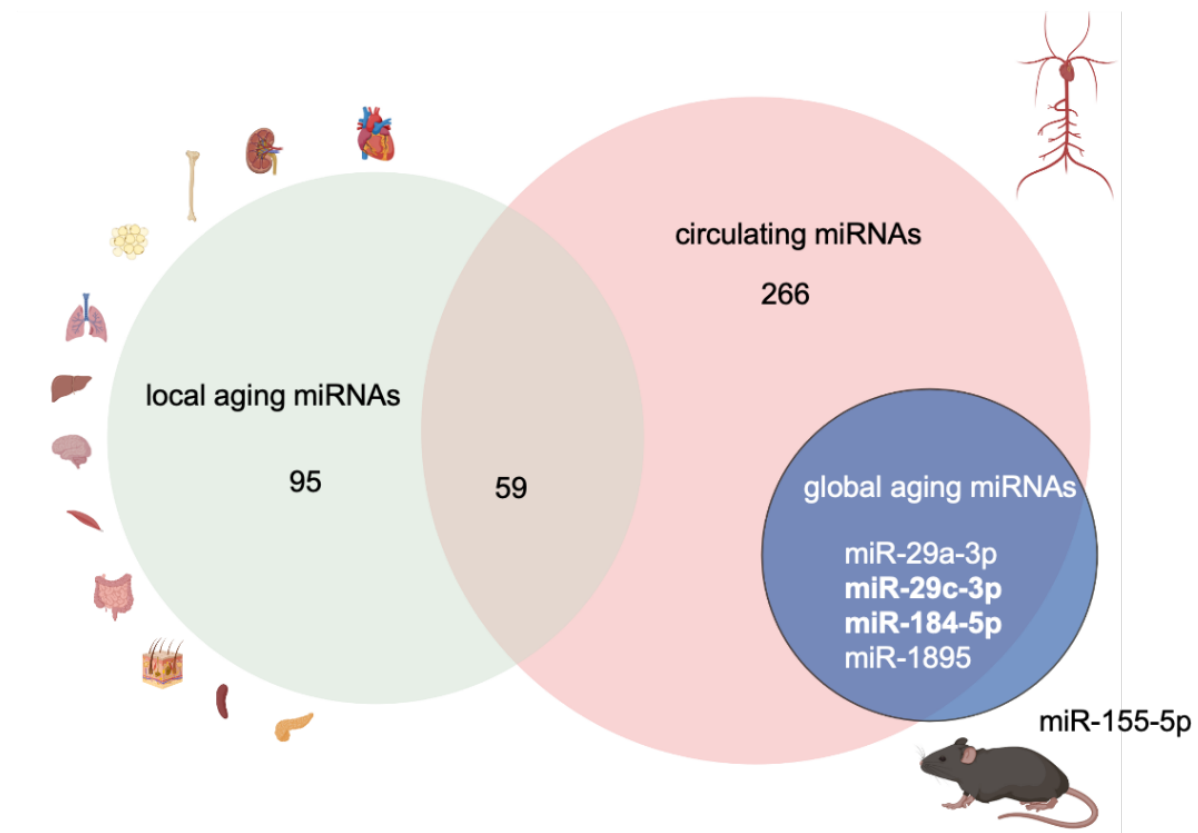


Figure 24: Overlap local and global aging miRNAs with circulating miRNAs. Venn diagram for local aging miRNAs from all 16 tissues and global aging miRNAs from the aging cohort and circulating miRNAs from the circulatory cohort; created with BioRender¹.

5.8 miR-29 family target validation

Our analysis suggested that miR-29 family members, miR-29a-3p and miR-29c-3p, together with the other global aging miRNAs regulate essential aging processes resulting in the aging phenotype. The predictions of miRNA-mRNA interactions suggested that especially targets in ECM related pathways were important mediators and their regulation is known to play a causal role in aging processes. mRNAs for *Eln*, *Adam12*, *Col1a1* and *Col3a1* have already been validated as targets of the miR-29 family. All predicted mRNA targets for miR-29a-3p and miR-29c-3p were examined for at least 7mer binding sites in their 3'UTR regions. All target mRNAs that fulfilled these criteria were tested in luciferase assay experiments to validate the regulatory function of the miR-29 family. Luciferase assays are used to determine post-transcriptional regulation of miRNAs on target mRNAs. Predicted 3'UTR target sites of the mRNA were cloned downstream of a firefly luciferase reporter (pMIR-RNL-TK). This construct was transfected together with a miRNA overexpression vector (pSG5-miR-29a) into HEK293T cells. By measuring luciferase activity in the cell lysates, the regulatory capacities of the miRNA on its predicted targets were determined. A reduction of RLU (relative light units) under 60% was set as high confidence identification of miRNA-mRNA regulation, reduction of under 80% was set as low confidence. Positive control of luciferase assay experiments were also conducted (Supplemental Figure 12).

Adamts17 and *Lox* were validated as targets of the miR-29 family via luciferase assay experiments with high confidence and *Vash1* with low confidence (Figure 25). For *Adamts17* even two binding sites within the 3'UTR could be validated as regulated by miR-29 family members. One other predicted target, namely *Aplnr* could not be validated via luciferase assays. *Lox*, which crosslinks elastin and collagens, plays a crucial role in

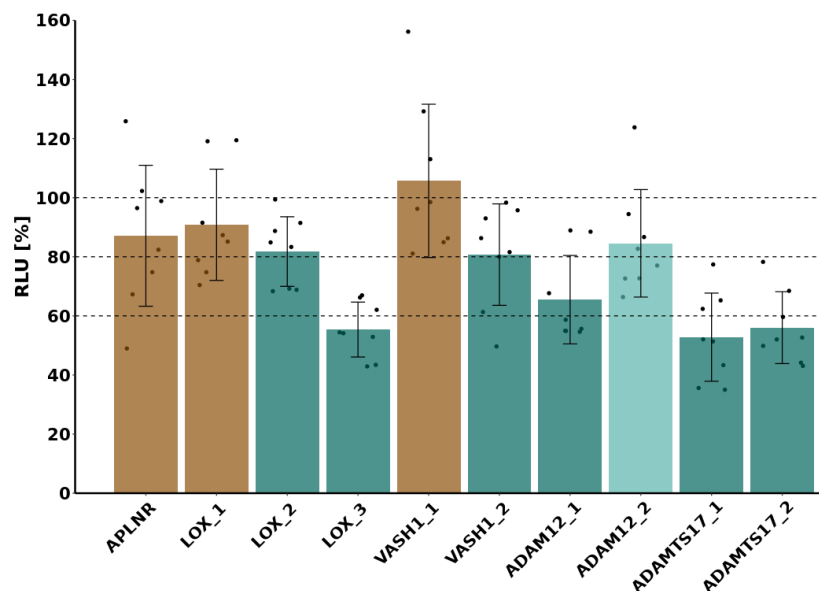


Figure 25: Luciferase assay results.

Validation of LOX_3, ADAMTS17_1 and ADAMTS17_2 as high confidence targets; VASH1_2 and LOX_2 as low confidence targets¹.

5.9 Region-specific brain aging^a

As aging is the main risk factor to suffer from major neurodegenerative diseases, like AD and PD as well as cognitive dysfunction, understanding the underlying mechanisms is crucial for the development of effective therapies. Previous studies suggest that aging impacts the brain in a region-specific manner⁸⁴. Region-specific expression changes were likely masked in our initial aging cohort as we looked at the expression changes of non-

coding RNA in the brain only with bulk sequencing data from whole brain samples. Therefore, now samples from 15 defined regions were collected. Bulk sequencing data from each region was generated and analyzed, to uncover the regions driving the peak expression of certain miRNAs at 12 and 18 months of age. We collected samples at 3 months as a young reference, middle aged (12,15,18 and 21 months) and aged samples (26 and

28 months) (Figure 27). The following regions were collected: corpus callosum, choroid plexus, neurogenic subventricular zone (SVZ), hippocampus anterior and posterior, hypothalamus, thalamus, caudate putamen, pons, medulla, cerebellum, olfactory bulb and three cortical regions, namely, motor, entorhinal and visual cortex (Appendix B, Table 2). Regions were defined and collected using visual landmarks and referencing the Allan Brain Atlas. This study is the first NGS study looking at region-specific miRNA expression patterns in the brain.

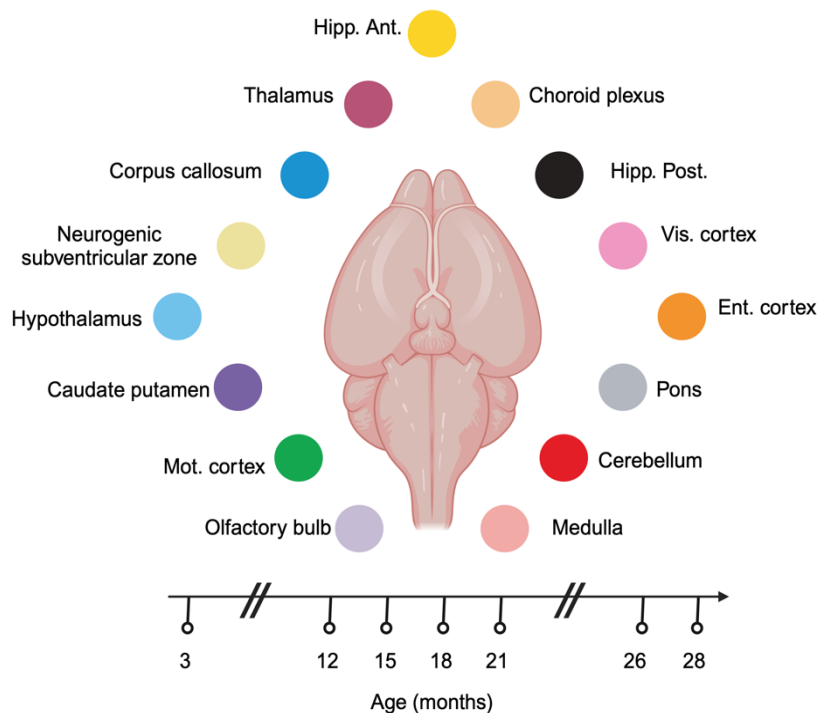


Figure 27: Study set up brain aging cohort.

Sample collection of 15 different brain regions at seven different ages, color code as indicated; Created with BioRender.

^a The following work has been conducted as a close collaboration with Annika Engel, who provided the main part of the analysis of this data set.

5.9.1 Region-specific miRNA expression patterns in brain

First, we identified strong region-specific signatures of miRNA expression in the different brain regions solely analyzing the expression of the adult mice (ages: 3, 12 and 15 months) without considering the age effect. Clustering all expressed miRNAs in an UMAP exhibited a clear separation driven by region identity (Figure 28). Exceptions, like the mixed clustering of hippocampus anterior and posterior can be explained by their anatomical and functional proximity.

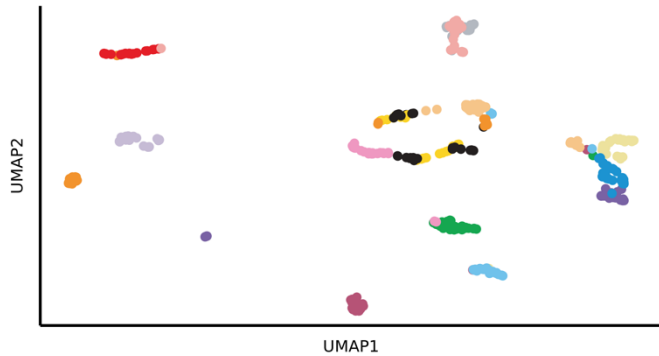


Figure 28: UMAP of all samples of the brain aging cohort overall expressed miRNAs.

Each dot represents a sample, colored by brain regions as indicated in Figure 27

All regions were clustered into four clusters based on the expression of the 75 miRNAs with the highest absolute coefficient of variation overall regions. These clusters are visualized as a binarized heatmap only for miRNAs exceeding the threshold of 75 rpmmm (reads per million mapped to miRNAs) in at least one region (Figure 29). The strongest region-specific signature was observed in the

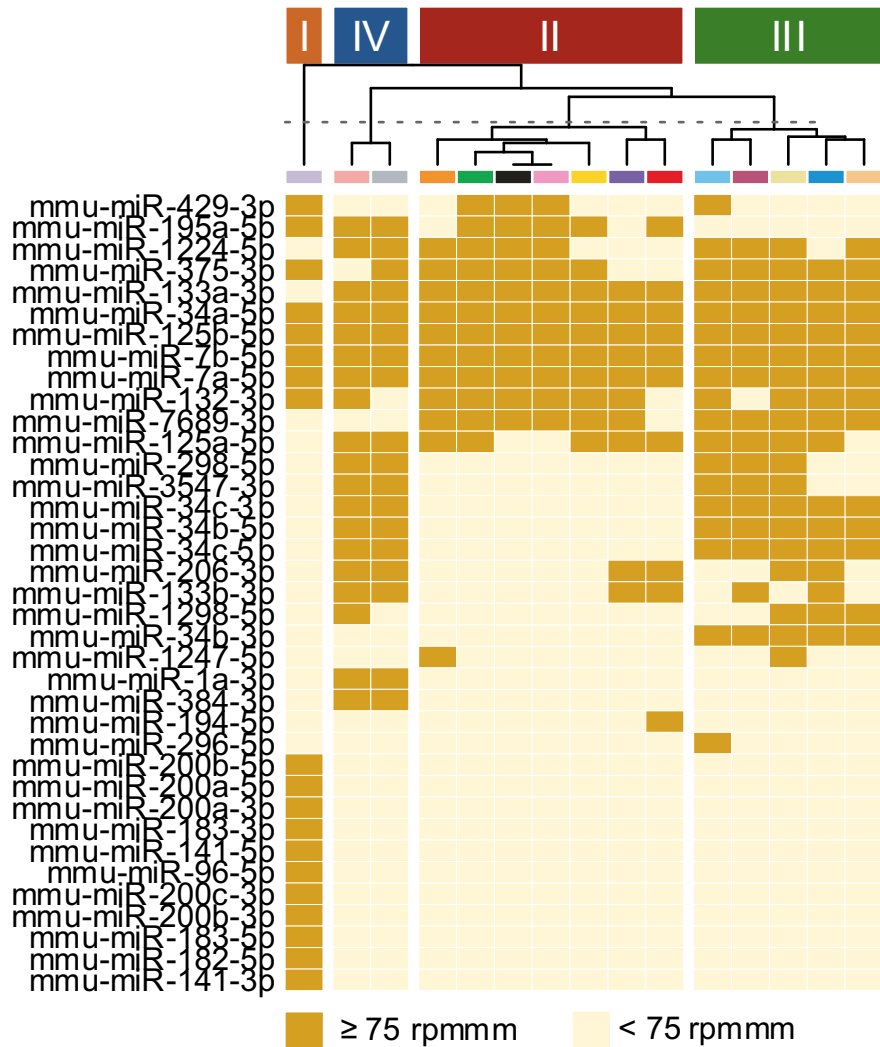


Figure 29: Binarized heatmap of most variable region-specific miRNAs overall brain regions.

Regions clustered into four clusters, binarized using threshold of 75 reads per million mapped to miRNAs.

olfactory bulb, as it clustered by itself. Eleven miRNAs were exclusively expressed in this region (threshold median expression ≥ 75 rpmm). Within these miRNAs were miR-200a-5p, miR-200a-3p, miR-200b-5p, miR-200b-3p and miR-200c-3p. MiR-200 family members have been reported in the olfactory bulb as crucial for neuronal maturation during postnatal development, mediating this effect through targeting *Zeb2*¹⁰⁵. Pons and medulla show an equally strong region-specific signature of miR-1a-3p and miR-384-3p expression.

5.9.2 Brain miRNA miR-9

MiR-9 family members were previously extensively studied in the brain and showed brain-specific expression¹⁰⁶. In our data miR-9-5p is highly expressed in all regions, but to varying extent. A median expression of over 150k rpmm of miR-9 was stably detected in the olfactory bulb over all ages. In contrast, in pons and medulla the median expression was below 50k

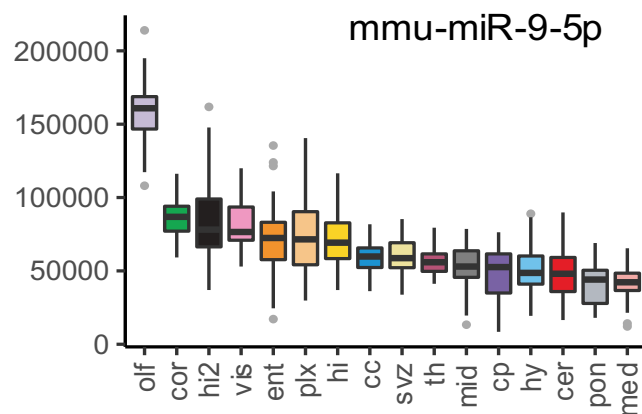


Figure 30: Median miR-9-5p expression in reads per million mapped for each brain region over all ages.

(Figure 30). In most regions, like in the olfactory bulb the miR-9-expression was stable during aging. In contrast, expression decreased in pons, hippocampus anterior, and ent. cortex over the lifespan (Appendix A, Supplemental Figure 13). As miR-9-5p is known to be involved in neurogenesis, axon development, differentiation and proliferation of neural progenitor cells¹⁰⁶, further investigation of functional consequences of the region-specific expression of this miRNA could yield more insight into these mechanisms.

5.9.3 Sex-specific signatures of miRNA expression in brain regions

Male and female biological replicates were collected for the dataset until the age of 21 months. Brain region identity was responsible for over half of the variation within the data set (55.1%, Appendix A, Supplemental Figure 14). Aging, as an independent factor, introduced 0.6% of variation within the entire dataset and in combination with the brain regions 3.9%. But sex was also responsible for 0.2% of the variation and in combination with the brain region for 3.1%. The relation of variation percentage of age and sex and their combination per region was visualized in a scatterplot (Figure 31). Region-wise analysis of variation shares revealed that for four regions the variation

introduced by sex identity was above 10% and bigger than the share introduced by aging. For mot. cortex and caudate putamen the variation share of sex were 18.8% and 21.2%, respectively. Especially for the caudate putamen sex dominated over age, which was only responsible for 5% of variation. Sex differences in pathologies as well as neural properties and associated mechanisms

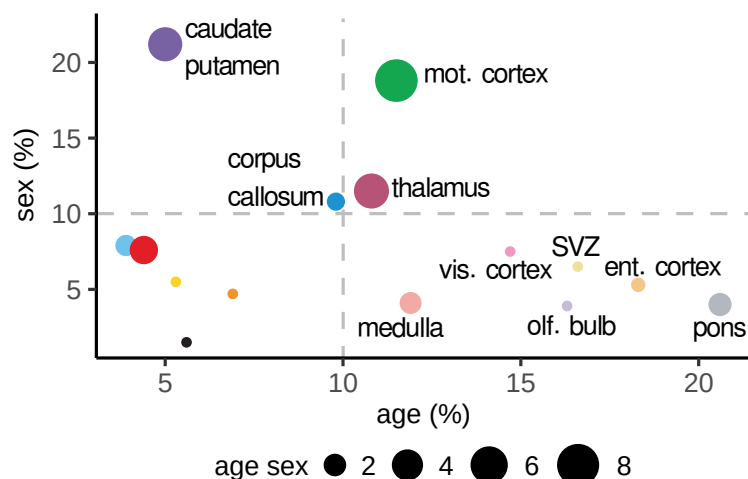


Figure 31: Percentage of variation introduced by age and sex in each region.

PVCA of each region for sex and age, percentage of each factor for each region, size indicated as percentage of combination of age and sex, colors coded for regions as indicated in Figure 27

have been reported previously for this region¹⁰⁷, e.g. in humans different fiber connection strength have been observed¹⁰⁸. Thalamus and corpus callosum also exhibited sex specific signatures.

More than 10% of variation in six tissues was explainable by age, for these tissues the sex was responsible for less than 10% of variation. These regions, namely, choroid plexus, subventricular zone, olfactory bulb, vis. cortex, medulla and most prominently pons, with 20.6% of variation explainable by age, were especially interesting for the main research question whether age-related expression changes in the brain occur region specifically.

5.9.4 Linear miRNA aging signatures

Next, we assessed the relation of miRNA expression in each brain region by calculating the Spearman rank correlation with age over all samples. MiRNAs with correlation values exceeding the interval between -0.5 and 0.5 were deemed (anti-) correlated with age. We observed region-specific correlations with age for large miRNA sets, as visible in the heatmap of (anti-)correlated miRNA per region (Figure 32). In the vis. cortex 63 miRNAs were positively correlated with age and in pons 84 miRNAs were anticorrelated. Using miEAA⁹⁸, we determined that the miRNAs uniquely positively correlated with age in vis. cortex are enriched for miRNAs associated with the mTOR signaling pathway. A reduction of this signaling pathway can extend the lifespan in various model organisms, furthermore it's deregulation may cause neurodegeneration^{109,110}. For example, miR-93, increasing with age in vis. cortex, is linked to TOR signaling in gliomas as an oncogenic miRNA¹¹¹. Cellular senescence and

neuron maturation are amongst the enriched pathways regulated by miRNAs uniquely anticorrelated with age in pons. Further investigation of these miRNAs and their respective targets in these pathways could relate miRNA expression changes to aging phenotypes.

Few miRNAs were correlated with age in multiple regions. MiR-155-5p and miR-146a-5p were correlated in seven different regions, exhibiting a strong aging signature independent from

regions. MiR-10a-5p was correlated with age in three different regions. Respectively, two miRNAs are anti-correlated with age in three regions, namely miR-322-5p, miR-669c-5p. MiR-669l-5p was even anticorrelated with age in four regions. As miR-155 and miR-146a are both known neuroinflammatory regulators also implicated in neurodegenerative disease, these miRNAs and their functions during brain aging are interesting targets for further investigations¹¹².

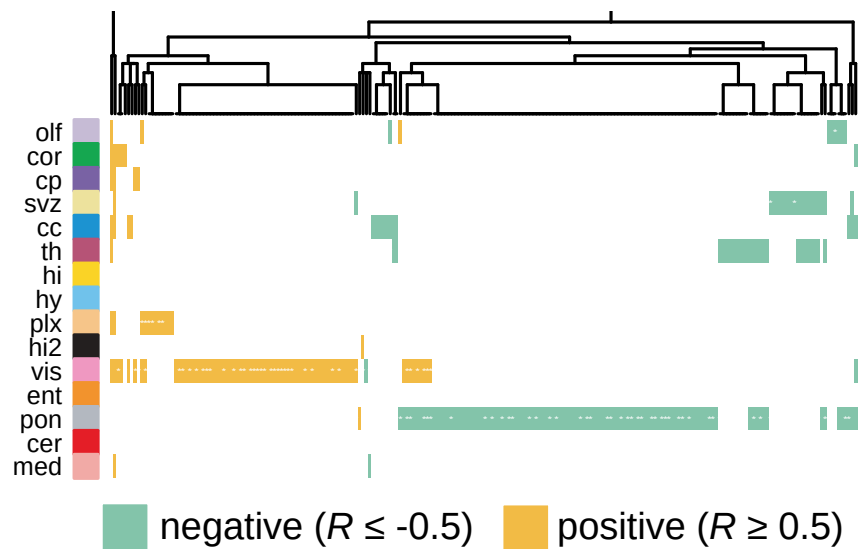


Figure 32: Heatmap of spearman rank correlation with age for each miRNA

Spearman rank correlation (R) calculated between miRNA expression in each region and respective age, color coded for miRNAs anticorrelated with age in green and correlated with age in yellow.

6 Discussion

Understanding microRNA expression patterns in all tissues and the respective changes of these patterns during aging will make miRNAs usable either as biomarkers or as potential therapeutic targets. The existing mRNA TMS and parabiosis transcriptome data sets were extended with the ncRNA expression patterns in this study. The combination of these data sets with each other allowed to reveal potential regulatory mechanisms and interactions between these two layers of gene expression. Initially, tissue-specific aging trajectories of miRNA expression were reported for ten out of the 20 clusters of the whole organism trajectory clustering. Interestingly, miRNAs related to the insulin resistance pathway were predominantly found in clusters of adipose tissue trajectories. A regulation of gene expression that is caused by the altered miRNA expression in these tissues could be causal to deregulated nutrient sensing. The identification of local aging miRNAs offers a framework for experts in the respective fields to illuminate the effects of these miRNA expression pattern changes in each tissue and eventually solve the contribution of the tissue related pathway regulation on organismal aging.

In contrast to local aging miRNAs, we identified global aging miRNAs, five correlated and three anticorrelated with age. The targets of these miRNAs link their expression changes to known pathways altered in aging. Furthermore, we could show that these aging-correlated miRNAs were presented in higher amounts in the circulation than local aging miRNAs. This higher presence and their reversed organ-specific expression patterns during heterochronic parabiosis are indicators, that they could play a causal role in aging processes. Especially the miR-29 family is an interesting target for further studies, as miR-29a-3p and miR-29c-3p are global aging miRNAs. Identification and validation of miR-29 targets *Lox* and *Adamts17* in our study link miR-29 expression changes further to ECM damage. *Adamts17*, is a protease, whose impairment through mutation causes Weil-Marchesani syndrome in humans. The syndrome is a connective tissue disorder and patients exhibit thick skin and joint stiffness¹¹³. A dysregulation of this protein caused by miR-29 expression increase could therefore also lead to age related symptoms like joint stiffness. *Lox* mediates oxidation of lysine residues in collagen and elastin. This enzymatic process triggers the establishment of covalent cross-links, consequently enhancing the structural stability of these fibrous proteins and thereby playing a crucial role in formation and repair of ECM. Deregulation of this protein is linked to inflammatory diseases, fibrosis and cancer¹¹⁴. Collagen and elastin themselves are also regulated by miR-29. MiR-29-mediated elastin downregulation in vascular smooth muscle cells leads to vascular calcification, increasing the likelihood of cardiovascular mortality¹¹⁵. Collagens (*Col1A1*, *Col1A2*,

Col3A1) are regulated by miR-29 directly post transcription, thereby regulating multiple profibrotic molecules in different cell types^{116,117}. For all 20 collagens conserved binding sites in the 3'UTR were predicted for miR-29 exclusively. These binding site predictions were not driven by broad sequence similarities, therefore highlighting the regulatory function of this miRNA family¹¹⁸. Previously, miR-29 family members were shown to target at least 16 different extracellular matrix genes¹¹⁸, relating its expression changes further to fibrosis development in heart, kidney, lung, liver and systemic sclerosis. Fibrosis is one disease phenotype tightly linked to aging via e.g. cellular senescence⁹.

The relation of miRNAs and mRNAs in this study is only analyzed and validated regarding the regulatory capacities of miRNAs to perform gene silencing. Other modes of action as regulators of gene expression are miRNA-mediated translational activation and (post-)transcriptional gene regulation within the nucleus⁶³. Further studies can use these datasets in combination with proteome data to illuminate other mode of actions and their implications of the complex processes composing the phenomenon aging. Furthermore, in heterochronic parabiosis various miRNAs over different tissues were deregulated uniquely in rejuvenation. These results in combination with the single-cell transcriptome data of another parabiosis cohort⁸⁶ that revealed the activation of novel pathways, mainly in the electron transport chain call for further experiments exploring the underlying mechanisms and interplay of miRNA and mRNA expression changes. Other bioinformatic tools could also be used to predict miRNA-mRNA interactions, like PicTar⁷⁰ and MBSTAR⁷² potentially identifying new targets below our chosen threshold and investigating their implications in aging.

miR-29 family members have been previously identified as upregulated in age in certain tissues. In muscle, they have been found to be upregulated in aging rodents and a mouse progeria model^{119,120}. Targets of miR-29 in skeletal muscle are *IGf1*, *P85a* and *Bmyb*, which are mediators of muscle growth and proliferation. A downregulation of these targets mediated through miR-29a/b may lead to muscle loss⁸¹. Another tissue in which miR-29 family members have been reported with an age-associated upregulation is the brain. This upregulation has been shown to lead to microglia dysregulation and thereby increase neuroinflammation¹²¹.

Completing the picture of this upregulation trend of miR-29 family members with our data, we can show that miR-29a-3p and miR-29c-3p expression is increasing in all tissues during aging. MiR-29 family expression increase is triggered in response to DNA damage¹¹⁹. As DNA damage is accumulating during aging, the p53 signaling pathway is activated. This could lead to an abnormal activation of miR-29 expression, which through downregulation of its targets, results in increasing cell senescence and apoptosis and ultimately in loss of tissue and organism-wide homeostasis. Another

relation between miR-29c-3p increase and the hallmarks of aging is the known role of miR-29c-3p as a negative regulator of RAG1 in B-cells in mouse and human¹²². MiR-29c-3p overexpression causes thereby a reduction of the V(D)J recombination. This immune system shaping process is responsible for clearance of infectious agents and potentially malignant or infectious cells⁵. This regulation mechanisms links global miR-29c-3p increase to immune senescence, which worsens the aging phenotype. Increasing miR-29 family member levels likely don't act exclusively in a systematic manner in the entire organism but also on a cellular level. As the TGF- β /Smad pathway regulates cellular senescence in parts through the loss of H4K20me3, which is mediated through miR-29¹²³.

A recent preprint has proven the causal relationship between expression changes of miR-29 family members during aging and aging phenotypes¹²⁴. This study showed that the partial loss of miR-29 expression in a progeria model, namely *Zmpste24*^{-/-}, results in an extension of the lifespan. Furthermore, they generated a mouse strain overexpressing miR-29, which exhibited aging-related phenotypes such as senescence, kyphosis, osteoporosis, alopecia and resulted ultimately in early lethality. Their analysis of transcriptomic changes in these two models showed the same gene regulation patterns of extracellular matrix, inflammation and fatty acid metabolism as we observed in our data^{1,124}. This study adds the functional proof missing from our study to show that miRNA expression changes of miR-29 are causal to the development or reversion of aging phenotypes¹²⁴. Another preprint assessed the effect of miR-29a reduction in AD model (5XFAD) and wild type and found improved memory measures as well as reduced beta-amyloid deposition¹²⁵. These results validate miR-29 as a master regulator controlling gene expression of aging-related phenotypes. In humans, the increase of miR-29a-3p expression was significantly associated with fast cognitive decline¹²⁶.

For the other global aging miRNAs identified in our study this causal relationship to aging has not been established yet, therefore future studies should focus on validating the effects of these miRNAs. A next promising target could be miR-184-3p, as this miRNA showed a reversion of aging expression patterns in liver during heterochronic parabiosis. Moreover, an overexpression of this miRNA showed a lifespan shortening in both genders, that was not influenced by diet changes in neither gender in *Drosophila melanogaster*¹²⁷. One global aging miRNA, which expression decreased with aging and was observed increased in GAT in heterochronic parabiosis was miR-300. This miRNA improves stemness signatures, by significantly increasing *Oct4* levels¹²⁸. Induced OSKM expression, which *Oct4* is a part of, extends lifespan in progeria models⁴⁰. Increased miR-300 expression also reduces senescence

progression¹²⁸; therefore, a reduction of this miRNA could also be causal for the aging phenotype and is an interesting target for functional validation as a global aging miRNA.

Since miRNA expression regulation on genetic levels is a complicated and time intensive challenge and the read out of the manipulation is a lifespan alteration, these experiments were out of the scope of this work. Even though it has been shown that miR-29 expression plays a causal role as an aging regulator¹²⁴, the entire organismal mechanisms underlying the phenotype changes remain unclear. There are indications that associate miR-29 family members with increasing oxidative stress and imbalanced iron homeostasis during aging¹²⁹. Future studies should focus solving the question whether elevated expression levels observed in plasma and EVs originate mainly from one tissue or multiple tissues and which cell type mainly expressed and secreted this miRNA. Furthermore, target studies of miR-29 family members in different tissues can determine whether mediated effects in all tissues occur in the same manner by targeting the same mRNAs in all cell types or if targets vary over cell types and tissues.

A limitation of this work is that all results are based on the analysis of bulk tissue samples and therefore a cell-type specific analysis of expression changes was not possible. The expression changes in the global miRNAs could be driven by a deregulation of their expression in one cell type over all tissues or various cell types in different tissues. Single-cell miRNA data could clarify this question, but to date there is currently no gold standard method for single-cell miRNA sequencing (sc-miRNA sequencing) available. Sc-miRNA sequencing is mostly plate based and therefore does not reach the high throughput quantities that are already possible with mRNA sequencing¹³⁰. Another limitation of sc-miRNA sequencing is that in e.g. smart-Seq-total only low counts of miRNA reads were detected when analyzing miRNA expression simultaneously with mRNA expression¹³¹. An optimization of these methods would yield not only in the possible discrimination of cell-type specific miRNA expression patterns but could also improve miRNA-mRNA interaction prediction. Currently with these data sets an estimate of interaction is proposed, as we find these expression patterns within a tissue. Since the probability of miRNAs and mRNAs interacting with each other within a cell is higher, data derived from one cell could increase the reliability of predictions.

In addition to sc-miRNA data, sequencing data of miRNA cargo exported from different cell types in EVs would further complete the picture of molecular aging mechanisms. Collecting expression data of miRNAs in EVs in combination with cell-type specific or sc-miRNA expression data would answer remaining research questions. Are the measured miRNA expression changes caused by tissue expression or are the global aging miRNA mainly expressed in a specific cell type in one tissue which secretes these into the tissues and eventually the plasma? Multiple studies have focused on the

potential of miRNAs as biomarkers for disease as their expression in extracellular fluids changes with different phenotypes⁷⁷. But the functional consequences of the miRNA changes in circulating fluids like blood or cerebrospinal fluid are not yet completely understood. Their capacities to target specific cells during aging and change their transcriptome is yet to be revealed. Especially in the aging context, that is known for altered intercellular communication the effect of altered systemic factors like miRNAs is interesting as these alternations not only hint to altered cellular communication but also altered communication between tissues. miRNAs remain an interesting target as they are stable for an amount of up to 4 days at room temperature⁶³.

Previous studies have shown that miRNAs transferred via exosomes mediated biological functions. For instance, miR-105 which is secreted from breast cancer cells targets tight junction proteins in endothelial cells and thereby promotes metastasis⁶³. MiRNAs harboring specific sequences, EXOmotifs, are more likely secreted in EVs and inhibit target genes in recipient cells more effectively¹³². Within the mature sequence of miR-29c-3p is a sequence (CUGGUG) very similar to an EXOmotif (CNGGNC). This is another indication that elevated miR-29 levels in the circulating fraction have functional implications.

Constraints during small RNA library construction are a limitation of this study. Adapter ligation bias, polymerase chain reaction amplification bias, adapter dimer contamination, barcode bias together with the impact of RNA degradation are challenges that are yet to overcome^{79,133,134}. Especially, RNA degradation posed a major challenge for data interpretation for lncRNAs, snoRNAs, snRNAs, tRNAs, rRNAs and scaRNAs. The expression of these RNA classes was just inferred from the reads of fragments mapping to reference sequences. Furthermore, the reference database for piRNAs, whose length allows for analysis of the full-length sequence must be used carefully. Conceivably, a significant portion of the sequences annotated in this database describe fragments with a biogenesis separate of the PIWI pathway. Likely, most reads from somatic tissue mapping to these sequences rather represent piRNA-sized fragments of various other non-coding RNAs⁹⁶. To account for this fact, we filtered the piRNAs mapping to the reference data set for only piRNAs encoded in prepachytene genomic loci, as these are likely real piwi-interacting RNAs expressed in the somatic tissues. Nevertheless, looking into the detected RNAs in our data set that are probably falsely annotated could give interesting insight into fragmentation patterns and functions of other ncRNAs as these piRNA-like small RNAs are also known to play important regulatory roles in the somatic tissue¹³⁵. Our analysis mainly focused on the miRNA data interpretation, as the protocol is optimized exactly for the size of mature miRNAs.

We identified new region-specific miRNA expression signatures for different brain regions, especially the olfactory bulb showed distinct miRNA expression patterns. Five out of the eleven miRNAs that were exclusively expressed in the olfactory bulb were members of the miR-200 family. This miRNA family was previously reported to play a crucial role in neurogenesis^{105,136}. Newly identified region-specific miRNAs from our analysis are therefore interesting targets to study for region specific functionalities. Especially miR-9, which is well known for its crucial role in neuronal development¹³⁷ is an interesting target for further investigation, as its expression has not been described as region-specific in the brain before.

The highly detailed analysis of miRNA expression patterns in brain regions during aging revealed – apart from previously unknown region-specific miRNA - expression patterns, miRNAs increasing with age in multiple brain regions. Especially miR-155-5p, which we identified as a global aging miRNA before, is an interesting target to further study in the aging brain context. Increased secretion of miR-155-5p from microglia mediates inflammatory neuronal cell death and therefore plays a proinflammatory role¹³⁸. In the disease context (AD), miR-155 together with interferon- γ signaling mediates a protective microglial state¹³⁹. Determining which cell type is responsible for the increase of miR-155 expression in the bulk data and if this miRNA is secreted will give a better insight which mechanisms mediate functional consequences of expression changes.

Mapping bulk expression to cell-type data could be done via purifying one cell-type (e.g., through immunopanning or FACS sorting) to avoid the issues of sc-miRNA sequencing. Microglia RNA expression was analyzed after isolation via immunopanning for developmental ages up to 8 weeks previously. This analysis revealed miRNA-mRNA networks coregulating important CNS processes, centered around miR-146a-5p and miR-10a-5p amongst others¹⁴⁰. These two miRNAs and miR-155-5p, already known as regulators of activated microglia, were all deregulated with aging in multiple regions within our data, indicating, that a change in microglial miRNA expression could be the main driver of age-related bulk expression changes. In the brain likewise in the whole organism not only cellular expression of aging miRNAs is interesting but also their secretion and effects in recipient cells are interesting targets for investigation.

Investigation of miRNA cargo secreted from one specific cell type has to be done *in vitro*, either via isolating primary cells from tissue or using cell culture models, e.g. the BV-2 cell line for microglia. The EV content of this cell line has been studied in various conditions already and is therefore promising for further investigations also in the aging context¹⁴¹. Doxorubicin-induced cell senescence has been used to generate senescent microglia¹⁴². Doxorubicin-induced and untreated BV-2 cells could be used as

a model for secretion of aged/senescent and young microglia to determine if miRNA cargo in EVs is altered during aging.

Mouse models give meaningful insight into the role of miRNAs in aging processes, as they are closer related to humans than other well established model organisms for miRNA research, like *C. elegans* (worm), *D. melanogaster* (fly) and *D. rerio* (fish)¹⁴³. Maintenance of mice is inexpensive and easy, additionally, their lifespan is still comparably short. 60% of mouse miRNA loci are evolutionary conserved between human and mouse¹⁴³. This conservation, together with the strong sequence conservation of global aging markers, like miR-29 between mouse and humans are good indicators, that core biological processes are conserved between species. However, key differences also exist and can lead to limited success in clinical applications.

Within the recent preprint that analyzed the effects of transgenic modification of miR-29 expression¹²⁴, macaque data was included. This data showed an increase of miR-29 expression in liver during aging. These findings support the hypothesis that the global aging miRNAs are conserved between species up to humans. Macaques, as nonhuman primates are a valuable resource for biomedical research¹⁴⁴, because they share main aspects of physiology and lifestyle with humans, namely social intelligence, development and especially brain organization¹⁴⁵. They have been proposed as versatile models for studying aging and neurodegeneration to bridge the gap between rodent research and human clinical trials^{144,145}. During aging, rhesus macaques and humans exhibit strong similarities of transcriptomic and epigenetic signatures in peripheral immune aging¹⁴⁶. Replicating mouse-based findings in macaques before moving on to human trials has been proposed to increase success rates of trials and thereby reduce cost and time investment. In addition, novel miRNAs involved in brain development were found in macaques, that were absent in rodents¹⁴⁷. Therefore, we could potentially discover novel aging miRNAs that are absent in rodents, by studying the miRNA expression patterns during aging in macaques. Likely these miRNAs could also play a role in human aging, due to the close phylogenetic relationship. Additional studies in macaques would solidify the results and give additional strong indication that the global aging makers are relevant therapeutical targets.

Since the early 1980s research with antisense oligonucleotides (ASOs) that inhibit protein synthesis as first RNA therapeutics, has expanded to using siRNA to silence human genes in the early 2000s and recently two SARS-CoV-2 mRNA vaccines were approved¹⁴⁸. Even though no miRNA drugs have been approved for clinical use yet, three siRNA drugs, using similar mechanisms as miRNA drugs, are FDA approved already and an additional seven candidates are in Phase III clinical trials.

Several miRNA related therapeutics are currently tested in early clinical trials. Their mode of action can either be as anti-miR, reducing the effect of the miRNA or as miRNA mimic, enhancing the effect of the miRNA. Different body applications, like subcutaneous and intravenous injection, as well as different uptake modes, e.g. vehicle transfer or biomolecule conjugation are under investigation⁶¹. A reduction of miR-29 expression through partial deletion as performed in the mouse model is not feasible in humans. Therefore, reduction of miRNA expression has to be achieved in alternative manner, by e.g. using miRNA sponges or antisense oligonucleotides (anti-miRs)¹⁴⁹. An interesting target to start therapeutic research would be the anti-miR-29. This anti-miR has been used previously in a study of the miRNA-29 mimic (Remlarsen) for proof-of-concept experiments. The results showed that intradermal injection of anti-miR-29 resulted in an upregulation of collagen and extracellular matrix pathways¹⁵⁰. As we identified these pathways to be implicated in aging this anti-miR could serve as a starting point for a therapeutic application. In further studies safe and effective delivery strategies must be explored for all organs, as our data suggests a deregulation of this miRNA in all tissues during aging^{1,151}.

Apart from the biological findings involving the identification of global, local and brain-region-specific aging miRNAs, the data created in this work can be used as a reference atlas for other researchers studying small non-coding RNAs in all major tissues during aging. Especially, emerging regulatory fragments of non-coding RNAs like tRNA-derived fragments can be extracted from this data set. These fragments, called tRFs, have a length of 14 to 50 nucleotides and therefore perfectly fit the length of reads enriched during library preparation protocol⁸⁸. Currently, the state-of-the-art database for tRFs for mouse is based on an analysis of 100 small RNA libraries from 2015¹⁵². Another limitation is that no standard nomenclature of tRFs exists today. Using the additional sequencing data created within this study to develop an updated reference database for tRFs in mouse including a standardized nomenclature as well as a prediction of functional tRFs would benefit this field of research. Using this database for alignment, the expression shifts of tRFs during aging could be illuminated. Expression changes of tRFs in human CSF (cerebrospinal fluid) have been observed in aging and age-related diseases¹⁵³. Studying these expression changes in mouse tissue and interventions will lead to a better understanding of the regulatory mechanisms of tRFs.

One main limitation of this study in particular is whether it really has relevance for human aging and aging interventions. As already mentioned, mouse-based findings must be replicated in (non-) human primates to increase the chance of successful clinical trials¹⁴⁴. The translation of pharmaceutical compounds from preclinical animal

trials to efficacious human therapies continues to exhibit a persistent failure rate exceeding 92% and this rate is even higher for age-related diseases, like AD with 99%¹⁵⁴. But collecting human samples for a similar study would pose major challenges not only due to the scarcity of human tissue, but also other factors such as varying post-mortem intervals, leading to RNA quality issues¹⁵⁵. To collect enough human samples likely multiple clinical centers would have to be involved and standard operating procedures would have to be implemented to reduce batch effects caused by different sampling techniques. Furthermore, cause of death as well as full medical history and drug treatment, would need to be collected to complete the meta data and be accounted for during analysis, to avoid bias in the collected data¹⁵⁶.

These challenges are hard to overcome, however another limitation of this study is that since all samples were collected from inbred mouse strains the genetic diversity of the human population is poorly reflected. This limitation could have been reduced by generating diverse mouse populations¹⁵⁷. Potential batch effects were introduced in this study, by combining findings from different mouse cohorts. The circulatory mouse cohort was the only cohort housed and dissected in Germany.

Moreover, a sex-specific analysis should be performed, analyzing the male and female samples completely separated from each other, as significant sex differences have been observed in previous studies in aging research in humans and animal models¹⁵⁸. Multiple samples were excluded due to quality control reasons, resulting in differing numbers of male and female replicates per time point over the organs. In several cases statistical analysis was only possible if male and female replicates were combined to exceed the threshold of a minimum of three replicates per time point per organ. Additional samples should be collected to ensure that for every time point in every tissue/ region at least three to four samples of each sex are available to perform reliable statistical analysis to check for sex-specific aging signatures across organs and brain regions.

7 Conclusion

The different data sets combined yielded great insight into the expression patterns of miRNAs during aging in different organs and their potential mode of action as regulators of the aging phenotype. The identified global and local aging miRNAs are interesting targets to study in therapeutic interventions to slow down the aging process. Next steps could be to initiate experiments further investigating the remaining global aging miRNAs. Experiments like those already performed for miR-29 family could validate the important role of the remaining global aging miRNAs in aging phenotypes using genetic engineering in wild type and progeria mouse models.

Additionally, to further explore the value of miRNAs as therapeutical targets, using the anti-miR-29, preclinical research could be started. For this anti-miR its regulatory effect on extracellular matrix pathways has already been proven¹⁵⁰. Toxicology and pharmacokinetics of the anti-miR-drug should be tested by applying it to aged mice. Phenotypical improvements should be monitored by e.g. using behavioral tests for cognitive function assessment and investigating cellular markers of aging. These tests should be combined with an assessment of transcriptomic changes occurring during anti-miR treatment to further elucidate the pathways affected by miR-29. Potentially, a combination of multiple anti-miRs of the global aging miRNAs could even yield more successful therapy approaches.

In parallel to these mouse experiments, data could be collected from macaques to fill the evolutionary gap between mouse and humans. Macaques offer great advantages as model organisms, as they exhibit similar physiology and lifestyle to humans¹⁴⁴. Issues of compromised RNA quality can be avoided as the take down of model organisms in contrast to human sampling can be scheduled and no extended or varying postmortem intervals are expected.

Similarly, to the global aging miRNAs, the effects of miR-155-5p and miR-146a expression changes during aging in the brain should be closer investigated. First, the origin of these expression changes should be illuminated. Using FACS sorting to sort all major cell types of the brain, namely neurons, astrocytes and microglia from young and aged mice should be performed. Analyzing the bulk cell type sequencing data will yield insight in cell type-dependent increasing expression patterns. If microglia are responsible for the increase of miR-155-5p in the aging brain it should be further assessed, if the miRNA is also exported via EVs. Previously, this miRNA has been shown to have a proinflammatory effect and is neurotoxic when exported from activated microglia¹³⁸. Experiments investigating the miRNA cargo of EVs of aged/senescent

microglia and their regulatory function could reveal the role of miRNAs in altered intercellular communication in the brain. Altered cellular communication as a hallmark of aging is another interesting therapeutic target. In summary, we identified global, local and brain-region-specific aging miRNAs in this study, which are promising targets for therapeutic aging interventions.

8 References

- 1 Wagner, V. *et al.* Characterizing expression changes in noncoding RNAs during aging and heterochronic parabiosis across mouse tissues. *Nat Biotechnol* (2023). <https://doi.org:10.1038/s41587-023-01751-6>
- 2 <<https://www.who.int/news-room/fact-sheets/detail/ageing-and-health>> (2023).
- 3 Harper, S. Economic and social implications of aging societies. *Science* **346**, 587-591 (2014). <https://doi.org:10.1126/science.1254405>
- 4 Guo, J. *et al.* Aging and aging-related diseases: from molecular mechanisms to interventions and treatments. *Signal Transduct Target Ther* **7**, 391 (2022). <https://doi.org:10.1038/s41392-022-01251-0>
- 5 Lopez-Otin, C., Blasco, M. A., Partridge, L., Serrano, M. & Kroemer, G. The hallmarks of aging. *Cell* **153**, 1194-1217 (2013). <https://doi.org:10.1016/j.cell.2013.05.039>
- 6 Cohen, A. A. *et al.* A complex systems approach to aging biology. *Nat Aging* **2**, 580-591 (2022). <https://doi.org:10.1038/s43587-022-00252-6>
- 7 Gems, D. The aging-disease false dichotomy: understanding senescence as pathology. *Front Genet* **6**, 212 (2015). <https://doi.org:10.3389/fgene.2015.00212>
- 8 Bulterijs, S., Hull, R. S., Bjork, V. C. & Roy, A. G. It is time to classify biological aging as a disease. *Front Genet* **6**, 205 (2015). <https://doi.org:10.3389/fgene.2015.00205>
- 9 Lopez-Otin, C., Blasco, M. A., Partridge, L., Serrano, M. & Kroemer, G. Hallmarks of aging: An expanding universe. *Cell* **186**, 243-278 (2023). <https://doi.org:10.1016/j.cell.2022.11.001>
- 10 Moskalev, A. A. *et al.* The role of DNA damage and repair in aging through the prism of Koch-like criteria. *Ageing Res Rev* **12**, 661-684 (2013). <https://doi.org:10.1016/j.arr.2012.02.001>
- 11 Tomas-Loba, A. *et al.* Telomerase reverse transcriptase delays aging in cancer-resistant mice. *Cell* **135**, 609-622 (2008). <https://doi.org:10.1016/j.cell.2008.09.034>
- 12 Bernardes de Jesus, B. *et al.* Telomerase gene therapy in adult and old mice delays aging and increases longevity without increasing cancer. *EMBO Mol Med* **4**, 691-704 (2012). <https://doi.org:10.1002/emmm.201200245>
- 13 Ghosh, T. S., Das, M., Jeffery, I. B. & O'Toole, P. W. Adjusting for age improves identification of gut microbiome alterations in multiple diseases. *Elife* **9** (2020). <https://doi.org:10.7554/eLife.50240>
- 14 Fransen, F. *et al.* Aged Gut Microbiota Contributes to Systemic Inflammation after Transfer to Germ-Free Mice. *Front Immunol* **8**, 1385 (2017). <https://doi.org:10.3389/fimmu.2017.01385>
- 15 Calderwood, S. K., Murshid, A. & Prince, T. The shock of aging: molecular chaperones and the heat shock response in longevity and aging--a mini-review. *Gerontology* **55**, 550-558 (2009). <https://doi.org:10.1159/000225957>

- 16 Bobkova, N. V. *et al.* Exogenous Hsp70 delays senescence and improves cognitive function in aging mice. *Proc Natl Acad Sci U S A* **112**, 16006-16011 (2015). <https://doi.org:10.1073/pnas.1516131112>
- 17 Levine, B. & Kroemer, G. Biological Functions of Autophagy Genes: A Disease Perspective. *Cell* **176**, 11-42 (2019). <https://doi.org:10.1016/j.cell.2018.09.048>
- 18 Pyo, J. O. *et al.* Overexpression of Atg5 in mice activates autophagy and extends lifespan. *Nat Commun* **4**, 2300 (2013). <https://doi.org:10.1038/ncomms3300>
- 19 Rodriguez-Matellan, A., Alcazar, N., Hernandez, F., Serrano, M. & Avila, J. In Vivo Reprogramming Ameliorates Aging Features in Dentate Gyrus Cells and Improves Memory in Mice. *Stem Cell Reports* **15**, 1056-1066 (2020). <https://doi.org:10.1016/j.stemcr.2020.09.010>
- 20 Collado, M., Blasco, M. A. & Serrano, M. Cellular senescence in cancer and aging. *Cell* **130**, 223-233 (2007). <https://doi.org:10.1016/j.cell.2007.07.003>
- 21 Budreviciute, A. *et al.* Management and Prevention Strategies for Non-communicable Diseases (NCDs) and Their Risk Factors. *Front Public Health* **8**, 574111 (2020). <https://doi.org:10.3389/fpubh.2020.574111>
- 22 Longo, M. *et al.* Diabetes and Aging: From Treatment Goals to Pharmacologic Therapy. *Front Endocrinol (Lausanne)* **10**, 45 (2019). <https://doi.org:10.3389/fendo.2019.00045>
- 23 Li, Z. *et al.* Aging and age-related diseases: from mechanisms to therapeutic strategies. *Biogerontology* **22**, 165-187 (2021). <https://doi.org:10.1007/s10522-021-09910-5>
- 24 DePinho, R. A. The age of cancer. *Nature* **408**, 248-254 (2000). <https://doi.org:10.1038/35041694>
- 25 Hanahan, D. & Weinberg, R. A. Hallmarks of cancer: the next generation. *Cell* **144**, 646-674 (2011). <https://doi.org:10.1016/j.cell.2011.02.013>
- 26 Laconi, E., Marongiu, F. & DeGregori, J. Cancer as a disease of old age: changing mutational and microenvironmental landscapes. *Br J Cancer* **122**, 943-952 (2020). <https://doi.org:10.1038/s41416-019-0721-1>
- 27 Ahima, R. S. Connecting obesity, aging and diabetes. *Nat Med* **15**, 996-997 (2009). <https://doi.org:10.1038/nm0909-996>
- 28 DeFronzo, R. A. *et al.* Type 2 diabetes mellitus. *Nat Rev Dis Primers* **1**, 15019 (2015). <https://doi.org:10.1038/nrdp.2015.19>
- 29 Bekris, L. M., Yu, C. E., Bird, T. D. & Tsuang, D. W. Genetics of Alzheimer disease. *J Geriatr Psychiatry Neurol* **23**, 213-227 (2010). <https://doi.org:10.1177/0891988710383571>
- 30 Hou, Y. *et al.* Ageing as a risk factor for neurodegenerative disease. *Nat Rev Neurol* **15**, 565-581 (2019). <https://doi.org:10.1038/s41582-019-0244-7>
- 31 Hwang, J. Y., Aromolaran, K. A. & Zukin, R. S. The emerging field of epigenetics in neurodegeneration and neuroprotection. *Nat Rev Neurosci* **18**, 347-361 (2017). <https://doi.org:10.1038/nrn.2017.46>
- 32 Keshavarz, M., Xie, K., Schaaf, K., Bano, D. & Ehninger, D. Targeting the "hallmarks of aging" to slow aging and treat age-related disease: fact

- or fiction? *Mol Psychiatry* **28**, 242-255 (2023).
<https://doi.org/10.1038/s41380-022-01680-x>
- 33 Reimers, C. D., Knapp, G. & Reimers, A. K. Does physical activity increase life expectancy? A review of the literature. *J Aging Res* **2012**, 243958 (2012). <https://doi.org/10.1155/2012/243958>
- 34 Navarro, A., Gomez, C., Lopez-Cepero, J. M. & Boveris, A. Beneficial effects of moderate exercise on mice aging: survival, behavior, oxidative stress, and mitochondrial electron transfer. *Am J Physiol Regul Integr Comp Physiol* **286**, R505-511 (2004).
<https://doi.org/10.1152/ajpregu.00208.2003>
- 35 De Miguel, Z. *et al.* Exercise plasma boosts memory and dampens brain inflammation via clusterin. *Nature* **600**, 494-499 (2021).
<https://doi.org/10.1038/s41586-021-04183-x>
- 36 Brett, J. O. *et al.* Exercise rejuvenates quiescent skeletal muscle stem cells in old mice through restoration of Cyclin D1. *Nat Metab* **2**, 307-317 (2020). <https://doi.org/10.1038/s42255-020-0190-0>
- 37 Madeo, F., Carmona-Gutierrez, D., Hofer, S. J. & Kroemer, G. Caloric Restriction Mimetics against Age-Associated Disease: Targets, Mechanisms, and Therapeutic Potential. *Cell Metab* **29**, 592-610 (2019).
<https://doi.org/10.1016/j.cmet.2019.01.018>
- 38 Green, C. L., Lamming, D. W. & Fontana, L. Molecular mechanisms of dietary restriction promoting health and longevity. *Nat Rev Mol Cell Biol* **23**, 56-73 (2022). <https://doi.org/10.1038/s41580-021-00411-4>
- 39 Ungvari, Z., Parrado-Fernandez, C., Csiszar, A. & de Cabo, R. Mechanisms underlying caloric restriction and lifespan regulation: implications for vascular aging. *Circ Res* **102**, 519-528 (2008).
<https://doi.org/10.1161/CIRCRESAHA.107.168369>
- 40 Ocampo, A. *et al.* In Vivo Amelioration of Age-Associated Hallmarks by Partial Reprogramming. *Cell* **167**, 1719-1733 e1712 (2016).
<https://doi.org/10.1016/j.cell.2016.11.052>
- 41 Takahashi, K. & Yamanaka, S. Induction of pluripotent stem cells from mouse embryonic and adult fibroblast cultures by defined factors. *Cell* **126**, 663-676 (2006). <https://doi.org/10.1016/j.cell.2006.07.024>
- 42 Browder, K. C. *et al.* In vivo partial reprogramming alters age-associated molecular changes during physiological aging in mice. *Nat Aging* **2**, 243-253 (2022). <https://doi.org/10.1038/s43587-022-00183-2>
- 43 Singh, P. B. & Zhakupova, A. Age reprogramming: cell rejuvenation by partial reprogramming. *Development* **149** (2022).
<https://doi.org/10.1242/dev.200755>
- 44 Arriola Apelo, S. I., Pumper, C. P., Baar, E. L., Cummings, N. E. & Lamming, D. W. Intermittent Administration of Rapamycin Extends the Life Span of Female C57BL/6J Mice. *J Gerontol A Biol Sci Med Sci* **71**, 876-881 (2016). <https://doi.org/10.1093/gerona/glw064>
- 45 Selvarani, R., Mohammed, S. & Richardson, A. Effect of rapamycin on aging and age-related diseases-past and future. *Geroscience* **43**, 1135-1158 (2021). <https://doi.org/10.1007/s11357-020-00274-1>
- 46 Martin-Montalvo, A. *et al.* Metformin improves healthspan and lifespan in mice. *Nat Commun* **4**, 2192 (2013). <https://doi.org/10.1038/ncomms3192>

- 47 Kulkarni, A. S., Gubbi, S. & Barzilai, N. Benefits of Metformin in Attenuating the Hallmarks of Aging. *Cell Metab* **32**, 15-30 (2020). <https://doi.org:10.1016/j.cmet.2020.04.001>
- 48 Chaib, S., Tchkonja, T. & Kirkland, J. L. Cellular senescence and senolytics: the path to the clinic. *Nat Med* **28**, 1556-1568 (2022). <https://doi.org:10.1038/s41591-022-01923-y>
- 49 Conboy, M. J., Conboy, I. M. & Rando, T. A. Heterochronic parabiosis: historical perspective and methodological considerations for studies of aging and longevity. *Aging Cell* **12**, 525-530 (2013). <https://doi.org:10.1111/accel.12065>
- 50 Brack, A. S. *et al.* Increased Wnt signaling during aging alters muscle stem cell fate and increases fibrosis. *Science* **317**, 807-810 (2007). <https://doi.org:10.1126/science.1144090>
- 51 Villeda, S. A. *et al.* The ageing systemic milieu negatively regulates neurogenesis and cognitive function. *Nature* **477**, 90-94 (2011). <https://doi.org:10.1038/nature10357>
- 52 Villeda, S. A. *et al.* Young blood reverses age-related impairments in cognitive function and synaptic plasticity in mice. *Nat Med* **20**, 659-663 (2014). <https://doi.org:10.1038/nm.3569>
- 53 Conese, M., Carbone, A., Beccia, E. & Angiolillo, A. The Fountain of Youth: A Tale of Parabiosis, Stem Cells, and Rejuvenation. *Open Med (Wars)* **12**, 376-383 (2017). <https://doi.org:10.1515/med-2017-0053>
- 54 Pandey, K. K. *et al.* Regulatory roles of tRNA-derived RNA fragments in human pathophysiology. *Mol Ther Nucleic Acids* **26**, 161-173 (2021). <https://doi.org:10.1016/j.omtn.2021.06.023>
- 55 Statello, L., Guo, C. J., Chen, L. L. & Huarte, M. Gene regulation by long non-coding RNAs and its biological functions. *Nat Rev Mol Cell Biol* **22**, 96-118 (2021). <https://doi.org:10.1038/s41580-020-00315-9>
- 56 Huang, Z. H., Du, Y. P., Wen, J. T., Lu, B. F. & Zhao, Y. snoRNAs: functions and mechanisms in biological processes, and roles in tumor pathophysiology. *Cell Death Discov* **8**, 259 (2022). <https://doi.org:10.1038/s41420-022-01056-8>
- 57 Deryusheva, S. & Gall, J. G. scaRNAs and snoRNAs: Are they limited to specific classes of substrate RNAs? *RNA* **25**, 17-22 (2019). <https://doi.org:10.1261/rna.068593.118>
- 58 Cech, T. R. & Steitz, J. A. The noncoding RNA revolution-trashing old rules to forge new ones. *Cell* **157**, 77-94 (2014). <https://doi.org:10.1016/j.cell.2014.03.008>
- 59 Morais, P., Adachi, H. & Yu, Y. T. Spliceosomal snRNA Epitranscriptomics. *Front Genet* **12**, 652129 (2021). <https://doi.org:10.3389/fgene.2021.652129>
- 60 Gurtan, A. M. & Sharp, P. A. The role of miRNAs in regulating gene expression networks. *J Mol Biol* **425**, 3582-3600 (2013). <https://doi.org:10.1016/j.jmb.2013.03.007>
- 61 Diener, C., Keller, A. & Meese, E. Emerging concepts of miRNA therapeutics: from cells to clinic. *Trends Genet* **38**, 613-626 (2022). <https://doi.org:10.1016/j.tig.2022.02.006>

- 62 Ni, W. J. & Leng, X. M. miRNA-Dependent Activation of mRNA Translation. *Microna* **5**, 83-86 (2016).
<https://doi.org:10.2174/2211536605666160825151201>
- 63 O'Brien, J., Hayder, H., Zayed, Y. & Peng, C. Overview of MicroRNA Biogenesis, Mechanisms of Actions, and Circulation. *Front Endocrinol (Lausanne)* **9**, 402 (2018). <https://doi.org:10.3389/fendo.2018.00402>
- 64 O'Brien, K., Breyne, K., Ughetto, S., Laurent, L. C. & Breakefield, X. O. RNA delivery by extracellular vesicles in mammalian cells and its applications. *Nat Rev Mol Cell Biol* **21**, 585-606 (2020).
<https://doi.org:10.1038/s41580-020-0251-y>
- 65 Keller, A. *et al.* Toward the blood-borne miRNome of human diseases. *Nat Methods* **8**, 841-843 (2011). <https://doi.org:10.1038/nmeth.1682>
- 66 Fehlmann, T., Ludwig, N., Backes, C., Meese, E. & Keller, A. Distribution of microRNA biomarker candidates in solid tissues and body fluids. *RNA Biol* **13**, 1084-1088 (2016).
<https://doi.org:10.1080/15476286.2016.1234658>
- 67 Lee, R. C., Feinbaum, R. L. & Ambros, V. The *C. elegans* heterochronic gene *lin-4* encodes small RNAs with antisense complementarity to *lin-14*. *Cell* **75**, 843-854 (1993). [https://doi.org:10.1016/0092-8674\(93\)90529-y](https://doi.org:10.1016/0092-8674(93)90529-y)
- 68 Gomes, C. P. *et al.* A Review of Computational Tools in microRNA Discovery. *Front Genet* **4**, 81 (2013).
<https://doi.org:10.3389/fgene.2013.00081>
- 69 Chen, L. *et al.* Trends in the development of miRNA bioinformatics tools. *Brief Bioinform* **20**, 1836-1852 (2019). <https://doi.org:10.1093/bib/bby054>
- 70 Shatoff, E. & Bundschuh, R. dsRBPBind: modeling the effect of RNA secondary structure on double-stranded RNA-protein binding. *Bioinformatics* **38**, 687-693 (2022).
<https://doi.org:10.1093/bioinformatics/btab724>
- 71 Agarwal, V., Bell, G. W., Nam, J. W. & Bartel, D. P. Predicting effective microRNA target sites in mammalian mRNAs. *Elife* **4** (2015).
<https://doi.org:10.7554/eLife.05005>
- 72 Bandyopadhyay, S., Ghosh, D., Mitra, R. & Zhao, Z. MBSTAR: multiple instance learning for predicting specific functional binding sites in microRNA targets. *Sci Rep* **5**, 8004 (2015).
<https://doi.org:10.1038/srep08004>
- 73 Rennie, W. *et al.* STarMirDB: A database of microRNA binding sites. *RNA Biol* **13**, 554-560 (2016).
<https://doi.org:10.1080/15476286.2016.1182279>
- 74 Miranda, K. C. *et al.* A pattern-based method for the identification of MicroRNA binding sites and their corresponding heteroduplexes. *Cell* **126**, 1203-1217 (2006). <https://doi.org:10.1016/j.cell.2006.07.031>
- 75 Chu, Y. W. *et al.* miRgo: integrating various off-the-shelf tools for identification of microRNA-target interactions by heterogeneous features and a novel evaluation indicator. *Sci Rep* **10**, 1466 (2020).
<https://doi.org:10.1038/s41598-020-58336-5>
- 76 Chen, Y. & Wang, X. miRDB: an online database for prediction of functional microRNA targets. *Nucleic Acids Res* **48**, D127-D131 (2020).
<https://doi.org:10.1093/nar/gkz757>

- 77 Fehlmann, T. *et al.* Common diseases alter the physiological age-related blood microRNA profile. *Nat Commun* **11**, 5958 (2020). <https://doi.org:10.1038/s41467-020-19665-1>
- 78 Keller, A. *et al.* miRNATissueAtlas2: an update to the human miRNA tissue atlas. *Nucleic Acids Res* **50**, D211-D221 (2022). <https://doi.org:10.1093/nar/gkab808>
- 79 Ludwig, N. *et al.* Bias in recent miRBase annotations potentially associated with RNA quality issues. *Sci Rep* **7**, 5162 (2017). <https://doi.org:10.1038/s41598-017-05070-0>
- 80 Du, W. W. *et al.* miR-17 extends mouse lifespan by inhibiting senescence signaling mediated by MKP7. *Cell Death Dis* **5**, e1355 (2014). <https://doi.org:10.1038/cddis.2014.305>
- 81 Kinser, H. E. & Pincus, Z. MicroRNAs as modulators of longevity and the aging process. *Hum Genet* **139**, 291-308 (2020). <https://doi.org:10.1007/s00439-019-02046-0>
- 82 Schaum, N. *et al.* Ageing hallmarks exhibit organ-specific temporal signatures. *Nature* **583**, 596-602 (2020). <https://doi.org:10.1038/s41586-020-2499-y>
- 83 Kern, F. *et al.* Ageing-associated small RNA cargo of extracellular vesicles. *RNA Biol* **20**, 482-494 (2023). <https://doi.org:10.1080/15476286.2023.2234713>
- 84 Hahn, O. *et al.* Atlas of the aging mouse brain reveals white matter as vulnerable foci. *Cell* **186**, 4117-4133 e4122 (2023). <https://doi.org:10.1016/j.cell.2023.07.027>
- 85 Fehlmann, T. *et al.* miRMaster 2.0: multi-species non-coding RNA sequencing analyses at scale. *Nucleic Acids Res* **49**, W397-W408 (2021). <https://doi.org:10.1093/nar/gkab268>
- 86 Palovics, R. *et al.* Molecular hallmarks of heterochronic parabiosis at single-cell resolution. *Nature* **603**, 309-314 (2022). <https://doi.org:10.1038/s41586-022-04461-2>
- 87 Fehlmann, T. *et al.* A high-resolution map of the human small non-coding transcriptome. *Bioinformatics* **34**, 1621-1628 (2018). <https://doi.org:10.1093/bioinformatics/btx814>
- 88 Yuan, Y. *et al.* tRNA-derived fragments as New Hallmarks of Aging and Age-related Diseases. *Aging Dis* **12**, 1304-1322 (2021). <https://doi.org:10.14336/AD.2021.0115>
- 89 Li, X. Z. *et al.* An ancient transcription factor initiates the burst of piRNA production during early meiosis in mouse testes. *Mol Cell* **50**, 67-81 (2013). <https://doi.org:10.1016/j.molcel.2013.02.016>
- 90 Ding, D. *et al.* TDRD5 binds piRNA precursors and selectively enhances pachytene piRNA processing in mice. *Nat Commun* **9**, 127 (2018). <https://doi.org:10.1038/s41467-017-02622-w>
- 91 Szklarczyk, D. *et al.* The STRING database in 2021: customizable protein-protein networks, and functional characterization of user-uploaded gene/measurement sets. *Nucleic Acids Res* **49**, D605-D612 (2021). <https://doi.org:10.1093/nar/gkaa1074>

- 92 Gerstner, N. *et al.* GeneTrail 3: advanced high-throughput enrichment analysis. *Nucleic Acids Res* **48**, W515-W520 (2020).
<https://doi.org:10.1093/nar/gkaa306>
- 93 Szczyrba, J. *et al.* Analysis of Argonaute Complex Bound mRNAs in DU145 Prostate Carcinoma Cells Reveals New miRNA Target Genes. *Prostate Cancer* **2017**, 4893921 (2017).
<https://doi.org:10.1155/2017/4893921>
- 94 Pan, H. *et al.* LncRNA LIFR-AS1 promotes proliferation and invasion of gastric cancer cell via miR-29a-3p/COL1A2 axis. *Cancer Cell Int* **21**, 7 (2021). <https://doi.org:10.1186/s12935-020-01644-7>
- 95 Kern, F. *et al.* Validation of human microRNA target pathways enables evaluation of target prediction tools. *Nucleic Acids Res* **49**, 127-144 (2021). <https://doi.org:10.1093/nar/gkaa1161>
- 96 Tosar, J. P., Rovira, C. & Cayota, A. Non-coding RNA fragments account for the majority of annotated piRNAs expressed in somatic non-gonadal tissues. *Commun Biol* **1**, 2 (2018). <https://doi.org:10.1038/s42003-017-0001-7>
- 97 Zhou, Z., Sun, B., Yu, D. & Bian, M. Roles of tRNA metabolism in aging and lifespan. *Cell Death Dis* **12**, 548 (2021).
<https://doi.org:10.1038/s41419-021-03838-x>
- 98 Kern, F. *et al.* miEAA 2.0: integrating multi-species microRNA enrichment analysis and workflow management systems. *Nucleic Acids Res* **48**, W521-W528 (2020). <https://doi.org:10.1093/nar/gkaa309>
- 99 van Rooij, E. *et al.* Dysregulation of microRNAs after myocardial infarction reveals a role of miR-29 in cardiac fibrosis. *Proc Natl Acad Sci U S A* **105**, 13027-13032 (2008).
<https://doi.org:10.1073/pnas.0805038105>
- 100 Mavrogenatou, E., Pratsinis, H., Papadopoulou, A., Karamanos, N. K. & Kletsas, D. Extracellular matrix alterations in senescent cells and their significance in tissue homeostasis. *Matrix Biol* **75-76**, 27-42 (2019).
<https://doi.org:10.1016/j.matbio.2017.10.004>
- 101 Tong, D. *et al.* MiR-487b suppressed inflammation and neuronal apoptosis in spinal cord injury by targeted Ifitm3. *Metab Brain Dis* **37**, 2405-2415 (2022). <https://doi.org:10.1007/s11011-022-01015-3>
- 102 Chen, X. *et al.* DNA methylation-regulated and tumor-suppressive roles of miR-487b in colorectal cancer via targeting MYC, SUZ12, and KRAS. *Cancer Med* **8**, 1694-1709 (2019). <https://doi.org:10.1002/cam4.2032>
- 103 Zhang, Y. *et al.* Hypothalamic stem cells control ageing speed partly through exosomal miRNAs. *Nature* **548**, 52-57 (2017).
<https://doi.org:10.1038/nature23282>
- 104 Selman, M. & Pardo, A. Fibroageing: An ageing pathological feature driven by dysregulated extracellular matrix-cell mechanobiology. *Ageing Res Rev* **70**, 101393 (2021). <https://doi.org:10.1016/j.arr.2021.101393>
- 105 Beclin, C. *et al.* miR-200 family controls late steps of postnatal forebrain neurogenesis via Zeb2 inhibition. *Sci Rep* **6**, 35729 (2016).
<https://doi.org:10.1038/srep35729>

- 106 Sim, S. E. *et al.* The Brain-Enriched MicroRNA miR-9-3p Regulates Synaptic Plasticity and Memory. *J Neurosci* **36**, 8641-8652 (2016). <https://doi.org/10.1523/JNEUROSCI.0630-16.2016>
- 107 Wong, J. E., Cao, J., Dorris, D. M. & Meitzen, J. Genetic sex and the volumes of the caudate-putamen, nucleus accumbens core and shell: original data and a review. *Brain Struct Funct* **221**, 4257-4267 (2016). <https://doi.org/10.1007/s00429-015-1158-9>
- 108 Lei, X. *et al.* Sex Differences in Fiber Connection between the Striatum and Subcortical and Cortical Regions. *Front Comput Neurosci* **10**, 100 (2016). <https://doi.org/10.3389/fncom.2016.00100>
- 109 Takei, N. & Nawa, H. mTOR signaling and its roles in normal and abnormal brain development. *Front Mol Neurosci* **7**, 28 (2014). <https://doi.org/10.3389/fnmol.2014.00028>
- 110 Garelick, M. G. & Kennedy, B. K. TOR on the brain. *Exp Gerontol* **46**, 155-163 (2011). <https://doi.org/10.1016/j.exger.2010.08.030>
- 111 Zhang, Y., Huang, B., Wang, H. Y., Chang, A. & Zheng, X. F. S. Emerging Role of MicroRNAs in mTOR Signaling. *Cell Mol Life Sci* **74**, 2613-2625 (2017). <https://doi.org/10.1007/s00018-017-2485-1>
- 112 Zingale, V. D., Gugliandolo, A. & Mazzon, E. MiR-155: An Important Regulator of Neuroinflammation. *Int J Mol Sci* **23** (2021). <https://doi.org/10.3390/ijms23010090>
- 113 Evans, D. R. *et al.* A novel pathogenic missense ADAMTS17 variant that impairs secretion causes Weill-Marchesani Syndrome with variably dysmorphic hand features. *Sci Rep* **10**, 10827 (2020). <https://doi.org/10.1038/s41598-020-66978-8>
- 114 Kumari, S., Panda, T. K. & Pradhan, T. Lysyl Oxidase: Its Diversity in Health and Diseases. *Indian J Clin Biochem* **32**, 134-141 (2017). <https://doi.org/10.1007/s12291-016-0576-7>
- 115 Sudo, R., Sato, F., Azechi, T. & Wachi, H. MiR-29-mediated elastin down-regulation contributes to inorganic phosphorus-induced osteoblastic differentiation in vascular smooth muscle cells. *Genes Cells* **20**, 1077-1087 (2015). <https://doi.org/10.1111/gtc.12311>
- 116 Mayer, U., Benditz, A. & Grassel, S. miR-29b regulates expression of collagens I and III in chondrogenically differentiating BMSC in an osteoarthritic environment. *Sci Rep* **7**, 13297 (2017). <https://doi.org/10.1038/s41598-017-13567-x>
- 117 Maurer, B. *et al.* MicroRNA-29, a key regulator of collagen expression in systemic sclerosis. *Arthritis Rheum* **62**, 1733-1743 (2010). <https://doi.org/10.1002/art.27443>
- 118 Kriegel, A. J., Liu, Y., Fang, Y., Ding, X. & Liang, M. The miR-29 family: genomics, cell biology, and relevance to renal and cardiovascular injury. *Physiol Genomics* **44**, 237-244 (2012). <https://doi.org/10.1152/physiolgenomics.00141.2011>
- 119 Ugalde, A. P. *et al.* Aging and chronic DNA damage response activate a regulatory pathway involving miR-29 and p53. *EMBO J* **30**, 2219-2232 (2011). <https://doi.org/10.1038/emboj.2011.124>

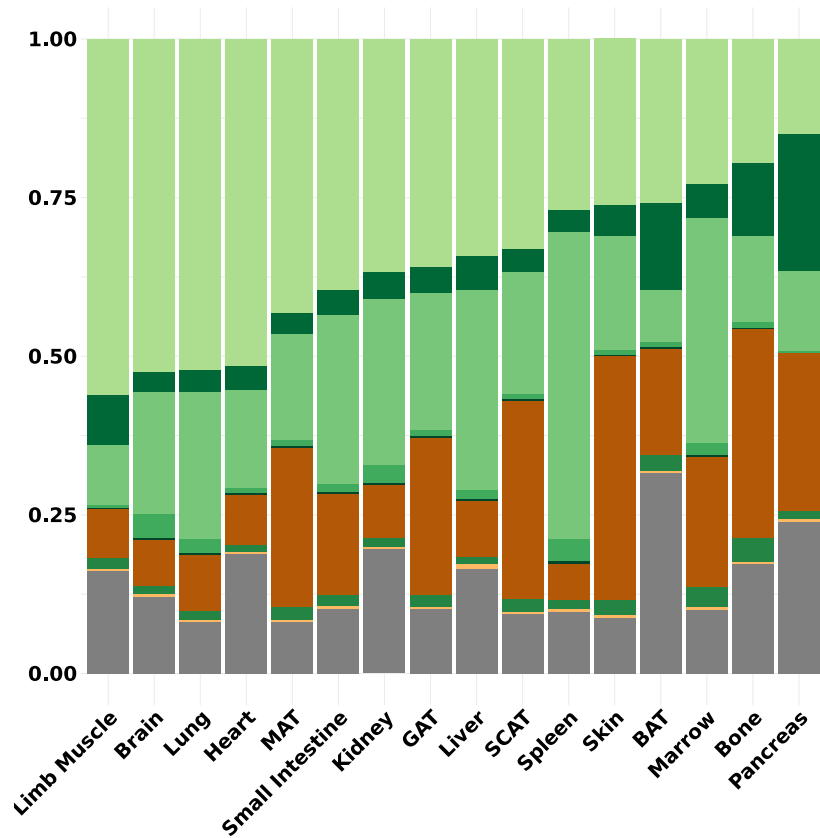
- 120 Hu, Z. *et al.* MicroRNA-29 induces cellular senescence in aging muscle through multiple signaling pathways. *Aging (Albany NY)* **6**, 160-175 (2014). <https://doi.org:10.18632/aging.100643>
- 121 Fenn, A. M. *et al.* Increased micro-RNA 29b in the aged brain correlates with the reduction of insulin-like growth factor-1 and fractalkine ligand. *Neurobiol Aging* **34**, 2748-2758 (2013). <https://doi.org:10.1016/j.neurobiolaging.2013.06.007>
- 122 Kumari, R. *et al.* MicroRNA miR-29c regulates RAG1 expression and modulates V(D)J recombination during B cell development. *Cell Rep* **36**, 109390 (2021). <https://doi.org:10.1016/j.celrep.2021.109390>
- 123 Lyu, G. *et al.* Addendum: TGF-beta signaling alters H4K20me3 status via miR-29 and contributes to cellular senescence and cardiac aging. *Nat Commun* **9**, 4134 (2018). <https://doi.org:10.1038/s41467-018-06710-3>
- 124 Vijay Swahari, A. N., Emilie Hollville, Yu-Han Hung, Matt Kanke, C. Lisa Kurtz, Xurde M. Caravia, Shenghui He, Janakiraman Krishnamurthy, Sahil Kapoor, Varun Prasad, Cornelius Flowers, Matt Beck, Jeanette Baran-Gale, Norman Sharpless, Carlos López-Otín, Praveen Sethupathy, Mohanish Deshmukh. *miR-29 is an important driver of aging-related phenotypes* (2022).
- 125 Mei, Z. *et al.* Lowering hippocampal miR-29a expression slows cognitive decline and reduces beta-amyloid deposition in 5xFAD mice. *Res Sq* (2023). <https://doi.org:10.21203/rs.3.rs-3235257/v1>
- 126 Wingo, A. P. *et al.* Brain microRNAs are associated with variation in cognitive trajectory in advanced age. *Transl Psychiatry* **12**, 47 (2022). <https://doi.org:10.1038/s41398-022-01806-3>
- 127 Gendron, C. M. & Pletcher, S. D. MicroRNAs mir-184 and let-7 alter *Drosophila* metabolism and longevity. *Aging Cell* **16**, 1434-1438 (2017). <https://doi.org:10.1111/accel.12673>
- 128 Cruz, F. M., Tome, M., Bernal, J. A. & Bernad, A. miR-300 mediates Bmi1 function and regulates differentiation in primitive cardiac progenitors. *Cell Death Dis* **6**, e1953 (2015). <https://doi.org:10.1038/cddis.2015.255>
- 129 Lettieri-Barbato, D., Aquilano, K., Punziano, C., Minopoli, G. & Faraonio, R. MicroRNAs, Long Non-Coding RNAs, and Circular RNAs in the Redox Control of Cell Senescence. *Antioxidants (Basel)* **11** (2022). <https://doi.org:10.3390/antiox11030480>
- 130 Hucker, S. M. *et al.* Single-cell microRNA sequencing method comparison and application to cell lines and circulating lung tumor cells. *Nat Commun* **12**, 4316 (2021). <https://doi.org:10.1038/s41467-021-24611-w>
- 131 Isakova, A., Neff, N. & Quake, S. R. Single-cell quantification of a broad RNA spectrum reveals unique noncoding patterns associated with cell types and states. *Proc Natl Acad Sci U S A* **118** (2021). <https://doi.org:10.1073/pnas.2113568118>
- 132 Garcia-Martin, R. *et al.* MicroRNA sequence codes for small extracellular vesicle release and cellular retention. *Nature* **601**, 446-451 (2022). <https://doi.org:10.1038/s41586-021-04234-3>

- 133 Raabe, C. A., Tang, T. H., Brosius, J. & Rozhdestvensky, T. S. Biases in small RNA deep sequencing data. *Nucleic Acids Res* **42**, 1414-1426 (2014). <https://doi.org:10.1093/nar/gkt1021>
- 134 Buschmann, D. *et al.* Toward reliable biomarker signatures in the age of liquid biopsies - how to standardize the small RNA-Seq workflow. *Nucleic Acids Res* **44**, 5995-6018 (2016). <https://doi.org:10.1093/nar/gkw545>
- 135 Yan, Z. *et al.* Widespread expression of piRNA-like molecules in somatic tissues. *Nucleic Acids Res* **39**, 6596-6607 (2011). <https://doi.org:10.1093/nar/gkr298>
- 136 Choi, P. S. *et al.* Members of the miRNA-200 family regulate olfactory neurogenesis. *Neuron* **57**, 41-55 (2008). <https://doi.org:10.1016/j.neuron.2007.11.018>
- 137 Coolen, M., Katz, S. & Bally-Cuif, L. miR-9: a versatile regulator of neurogenesis. *Front Cell Neurosci* **7**, 220 (2013). <https://doi.org:10.3389/fncel.2013.00220>
- 138 Cardoso, A. L., Guedes, J. R., Pereira de Almeida, L. & Pedroso de Lima, M. C. miR-155 modulates microglia-mediated immune response by down-regulating SOCS-1 and promoting cytokine and nitric oxide production. *Immunology* **135**, 73-88 (2012). <https://doi.org:10.1111/j.1365-2567.2011.03514.x>
- 139 Yin, Z. *et al.* Identification of a protective microglial state mediated by miR-155 and interferon-gamma signaling in a mouse model of Alzheimer's disease. *Nat Neurosci* **26**, 1196-1207 (2023). <https://doi.org:10.1038/s41593-023-01355-y>
- 140 Walsh, A. D. *et al.* Mouse microglia express unique miRNA-mRNA networks to facilitate age-specific functions in the developing central nervous system. *Commun Biol* **6**, 555 (2023). <https://doi.org:10.1038/s42003-023-04926-8>
- 141 Gabrielli, M., Raffaele, S., Fumagalli, M. & Verderio, C. The multiple faces of extracellular vesicles released by microglia: Where are we 10 years after? *Front Cell Neurosci* **16**, 984690 (2022). <https://doi.org:10.3389/fncel.2022.984690>
- 142 Marques, L., Johnson, A. A. & Stolzing, A. Doxorubicin generates senescent microglia that exhibit altered proteomes, higher levels of cytokine secretion, and a decreased ability to internalize amyloid beta. *Exp Cell Res* **395**, 112203 (2020). <https://doi.org:10.1016/j.yexcr.2020.112203>
- 143 Pal, A. S. & Kasinski, A. L. Animal Models to Study MicroRNA Function. *Adv Cancer Res* **135**, 53-118 (2017). <https://doi.org:10.1016/bs.acr.2017.06.006>
- 144 Gardner, M. B. & Luciw, P. A. Macaque models of human infectious disease. *ILAR J* **49**, 220-255 (2008). <https://doi.org:10.1093/ilar.49.2.220>
- 145 Lopez, M. S., Metzger, J. M. & Emborg, M. E. Identification of novel rhesus macaque microRNAs from naive whole blood. *Mol Biol Rep* **46**, 5511-5516 (2019). <https://doi.org:10.1007/s11033-019-04891-8>
- 146 Chiou, K. L. *et al.* Rhesus macaques as a tractable physiological model of human ageing. *Philos Trans R Soc Lond B Biol Sci* **375**, 20190612 (2020). <https://doi.org:10.1098/rstb.2019.0612>

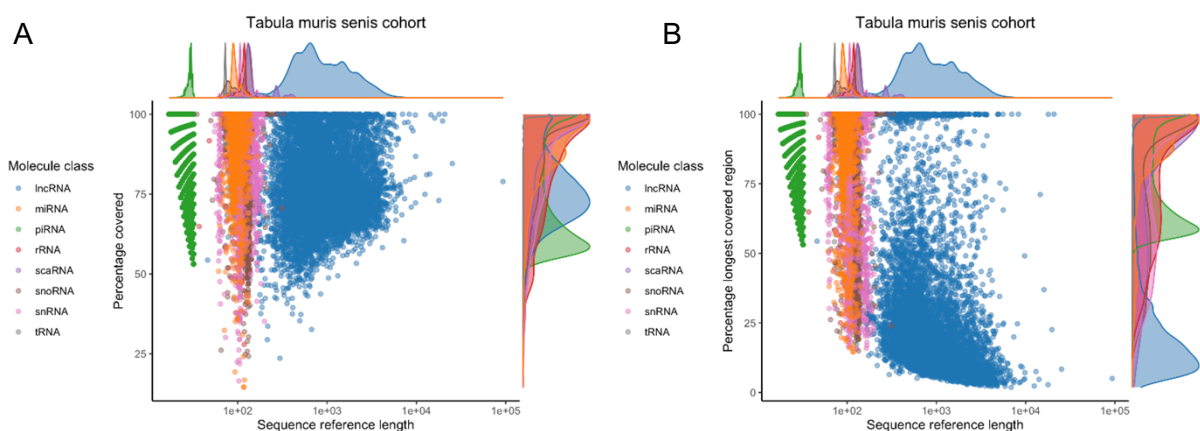
- 147 Arcila, M. L. *et al.* Novel primate miRNAs coevolved with ancient target genes in germinal zone-specific expression patterns. *Neuron* **81**, 1255-1262 (2014). <https://doi.org:10.1016/j.neuron.2014.01.017>
- 148 Zhu, Y., Zhu, L., Wang, X. & Jin, H. RNA-based therapeutics: an overview and prospectus. *Cell Death Dis* **13**, 644 (2022). <https://doi.org:10.1038/s41419-022-05075-2>
- 149 Jie, J. *et al.* Generation of MiRNA sponge constructs targeting multiple MiRNAs. *J Clin Lab Anal* **36**, e24527 (2022). <https://doi.org:10.1002/jcla.24527>
- 150 Gallant-Behm, C. L. *et al.* A MicroRNA-29 Mimic (Replarsen) Represses Extracellular Matrix Expression and Fibroplasia in the Skin. *J Invest Dermatol* **139**, 1073-1081 (2019). <https://doi.org:10.1016/j.jid.2018.11.007>
- 151 Broderick, J. A. & Zamore, P. D. MicroRNA therapeutics. *Gene Ther* **18**, 1104-1110 (2011). <https://doi.org:10.1038/gt.2011.50>
- 152 Kumar, P., Mudunuri, S. B., Anaya, J. & Dutta, A. tRFdb: a database for transfer RNA fragments. *Nucleic Acids Res* **43**, D141-145 (2015). <https://doi.org:10.1093/nar/gku1138>
- 153 Paldor, I. *et al.* Cerebrospinal fluid and blood profiles of transfer RNA fragments show age, sex, and Parkinson's disease-related changes. *J Neurochem* **164**, 671-683 (2023). <https://doi.org:10.1111/jnc.15723>
- 154 Marshall, L. J., Bailey, J., Cassotta, M., Herrmann, K. & Pistollato, F. Poor Translatability of Biomedical Research Using Animals - A Narrative Review. *Altern Lab Anim* **51**, 102-135 (2023). <https://doi.org:10.1177/02611929231157756>
- 155 Trabzuni, D. *et al.* Quality control parameters on a large dataset of regionally dissected human control brains for whole genome expression studies. *J Neurochem* **119**, 275-282 (2011). <https://doi.org:10.1111/j.1471-4159.2011.07432.x>
- 156 Grizzle, W. E., Bell, W. C. & Sexton, K. C. Issues in collecting, processing and storing human tissues and associated information to support biomedical research. *Cancer Biomark* **9**, 531-549 (2010). <https://doi.org:10.3233/CBM-2011-0183>
- 157 Koks, S. *et al.* Mouse models of ageing and their relevance to disease. *Mech Ageing Dev* **160**, 41-53 (2016). <https://doi.org:10.1016/j.mad.2016.10.001>
- 158 Hagg, S. & Jylhava, J. Sex differences in biological aging with a focus on human studies. *Elife* **10** (2021). <https://doi.org:10.7554/eLife.63425>

9 Appendix

9.1 Appendix A

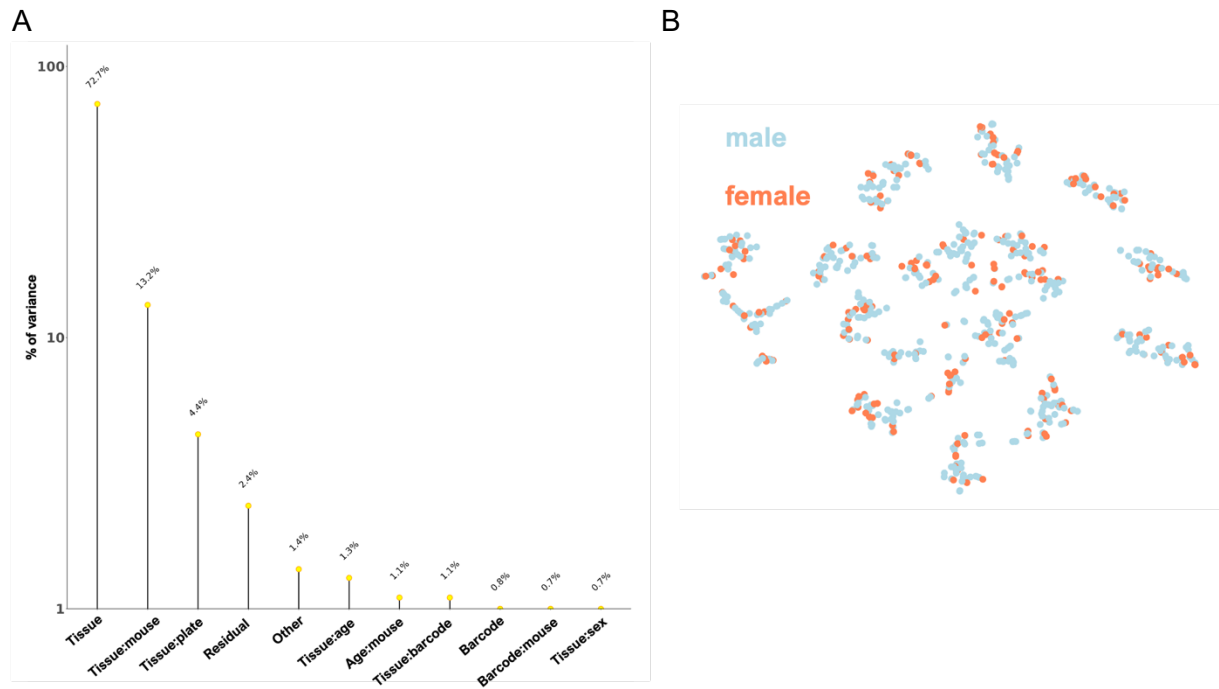


Supplemental Figure 1: Share of read distribution per tissue of detected ncRNAs per RNA class, color coded by RNA class¹.



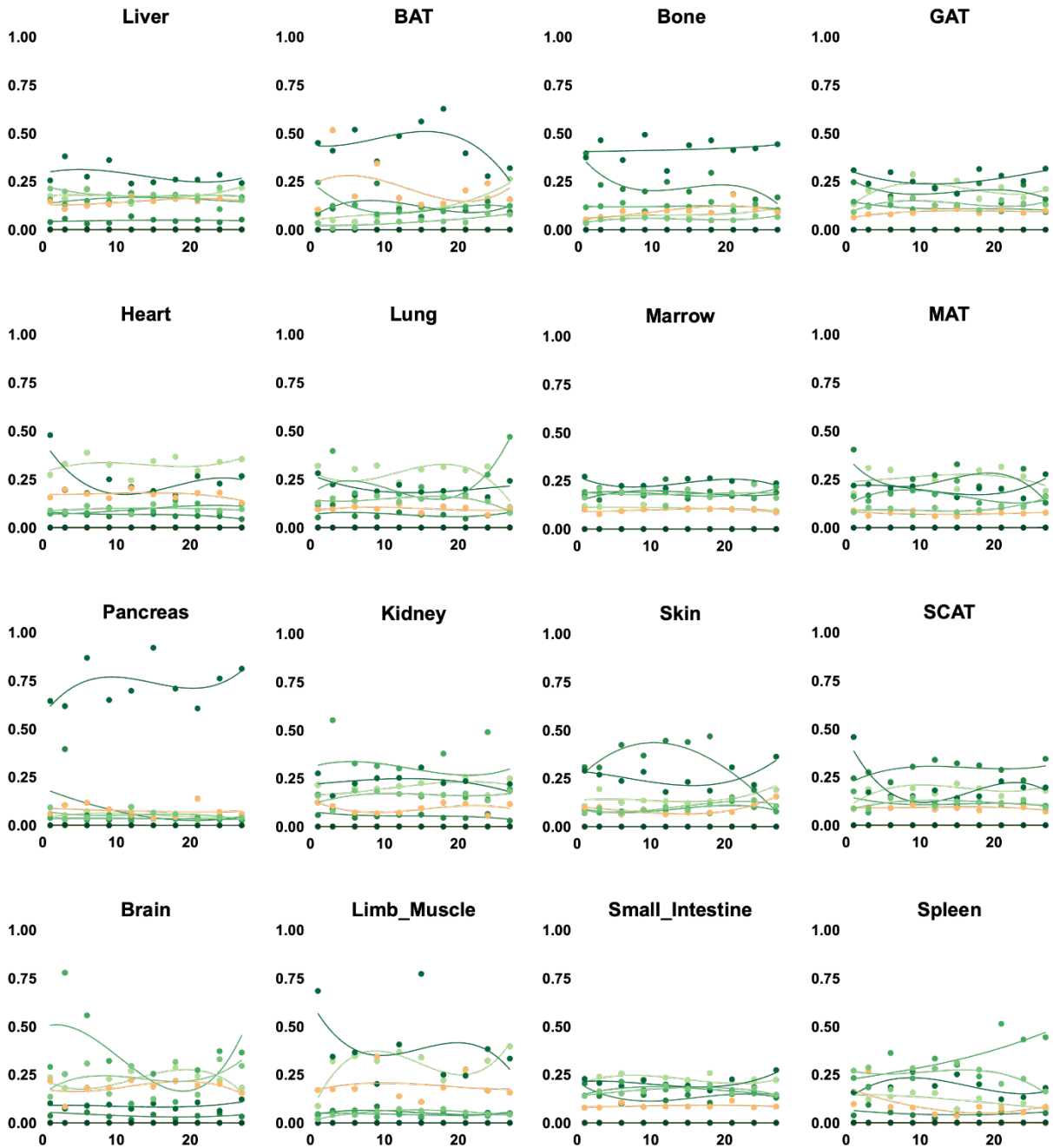
Supplemental Figure 2: Mapped read length analysis.

(A) Reference sequence length versus share of length covered by mapped reads, colored by RNA class for all raw reads in aging cohort, (B) Reference sequence length versus percentage of longest continuous mapped read calculated by connected reads for all ncRNAs detected in raw reads¹.



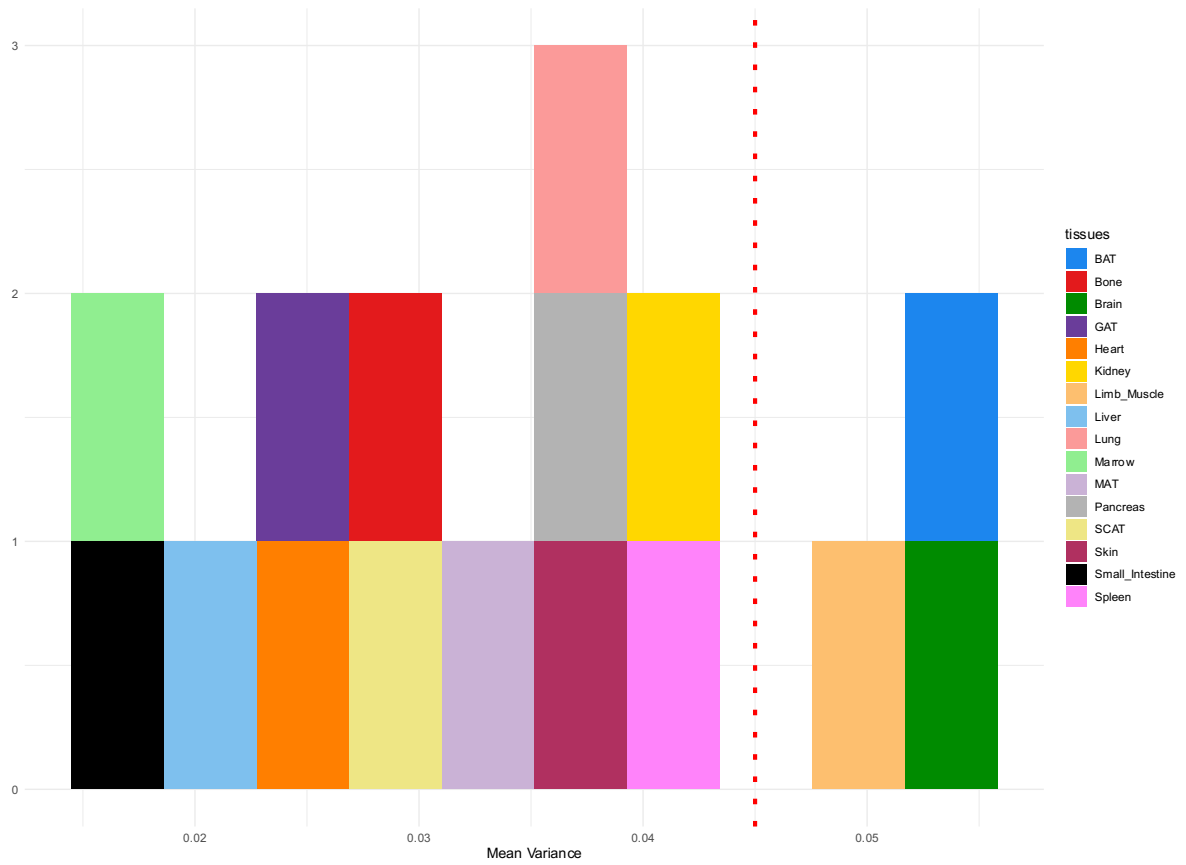
Supplemental Figure 3: Biological and technical parameters as drivers of variance.

(A) PVCA analysis determining tissue identity as major driver of variance over technical parameters (like barcode and plate) and other biological parameters (like sex), (B) tSNE clustering colored by sex, male in light blue and female in light red¹.

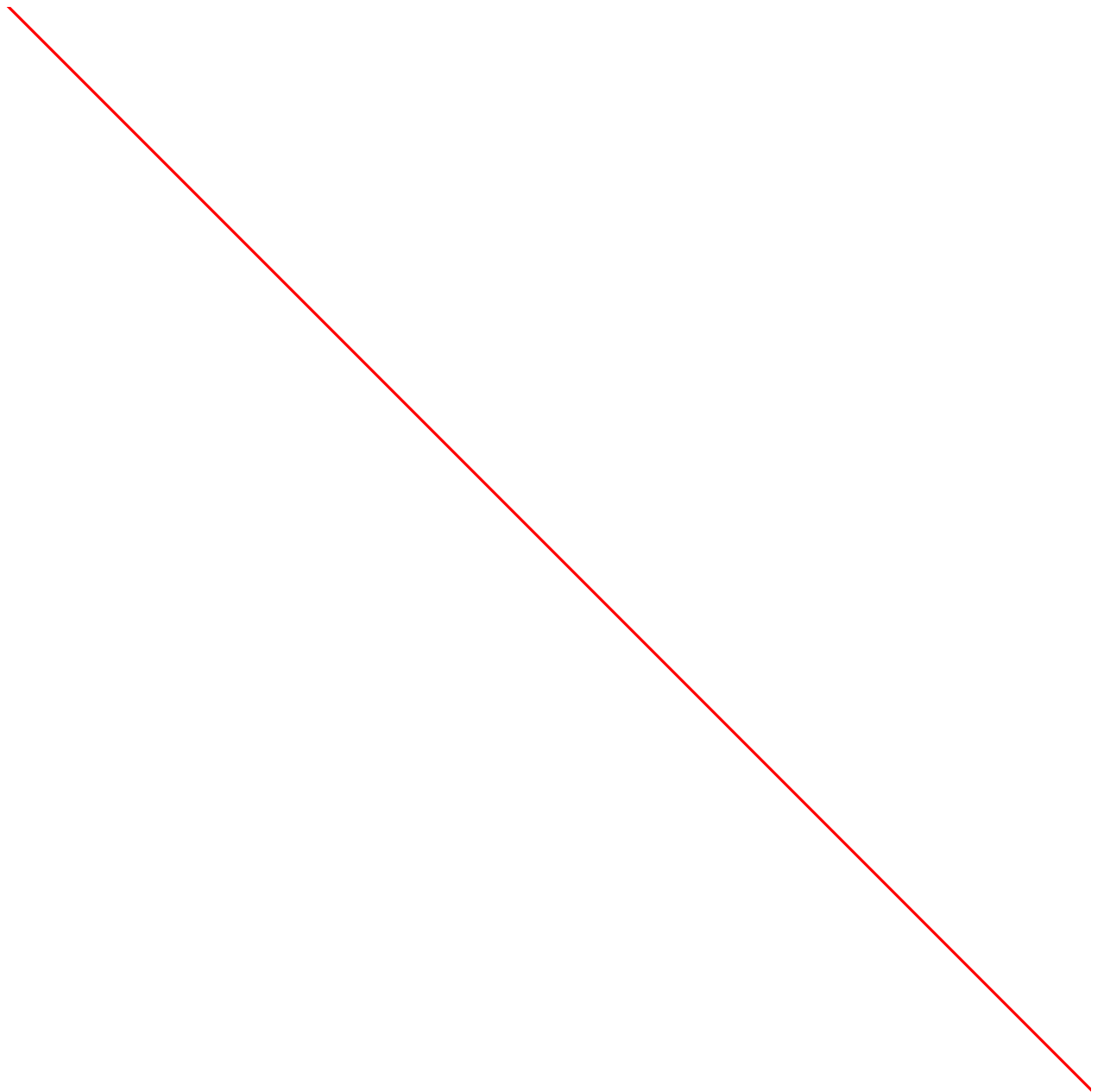


Supplemental Figure 4: Share counts per ncRNA class for each individual tissue after abundance filtering.

Mean share of ncRNA counts per tissue per timepoint grouped by ncRNA class after filtering for abundant ncRNAs in each tissue for all 16 tissues¹.

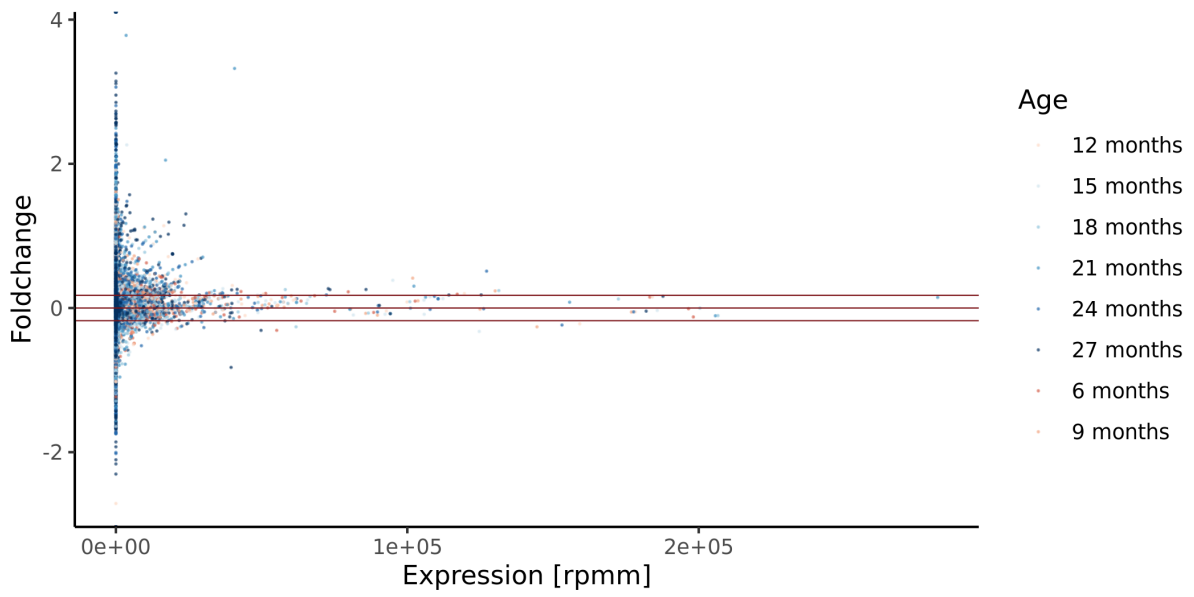


Supplemental Figure 5: Mean variance of ncRNA count shares per RNA class for each tissue¹.

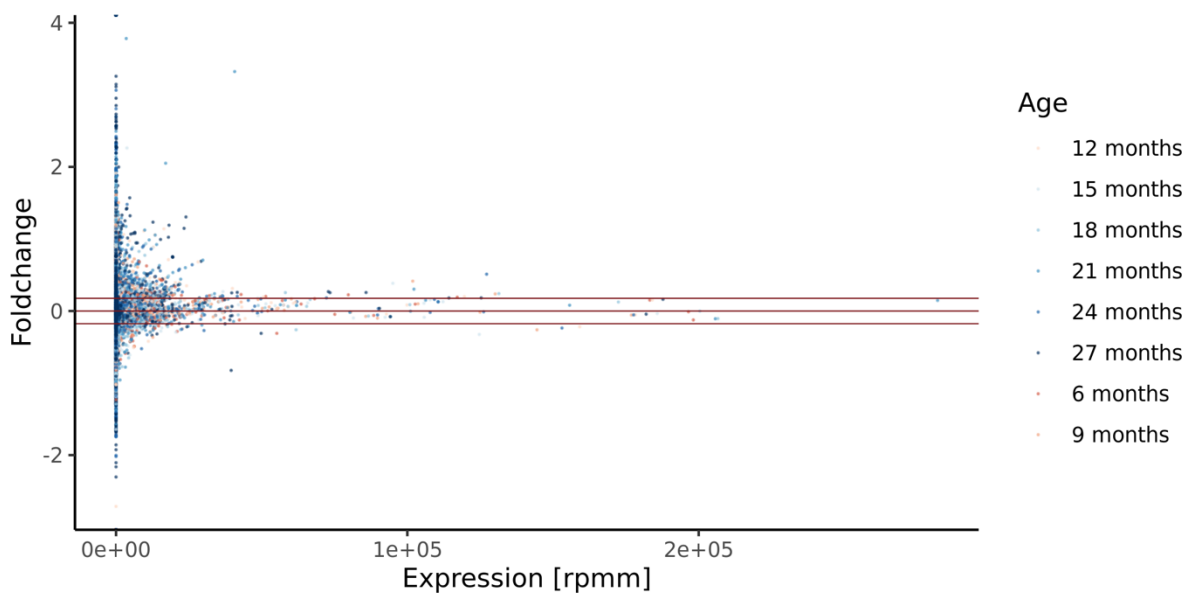


Supplemental Figure 6: Volcano plots of FC versus *P*-values for all tissues.

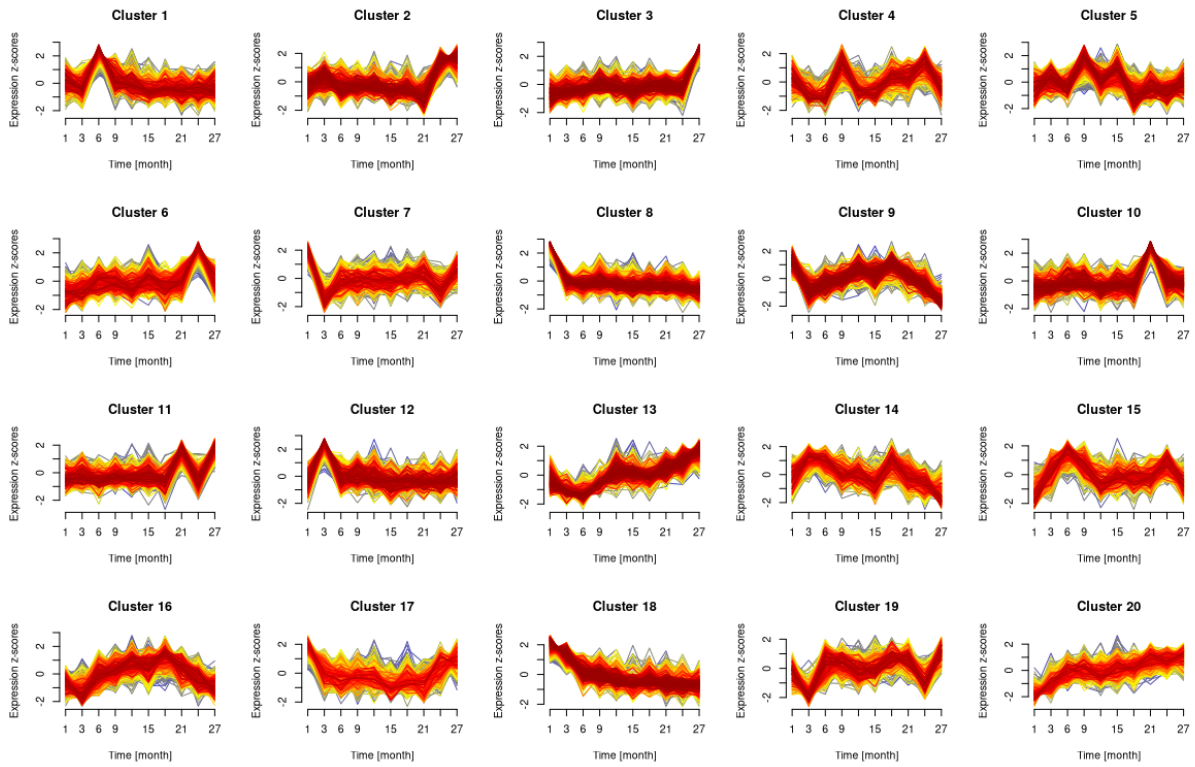
Foldchange calculated for 3 months versus all later ages per tissue for all locally expressed miRNAs plotted as $\log_2(\text{FC})$ versus $-\log_{10}(P\text{-value})$, colored by age¹.



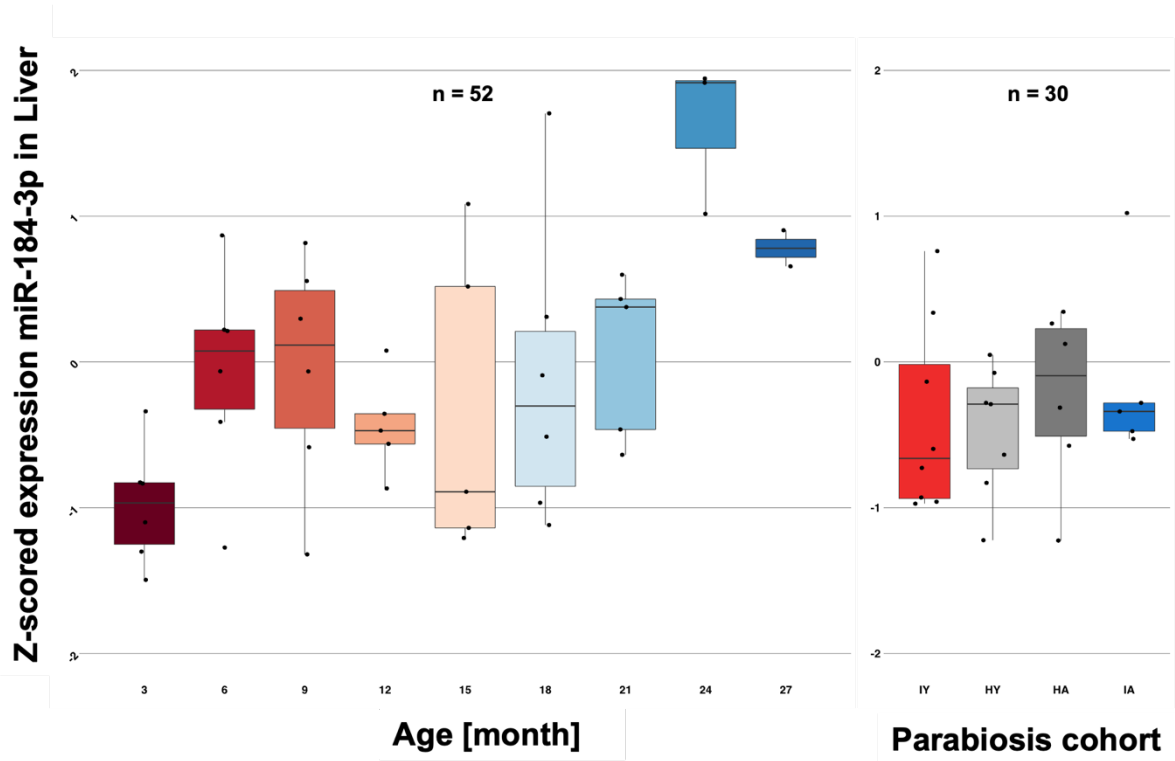
Supplemental Figure 7: Mean expression of all miRNA features after local filtering per time point per tissue versus foldchange calculated versus three months of age¹.



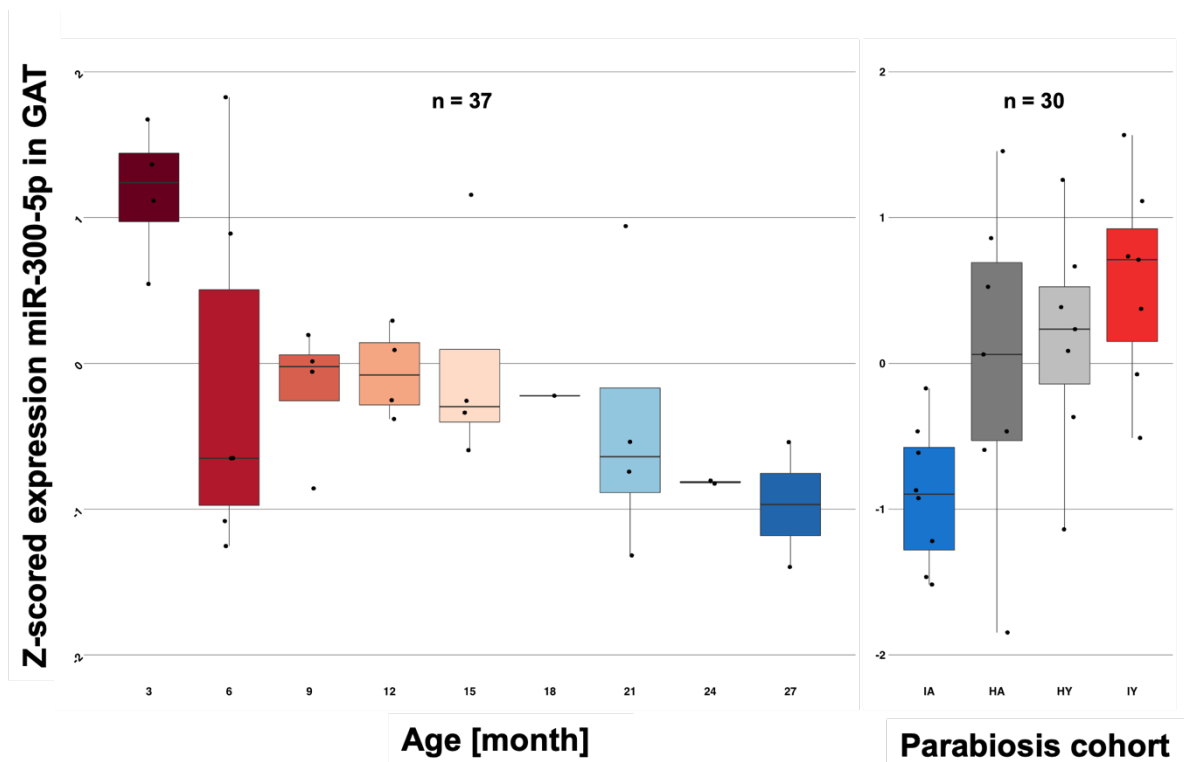
Supplemental Figure 8: Mean expression of all non-coding RNA features after local filtering per time point per tissue versus foldchange calculated versus three months of age¹.



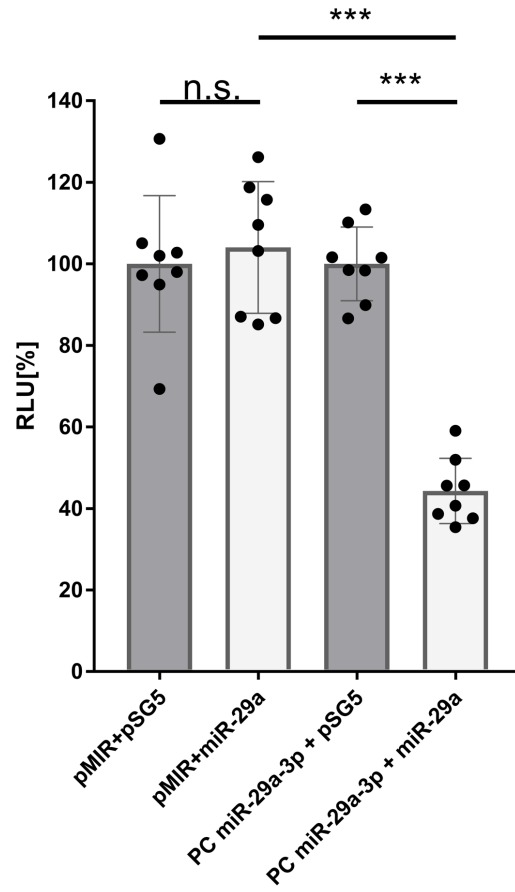
Supplemental Figure 9: Fuzzy c-means clustering in 20 clusters of all z-scored miRNA trajectories for all miRNAs expressed in each tissue¹.



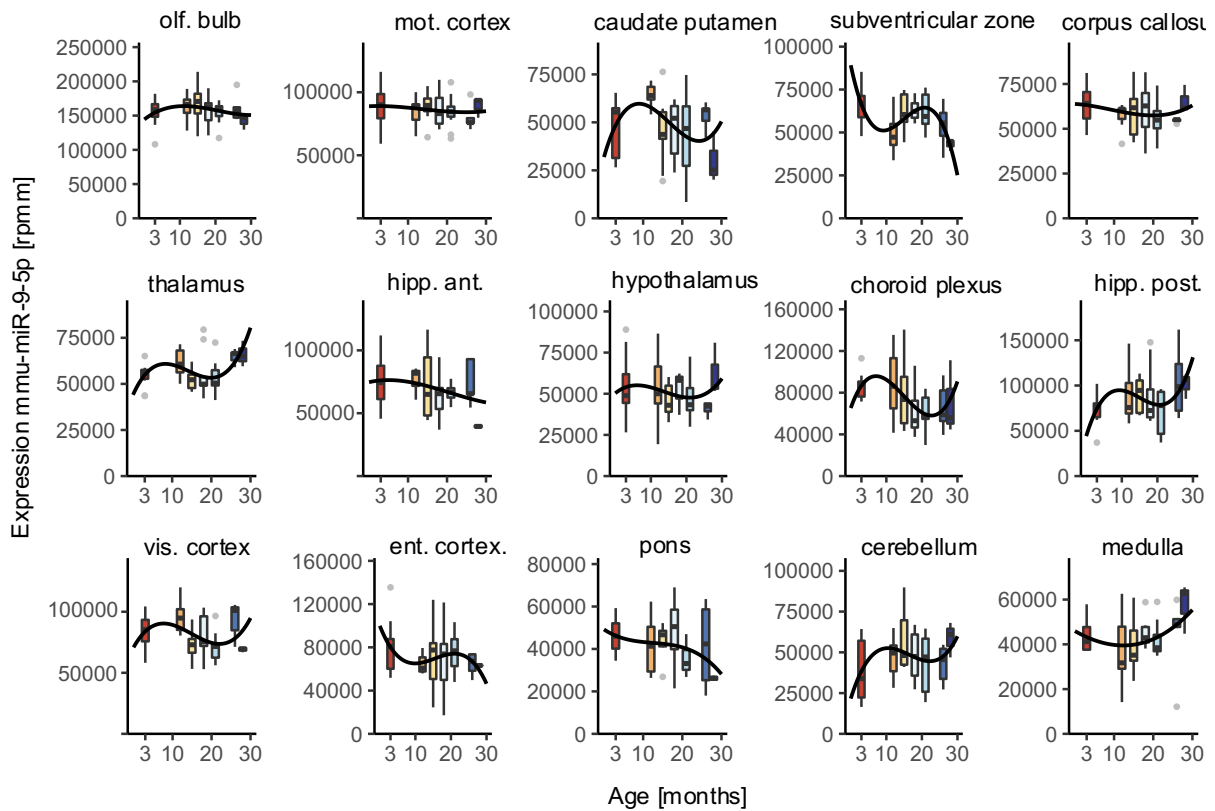
Supplemental Figure 10: Z-scored increasing expression patterns of miR-184-3p in liver for aging cohort and parabiosis cohort¹.



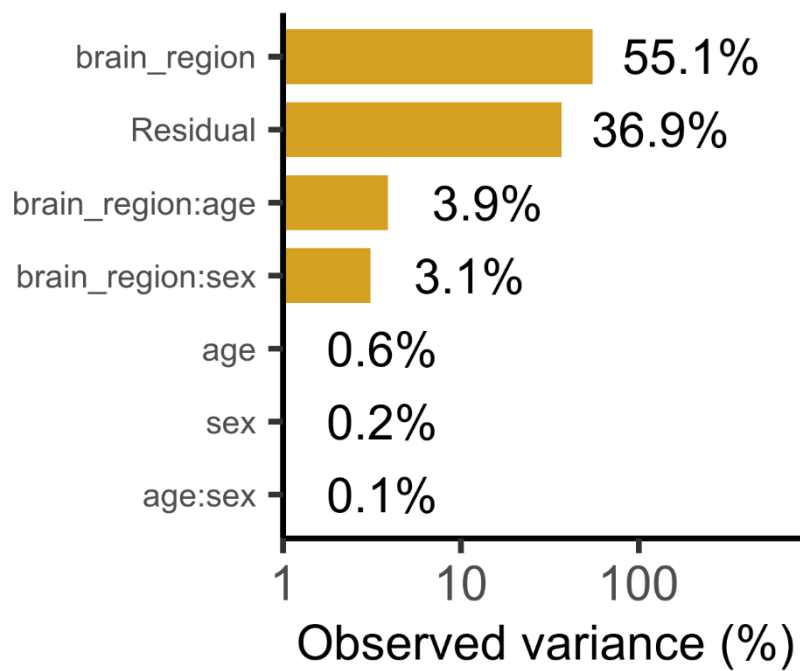
Supplemental Figure 11: Z-scored decreasing expression patterns of miR-300-5p in GAT for aging cohort and parabiosis cohort¹.



Supplemental Figure 12: Positive control Luciferase assay¹.



Supplemental Figure 13: Boxplot of expression of miR-9-5p over time in reads per mapped million versus age in month.



Supplemental Figure 14: PVCA brain aging cohort over all samples with both genders.

9.2 Appendix B

Table 1: Sample metadata table aging and parabiosis cohort¹.

Metadata for all samples analyzed in the aging (TMS) and parabiosis cohort

sample identifier	sample name	tissue	organism	strain	age	sex	cohort
BAT_19-m-27	BAT_19	BAT	Mus musculus	C57BL/6JN	27	m	TMS
Heart_4-m-21	Heart_04	Heart	Mus musculus	C57BL/6JN	21	m	TMS
Heart_9-f-3	Heart_09	Heart	Mus musculus	C57BL/6JN	3	f	TMS
Small_Intestine_30-m-12	Small_Intestine_30	Small_Intestine	Mus musculus	C57BL/6JN	12	m	TMS
Kidney_43-f-18	Kidney_43	Kidney	Mus musculus	C57BL/6JN	18	f	TMS
Kidney_16-f-18	Kidney_16	Kidney	Mus musculus	C57BL/6JN	18	f	TMS
Brain_1-m-21	Brain_01	Brain	Mus musculus	C57BL/6JN	21	m	TMS
Kidney_22-m-6	Kidney_22	Kidney	Mus musculus	C57BL/6JN	6	m	TMS
Liver_23-m-9	Liver_23	Liver	Mus musculus	C57BL/6JN	9	m	TMS
Liver_12-m-24	Liver_12	Liver	Mus musculus	C57BL/6JN	24	m	TMS
Brain_2-m-1	Brain_02	Brain	Mus musculus	C57BL/6JN	1	m	TMS
Lung_10-f-18	Lung_10	Lung	Mus musculus	C57BL/6JN	18	f	TMS
Heart_20-f-9	Heart_20	Heart	Mus musculus	C57BL/6JN	9	f	TMS
Kidney_18-m-9	Kidney_18	Kidney	Mus musculus	C57BL/6JN	9	m	TMS
Lung_23-m-3	Lung_23	Lung	Mus musculus	C57BL/6JN	3	m	TMS
Bone_22-m-21	Bone_22	Bone	Mus musculus	C57BL/6JN	21	m	TMS
MAT_28-f-12	MAT_28	MAT	Mus musculus	C57BL/6JN	12	f	TMS
Bone_49-m-9	Bone_49	Bone	Mus musculus	C57BL/6JN	9	m	TMS
Limb_Muscle_15-m-3	Limb_Muscle_15	Limb_Muscle	Mus musculus	C57BL/6JN	3	m	TMS
Marrow_16-m-15	Marrow_16	Marrow	Mus musculus	C57BL/6JN	15	m	TMS
Small_Intestine_15-m-24	Small_Intestine_15	Small_Intestine	Mus musculus	C57BL/6JN	24	m	TMS
Brain_24-f-9	Brain_24	Brain	Mus musculus	C57BL/6JN	9	f	TMS
Skin_24-m-21	Skin_24	Skin	Mus musculus	C57BL/6JN	21	m	TMS
SCAT_30-m-18	SCAT_30	SCAT	Mus musculus	C57BL/6JN	18	m	TMS
BAT_43-m-21	BAT_43	BAT	Mus musculus	C57BL/6JN	21	m	TMS
BAT_5-m-27	BAT_05	BAT	Mus musculus	C57BL/6JN	27	m	TMS
Bone_18-f-3	Bone_18	Bone	Mus musculus	C57BL/6JN	3	f	TMS
Skin_5-f-12	Skin_05	Skin	Mus musculus	C57BL/6JN	12	f	TMS
Spleen_3-m-24	Spleen_03	Spleen	Mus musculus	C57BL/6JN	24	m	TMS
GAT_24-f-15	GAT_24	GAT	Mus musculus	C57BL/6JN	15	f	TMS
Small_Intestine_2-f-21	Small_Intestine_02	Small_Intestine	Mus musculus	C57BL/6JN	21	f	TMS
SCAT_2-f-9	SCAT_02	SCAT	Mus musculus	C57BL/6JN	9	f	TMS
Marrow_2-f-21	Marrow_02	Marrow	Mus musculus	C57BL/6JN	21	f	TMS

Brain_53-m-9	Brain_53	Brain	Mus musculus	C57BL/6JN	9	m	TMS
Liver_17-m-21	Liver_17	Liver	Mus musculus	C57BL/6JN	21	m	TMS
Limb_Muscle_55-m-21	Limb_Muscle_55	Limb_Muscle	Mus musculus	C57BL/6JN	21	m	TMS
Kidney_46-f-1	Kidney_46	Kidney	Mus musculus	C57BL/6JN	1	f	TMS
Heart_28-m-1	Heart_28	Heart	Mus musculus	C57BL/6JN	1	m	TMS
MAT_8-m-3	MAT_08	MAT	Mus musculus	C57BL/6JN	3	m	TMS
Small_Intestine_1-m-18	Small_Intestine_01	Small_Intestine	Mus musculus	C57BL/6JN	18	m	TMS
SCAT_1-m-24	SCAT_01	SCAT	Mus musculus	C57BL/6JN	24	m	TMS
BAT_6-m-24	BAT_06	BAT	Mus musculus	C57BL/6JN	24	m	TMS
Liver_18-m-27	Liver_18	Liver	Mus musculus	C57BL/6JN	27	m	TMS
GAT_25-m-12	GAT_25	GAT	Mus musculus	C57BL/6JN	12	m	TMS
Pancreas_2-m-3	Pancreas_02	Pancreas	Mus musculus	C57BL/6JN	3	m	TMS
Spleen_1-m-3	Spleen_01	Spleen	Mus musculus	C57BL/6JN	3	m	TMS
Bone_19-m-9	Bone_19	Bone	Mus musculus	C57BL/6JN	9	m	TMS
Limb_Muscle_56-m-18	Limb_Muscle_56	Limb_Muscle	Mus musculus	C57BL/6JN	18	m	TMS
Lung_9-m-24	Lung_09	Lung	Mus musculus	C57BL/6JN	24	m	TMS
Heart_29-m-12	Heart_29	Heart	Mus musculus	C57BL/6JN	12	m	TMS
MAT_9-f-18	MAT_09	MAT	Mus musculus	C57BL/6JN	18	f	TMS
Skin_6-m-24	Skin_06	Skin	Mus musculus	C57BL/6JN	24	m	TMS
Small_Intestine_7-f-3	Small_Intestine_07	Small_Intestine	Mus musculus	C57BL/6JN	3	f	TMS
Spleen_11-f-3	Spleen_11	Spleen	Mus musculus	C57BL/6JN	3	f	TMS
Skin_14-f-18	Skin_14	Skin	Mus musculus	C57BL/6JN	18	f	TMS
BAT_8-f-1	BAT_08	BAT	Mus musculus	C57BL/6JN	1	f	TMS
Bone_6-m-12	Bone_06	Bone	Mus musculus	C57BL/6JN	12	m	TMS
Brain_3-m-1	Brain_03	Brain	Mus musculus	C57BL/6JN	1	m	TMS
GAT_8-m-1	GAT_08	GAT	Mus musculus	C57BL/6JN	1	m	TMS
Liver_29-f-6	Liver_29	Liver	Mus musculus	C57BL/6JN	6	f	TMS
Limb_Muscle_5-f-6	Limb_Muscle_05	Limb_Muscle	Mus musculus	C57BL/6JN	6	f	TMS
Marrow_1-m-27	Marrow_01	Marrow	Mus musculus	C57BL/6JN	27	m	TMS
Heart_8-m-1	Heart_08	Heart	Mus musculus	C57BL/6JN	1	m	TMS
Lung_12-m-9	Lung_12	Lung	Mus musculus	C57BL/6JN	9	m	TMS
Pancreas_22-f-9	Pancreas_22	Pancreas	Mus musculus	C57BL/6JN	9	f	TMS
MAT_5-f-3	MAT_05	MAT	Mus musculus	C57BL/6JN	3	f	TMS
SCAT_8-m-6	SCAT_08	SCAT	Mus musculus	C57BL/6JN	6	m	TMS
Marrow_8-m-6	Marrow_08	Marrow	Mus musculus	C57BL/6JN	6	m	TMS
MAT_10-m-6	MAT_10	MAT	Mus musculus	C57BL/6JN	6	m	TMS
Pancreas_21-m-15	Pancreas_21	Pancreas	Mus musculus	C57BL/6JN	15	m	TMS

BAT_9-m-9	BAT_09	BAT	Mus musculus	C57BL/6JN	9	m	TMS
Small_Intestine_8-m-15	Small_Intestine_08	Small Intestine	Mus musculus	C57BL/6JN	15	m	TMS
Spleen_10-m-27	Spleen_10	Spleen	Mus musculus	C57BL/6JN	27	m	TMS
Bone_5-m-3	Bone_05	Bone	Mus musculus	C57BL/6JN	3	m	TMS
GAT_5-m-9	GAT_05	GAT	Mus musculus	C57BL/6JN	9	m	TMS
Brain_5-m-9	Brain_05	Brain	Mus musculus	C57BL/6JN	9	m	TMS
Heart_7-m-24	Heart_07	Heart	Mus musculus	C57BL/6JN	24	m	TMS
Liver_28-m-3	Liver_28	Liver	Mus musculus	C57BL/6JN	3	m	TMS
Skin_12-m-15	Skin_12	Skin	Mus musculus	C57BL/6JN	15	m	TMS
Kidney_37-m-24	Kidney_37	Kidney	Mus musculus	C57BL/6JN	24	m	TMS
Lung_13-m-12	Lung_13	Lung	Mus musculus	C57BL/6JN	12	m	TMS
Kidney_20-m-27	Kidney_20	Kidney	Mus musculus	C57BL/6JN	27	m	TMS
Limb_Muscle_13-m-1	Limb_Muscle_13	Limb_Muscle	Mus musculus	C57BL/6JN	1	m	TMS
Marrow_18-m-9	Marrow_18	Marrow	Mus musculus	C57BL/6JN	9	m	TMS
BAT_35-m-18	BAT_35	BAT	Mus musculus	C57BL/6JN	18	m	TMS
MAT_25-f-18	MAT_25	MAT	Mus musculus	C57BL/6JN	18	f	TMS
Pancreas_29-m-1	Pancreas_29	Pancreas	Mus musculus	C57BL/6JN	1	m	TMS
SCAT_28-m-27	SCAT_28	SCAT	Mus musculus	C57BL/6JN	27	m	TMS
Lung_21-f-1	Lung_21	Lung	Mus musculus	C57BL/6JN	1	f	TMS
Skin_27-f-15	Skin_27	Skin	Mus musculus	C57BL/6JN	15	f	TMS
MAT_45-f-21	MAT_45	MAT	Mus musculus	C57BL/6JN	21	f	TMS
Liver_14-m-3	Liver_14	Liver	Mus musculus	C57BL/6JN	3	m	TMS
Small_Intestine_13-m-1	Small_Intestine_13	Small Intestine	Mus musculus	C57BL/6JN	1	m	TMS
Spleen_16-m-6	Spleen_16	Spleen	Mus musculus	C57BL/6JN	6	m	TMS
GAT_33-m-6	GAT_33	GAT	Mus musculus	C57BL/6JN	6	m	TMS
Heart_19-f-1	Heart_19	Heart	Mus musculus	C57BL/6JN	1	f	TMS
Kidney_19-f-15	Kidney_19	Kidney	Mus musculus	C57BL/6JN	15	f	TMS
Limb_Muscle_14-m-1	Limb_Muscle_14	Limb_Muscle	Mus musculus	C57BL/6JN	1	m	TMS
Lung_22-m-21	Lung_22	Lung	Mus musculus	C57BL/6JN	21	m	TMS
BAT_38-f-15	BAT_38	BAT	Mus musculus	C57BL/6JN	15	f	TMS
Marrow_17-m-27	Marrow_17	Marrow	Mus musculus	C57BL/6JN	27	m	TMS
MAT_26-f-9	MAT_26	MAT	Mus musculus	C57BL/6JN	9	f	TMS
Pancreas_28-f-18	Pancreas_28	Pancreas	Mus musculus	C57BL/6JN	18	f	TMS
Liver_10-m-21	Liver_10	Liver	Mus musculus	C57BL/6JN	21	m	TMS
SCAT_26-f-6	SCAT_26	SCAT	Mus musculus	C57BL/6JN	6	f	TMS
Bone_24-m-15	Bone_24	Bone	Mus musculus	C57BL/6JN	15	m	TMS
Small_Intestine_14-f-1	Small_Intestine_14	Small Intestine	Mus musculus	C57BL/6JN	1	f	TMS

Skin_26-m-18	Skin_26	Skin	Mus musculus	C57BL/6JN	18	m	TMS
Spleen_15-m-6	Spleen_15	Spleen	Mus musculus	C57BL/6JN	6	m	TMS
Brain_26-m-27	Brain_26	Brain	Mus musculus	C57BL/6JN	27	m	TMS
Heart_18-f-18	Heart_18	Heart	Mus musculus	C57BL/6JN	18	f	TMS
MAT_29-m-9	MAT_29	MAT	Mus musculus	C57BL/6JN	9	m	TMS
Bone_37-f-21	Bone_37	Bone	Mus musculus	C57BL/6JN	21	f	TMS
Small_Intestine_16-f-15	Small_Intestine_16	Small_Intestine	Mus musculus	C57BL/6JN	15	f	TMS
Lung_24-m-27	Lung_24	Lung	Mus musculus	C57BL/6JN	27	m	TMS
Marrow_15-f-1	Marrow_15	Marrow	Mus musculus	C57BL/6JN	1	f	TMS
Pancreas_26-m-21	Pancreas_26	Pancreas	Mus musculus	C57BL/6JN	21	m	TMS
Heart_21-m-24	Heart_21	Heart	Mus musculus	C57BL/6JN	24	m	TMS
Kidney_15-m-24	Kidney_15	Kidney	Mus musculus	C57BL/6JN	24	m	TMS
Liver_9-f-15	Liver_09	Liver	Mus musculus	C57BL/6JN	15	f	TMS
BAT_45-m-18	BAT_45	BAT	Mus musculus	C57BL/6JN	18	m	TMS
Limb_Muscle_16-m-27	Limb_Muscle_16	Limb_Muscle	Mus musculus	C57BL/6JN	27	m	TMS
Spleen_14-f-6	Spleen_14	Spleen	Mus musculus	C57BL/6JN	6	f	TMS
Skin_23-m-1	Skin_23	Skin	Mus musculus	C57BL/6JN	1	m	TMS
Brain_23-m-24	Brain_23	Brain	Mus musculus	C57BL/6JN	24	m	TMS
GAT_35-m-21	GAT_35	GAT	Mus musculus	C57BL/6JN	21	m	TMS
MAT_33-m-27	MAT_33	MAT	Mus musculus	C57BL/6JN	27	m	TMS
Lung_25-m-21	Lung_25	Lung	Mus musculus	C57BL/6JN	21	m	TMS
Pancreas_25-m-3	Pancreas_25	Pancreas	Mus musculus	C57BL/6JN	3	m	TMS
SCAT_39-m-18	SCAT_39	SCAT	Mus musculus	C57BL/6JN	18	m	TMS
Skin_22-m-3	Skin_22	Skin	Mus musculus	C57BL/6JN	3	m	TMS
Bone_21-m-24	Bone_21	Bone	Mus musculus	C57BL/6JN	24	m	TMS
BAT_46-f-18	BAT_46	BAT	Mus musculus	C57BL/6JN	18	f	TMS
Brain_22-m-15	Brain_22	Brain	Mus musculus	C57BL/6JN	15	m	TMS
Kidney_14-m-27	Kidney_14	Kidney	Mus musculus	C57BL/6JN	27	m	TMS
GAT_31-m-1	GAT_31	GAT	Mus musculus	C57BL/6JN	1	m	TMS
Liver_8-f-3	Liver_08	Liver	Mus musculus	C57BL/6JN	3	f	TMS
Marrow_14-m-12	Marrow_14	Marrow	Mus musculus	C57BL/6JN	12	m	TMS
Small_Intestine_17-m-6	Small_Intestine_17	Small_Intestine	Mus musculus	C57BL/6JN	6	m	TMS
Heart_30-m-21	Heart_30	Heart	Mus musculus	C57BL/6JN	21	m	TMS
Limb_Muscle_17-m-21	Limb_Muscle_17	Limb_Muscle	Mus musculus	C57BL/6JN	21	m	TMS
Bone_20-m-18	Bone_20	Bone	Mus musculus	C57BL/6JN	18	m	TMS
Brain_11-m-21	Brain_11	Brain	Mus musculus	C57BL/6JN	21	m	TMS
Heart_11-m-18	Heart_11	Heart	Mus musculus	C57BL/6JN	18	m	TMS

GAT_13-f-6	GAT_13	GAT	Mus musculus	C57BL/6JN	6	f	TMS
Lung_8-f-9	Lung_08	Lung	Mus musculus	C57BL/6JN	9	f	TMS
Pancreas_51-m-9	Pancreas_51	Pancreas	Mus musculus	C57BL/6JN	9	m	TMS
SCAT_18-m-24	SCAT_18	SCAT	Mus musculus	C57BL/6JN	24	m	TMS
Skin_18-m-3	Skin_18	Skin	Mus musculus	C57BL/6JN	3	m	TMS
Small_Intestine_23-m-15	Small_Intestine_23	Small_Intestine	Mus musculus	C57BL/6JN	15	m	TMS
Kidney_1-f-6	Kidney_01	Kidney	Mus musculus	C57BL/6JN	6	f	TMS
Spleen_31-m-21	Spleen_31	Spleen	Mus musculus	C57BL/6JN	21	m	TMS
Marrow_41-f-15	Marrow_41	Marrow	Mus musculus	C57BL/6JN	15	f	TMS
MAT_18-m-6	MAT_18	MAT	Mus musculus	C57BL/6JN	6	m	TMS
Limb_Muscle_12-f-9	Limb_Muscle_12	Limb_Muscle	Mus musculus	C57BL/6JN	9	f	TMS
Liver_3-m-9	Liver_05	Liver	Mus musculus	C57BL/6JN	9	m	TMS
Lung_1-f-9	Lung_01	Lung	Mus musculus	C57BL/6JN	9	f	TMS
Bone_11-m-24	Bone_11	Bone	Mus musculus	C57BL/6JN	24	m	TMS
Kidney_3-m-24	Kidney_03	Kidney	Mus musculus	C57BL/6JN	24	m	TMS
GAT_17-m-3	GAT_17	GAT	Mus musculus	C57BL/6JN	3	m	TMS
Bone_15-m-15	Bone_15	Bone	Mus musculus	C57BL/6JN	15	m	TMS
Marrow_42-m-27	Marrow_42	Marrow	Mus musculus	C57BL/6JN	27	m	TMS
Pancreas_50-f-21	Pancreas_50	Pancreas	Mus musculus	C57BL/6JN	21	f	TMS
SCAT_17-m-15	SCAT_17	SCAT	Mus musculus	C57BL/6JN	15	m	TMS
Limb_Muscle_11-m-3	Limb_Muscle_11	Limb_Muscle	Mus musculus	C57BL/6JN	3	m	TMS
Small_Intestine_22-m-18	Small_Intestine_22	Small_Intestine	Mus musculus	C57BL/6JN	18	m	TMS
Skin_20-m-3	Skin_20	Skin	Mus musculus	C57BL/6JN	3	m	TMS
Spleen_32-m-18	Spleen_32	Spleen	Mus musculus	C57BL/6JN	18	m	TMS
Liver_6-f-3	Liver_06	Liver	Mus musculus	C57BL/6JN	3	f	TMS
Heart_10-m-21	Heart_10	Heart	Mus musculus	C57BL/6JN	21	m	TMS
Heart_56-m-6	Heart_56	Heart	Mus musculus	C57BL/6JN	6	m	TMS
SCAT_55-f-15	SCAT_55	SCAT	Mus musculus	C57BL/6JN	15	f	TMS
Skin_47-m-15	Skin_47	Skin	Mus musculus	C57BL/6JN	15	m	TMS
Spleen_49-f-21	Spleen_49	Spleen	Mus musculus	C57BL/6JN	21	f	TMS
Marrow_54-m-24	Marrow_54	Marrow	Mus musculus	C57BL/6JN	24	m	TMS
Lung_49-m-18	Lung_49	Lung	Mus musculus	C57BL/6JN	18	m	TMS
GAT_36-f-3	GAT_36	GAT	Mus musculus	C57BL/6JN	3	f	TMS
Brain_16-m-1	Brain_16	Brain	Mus musculus	C57BL/6JN	1	m	TMS
Bone_51-m-12	Bone_51	Bone	Mus musculus	C57BL/6JN	12	m	TMS
Kidney_32-f-3	Kidney_32	Kidney	Mus musculus	C57BL/6JN	3	f	TMS
Liver_51-m-1	Liver_51	Liver	Mus musculus	C57BL/6JN	1	m	TMS

Limb_Muscle_47-m-1	Limb_Muscle_47	Limb_Muscle	Mus musculus	C57BL/6JN	1	m	TMS
Limb_Muscle_46-m-9	Limb_Muscle_46	Limb_Muscle	Mus musculus	C57BL/6JN	9	m	TMS
Heart_55-m-12	Heart_55	Heart	Mus musculus	C57BL/6JN	12	m	TMS
Brain_17-m-3	Brain_17	Brain	Mus musculus	C57BL/6JN	3	m	TMS
BAT_30-m-27	BAT_30	BAT	Mus musculus	C57BL/6JN	27	m	TMS
Marrow_53-m-3	Marrow_53	Marrow	Mus musculus	C57BL/6JN	3	m	TMS
MAT_49-f-12	MAT_49	MAT	Mus musculus	C57BL/6JN	12	f	TMS
Liver_52-m-12	Liver_52	Liver	Mus musculus	C57BL/6JN	12	m	TMS
Small_Intestine_51-m-9	Small_Intestine_51	Small_Intestine	Mus musculus	C57BL/6JN	9	m	TMS
Pancreas_46-f-3	Pancreas_46	Pancreas	Mus musculus	C57BL/6JN	3	f	TMS
Lung_50-m-24	Lung_50	Lung	Mus musculus	C57BL/6JN	24	m	TMS
Kidney_35-f-21	Kidney_35	Kidney	Mus musculus	C57BL/6JN	21	f	TMS
GAT_49-f-3	GAT_49	GAT	Mus musculus	C57BL/6JN	3	f	TMS
Bone_53-m-3	Bone_53	Bone	Mus musculus	C57BL/6JN	3	m	TMS
Spleen_50-m-12	Spleen_50	Spleen	Mus musculus	C57BL/6JN	12	m	TMS
SCAT_53-m-9	SCAT_53	SCAT	Mus musculus	C57BL/6JN	9	m	TMS
Brain_44-m-18	Brain_44	Brain	Mus musculus	C57BL/6JN	18	m	TMS
Liver_50-m-6	Liver_50	Liver	Mus musculus	C57BL/6JN	6	m	TMS
Bone_46-m-1	Bone_46	Bone	Mus musculus	C57BL/6JN	1	m	TMS
Spleen_44-m-21	Spleen_44	Spleen	Mus musculus	C57BL/6JN	21	m	TMS
Spleen_46-m-15	Spleen_46	Spleen	Mus musculus	C57BL/6JN	15	m	TMS
Bone_42-f-3	Bone_42	Bone	Mus musculus	C57BL/6JN	3	f	TMS
Marrow_48-f-18	Marrow_48	Marrow	Mus musculus	C57BL/6JN	18	f	TMS
Small_Intestine_50-f-6	Small_Intestine_50	Small_Intestine	Mus musculus	C57BL/6JN	6	f	TMS
Lung_44-m-15	Lung_44	Lung	Mus musculus	C57BL/6JN	15	m	TMS
Heart_48-m-18	Heart_48	Heart	Mus musculus	C57BL/6JN	18	m	TMS
Bone_44-m-27	Bone_44	Bone	Mus musculus	C57BL/6JN	27	m	TMS
Heart_40-f-1	Heart_40	Heart	Mus musculus	C57BL/6JN	1	f	TMS
Brain_43-m-21	Brain_43	Brain	Mus musculus	C57BL/6JN	21	m	TMS
Pancreas_38-m-21	Pancreas_38	Pancreas	Mus musculus	C57BL/6JN	21	m	TMS
Liver_46-m-6	Liver_46	Liver	Mus musculus	C57BL/6JN	6	m	TMS
Skin_39-m-9	Skin_39	Skin	Mus musculus	C57BL/6JN	9	m	TMS
Limb_Muscle_39-m-12	Limb_Muscle_39	Limb_Muscle	Mus musculus	C57BL/6JN	12	m	TMS
Marrow_30-f-9	Marrow_30	Marrow	Mus musculus	C57BL/6JN	9	f	TMS
Bone_33-m-21	Bone_33	Bone	Mus musculus	C57BL/6JN	21	m	TMS
Small_Intestine_39-m-1	Small_Intestine_39	Small_Intestine	Mus musculus	C57BL/6JN	1	m	TMS
Lung_36-f-1	Lung_36	Lung	Mus musculus	C57BL/6JN	1	f	TMS

Spleen_34-m-27	Spleen_34	Spleen	Musculus	C57BL/6JN	27	m	TMS
Heart_38-f-21	Heart_38	Heart	Musculus	C57BL/6JN	21	f	TMS
Bone_38-f-15	Bone_38	Bone	Musculus	C57BL/6JN	15	f	TMS
Small_Intestine_45-m-21	Small_Intestine_45	Small_Intestine	Musculus	C57BL/6JN	21	m	TMS
Marrow_43-m-6	Marrow_43	Marrow	Musculus	C57BL/6JN	6	m	TMS
Brain_35-m-3	Brain_35	Brain	Musculus	C57BL/6JN	3	m	TMS
Skin_44-m-3	Skin_44	Skin	Musculus	C57BL/6JN	3	m	TMS
Small_Intestine_49-m-21	Small_Intestine_49	Small_Intestine	Musculus	C57BL/6JN	21	m	TMS
Spleen_43-f-18	Spleen_43	Spleen	Musculus	C57BL/6JN	18	f	TMS
Spleen_45-m-15	Spleen_45	Spleen	Musculus	C57BL/6JN	15	m	TMS
Bone_48-m-12	Bone_48	Bone	Musculus	C57BL/6JN	12	m	TMS
Spleen_47-m-18	Spleen_47	Spleen	Musculus	C57BL/6JN	18	m	TMS
Heart_45-f-18	Heart_45	Heart	Musculus	C57BL/6JN	18	f	TMS
Spleen_56-m-6	Spleen_56	Spleen	Musculus	C57BL/6JN	6	m	TMS
Liver_49-m-6	Liver_49	Liver	Musculus	C57BL/6JN	6	m	TMS
Brain_45-m-6	Brain_45	Brain	Musculus	C57BL/6JN	6	m	TMS
Brain_42-f-15	Brain_42	Brain	Musculus	C57BL/6JN	15	f	TMS
Lung_45-f-3	Lung_45	Lung	Musculus	C57BL/6JN	3	f	TMS
Heart_46-f-21	Heart_46	Heart	Musculus	C57BL/6JN	21	f	TMS
Heart_43-f-9	Heart_43	Heart	Musculus	C57BL/6JN	9	f	TMS
Marrow_45-m-3	Marrow_45	Marrow	Musculus	C57BL/6JN	3	m	TMS
Small_Intestine_48-f-6	Small_Intestine_48	Small_Intestine	Musculus	C57BL/6JN	6	f	TMS
Bone_55-m-15	Bone_55	Bone	Musculus	C57BL/6JN	15	m	TMS
Brain_21-m-15	Brain_21	Brain	Musculus	C57BL/6JN	15	m	TMS
BAT_34-m-27	BAT_34	BAT	Musculus	C57BL/6JN	27	m	TMS
GAT_56-m-15	GAT_56	GAT	Musculus	C57BL/6JN	15	m	TMS
SCAT_47-f-21	SCAT_47	SCAT	Musculus	C57BL/6JN	21	f	TMS
Kidney_55-m-12	Kidney_55	Kidney	Musculus	C57BL/6JN	12	m	TMS
Spleen_54-m-21	Spleen_54	Spleen	Musculus	C57BL/6JN	21	m	TMS
Small_Intestine_55-m-15	Small_Intestine_55	Small_Intestine	Musculus	C57BL/6JN	15	m	TMS
Skin_55-f-1	Skin_55	Skin	Musculus	C57BL/6JN	1	f	TMS
Skin_7-f-12	Skin_07	Skin	Musculus	C57BL/6JN	12	f	TMS
Marrow_50-m-15	Marrow_50	Marrow	Musculus	C57BL/6JN	15	m	TMS
MAT_53-m-27	MAT_53	MAT	Musculus	C57BL/6JN	27	m	TMS
Liver_56-m-6	Liver_56	Liver	Musculus	C57BL/6JN	6	m	TMS
Limb_Muscle_40-f-3	Limb_Muscle_40	Limb_Muscle	Musculus	C57BL/6JN	3	f	TMS
Heart_50-m-15	Heart_50	Heart	Musculus	C57BL/6JN	15	m	TMS

MAT_24-m-9	MAT_24	MAT	Mus musculus	C57BL/6JN	9	m	TMS
Spleen_55-f-9	Spleen_55	Spleen	Mus musculus	C57BL/6JN	9	f	TMS
Lung_38-f-6	Lung_38	Lung	Mus musculus	C57BL/6JN	6	f	TMS
Lung_40-m-24	Lung_40	Lung	Mus musculus	C57BL/6JN	24	m	TMS
SCAT_9-f-18	SCAT_09	SCAT	Mus musculus	C57BL/6JN	18	f	TMS
Kidney_34-m-27	Kidney_34	Kidney	Mus musculus	C57BL/6JN	27	m	TMS
Liver_22-m-18	Liver_22	Liver	Mus musculus	C57BL/6JN	18	m	TMS
Spleen_28-f-6	Spleen_28	Spleen	Mus musculus	C57BL/6JN	6	f	TMS
GAT_51-f-12	GAT_51	GAT	Mus musculus	C57BL/6JN	12	f	TMS
Liver_21-f-6	Liver_21	Liver	Mus musculus	C57BL/6JN	6	f	TMS
SCAT_35-m-6	SCAT_35	SCAT	Mus musculus	C57BL/6JN	6	m	TMS
Small_Intestine_29-m-3	Small_Intestine_29	Small_Intestine	Mus musculus	C57BL/6JN	3	m	TMS
Spleen_36-m-12	Spleen_36	Spleen	Mus musculus	C57BL/6JN	12	m	TMS
Lung_31-m-15	Lung_31	Lung	Mus musculus	C57BL/6JN	15	m	TMS
MAT_23-m-12	MAT_23	MAT	Mus musculus	C57BL/6JN	12	m	TMS
SCAT_54-m-9	SCAT_54	SCAT	Mus musculus	C57BL/6JN	9	m	TMS
MAT_15-m-18	MAT_15	MAT	Mus musculus	C57BL/6JN	18	m	TMS
MAT_22-f-6	MAT_22	MAT	Mus musculus	C57BL/6JN	6	f	TMS
Lung_54-m-27	Lung_54	Lung	Mus musculus	C57BL/6JN	27	m	TMS
Lung_43-m-15	Lung_43	Lung	Mus musculus	C57BL/6JN	15	m	TMS
Lung_56-m-9	Lung_56	Lung	Mus musculus	C57BL/6JN	9	m	TMS
Liver_3-m-15	Liver_03	Liver	Mus musculus	C57BL/6JN	15	m	TMS
Spleen_35-m-18	Spleen_35	Spleen	Mus musculus	C57BL/6JN	18	m	TMS
Spleen_26-m-27	Spleen_26	Spleen	Mus musculus	C57BL/6JN	27	m	TMS
Small_Intestine_26-m-18	Small_Intestine_26	Small_Intestine	Mus musculus	C57BL/6JN	18	m	TMS
Kidney_10-m-9	Kidney_10	Kidney	Mus musculus	C57BL/6JN	9	m	TMS
Small_Intestine_40-m-12	Small_Intestine_40	Small_Intestine	Mus musculus	C57BL/6JN	12	m	TMS
Small_Intestine_21-m-6	Small_Intestine_21	Small_Intestine	Mus musculus	C57BL/6JN	6	m	TMS
Kidney_12-m-12	Kidney_12	Kidney	Mus musculus	C57BL/6JN	12	m	TMS
SCAT_51-f-12	SCAT_51	SCAT	Mus musculus	C57BL/6JN	12	f	TMS
GAT_15-m-12	GAT_15	GAT	Mus musculus	C57BL/6JN	12	m	TMS
Kidney_36-f-1	Kidney_36	Kidney	Mus musculus	C57BL/6JN	1	f	TMS
Liver_19-m-9	Liver_19	Liver	Mus musculus	C57BL/6JN	9	m	TMS
Liver_39-m-12	Liver_39	Liver	Mus musculus	C57BL/6JN	12	m	TMS
SCAT_14-f-21	SCAT_14	SCAT	Mus musculus	C57BL/6JN	21	f	TMS
Kidney_33-m-15	Kidney_33	Kidney	Mus musculus	C57BL/6JN	15	m	TMS
Pancreas_20-m-15	Pancreas_20	Pancreas	Mus musculus	C57BL/6JN	15	m	TMS

Skin_49-m-18	Skin_49	Skin	Musculus	C57BL/6JN	18	m	TMS
Heart_12-m-24	Heart_12	Heart	Musculus	C57BL/6JN	24	m	TMS
MAT_54-m-9	MAT_54	MAT	Musculus	C57BL/6JN	9	m	TMS
Limb_Muscle_6-m-24	Limb_Muscle_06	Limb_Muscle	Musculus	C57BL/6JN	24	m	TMS
SCAT_5-m-3	SCAT_05	SCAT	Musculus	C57BL/6JN	3	m	TMS
MAT_7-m-24	MAT_07	MAT	Musculus	C57BL/6JN	24	m	TMS
MAT_2-f-9	MAT_02	MAT	Musculus	C57BL/6JN	9	f	TMS
Marrow_24-f-6	Marrow_24	Marrow	Musculus	C57BL/6JN	6	f	TMS
Liver_43-m-12	Liver_43	Liver	Musculus	C57BL/6JN	12	m	TMS
Kidney_29-m-21	Kidney_29	Kidney	Musculus	C57BL/6JN	21	m	TMS
Kidney_44-m-1	Kidney_44	Kidney	Musculus	C57BL/6JN	1	m	TMS
Brain_8-f-12	Brain_08	Brain	Musculus	C57BL/6JN	12	f	TMS
Heart_16-m-3	Heart_16	Heart	Musculus	C57BL/6JN	3	m	TMS
Marrow_49-m-1	Marrow_49	Marrow	Musculus	C57BL/6JN	1	m	TMS
MAT_55-m-6	MAT_55	MAT	Musculus	C57BL/6JN	6	m	TMS
Heart_41-m-27	Heart_41	Heart	Musculus	C57BL/6JN	27	m	TMS
Marrow_6-m-12	Marrow_06	Marrow	Musculus	C57BL/6JN	12	m	TMS
SCAT_50-m-21	SCAT_50	SCAT	Musculus	C57BL/6JN	21	m	TMS
GAT_22-m-24	GAT_22	GAT	Musculus	C57BL/6JN	24	m	TMS
Limb_Muscle_19-m-12	Limb_Muscle_19	Limb_Muscle	Musculus	C57BL/6JN	12	m	TMS
Liver_7-m-24	Liver_07	Liver	Musculus	C57BL/6JN	24	m	TMS
Lung_26-m-27	Lung_26	Lung	Musculus	C57BL/6JN	27	m	TMS
Marrow_13-f-9	Marrow_13	Marrow	Musculus	C57BL/6JN	9	f	TMS
Kidney_13-m-21	Kidney_13	Kidney	Musculus	C57BL/6JN	21	m	TMS
Heart_31-m-9	Heart_31	Heart	Musculus	C57BL/6JN	9	m	TMS
MAT_34-m-24	MAT_34	MAT	Musculus	C57BL/6JN	24	m	TMS
Pancreas_24-m-18	Pancreas_24	Pancreas	Musculus	C57BL/6JN	18	m	TMS
SCAT_40-m-9	SCAT_40	SCAT	Musculus	C57BL/6JN	9	m	TMS
Bone_25-f-18	Bone_25	Bone	Musculus	C57BL/6JN	18	f	TMS
Skin_21-m-6	Skin_21	Skin	Musculus	C57BL/6JN	6	m	TMS
Small_Intestine_18-m-24	Small_Intestine_18	Small_Intestine	Musculus	C57BL/6JN	24	m	TMS
Spleen_13-f-15	Spleen_13	Spleen	Musculus	C57BL/6JN	15	f	TMS
GAT_30-f-9	GAT_30	GAT	Musculus	C57BL/6JN	9	f	TMS
Limb_Muscle_21-f-1	Limb_Muscle_21	Limb_Muscle	Musculus	C57BL/6JN	1	f	TMS
Lung_27-m-3	Lung_27	Lung	Musculus	C57BL/6JN	3	m	TMS
Liver_35-m-3	Liver_35	Liver	Musculus	C57BL/6JN	3	m	TMS
Kidney_30-m-18	Kidney_30	Kidney	Musculus	C57BL/6JN	18	m	TMS

BAT_50-f-3	BAT_50	BAT	Mus musculus	C57BL/6JN	3	f	TMS
Marrow_25-m-18	Marrow_25	Marrow	Mus musculus	C57BL/6JN	18	m	TMS
MAT_35-m-1	MAT_35	MAT	Mus musculus	C57BL/6JN	1	m	TMS
Pancreas_36-m-12	Pancreas_36	Pancreas	Mus musculus	C57BL/6JN	12	m	TMS
SCAT_46-m-15	SCAT_46	SCAT	Mus musculus	C57BL/6JN	15	m	TMS
Spleen_17-m-3	Spleen_17	Spleen	Mus musculus	C57BL/6JN	3	m	TMS
Limb_Muscle_33-m-15	Limb_Muscle_33	Limb_Muscle	Mus musculus	C57BL/6JN	15	m	TMS
Small_Intestine_36-f-9	Small_Intestine_36	Small_Intestine	Mus musculus	C57BL/6JN	9	f	TMS
Skin_28-m-27	Skin_28	Skin	Mus musculus	C57BL/6JN	27	m	TMS
Brain_32-f-15	Brain_32	Brain	Mus musculus	C57BL/6JN	15	f	TMS
Heart_42-m-1	Heart_42	Heart	Mus musculus	C57BL/6JN	1	m	TMS
Limb_Muscle_22-f-15	Limb_Muscle_22	Limb_Muscle	Mus musculus	C57BL/6JN	15	f	TMS
Marrow_23-m-1	Marrow_23	Marrow	Mus musculus	C57BL/6JN	1	m	TMS
MAT_37-m-24	MAT_37	MAT	Mus musculus	C57BL/6JN	24	m	TMS
Lung_28-m-6	Lung_28	Lung	Mus musculus	C57BL/6JN	6	m	TMS
Brain_31-f-6	Brain_31	Brain	Mus musculus	C57BL/6JN	6	f	TMS
Liver_34-m-21	Liver_34	Liver	Mus musculus	C57BL/6JN	21	m	TMS
SCAT_45-m-21	SCAT_45	SCAT	Mus musculus	C57BL/6JN	21	m	TMS
Small_Intestine_35-f-15	Small_Intestine_34	Small_Intestine	Mus musculus	C57BL/6JN	3	m	TMS
Spleen_18-m-1	Spleen_18	Spleen	Mus musculus	C57BL/6JN	1	m	TMS
Liver_47-f-18	Liver_47	Liver	Mus musculus	C57BL/6JN	18	f	TMS
Liver_37-m-1	Liver_37	Liver	Mus musculus	C57BL/6JN	1	m	TMS
Skin_30-m-12	Skin_30	Skin	Mus musculus	C57BL/6JN	12	m	TMS
Pancreas_34-m-24	Pancreas_34	Pancreas	Mus musculus	C57BL/6JN	24	m	TMS
MAT_38-m-21	MAT_38	MAT	Mus musculus	C57BL/6JN	21	m	TMS
Kidney_28-m-1	Kidney_28	Kidney	Mus musculus	C57BL/6JN	1	m	TMS
Lung_29-m-3	Lung_29	Lung	Mus musculus	C57BL/6JN	3	m	TMS
SCAT_44-m-15	SCAT_44	SCAT	Mus musculus	C57BL/6JN	15	m	TMS
Small_Intestine_34-m-3	Small_Intestine_33	Small_Intestine	Mus musculus	C57BL/6JN	24	m	TMS
Spleen_19-m-24	Spleen_19	Spleen	Mus musculus	C57BL/6JN	24	m	TMS
Limb_Muscle_23-m-24	Limb_Muscle_23	Limb_Muscle	Mus musculus	C57BL/6JN	24	m	TMS
Lung_46-m-12	Lung_46	Lung	Mus musculus	C57BL/6JN	12	m	TMS
BAT_54-f-3	BAT_54	BAT	Mus musculus	C57BL/6JN	3	f	TMS
Liver_33-f-15	Liver_33	Liver	Mus musculus	C57BL/6JN	15	f	TMS
Heart_34-m-9	Heart_34	Heart	Mus musculus	C57BL/6JN	9	m	TMS
Kidney_31-m-6	Kidney_31	Kidney	Mus musculus	C57BL/6JN	6	m	TMS
Marrow_22-f-12	Marrow_22	Marrow	Mus musculus	C57BL/6JN	12	f	TMS

Brain_30-m-21	Brain_30	Brain	Mus musculus	C57BL/6JN	21	m	TMS
Kidney_27-f-12	Kidney_27	Kidney	Mus musculus	C57BL/6JN	12	f	TMS
Brain_29-m-27	Brain_29	Brain	Mus musculus	C57BL/6JN	27	m	TMS
Marrow_44-m-1	Marrow_44	Marrow	Mus musculus	C57BL/6JN	1	m	TMS
Kidney_25-m-9	Kidney_25	Kidney	Mus musculus	C57BL/6JN	9	m	TMS
MAT_40-m-24	MAT_40	MAT	Mus musculus	C57BL/6JN	24	m	TMS
SCAT_42-m-27	SCAT_42	SCAT	Mus musculus	C57BL/6JN	27	m	TMS
Marrow_21-m-3	Marrow_21	Marrow	Mus musculus	C57BL/6JN	3	m	TMS
Liver_32-m-21	Liver_32	Liver	Mus musculus	C57BL/6JN	21	m	TMS
Small_Intestine_32-m-15	Small_Intestine_32	Small_Intestine	Mus musculus	C57BL/6JN	15	m	TMS
Pancreas_44-m-24	Pancreas_44	Pancreas	Mus musculus	C57BL/6JN	24	m	TMS
Skin_32-m-6	Skin_32	Skin	Mus musculus	C57BL/6JN	6	m	TMS
Spleen_20-m-9	Spleen_20	Spleen	Mus musculus	C57BL/6JN	9	m	TMS
Pancreas_32-m-1	Pancreas_32	Pancreas	Mus musculus	C57BL/6JN	1	m	TMS
Lung_30-f-15	Lung_30	Lung	Mus musculus	C57BL/6JN	15	f	TMS
Bone_26-m-6	Bone_26	Bone	Mus musculus	C57BL/6JN	6	m	TMS
Limb_Muscle_25-m-18	Limb_Muscle_25	Limb_Muscle	Mus musculus	C57BL/6JN	18	m	TMS
Lung_32-m-1	Lung_32	Lung	Mus musculus	C57BL/6JN	1	m	TMS
Heart_33-f-3	Heart_33	Heart	Mus musculus	C57BL/6JN	3	f	TMS
Bone_27-m-21	Bone_27	Bone	Mus musculus	C57BL/6JN	21	m	TMS
MAT_46-m-21	MAT_46	MAT	Mus musculus	C57BL/6JN	21	m	TMS
Brain_28-f-1	Brain_28	Brain	Mus musculus	C57BL/6JN	1	f	TMS
Spleen_21-f-21	Spleen_21	Spleen	Mus musculus	C57BL/6JN	21	f	TMS
Marrow_20-m-24	Marrow_20	Marrow	Mus musculus	C57BL/6JN	24	m	TMS
Liver_31-f-9	Liver_31	Liver	Mus musculus	C57BL/6JN	9	f	TMS
Limb_Muscle_26-f-9	Limb_Muscle_26	Limb_Muscle	Mus musculus	C57BL/6JN	9	f	TMS
MAT_41-m-15	MAT_41	MAT	Mus musculus	C57BL/6JN	15	m	TMS
SCAT_41-m-12	SCAT_41	SCAT	Mus musculus	C57BL/6JN	12	m	TMS
Brain_46-m-24	Brain_46	Brain	Mus musculus	C57BL/6JN	24	m	TMS
Kidney_24-m-12	Kidney_24	Kidney	Mus musculus	C57BL/6JN	12	m	TMS
Pancreas_31-m-18	Pancreas_31	Pancreas	Mus musculus	C57BL/6JN	18	m	TMS
Marrow_19-m-18	Marrow_19	Marrow	Mus musculus	C57BL/6JN	18	m	TMS
Skin_34-f-18	Skin_34	Skin	Mus musculus	C57BL/6JN	18	f	TMS
Small_Intestine_19-f-18	Small_Intestine_19	Small_Intestine	Mus musculus	C57BL/6JN	18	f	TMS
Heart_32-f-15	Heart_32	Heart	Mus musculus	C57BL/6JN	15	f	TMS
Marrow_46-f-6	Marrow_46	Marrow	Mus musculus	C57BL/6JN	6	f	TMS
Pancreas_30-m-12	Pancreas_30	Pancreas	Mus musculus	C57BL/6JN	12	m	TMS

Brain_27-m-15	Brain_27	Brain	Musculus	C57BL/6JN	15	m	TMS
Bone_28-f-1	Bone_28	Bone	Musculus	C57BL/6JN	1	f	TMS
Kidney_21-m-15	Kidney_21	Kidney	Musculus	C57BL/6JN	15	m	TMS
Lung_33-f-3	Lung_33	Lung	Musculus	C57BL/6JN	3	f	TMS
Liver_20-m-3	Liver_20	Liver	Musculus	C57BL/6JN	3	m	TMS
Limb_Muscle_29-m-9	Limb_Muscle_29	Limb_Muscle	Musculus	C57BL/6JN	9	m	TMS
Spleen_22-m-9	Spleen_22	Spleen	Musculus	C57BL/6JN	9	m	TMS
Marrow_26-f-3	Marrow_26	Marrow	Musculus	C57BL/6JN	3	f	TMS
Pancreas_41-f-15	Pancreas_41	Pancreas	Musculus	C57BL/6JN	15	f	TMS
Skin_35-f-3	Skin_35	Skin	Musculus	C57BL/6JN	3	f	TMS
Limb_Muscle_36-m-15	Limb_Muscle_36	Limb_Muscle	Musculus	C57BL/6JN	15	m	TMS
Brain_38-f-12	Brain_38	Brain	Musculus	C57BL/6JN	12	f	TMS
Small_Intestine_43-m-18	Small_Intestine_43	Small_Intestine	Musculus	C57BL/6JN	18	m	TMS
Lung_42-m-27	Lung_42	Lung	Musculus	C57BL/6JN	27	m	TMS
Marrow_34-f-18	Marrow_34	Marrow	Musculus	C57BL/6JN	18	f	TMS
Marrow_27-m-15	Marrow_27	Marrow	Musculus	C57BL/6JN	15	m	TMS
Liver_44-m-18	Liver_44	Liver	Musculus	C57BL/6JN	18	m	TMS
Bone_29-m-6	Bone_29	Bone	Musculus	C57BL/6JN	6	m	TMS
Lung_48-f-15	Lung_48	Lung	Musculus	C57BL/6JN	15	f	TMS
Pancreas_43-m-1	Pancreas_43	Pancreas	Musculus	C57BL/6JN	1	m	TMS
Spleen_23-m-1	Spleen_23	Spleen	Musculus	C57BL/6JN	1	m	TMS
Lung_41-m-6	Lung_41	Lung	Musculus	C57BL/6JN	6	m	TMS
Heart_39-m-1	Heart_39	Heart	Musculus	C57BL/6JN	1	m	TMS
Small_Intestine_42-m-24	Small_Intestine_42	Small_Intestine	Musculus	C57BL/6JN	24	m	TMS
Pancreas_40-f-6	Pancreas_40	Pancreas	Musculus	C57BL/6JN	6	f	TMS
Marrow_28-m-6	Marrow_28	Marrow	Musculus	C57BL/6JN	6	m	TMS
Spleen_24-m-1	Spleen_24	Spleen	Musculus	C57BL/6JN	1	m	TMS
Bone_31-m-21	Bone_31	Bone	Musculus	C57BL/6JN	21	m	TMS
Skin_45-m-1	Skin_45	Skin	Musculus	C57BL/6JN	1	m	TMS
Marrow_33-m-18	Marrow_33	Marrow	Musculus	C57BL/6JN	18	m	TMS
Marrow_35-m-1	Marrow_35	Marrow	Musculus	C57BL/6JN	1	m	TMS
Lung_39-m-3	Lung_39	Lung	Musculus	C57BL/6JN	3	m	TMS
Brain_37-m-27	Brain_37	Brain	Musculus	C57BL/6JN	27	m	TMS
Heart_37-f-12	Heart_37	Heart	Musculus	C57BL/6JN	12	f	TMS
Liver_45-m-27	Liver_45	Liver	Musculus	C57BL/6JN	27	m	TMS
Limb_Muscle_37-m-27	Limb_Muscle_37	Limb_Muscle	Musculus	C57BL/6JN	27	m	TMS
Skin_37-m-1	Skin_37	Skin	Musculus	C57BL/6JN	1	m	TMS

Bone_32-m-1	Bone_32	Bone	Mus musculus	C57BL/6JN	1	m	TMS
Skin_38-m-6	Skin_38	Skin	Mus musculus	C57BL/6JN	6	m	TMS
Small_Intestine_41-m-1	Small_Intestine_41	Small_Intestine	Mus musculus	C57BL/6JN	1	m	TMS
Limb_Muscle_38-m-9	Limb_Muscle_38	Limb_Muscle	Mus musculus	C57BL/6JN	9	m	TMS
Pancreas_39-m-12	Pancreas_39	Pancreas	Mus musculus	C57BL/6JN	12	m	TMS
Marrow_36-m-12	Marrow_36	Marrow	Mus musculus	C57BL/6JN	12	m	TMS
Brain_36-m-24	Brain_36	Brain	Mus musculus	C57BL/6JN	24	m	TMS
Lung_47-m-6	Lung_47	Lung	Mus musculus	C57BL/6JN	6	m	TMS
Skin_46-m-15	Skin_46	Skin	Mus musculus	C57BL/6JN	15	m	TMS
Lung_37-f-6	Lung_37	Lung	Mus musculus	C57BL/6JN	6	f	TMS
Spleen_25-m-9	Spleen_25	Spleen	Mus musculus	C57BL/6JN	9	m	TMS
Heart_49-f-6	Heart_49	Heart	Mus musculus	C57BL/6JN	6	f	TMS
Brain_39-m-12	Brain_39	Brain	Mus musculus	C57BL/6JN	12	m	TMS
Pancreas_42-f-9	Pancreas_42	Pancreas	Mus musculus	C57BL/6JN	9	f	TMS
Marrow_29-m-21	Marrow_29	Marrow	Mus musculus	C57BL/6JN	21	m	TMS
Lung_35-m-18	Lung_35	Lung	Mus musculus	C57BL/6JN	18	m	TMS
Small_Intestine_38-m-9	Small_Intestine_38	Small_Intestine	Mus musculus	C57BL/6JN	9	m	TMS
Spleen_37-f-1	Spleen_37	Spleen	Mus musculus	C57BL/6JN	1	f	TMS
Heart_35-m-6	Heart_35	Heart	Mus musculus	C57BL/6JN	6	m	TMS
Brain_34-f-3	Brain_34	Brain	Mus musculus	C57BL/6JN	3	f	TMS
Skin_40-m-9	Skin_40	Skin	Mus musculus	C57BL/6JN	9	m	TMS
Bone_34-m-27	Bone_34	Bone	Mus musculus	C57BL/6JN	27	m	TMS
Bone_39-m-6	Bone_39	Bone	Mus musculus	C57BL/6JN	6	m	TMS
Brain_41-m-15	Brain_41	Brain	Mus musculus	C57BL/6JN	15	m	TMS
Small_Intestine_46-m-12	Small_Intestine_46	Small_Intestine	Mus musculus	C57BL/6JN	12	m	TMS
Spleen_42-m-18	Spleen_42	Spleen	Mus musculus	C57BL/6JN	18	m	TMS
Small_Intestine_44-m-21	Small_Intestine_44	Small_Intestine	Mus musculus	C57BL/6JN	21	m	TMS
Pancreas_37-f-12	Pancreas_37	Pancreas	Mus musculus	C57BL/6JN	12	f	TMS
Marrow_31-m-24	Marrow_31	Marrow	Mus musculus	C57BL/6JN	24	m	TMS
Liver_38-m-15	Liver_38	Liver	Mus musculus	C57BL/6JN	15	m	TMS
Spleen_39-m-9	Spleen_39	Spleen	Mus musculus	C57BL/6JN	9	m	TMS
Heart_36-m-12	Heart_36	Heart	Mus musculus	C57BL/6JN	12	m	TMS
Liver_40-m-15	Liver_40	Liver	Mus musculus	C57BL/6JN	15	m	TMS
Bone_41-m-27	Bone_41	Bone	Mus musculus	C57BL/6JN	27	m	TMS
Brain_40-m-6	Brain_40	Brain	Mus musculus	C57BL/6JN	6	m	TMS
Spleen_40-m-24	Spleen_40	Spleen	Mus musculus	C57BL/6JN	24	m	TMS
Small_Intestine_37-f-21	Small_Intestine_37	Small_Intestine	Mus musculus	C57BL/6JN	21	f	TMS

Skin_43-m-6	Skin_43	Skin	Musculus	C57BL/6JN	6	m	TMS
Marrow_32-m-12	Marrow_32	Marrow	Musculus	C57BL/6JN	12	m	TMS
Brain_33-f-9	Brain_33	Brain	Musculus	C57BL/6JN	9	f	TMS
MAT_44-f-6	MAT_44	MAT	Musculus	C57BL/6JN	6	f	TMS
Bone_36-f-6	Bone_36	Bone	Musculus	C57BL/6JN	6	f	TMS
Spleen_41-m-12	Spleen_41	Spleen	Musculus	C57BL/6JN	12	m	TMS
Small_Intestine_47-m-12	Small_Intestine_47	Small_Intestine	Musculus	C57BL/6JN	12	m	TMS
MAT_11-m-18	MAT_11	MAT	Musculus	C57BL/6JN	18	m	TMS
BAT_10-m-15	BAT_10	BAT	Musculus	C57BL/6JN	15	m	TMS
Liver_27-f-12	Liver_27	Liver	Musculus	C57BL/6JN	12	f	TMS
SCAT_11-m-18	SCAT_11	SCAT	Musculus	C57BL/6JN	18	m	TMS
Brain_6-m-9	Brain_06	Brain	Musculus	C57BL/6JN	9	m	TMS
Small_Intestine_9-f-12	Small_Intestine_09	Small_Intestine	Musculus	C57BL/6JN	12	f	TMS
Skin_11-m-18	Skin_11	Skin	Musculus	C57BL/6JN	18	m	TMS
Pancreas_19-m-27	Pancreas_19	Pancreas	Musculus	C57BL/6JN	27	m	TMS
Bone_4-f-15	Bone_04	Bone	Musculus	C57BL/6JN	15	f	TMS
Kidney_38-m-21	Kidney_38	Kidney	Musculus	C57BL/6JN	21	m	TMS
GAT_4-m-24	GAT_04	GAT	Musculus	C57BL/6JN	24	m	TMS
Heart_6-m-24	Heart_06	Heart	Musculus	C57BL/6JN	24	m	TMS
Limb_Muscle_4-f-18	Limb_Muscle_04	Limb_Muscle	Musculus	C57BL/6JN	18	f	TMS
Lung_14-f-21	Lung_14	Lung	Musculus	C57BL/6JN	21	f	TMS
Marrow_9-m-15	Marrow_09	Marrow	Musculus	C57BL/6JN	15	m	TMS
Brain_7-m-1	Brain_07	Brain	Musculus	C57BL/6JN	1	m	TMS
SCAT_13-f-18	SCAT_13	SCAT	Musculus	C57BL/6JN	18	f	TMS
Spleen_9-m-21	Spleen_09	Spleen	Musculus	C57BL/6JN	21	m	TMS
Kidney_39-m-18	Kidney_39	Kidney	Musculus	C57BL/6JN	18	m	TMS
Pancreas_18-f-1	Pancreas_18	Pancreas	Musculus	C57BL/6JN	1	f	TMS
Skin_9-m-27	Skin_09	Skin	Musculus	C57BL/6JN	27	m	TMS
Liver_26-m-18	Liver_26	Liver	Musculus	C57BL/6JN	18	m	TMS
Limb_Muscle_3-m-12	Limb_Muscle_03	Limb_Muscle	Musculus	C57BL/6JN	12	m	TMS
Lung_15-m-21	Lung_15	Lung	Musculus	C57BL/6JN	21	m	TMS
GAT_3-m-6	GAT_03	GAT	Musculus	C57BL/6JN	6	m	TMS
Bone_3-m-27	Bone_03	Bone	Musculus	C57BL/6JN	27	m	TMS
BAT_11-m-15	BAT_11	BAT	Musculus	C57BL/6JN	15	m	TMS
Marrow_10-f-15	Marrow_10	Marrow	Musculus	C57BL/6JN	15	f	TMS
MAT_12-m-3	MAT_12	MAT	Musculus	C57BL/6JN	3	m	TMS
Small_Intestine_11-m-3	Small_Intestine_11	Small_Intestine	Musculus	C57BL/6JN	3	m	TMS

Spleen_8-f-15	Spleen_08	Spleen	Musculus	C57BL/6JN	15	f	TMS
Skin_8-m-21	Skin_08	Skin	Musculus	C57BL/6JN	21	m	TMS
Pancreas_17-f-1	Pancreas_17	Pancreas	Musculus	C57BL/6JN	1	f	TMS
Kidney_40-f-12	Kidney_40	Kidney	Musculus	C57BL/6JN	12	f	TMS
BAT_13-m-6	BAT_13	BAT	Musculus	C57BL/6JN	6	m	TMS
Brain_10-m-18	Brain_10	Brain	Musculus	C57BL/6JN	18	m	TMS
Heart_5-m-18	Heart_05	Heart	Musculus	C57BL/6JN	18	m	TMS
MAT_14-m-9	MAT_14	MAT	Musculus	C57BL/6JN	9	m	TMS
Liver_25-m-18	Liver_25	Liver	Musculus	C57BL/6JN	18	m	TMS
Lung_16-m-9	Lung_16	Lung	Musculus	C57BL/6JN	9	m	TMS
Limb_Muscle_2-m-18	Limb_Muscle_02	Limb_Muscle	Musculus	C57BL/6JN	18	m	TMS
Bone_2-m-3	Bone_02	Bone	Musculus	C57BL/6JN	3	m	TMS
Marrow_11-m-3	Marrow_11	Marrow	Musculus	C57BL/6JN	3	m	TMS
SCAT_15-m-1	SCAT_15	SCAT	Musculus	C57BL/6JN	1	m	TMS
Heart_3-m-6	Heart_03	Heart	Musculus	C57BL/6JN	6	m	TMS
Marrow_12-m-24	Marrow_12	Marrow	Musculus	C57BL/6JN	24	m	TMS
Pancreas_16-m-9	Pancreas_16	Pancreas	Musculus	C57BL/6JN	9	m	TMS
SCAT_16-m-3	SCAT_16	SCAT	Musculus	C57BL/6JN	3	m	TMS
Small_Intestine_12-m-6	Small_Intestine_12	Small_Intestine	Musculus	C57BL/6JN	6	m	TMS
Spleen_4-m-6	Spleen_04	Spleen	Musculus	C57BL/6JN	6	m	TMS
Lung_17-f-12	Lung_17	Lung	Musculus	C57BL/6JN	12	f	TMS
Brain_9-m-27	Brain_09	Brain	Musculus	C57BL/6JN	27	m	TMS
Limb_Muscle_1-f-15	Limb_Muscle_01	Limb_Muscle	Musculus	C57BL/6JN	15	f	TMS
Kidney_41-m-24	Kidney_41	Kidney	Musculus	C57BL/6JN	24	m	TMS
GAT_1-f-21	GAT_01	GAT	Musculus	C57BL/6JN	21	f	TMS
BAT_12-m-18	BAT_12	BAT	Musculus	C57BL/6JN	18	m	TMS
BAT_31-m-12	BAT_31	BAT	Musculus	C57BL/6JN	12	m	TMS
Spleen_51-m-15	Spleen_51	Spleen	Musculus	C57BL/6JN	15	m	TMS
Bone_52-m-18	Bone_52	Bone	Musculus	C57BL/6JN	18	m	TMS
Liver_53-m-24	Liver_53	Liver	Musculus	C57BL/6JN	24	m	TMS
Limb_Muscle_45-m-3	Limb_Muscle_45	Limb_Muscle	Musculus	C57BL/6JN	3	m	TMS
Pancreas_23-m-6	Pancreas_23	Pancreas	Musculus	C57BL/6JN	6	m	TMS
Skin_51-m-18	Skin_51	Skin	Musculus	C57BL/6JN	18	m	TMS
GAT_52-m-27	GAT_52	GAT	Musculus	C57BL/6JN	27	m	TMS
Lung_51-m-9	Lung_51	Lung	Musculus	C57BL/6JN	9	m	TMS
Marrow_52-m-21	Marrow_52	Marrow	Musculus	C57BL/6JN	21	m	TMS
Kidney_52-f-6	Kidney_52	Kidney	Musculus	C57BL/6JN	6	f	TMS

MAT_50-f-15	MAT_50	MAT	Mus musculus	C57BL/6JN	15	f	TMS
Small_Intestine_52-m-3	Small_Intestine_52	Small Intestine	Mus musculus	C57BL/6JN	3	m	TMS
Heart_54-m-21	Heart_54	Heart	Mus musculus	C57BL/6JN	21	m	TMS
Brain_18-f-6	Brain_18	Brain	Mus musculus	C57BL/6JN	6	f	TMS
Limb_Muscle_43-m-15	Limb_Muscle_43	Limb_Muscle	Mus musculus	C57BL/6JN	15	m	TMS
Heart_53-f-15	Heart_53	Heart	Mus musculus	C57BL/6JN	15	f	TMS
Brain_19-f-1	Brain_19	Brain	Mus musculus	C57BL/6JN	1	f	TMS
BAT_32-f-9	BAT_32	BAT	Mus musculus	C57BL/6JN	9	f	TMS
Liver_54-f-1	Liver_54	Liver	Mus musculus	C57BL/6JN	1	f	TMS
Bone_54-m-9	Bone_54	Bone	Mus musculus	C57BL/6JN	9	m	TMS
Skin_53-m-12	Skin_53	Skin	Mus musculus	C57BL/6JN	12	m	TMS
Small_Intestine_53-f-1	Small_Intestine_53	Small Intestine	Mus musculus	C57BL/6JN	1	f	TMS
Pancreas_47-f-18	Pancreas_47	Pancreas	Mus musculus	C57BL/6JN	18	f	TMS
SCAT_49-m-9	SCAT_49	SCAT	Mus musculus	C57BL/6JN	9	m	TMS
Kidney_53-m-18	Kidney_53	Kidney	Mus musculus	C57BL/6JN	18	m	TMS
GAT_53-m-15	GAT_53	GAT	Mus musculus	C57BL/6JN	15	m	TMS
Lung_52-f-18	Lung_52	Lung	Mus musculus	C57BL/6JN	18	f	TMS
Spleen_52-m-27	Spleen_52	Spleen	Mus musculus	C57BL/6JN	27	m	TMS
Marrow_51-m-9	Marrow_51	Marrow	Mus musculus	C57BL/6JN	9	m	TMS
SCAT_48-m-3	SCAT_48	SCAT	Mus musculus	C57BL/6JN	3	m	TMS
Bone_56-m-9	Bone_56	Bone	Mus musculus	C57BL/6JN	9	m	TMS
BAT_33-f-12	BAT_33	BAT	Mus musculus	C57BL/6JN	12	f	TMS
GAT_55-m-6	GAT_55	GAT	Mus musculus	C57BL/6JN	6	m	TMS
Limb_Muscle_41-f-21	Limb_Muscle_41	Limb_Muscle	Mus musculus	C57BL/6JN	21	f	TMS
Kidney_56-f-9	Kidney_56	Kidney	Mus musculus	C57BL/6JN	9	f	TMS
Small_Intestine_54-m-1	Small_Intestine_54	Small Intestine	Mus musculus	C57BL/6JN	1	m	TMS
Skin_54-f-3	Skin_54	Skin	Mus musculus	C57BL/6JN	3	f	TMS
Liver_55-f-1	Liver_55	Liver	Mus musculus	C57BL/6JN	1	f	TMS
Brain_20-f-21	Brain_20	Brain	Mus musculus	C57BL/6JN	21	f	TMS
Lung_53-m-18	Lung_53	Lung	Mus musculus	C57BL/6JN	18	m	TMS
MAT_51-f-15	MAT_51	MAT	Mus musculus	C57BL/6JN	15	f	TMS
Pancreas_48-m-21	Pancreas_48	Pancreas	Mus musculus	C57BL/6JN	21	m	TMS
Heart_52-m-9	Heart_52	Heart	Mus musculus	C57BL/6JN	9	m	TMS
Spleen_53-m-24	Spleen_53	Spleen	Mus musculus	C57BL/6JN	24	m	TMS
SCAT_56-f-1	SCAT_56	SCAT	Mus musculus	C57BL/6JN	1	f	TMS
Pancreas_56-m-18	Pancreas_56	Pancreas	Mus musculus	C57BL/6JN	18	m	TMS
MAT_52-m-15	MAT_52	MAT	Mus musculus	C57BL/6JN	15	m	TMS

Marrow_55-m-6	Marrow_55	Marrow	Musculus	C57BL/6JN	6	m	TMS
Spleen_12-m-15	Spleen_12	Spleen	Musculus	C57BL/6JN	15	m	TMS
Lung_55-m-6	Lung_55	Lung	Musculus	C57BL/6JN	6	m	TMS
Liver_42-m-12	Liver_42	Liver	Musculus	C57BL/6JN	12	m	TMS
Limb_Muscle_48-m-9	Limb_Muscle_48	Limb_Muscle	Musculus	C57BL/6JN	9	m	TMS
Kidney_42-f-15	Kidney_42	Kidney	Musculus	C57BL/6JN	15	f	TMS
Heart_23-m-15	Heart_23	Heart	Musculus	C57BL/6JN	15	m	TMS
GAT_28-f-21	GAT_28	GAT	Musculus	C57BL/6JN	21	f	TMS
Brain_48-m-12	Brain_48	Brain	Musculus	C57BL/6JN	12	m	TMS
Small_Intestine_56-m-21	Small_Intestine_56	Small_Intestine	Musculus	C57BL/6JN	21	m	TMS
Skin_50-m-15	Skin_50	Skin	Musculus	C57BL/6JN	15	m	TMS
Heart_24-m-27	Heart_24	Heart	Musculus	C57BL/6JN	27	m	TMS
Kidney_51-m-9	Kidney_51	Kidney	Musculus	C57BL/6JN	9	m	TMS
Limb_Muscle_49-f-3	Limb_Muscle_49	Limb_Muscle	Musculus	C57BL/6JN	3	f	TMS
Liver_13-m-27	Liver_13	Liver	Musculus	C57BL/6JN	27	m	TMS
BAT_1-m-24	BAT_01	BAT	Musculus	C57BL/6JN	24	m	TMS
Lung_4-m-24	Lung_04	Lung	Musculus	C57BL/6JN	24	m	TMS
Marrow_7-m-21	Marrow_07	Marrow	Musculus	C57BL/6JN	21	m	TMS
MAT_1-m-3	MAT_01	MAT	Musculus	C57BL/6JN	3	m	TMS
SCAT_7-m-15	SCAT_07	SCAT	Musculus	C57BL/6JN	15	m	TMS
Pancreas_14-m-27	Pancreas_14	Pancreas	Musculus	C57BL/6JN	27	m	TMS
Bone_13-m-3	Bone_13	Bone	Musculus	C57BL/6JN	3	m	TMS
Skin_1-f-6	Skin_01	Skin	Musculus	C57BL/6JN	6	f	TMS
Spleen_7-f-12	Spleen_07	Spleen	Musculus	C57BL/6JN	12	f	TMS
Small_Intestine_6-f-12	Small_Intestine_06	Small_Intestine	Musculus	C57BL/6JN	12	f	TMS
Brain_49-m-6	Brain_49	Brain	Musculus	C57BL/6JN	6	m	TMS
Lung_5-m-12	Lung_05	Lung	Musculus	C57BL/6JN	12	m	TMS
MAT_4-m-1	MAT_04	MAT	Musculus	C57BL/6JN	1	m	TMS
Skin_2-m-27	Skin_02	Skin	Musculus	C57BL/6JN	27	m	TMS
Bone_14-m-6	Bone_14	Bone	Musculus	C57BL/6JN	6	m	TMS
Kidney_50-m-27	Kidney_50	Kidney	Musculus	C57BL/6JN	27	m	TMS
Limb_Muscle_51-m-6	Limb_Muscle_51	Limb_Muscle	Musculus	C57BL/6JN	6	m	TMS
Marrow_5-f-12	Marrow_05	Marrow	Musculus	C57BL/6JN	12	f	TMS
Pancreas_13-m-6	Pancreas_13	Pancreas	Musculus	C57BL/6JN	6	m	TMS
Spleen_6-f-3	Spleen_06	Spleen	Musculus	C57BL/6JN	3	f	TMS
GAT_19-f-9	GAT_19	GAT	Musculus	C57BL/6JN	9	f	TMS
Small_Intestine_5-m-27	Small_Intestine_05	Small_Intestine	Musculus	C57BL/6JN	27	m	TMS

SCAT_6-f-9	SCAT_06	SCAT	Mus musculus	C57BL/6JN	9	f	TMS
BAT_2-f-21	BAT_02	BAT	Mus musculus	C57BL/6JN	21	f	TMS
Heart_25-f-6	Heart_25	Heart	Mus musculus	C57BL/6JN	6	f	TMS
Brain_50-f-3	Brain_50	Brain	Mus musculus	C57BL/6JN	3	f	TMS
Limb_Muscle_53-m-27	Limb_Muscle_53	Limb_Muscle	Mus musculus	C57BL/6JN	27	m	TMS
GAT_20-f-1	GAT_20	GAT	Mus musculus	C57BL/6JN	1	f	TMS
SCAT_4-m-12	SCAT_04	SCAT	Mus musculus	C57BL/6JN	12	m	TMS
Brain_51-f-18	Brain_51	Brain	Mus musculus	C57BL/6JN	18	f	TMS
Skin_3-f-15	Skin_03	Skin	Mus musculus	C57BL/6JN	15	f	TMS
Small_Intestine_4-m-27	Small_Intestine_04	Small_Intestine	Mus musculus	C57BL/6JN	27	m	TMS
Spleen_5-m-12	Spleen_05	Spleen	Mus musculus	C57BL/6JN	12	m	TMS
Kidney_48-m-21	Kidney_48	Kidney	Mus musculus	C57BL/6JN	21	m	TMS
Marrow_4-m-9	Marrow_04	Marrow	Mus musculus	C57BL/6JN	9	m	TMS
Liver_15-m-1	Liver_15	Liver	Mus musculus	C57BL/6JN	1	m	TMS
Bone_16-m-1	Bone_16	Bone	Mus musculus	C57BL/6JN	1	m	TMS
BAT_3-f-15	BAT_03	BAT	Mus musculus	C57BL/6JN	15	f	TMS
Pancreas_12-m-15	Pancreas_12	Pancreas	Mus musculus	C57BL/6JN	15	m	TMS
Lung_6-f-12	Lung_06	Lung	Mus musculus	C57BL/6JN	12	f	TMS
Heart_26-m-3	Heart_26	Heart	Mus musculus	C57BL/6JN	3	m	TMS
Skin_4-m-9	Skin_04	Skin	Mus musculus	C57BL/6JN	9	m	TMS
BAT_4-m-12	BAT_04	BAT	Mus musculus	C57BL/6JN	12	m	TMS
Liver_16-m-27	Liver_16	Liver	Mus musculus	C57BL/6JN	27	m	TMS
Heart_27-m-12	Heart_27	Heart	Mus musculus	C57BL/6JN	12	m	TMS
Lung_11-m-18	Lung_11	Lung	Mus musculus	C57BL/6JN	18	m	TMS
SCAT_3-m-18	SCAT_03	SCAT	Mus musculus	C57BL/6JN	18	m	TMS
Small_Intestine_3-m-9	Small_Intestine_03	Small_Intestine	Mus musculus	C57BL/6JN	9	m	TMS
Bone_17-m-18	Bone_17	Bone	Mus musculus	C57BL/6JN	18	m	TMS
Limb_Muscle_54-m-6	Limb_Muscle_54	Limb_Muscle	Mus musculus	C57BL/6JN	6	m	TMS
GAT_21-m-3	GAT_21	GAT	Mus musculus	C57BL/6JN	3	m	TMS
Kidney_47-m-3	Kidney_47	Kidney	Mus musculus	C57BL/6JN	3	m	TMS
Pancreas_11-m-21	Pancreas_11	Pancreas	Mus musculus	C57BL/6JN	21	m	TMS
Marrow_3-m-9	Marrow_03	Marrow	Mus musculus	C57BL/6JN	9	m	TMS
Brain_52-f-18	Brain_52	Brain	Mus musculus	C57BL/6JN	18	f	TMS
MAT_6-m-18	MAT_06	MAT	Mus musculus	C57BL/6JN	18	m	TMS
GAT_10-m-1	GAT_10	GAT	Mus musculus	C57BL/6JN	1	m	TMS
Heart_17-m-15	Heart_17	Heart	Mus musculus	C57BL/6JN	15	m	TMS
Kidney_9-m-1	Kidney_09	Kidney	Mus musculus	C57BL/6JN	1	m	TMS

Liver_1-f-18	Liver_01	Liver	Mus musculus	C57BL/6JN	18	f	TMS
Marrow_37-m-27	Marrow_37	Marrow	Mus musculus	C57BL/6JN	27	m	TMS
Pancreas_55-m-6	Pancreas_55	Pancreas	Mus musculus	C57BL/6JN	6	m	TMS
SCAT_23-f-15	SCAT_23	SCAT	Mus musculus	C57BL/6JN	15	f	TMS
Lung_20-m-15	Lung_20	Lung	Mus musculus	C57BL/6JN	15	m	TMS
MAT_21-m-1	MAT_21	MAT	Mus musculus	C57BL/6JN	1	m	TMS
Bone_7-f-1	Bone_07	Bone	Mus musculus	C57BL/6JN	1	f	TMS
Skin_15-f-9	Skin_15	Skin	Mus musculus	C57BL/6JN	9	f	TMS
Spleen_33-f-1	Spleen_33	Spleen	Mus musculus	C57BL/6JN	1	f	TMS
Small_Intestine_27-f-18	Small_Intestine_27	Small_Intestine	Mus musculus	C57BL/6JN	18	f	TMS
BAT_17-m-18	BAT_17	BAT	Mus musculus	C57BL/6JN	18	m	TMS
Brain_15-m-12	Brain_15	Brain	Mus musculus	C57BL/6JN	12	m	TMS
GAT_11-f-12	GAT_11	GAT	Mus musculus	C57BL/6JN	12	f	TMS
Heart_15-m-27	Heart_15	Heart	Mus musculus	C57BL/6JN	27	m	TMS
Kidney_11-f-3	Kidney_11	Kidney	Mus musculus	C57BL/6JN	3	f	TMS
Limb_Muscle_8-m-21	Limb_Muscle_08	Limb_Muscle	Mus musculus	C57BL/6JN	21	m	TMS
BAT_18-m-9	BAT_18	BAT	Mus musculus	C57BL/6JN	9	m	TMS
Pancreas_54-m-3	Pancreas_54	Pancreas	Mus musculus	C57BL/6JN	3	m	TMS
Skin_16-m-24	Skin_16	Skin	Mus musculus	C57BL/6JN	24	m	TMS
Lung_19-m-1	Lung_19	Lung	Mus musculus	C57BL/6JN	1	m	TMS
Marrow_38-m-18	Marrow_38	Marrow	Mus musculus	C57BL/6JN	18	m	TMS
SCAT_21-m-27	SCAT_21	SCAT	Mus musculus	C57BL/6JN	27	m	TMS
Limb_Muscle_30-m-12	Limb_Muscle_30	Limb_Muscle	Mus musculus	C57BL/6JN	12	m	TMS
MAT_20-m-15	MAT_20	MAT	Mus musculus	C57BL/6JN	15	m	TMS
Small_Intestine_28-m-27	Small_Intestine_28	Small_Intestine	Mus musculus	C57BL/6JN	27	m	TMS
Spleen_27-f-18	Spleen_27	Spleen	Mus musculus	C57BL/6JN	18	f	TMS
Brain_13-m-9	Brain_13	Brain	Mus musculus	C57BL/6JN	9	m	TMS
Heart_14-m-18	Heart_14	Heart	Mus musculus	C57BL/6JN	18	m	TMS
Kidney_7-m-15	Kidney_07	Kidney	Mus musculus	C57BL/6JN	15	m	TMS
Limb_Muscle_9-m-3	Limb_Muscle_09	Limb_Muscle	Mus musculus	C57BL/6JN	3	m	TMS
Liver_2-f-9	Liver_02	Liver	Mus musculus	C57BL/6JN	9	f	TMS
BAT_22-m-21	BAT_22	BAT	Mus musculus	C57BL/6JN	21	m	TMS
Skin_17-m-9	Skin_17	Skin	Mus musculus	C57BL/6JN	9	m	TMS
Spleen_29-m-3	Spleen_29	Spleen	Mus musculus	C57BL/6JN	3	m	TMS
Small_Intestine_25-f-9	Small_Intestine_25	Small_Intestine	Mus musculus	C57BL/6JN	9	f	TMS
Lung_18-m-1	Lung_18	Lung	Mus musculus	C57BL/6JN	1	m	TMS
MAT_19-m-21	MAT_19	MAT	Mus musculus	C57BL/6JN	21	m	TMS

Bone_10-m-12	Bone_10	Bone	Musculus	C57BL/6JN	12	m	TMS
Marrow_39-f-21	Marrow_39	Marrow	Musculus	C57BL/6JN	21	f	TMS
SCAT_20-m-12	SCAT_20	SCAT	Musculus	C57BL/6JN	12	m	TMS
Brain_14-m-12	Brain_14	Brain	Musculus	C57BL/6JN	12	m	TMS
Brain_12-f-21	Brain_12	Brain	Musculus	C57BL/6JN	21	f	TMS
GAT_12-m-6	GAT_12	GAT	Musculus	C57BL/6JN	6	m	TMS
Kidney_4-m-18	Kidney_04	Kidney	Musculus	C57BL/6JN	18	m	TMS
Liver_4-f-21	Liver_04	Liver	Musculus	C57BL/6JN	21	f	TMS
Limb_Muscle_10-m-18	Limb_Muscle_10	Limb_Muscle	Musculus	C57BL/6JN	18	m	TMS
MAT_17-m-3	MAT_17	MAT	Musculus	C57BL/6JN	3	m	TMS
BAT_23-m-24	BAT_23	BAT	Musculus	C57BL/6JN	24	m	TMS
Heart_13-m-15	Heart_13	Heart	Musculus	C57BL/6JN	15	m	TMS
Lung_2-m-21	Lung_02	Lung	Musculus	C57BL/6JN	21	m	TMS
Small_Intestine_24-f-3	Small_Intestine_24	Small_Intestine	Musculus	C57BL/6JN	3	f	TMS
Spleen_30-m-3	Spleen_30	Spleen	Musculus	C57BL/6JN	3	m	TMS
SCAT_19-m-24	SCAT_19	SCAT	Musculus	C57BL/6JN	24	m	TMS
Marrow_40-m-21	Marrow_40	Marrow	Musculus	C57BL/6JN	21	m	TMS
Skin_19-m-1	Skin_19	Skin	Musculus	C57BL/6JN	1	m	TMS
Pancreas_9-m-24	Pancreas_09	Pancreas	Musculus	C57BL/6JN	24	m	TMS
Skin_52-f-6	Skin_52	Skin	Musculus	C57BL/6JN	6	f	TMS
MAT_43-m-12	MAT_43	MAT	Musculus	C57BL/6JN	12	m	TMS
GAT_9-m-9	GAT_09	GAT	Musculus	C57BL/6JN	9	m	TMS
Kidney_17-m-1	Kidney_17	Kidney	Musculus	C57BL/6JN	1	m	TMS
Kidney_8-m-3	Kidney_08	Kidney	Musculus	C57BL/6JN	3	m	TMS
Brain_25-m-6	Brain_25	Brain	Musculus	C57BL/6JN	6	m	TMS
Limb_Muscle_42-m-6	Limb_Muscle_42	Limb_Muscle	Musculus	C57BL/6JN	6	m	TMS
MAT_30-m-12	MAT_30	MAT	Musculus	C57BL/6JN	12	m	TMS
BAT_7-m-15	BAT_07	BAT	Musculus	C57BL/6JN	15	m	TMS
Liver_36-m-9	Liver_36	Liver	Musculus	C57BL/6JN	9	m	TMS
Heart_47-m-9	Heart_47	Heart	Musculus	C57BL/6JN	9	m	TMS
Lung_7-m-1	Lung_07	Lung	Musculus	C57BL/6JN	1	m	TMS
Kidney_26-m-15	Kidney_26	Kidney	Musculus	C57BL/6JN	15	m	TMS
Pancreas_1-f-15	Pancreas_01	Pancreas	Musculus	C57BL/6JN	15	f	TMS
SCAT_52-m-6	SCAT_52	SCAT	Musculus	C57BL/6JN	6	m	TMS
Spleen_48-m-1	Spleen_48	Spleen	Musculus	C57BL/6JN	1	m	TMS
GAT_16-m-3	GAT_16	GAT	Musculus	C57BL/6JN	3	m	TMS
Spleen_38-f-12	Spleen_38	Spleen	Musculus	C57BL/6JN	12	f	TMS

Kidney_23-m-3	Kidney_23	Kidney	Mus musculus	C57BL/6JN	3	m	TMS
BAT_36-f-21	BAT_36	BAT	Mus musculus	C57BL/6JN	21	f	TMS
Lung_3-m-12	Lung_03	Lung	Mus musculus	C57BL/6JN	12	m	TMS
Heart_51-m-6	Heart_51	Heart	Mus musculus	C57BL/6JN	6	m	TMS
SCAT_43-m-3	SCAT_43	SCAT	Mus musculus	C57BL/6JN	3	m	TMS
Skin_25-m-27	Skin_25	Skin	Mus musculus	C57BL/6JN	27	m	TMS
MAT_56-m-18	MAT_56	MAT	Mus musculus	C57BL/6JN	18	m	TMS
GAT_14-f-6	GAT_14	GAT	Mus musculus	C57BL/6JN	6	f	TMS
GAT_23-m-15	GAT_23	GAT	Mus musculus	C57BL/6JN	15	m	TMS
Pancreas_6-m-6	Pancreas_06	Pancreas	Mus musculus	C57BL/6JN	6	m	TMS
Kidney_54-m-6	Kidney_54	Kidney	Mus musculus	C57BL/6JN	6	m	TMS
Limb_Muscle_50-f-6	Limb_Muscle_50	Limb_Muscle	Mus musculus	C57BL/6JN	6	f	TMS
Limb_Muscle_18-m-6	Limb_Muscle_18	Limb_Muscle	Mus musculus	C57BL/6JN	6	m	TMS
Limb_Muscle_28-f-21	Limb_Muscle_28	Limb_Muscle	Mus musculus	C57BL/6JN	21	f	TMS
MAT_31-m-27	MAT_31	MAT	Mus musculus	C57BL/6JN	27	m	TMS
GAT_50-m-1	GAT_50	GAT	Mus musculus	C57BL/6JN	1	m	TMS
Bone_50-f-6	Bone_50	Bone	Mus musculus	C57BL/6JN	6	f	TMS
Marrow_47-f-1	Marrow_47	Marrow	Mus musculus	C57BL/6JN	1	f	TMS
GAT_26-f-18	GAT_26	GAT	Mus musculus	C57BL/6JN	18	f	TMS
Pancreas_10-f-3	Pancreas_10	Pancreas	Mus musculus	C57BL/6JN	3	f	TMS
Bone_35-m-24	Bone_35	Bone	Mus musculus	C57BL/6JN	24	m	TMS
SCAT_31-m-21	SCAT_31	SCAT	Mus musculus	C57BL/6JN	21	m	TMS
Pancreas_8-m-9	Pancreas_08	Pancreas	Mus musculus	C57BL/6JN	9	m	TMS
Marrow_56-f-3	Marrow_56	Marrow	Mus musculus	C57BL/6JN	3	f	TMS
Limb_Muscle_52-f-12	Limb_Muscle_52	Limb_Muscle	Mus musculus	C57BL/6JN	12	f	TMS
Skin_29-f-9	Skin_29	Skin	Mus musculus	C57BL/6JN	9	f	TMS
MAT_32-f-21	MAT_32	MAT	Mus musculus	C57BL/6JN	21	f	TMS
Bone_45-m-15	Bone_45	Bone	Mus musculus	C57BL/6JN	15	m	TMS
GAT_29-m-27	GAT_29	GAT	Mus musculus	C57BL/6JN	27	m	TMS
GAT_54-m-21	GAT_54	GAT	Mus musculus	C57BL/6JN	21	m	TMS
SCAT_27-m-21	SCAT_27	SCAT	Mus musculus	C57BL/6JN	21	m	TMS
Bone_12-m-1	Bone_12	Bone	Mus musculus	C57BL/6JN	1	m	TMS
Heart_2-m-3	Heart_02	Heart	Mus musculus	C57BL/6JN	3	m	TMS
Pancreas_35-m-27	Pancreas_35	Pancreas	Mus musculus	C57BL/6JN	27	m	TMS
Liver_41-m-1	Liver_41	Liver	Mus musculus	C57BL/6JN	1	m	TMS
GAT_10A	GAT_10A	GAT	Mus musculus	C57BL/6J	4,5	m	Parabiosis
GAT_10B	GAT_10B	GAT	Mus musculus	C57BL/6J	4,5	m	Parabiosis

GAT_11A	GAT_11A	GAT	Mus musculus	C57BL/6J	19	m	Parabiosis
GAT_11B	GAT_11B	GAT	Mus musculus	C57BL/6-Tg(UBC-GFP)30Scha/J	4	m	Parabiosis
GAT_12A	GAT_12A	GAT	Mus musculus	C57BL/6J	19	m	Parabiosis
GAT_12B	GAT_12B	GAT	Mus musculus	C57BL/6-Tg(UBC-GFP)30Scha/J	4	m	Parabiosis
GAT_14A	GAT_14A	GAT	Mus musculus	C57BL/6J	19	m	Parabiosis
GAT_14B	GAT_14B	GAT	Mus musculus	C57BL/6-Tg(UBC-GFP)30Scha/J	4	m	Parabiosis
GAT_15A	GAT_15A	GAT	Mus musculus	C57BL/6J	3	m	Parabiosis
GAT_15B	GAT_15B	GAT	Mus musculus	C57BL/6J	3	m	Parabiosis
GAT_16A	GAT_16A	GAT	Mus musculus	C57BL/6J	3	m	Parabiosis
GAT_16B	GAT_16B	GAT	Mus musculus	C57BL/6J	3	m	Parabiosis
GAT_17A	GAT_17A	GAT	Mus musculus	C57BL/6J	4,5	m	Parabiosis
GAT_17B	GAT_17B	GAT	Mus musculus	C57BL/6J	4,5	m	Parabiosis
GAT_19A	GAT_19A	GAT	Mus musculus	C57BL/6JN	19	m	Parabiosis
GAT_19B	GAT_19B	GAT	Mus musculus	C57BL/6JN	19	m	Parabiosis
GAT_1A	GAT_1A	GAT	Mus musculus	C57BL/6J	19	m	Parabiosis
GAT_1B	GAT_1B	GAT	Mus musculus	C57BL/6-Tg(UBC-GFP)30Scha/J	4	m	Parabiosis
GAT_20A	GAT_20A	GAT	Mus musculus	C57BL/6JN	19	m	Parabiosis
GAT_20B	GAT_20B	GAT	Mus musculus	C57BL/6-Tg(UBC-GFP)30Scha/J	4	m	Parabiosis
GAT_2A	GAT_2A	GAT	Mus musculus	C57BL/6J	19	m	Parabiosis
GAT_2B	GAT_2B	GAT	Mus musculus	C57BL/6-Tg(UBC-GFP)30Scha/J	4	m	Parabiosis
GAT_5A	GAT_5A	GAT	Mus musculus	C57BL/6J	19	m	Parabiosis
GAT_5B	GAT_5B	GAT	Mus musculus	C57BL/6-Tg(UBC-GFP)30Scha/J	4	m	Parabiosis
GAT_6A	GAT_6A	GAT	Mus musculus	C57BL/6J	19	m	Parabiosis
GAT_6B	GAT_6B	GAT	Mus musculus	C57BL/6J	19	m	Parabiosis
GAT_7A	GAT_7A	GAT	Mus musculus	C57BL/6J	19	m	Parabiosis
GAT_7B	GAT_7B	GAT	Mus musculus	C57BL/6J	19	m	Parabiosis
GAT_9A	GAT_9A	GAT	Mus musculus	C57BL/6J	19	m	Parabiosis
GAT_9B	GAT_9B	GAT	Mus musculus	C57BL/6J	19	m	Parabiosis
H_10A	H_10A	Heart	Mus musculus	C57BL/6J	4,5	m	Parabiosis
H_10B	H_10B	Heart	Mus musculus	C57BL/6J	4,5	m	Parabiosis

H_11A	H_11A	Heart	Mus musculus	C57BL/6J	19	m	Parabiosis
H_11B	H_11B	Heart	Mus musculus	C57BL/6-Tg(UBC-GFP)30Scha/J	4	m	Parabiosis
H_12A	H_12A	Heart	Mus musculus	C57BL/6J	19	m	Parabiosis
H_12B	H_12B	Heart	Mus musculus	C57BL/6-Tg(UBC-GFP)30Scha/J	4	m	Parabiosis
H_14A	H_14A	Heart	Mus musculus	C57BL/6J	19	m	Parabiosis
H_14B	H_14B	Heart	Mus musculus	C57BL/6-Tg(UBC-GFP)30Scha/J	4	m	Parabiosis
H_15A	H_15A	Heart	Mus musculus	C57BL/6J	3	m	Parabiosis
H_15B	H_15B	Heart	Mus musculus	C57BL/6J	3	m	Parabiosis
H_16A	H_16A	Heart	Mus musculus	C57BL/6J	3	m	Parabiosis
H_16B	H_16B	Heart	Mus musculus	C57BL/6J	3	m	Parabiosis
H_17A	H_17A	Heart	Mus musculus	C57BL/6J	4,5	m	Parabiosis
H_17B	H_17B	Heart	Mus musculus	C57BL/6J	4,5	m	Parabiosis
H_19A	H_19A	Heart	Mus musculus	C57BL/6JN	19	m	Parabiosis
H_19B	H_19B	Heart	Mus musculus	C57BL/6JN	19	m	Parabiosis
H_1A	H_1A	Heart	Mus musculus	C57BL/6J	19	m	Parabiosis
H_1B	H_1B	Heart	Mus musculus	C57BL/6-Tg(UBC-GFP)30Scha/J	4	m	Parabiosis
H_20A	H_20A	Heart	Mus musculus	C57BL/6JN	19	m	Parabiosis
H_20B	H_20B	Heart	Mus musculus	C57BL/6-Tg(UBC-GFP)30Scha/J	4	m	Parabiosis
H_2A	H_2A	Heart	Mus musculus	C57BL/6J	19	m	Parabiosis
H_2B	H_2B	Heart	Mus musculus	C57BL/6-Tg(UBC-GFP)30Scha/J	4	m	Parabiosis
H_5A	H_5A	Heart	Mus musculus	C57BL/6J	19	m	Parabiosis
H_5B	H_5B	Heart	Mus musculus	C57BL/6-Tg(UBC-GFP)30Scha/J	4	m	Parabiosis
H_6A	H_6A	Heart	Mus musculus	C57BL/6J	19	m	Parabiosis
H_6B	H_6B	Heart	Mus musculus	C57BL/6J	19	m	Parabiosis
H_7A	H_7A	Heart	Mus musculus	C57BL/6J	19	m	Parabiosis
H_7B	H_7B	Heart	Mus musculus	C57BL/6J	19	m	Parabiosis
H_9A	H_9A	Heart	Mus musculus	C57BL/6J	19	m	Parabiosis
H_9B	H_9B	Heart	Mus musculus	C57BL/6J	19	m	Parabiosis
K_10A	K_10A	Kidney	Mus musculus	C57BL/6J	4,5	m	Parabiosis
K_10B	K_10B	Kidney	Mus musculus	C57BL/6J	4,5	m	Parabiosis

K_11A	K_11A	Kidney	Mus musculus	C57BL/6J	19	m	Parabiosis
K_11B	K_11B	Kidney	Mus musculus	C57BL/6-Tg(UBC-GFP)30Scha/J	4	m	Parabiosis
K_12A	K_12A	Kidney	Mus musculus	C57BL/6J	19	m	Parabiosis
K_12B	K_12B	Kidney	Mus musculus	C57BL/6-Tg(UBC-GFP)30Scha/J	4	m	Parabiosis
K_14A	K_14A	Kidney	Mus musculus	C57BL/6J	19	m	Parabiosis
K_14B	K_14B	Kidney	Mus musculus	C57BL/6-Tg(UBC-GFP)30Scha/J	4	m	Parabiosis
K_15A	K_15A	Kidney	Mus musculus	C57BL/6J	3	m	Parabiosis
K_15B	K_15B	Kidney	Mus musculus	C57BL/6J	3	m	Parabiosis
K_16A	K_16A	Kidney	Mus musculus	C57BL/6J	3	m	Parabiosis
K_16B	K_16B	Kidney	Mus musculus	C57BL/6J	3	m	Parabiosis
K_17A	K_17A	Kidney	Mus musculus	C57BL/6J	4,5	m	Parabiosis
K_17B	K_17B	Kidney	Mus musculus	C57BL/6J	4,5	m	Parabiosis
K_19A	K_19A	Kidney	Mus musculus	C57BL/6JN	19	m	Parabiosis
K_19B	K_19B	Kidney	Mus musculus	C57BL/6JN	19	m	Parabiosis
K_1A	K_1A	Kidney	Mus musculus	C57BL/6J	19	m	Parabiosis
K_1B	K_1B	Kidney	Mus musculus	C57BL/6-Tg(UBC-GFP)30Scha/J	4	m	Parabiosis
K_20A	K_20A	Kidney	Mus musculus	C57BL/6JN	19	m	Parabiosis
K_20B	K_20B	Kidney	Mus musculus	C57BL/6-Tg(UBC-GFP)30Scha/J	4	m	Parabiosis
K_2B	K_2B	Kidney	Mus musculus	C57BL/6-Tg(UBC-GFP)30Scha/J	4	m	Parabiosis
K_5A	K_5A	Kidney	Mus musculus	C57BL/6J	19	m	Parabiosis
K_5B	K_5B	Kidney	Mus musculus	C57BL/6-Tg(UBC-GFP)30Scha/J	4	m	Parabiosis
K_6A	K_6A	Kidney	Mus musculus	C57BL/6J	19	m	Parabiosis
K_6B	K_6B	Kidney	Mus musculus	C57BL/6J	19	m	Parabiosis
K_7A	K_7A	Kidney	Mus musculus	C57BL/6J	19	m	Parabiosis
K_7B	K_7B	Kidney	Mus musculus	C57BL/6J	19	m	Parabiosis
K_9A	K_9A	Kidney	Mus musculus	C57BL/6J	19	m	Parabiosis
K_9B	K_9B	Kidney	Mus musculus	C57BL/6J	19	m	Parabiosis
L_10A	L_10A	Liver	Mus musculus	C57BL/6J	4,5	m	Parabiosis
L_10B	L_10B	Liver	Mus musculus	C57BL/6J	4,5	m	Parabiosis
L_11A	L_11A	Liver	Mus musculus	C57BL/6J	19	m	Parabiosis

L_11B	L_11B	Liver	Mus musculus	C57BL/6-Tg(UBC-GFP)30Scha/J	4	m	Parabiosis
L_12A	L_12A	Liver	Mus musculus	C57BL/6J	19	m	Parabiosis
L_12B	L_12B	Liver	Mus musculus	C57BL/6-Tg(UBC-GFP)30Scha/J	4	m	Parabiosis
L_14A	L_14A	Liver	Mus musculus	C57BL/6J	19	m	Parabiosis
L_14B	L_14B	Liver	Mus musculus	C57BL/6-Tg(UBC-GFP)30Scha/J	4	m	Parabiosis
L_15A	L_15A	Liver	Mus musculus	C57BL/6J	3	m	Parabiosis
L_15B	L_15B	Liver	Mus musculus	C57BL/6J	3	m	Parabiosis
L_16A	L_16A	Liver	Mus musculus	C57BL/6J	3	m	Parabiosis
L_16B	L_16B	Liver	Mus musculus	C57BL/6J	3	m	Parabiosis
L_17A	L_17A	Liver	Mus musculus	C57BL/6J	4,5	m	Parabiosis
L_17B	L_17B	Liver	Mus musculus	C57BL/6J	4,5	m	Parabiosis
L_19A	L_19A	Liver	Mus musculus	C57BL/6JN	19	m	Parabiosis
L_19B	L_19B	Liver	Mus musculus	C57BL/6JN	19	m	Parabiosis
L_1A	L_1A	Liver	Mus musculus	C57BL/6J	19	m	Parabiosis
L_1B	L_1B	Liver	Mus musculus	C57BL/6-Tg(UBC-GFP)30Scha/J	4	m	Parabiosis
L_20A	L_20A	Liver	Mus musculus	C57BL/6JN	19	m	Parabiosis
L_20B	L_20B	Liver	Mus musculus	C57BL/6-Tg(UBC-GFP)30Scha/J	4	m	Parabiosis
L_2A	L_2A	Liver	Mus musculus	C57BL/6J	19	m	Parabiosis
L_2B	L_2B	Liver	Mus musculus	C57BL/6-Tg(UBC-GFP)30Scha/J	4	m	Parabiosis
L_5A	L_5A	Liver	Mus musculus	C57BL/6J	19	m	Parabiosis
L_5B	L_5B	Liver	Mus musculus	C57BL/6-Tg(UBC-GFP)30Scha/J	4	m	Parabiosis
L_6A	L_6A	Liver	Mus musculus	C57BL/6J	19	m	Parabiosis
L_6B	L_6B	Liver	Mus musculus	C57BL/6J	19	m	Parabiosis
L_7A	L_7A	Liver	Mus musculus	C57BL/6J	19	m	Parabiosis
L_7B	L_7B	Liver	Mus musculus	C57BL/6J	19	m	Parabiosis
L_9A	L_9A	Liver	Mus musculus	C57BL/6J	19	m	Parabiosis
L_9B	L_9B	Liver	Mus musculus	C57BL/6J	19	m	Parabiosis
MAT_10A	MAT_10A	MAT	Mus musculus	C57BL/6J	4,5	m	Parabiosis
MAT_10B	MAT_10B	MAT	Mus musculus	C57BL/6J	4,5	m	Parabiosis
MAT_11A	MAT_11A	MAT	Mus musculus	C57BL/6J	19	m	Parabiosis

MAT_11B	MAT_11B	MAT	Mus musculus	C57BL/6-Tg(UBC-GFP)30Scha/J	4	m	Parabiosis
MAT_12A	MAT_12A	MAT	Mus musculus	C57BL/6J	19	m	Parabiosis
MAT_14B	MAT_14B	MAT	Mus musculus	C57BL/6-Tg(UBC-GFP)30Scha/J	4	m	Parabiosis
MAT_15A	MAT_15A	MAT	Mus musculus	C57BL/6J	3	m	Parabiosis
MAT_15B	MAT_15B	MAT	Mus musculus	C57BL/6J	3	m	Parabiosis
MAT_16A	MAT_16A	MAT	Mus musculus	C57BL/6J	3	m	Parabiosis
MAT_16B	MAT_16B	MAT	Mus musculus	C57BL/6J	3	m	Parabiosis
MAT_17A	MAT_17A	MAT	Mus musculus	C57BL/6J	4,5	m	Parabiosis
MAT_17B	MAT_17B	MAT	Mus musculus	C57BL/6J	4,5	m	Parabiosis
MAT_19A	MAT_19A	MAT	Mus musculus	C57BL/6JN	19	m	Parabiosis
MAT_19B	MAT_19B	MAT	Mus musculus	C57BL/6JN	19	m	Parabiosis
MAT_1A	MAT_1A	MAT	Mus musculus	C57BL/6J	19	m	Parabiosis
MAT_1B	MAT_1B	MAT	Mus musculus	C57BL/6-Tg(UBC-GFP)30Scha/J	4	m	Parabiosis
MAT_20A	MAT_20A	MAT	Mus musculus	C57BL/6JN	19	m	Parabiosis
MAT_20B	MAT_20B	MAT	Mus musculus	C57BL/6-Tg(UBC-GFP)30Scha/J	4	m	Parabiosis
MAT_2A	MAT_2A	MAT	Mus musculus	C57BL/6J	19	m	Parabiosis
MAT_2B	MAT_2B	MAT	Mus musculus	C57BL/6-Tg(UBC-GFP)30Scha/J	4	m	Parabiosis
MAT_5A	MAT_5A	MAT	Mus musculus	C57BL/6J	19	m	Parabiosis
MAT_5B	MAT_5B	MAT	Mus musculus	C57BL/6-Tg(UBC-GFP)30Scha/J	4	m	Parabiosis
MAT_6A	MAT_6A	MAT	Mus musculus	C57BL/6J	19	m	Parabiosis
MAT_6B	MAT_6B	MAT	Mus musculus	C57BL/6J	19	m	Parabiosis
MAT_7A	MAT_7A	MAT	Mus musculus	C57BL/6J	19	m	Parabiosis
MAT_7B	MAT_7B	MAT	Mus musculus	C57BL/6J	19	m	Parabiosis
MAT_9A	MAT_9A	MAT	Mus musculus	C57BL/6J	19	m	Parabiosis
TA_10A	TA_10A	Limb_Muscle	Mus musculus	C57BL/6J	4,5	m	Parabiosis
TA_10B	TA_10B	Limb_Muscle	Mus musculus	C57BL/6J	4,5	m	Parabiosis
TA_11A	TA_11A	Limb_Muscle	Mus musculus	C57BL/6J	19	m	Parabiosis
TA_11B	TA_11B	Limb_Muscle	Mus musculus	C57BL/6-Tg(UBC-GFP)30Scha/J	4	m	Parabiosis
TA_12A	TA_12A	Limb_Muscle	Mus musculus	C57BL/6J	19	m	Parabiosis
TA_12B	TA_12B	Limb_Muscle	Mus musculus	C57BL/6-Tg(UBC-GFP)30Scha/J	4	m	Parabiosis

TA_14A	TA_14A	Limb_Muscle	Mus musculus	C57BL/6J	19	m	Parabiosis
TA_14B	TA_14B	Limb_Muscle	Mus musculus	C57BL/6-Tg(UBC-GFP)30Scha/J	4	m	Parabiosis
TA_15A	TA_15A	Limb_Muscle	Mus musculus	C57BL/6J	3	m	Parabiosis
TA_15B	TA_15B	Limb_Muscle	Mus musculus	C57BL/6J	3	m	Parabiosis
TA_16A	TA_16A	Limb_Muscle	Mus musculus	C57BL/6J	3	m	Parabiosis
TA_16B	TA_16B	Limb_Muscle	Mus musculus	C57BL/6J	3	m	Parabiosis
TA_17A	TA_17A	Limb_Muscle	Mus musculus	C57BL/6J	4,5	m	Parabiosis
TA_17B	TA_17B	Limb_Muscle	Mus musculus	C57BL/6J	4,5	m	Parabiosis
TA_19A	TA_19A	Limb_Muscle	Mus musculus	C57BL/6JN	19	m	Parabiosis
TA_19B	TA_19B	Limb_Muscle	Mus musculus	C57BL/6JN	19	m	Parabiosis
TA_1A	TA_1A	Limb_Muscle	Mus musculus	C57BL/6J	19	m	Parabiosis
TA_1B	TA_1B	Limb_Muscle	Mus musculus	C57BL/6-Tg(UBC-GFP)30Scha/J	4	m	Parabiosis
TA_20A	TA_20A	Limb_Muscle	Mus musculus	C57BL/6JN	19	m	Parabiosis
TA_20B	TA_20B	Limb_Muscle	Mus musculus	C57BL/6-Tg(UBC-GFP)30Scha/J	4	m	Parabiosis
TA_2A	TA_2A	Limb_Muscle	Mus musculus	C57BL/6J	19	m	Parabiosis
TA_2B	TA_2B	Limb_Muscle	Mus musculus	C57BL/6-Tg(UBC-GFP)30Scha/J	4	m	Parabiosis
TA_5A	TA_5A	Limb_Muscle	Mus musculus	C57BL/6J	19	m	Parabiosis
TA_5B	TA_5B	Limb_Muscle	Mus musculus	C57BL/6-Tg(UBC-GFP)30Scha/J	4	m	Parabiosis
TA_6A	TA_6A	Limb_Muscle	Mus musculus	C57BL/6J	19	m	Parabiosis
TA_6B	TA_6B	Limb_Muscle	Mus musculus	C57BL/6J	19	m	Parabiosis
TA_7A	TA_7A	Limb_Muscle	Mus musculus	C57BL/6J	19	m	Parabiosis
TA_7B	TA_7B	Limb_Muscle	Mus musculus	C57BL/6J	19	m	Parabiosis
TA_9A	TA_9A	Limb_Muscle	Mus musculus	C57BL/6J	19	m	Parabiosis
TA_9B	TA_9B	Limb_Muscle	Mus musculus	C57BL/6J	19	m	Parabiosis

Table 2: Sample metadata table brain aging cohort¹.

Metadata for all samples analyzed in the brain aging cohort.

sample identifier	cohort	brain region	age	sex	strain	organism
CA1_olf_1	CA1	Olfactory bulb	12	f	C57BL/6JN	Mus musculus
CA1_olf_2	CA1	Olfactory bulb	26	m	C57BL/6JN	Mus musculus
CA1_olf_3	CA1	Olfactory bulb	12	m	C57BL/6JN	Mus musculus
CA1_olf_4	CA1	Olfactory bulb	12	f	C57BL/6JN	Mus musculus
CA1_olf_5	CA1	Olfactory bulb	26	m	C57BL/6JN	Mus musculus
CA1_olf_6	CA1	Olfactory bulb	12	m	C57BL/6JN	Mus musculus
CA1_olf_7	CA1	Olfactory bulb	12	f	C57BL/6JN	Mus musculus
CA1_olf_8	CA1	Olfactory bulb	26	m	C57BL/6JN	Mus musculus
CA1_cor_22	CA1	Motor cortex	15	m	C57BL/6JN	Mus musculus
CA1_cor_23	CA1	Motor cortex	18	m	C57BL/6JN	Mus musculus
CA1_cor_24	CA1	Motor cortex	21	m	C57BL/6JN	Mus musculus
CA1_cor_25	CA1	Motor cortex	3	m	C57BL/6JN	Mus musculus
CA1_cor_26	CA1	Motor cortex	15	m	C57BL/6JN	Mus musculus
CA1_cor_27	CA1	Motor cortex	18	m	C57BL/6JN	Mus musculus
CA1_cor_28	CA1	Motor cortex	21	m	C57BL/6JN	Mus musculus
CA1_cor_29	CA1	Motor cortex	3	m	C57BL/6JN	Mus musculus
CA1_olf_17	CA1	Olfactory bulb	3	m	C57BL/6JN	Mus musculus
CA1_olf_18	CA1	Olfactory bulb	15	m	C57BL/6JN	Mus musculus
CA1_olf_19	CA1	Olfactory bulb	18	m	C57BL/6JN	Mus musculus
CA1_olf_20	CA1	Olfactory bulb	21	m	C57BL/6JN	Mus musculus
CA1_olf_21	CA1	Olfactory bulb	3	m	C57BL/6JN	Mus musculus
CA1_olf_22	CA1	Olfactory bulb	15	m	C57BL/6JN	Mus musculus
CA1_olf_23	CA1	Olfactory bulb	18	m	C57BL/6JN	Mus musculus
CA1_olf_24	CA1	Olfactory bulb	21	m	C57BL/6JN	Mus musculus
CA1_cor_30	CA1	Motor cortex	15	m	C57BL/6JN	Mus musculus
CA1_cor_31	CA1	Motor cortex	18	m	C57BL/6JN	Mus musculus
CA1_cor_32	CA1	Motor cortex	21	m	C57BL/6JN	Mus musculus
CA1_cor_33	CA1	Motor cortex	3	m	C57BL/6JN	Mus musculus
CA1_cor_34	CA1	Motor cortex	15	m	C57BL/6JN	Mus musculus
CA1_cor_35	CA1	Motor cortex	18	m	C57BL/6JN	Mus musculus
CA1_cor_36	CA1	Motor cortex	21	m	C57BL/6JN	Mus musculus
CA1_cor_37	CA1	Motor cortex	3	f	C57BL/6JN	Mus musculus
CA1_olf_33	CA1	Olfactory bulb	3	m	C57BL/6JN	Mus musculus
CA1_olf_34	CA1	Olfactory bulb	15	m	C57BL/6JN	Mus musculus
CA1_olf_35	CA1	Olfactory bulb	18	m	C57BL/6JN	Mus musculus
CA1_olf_36	CA1	Olfactory bulb	21	m	C57BL/6JN	Mus musculus
CA1_olf_37	CA1	Olfactory bulb	3	f	C57BL/6JN	Mus musculus
CA1_olf_38	CA1	Olfactory bulb	15	f	C57BL/6JN	Mus musculus
CA1_olf_39	CA1	Olfactory bulb	18	f	C57BL/6JN	Mus musculus
CA1_olf_40	CA1	Olfactory bulb	21	f	C57BL/6JN	Mus musculus

CA1_olf_41	CA1	Olfactory bulb	3	f	C57BL/6JN	Mus musculus
CA1_olf_42	CA1	Olfactory bulb	15	f	C57BL/6JN	Mus musculus
CA1_olf_43	CA1	Olfactory bulb	18	f	C57BL/6JN	Mus musculus
CA1_olf_44	CA1	Olfactory bulb	21	f	C57BL/6JN	Mus musculus
CA1_olf_45	CA1	Olfactory bulb	3	f	C57BL/6JN	Mus musculus
CA1_olf_46	CA1	Olfactory bulb	15	f	C57BL/6JN	Mus musculus
CA1_olf_47	CA1	Olfactory bulb	18	f	C57BL/6JN	Mus musculus
CA1_olf_48	CA1	Olfactory bulb	21	f	C57BL/6JN	Mus musculus
CA1_olf_49	CA1	Olfactory bulb	3	f	C57BL/6JN	Mus musculus
CA1_olf_50	CA1	Olfactory bulb	15	f	C57BL/6JN	Mus musculus
CA1_olf_51	CA1	Olfactory bulb	18	f	C57BL/6JN	Mus musculus
CA1_olf_52	CA1	Olfactory bulb	21	f	C57BL/6JN	Mus musculus
CA1_olf_53	CA1	Olfactory bulb	3	f	C57BL/6JN	Mus musculus
CA1_olf_54	CA1	Olfactory bulb	15	f	C57BL/6JN	Mus musculus
CA1_olf_55	CA1	Olfactory bulb	18	f	C57BL/6JN	Mus musculus
CA1_olf_56	CA1	Olfactory bulb	21	f	C57BL/6JN	Mus musculus
CA1_olf_57	CA1	Olfactory bulb	28	m	C57BL/6JN	Mus musculus
CA1_olf_58	CA1	Olfactory bulb	28	m	C57BL/6JN	Mus musculus
CA1_olf_59	CA1	Olfactory bulb	28	m	C57BL/6JN	Mus musculus
CA1_cor_1	CA1	Motor cortex	12	f	C57BL/6JN	Mus musculus
CA1_cor_2	CA1	Motor cortex	26	m	C57BL/6JN	Mus musculus
CA1_cor_3	CA1	Motor cortex	12	m	C57BL/6JN	Mus musculus
CA1_cor_4	CA1	Motor cortex	12	f	C57BL/6JN	Mus musculus
CA1_cor_5	CA1	Motor cortex	26	m	C57BL/6JN	Mus musculus
CA1_olf_9	CA1	Olfactory bulb	12	m	C57BL/6JN	Mus musculus
CA1_olf_10	CA1	Olfactory bulb	12	f	C57BL/6JN	Mus musculus
CA1_olf_11	CA1	Olfactory bulb	26	m	C57BL/6JN	Mus musculus
CA1_olf_13	CA1	Olfactory bulb	12	f	C57BL/6JN	Mus musculus
CA1_olf_14	CA1	Olfactory bulb	26	m	C57BL/6JN	Mus musculus
CA1_olf_15	CA1	Olfactory bulb	12	m	C57BL/6JN	Mus musculus
CA1_olf_16	CA1	Olfactory bulb	21	m	C57BL/6JN	Mus musculus
CA1_cor_6	CA1	Motor cortex	12	m	C57BL/6JN	Mus musculus
CA1_cor_7	CA1	Motor cortex	12	f	C57BL/6JN	Mus musculus
CA1_cor_8	CA1	Motor cortex	26	m	C57BL/6JN	Mus musculus
CA1_cor_9	CA1	Motor cortex	12	m	C57BL/6JN	Mus musculus
CA1_cor_10	CA1	Motor cortex	12	f	C57BL/6JN	Mus musculus
CA1_cor_11	CA1	Motor cortex	26	m	C57BL/6JN	Mus musculus
CA1_cor_12	CA1	Motor cortex	12	m	C57BL/6JN	Mus musculus
CA1_cor_13	CA1	Motor cortex	12	f	C57BL/6JN	Mus musculus
CA1_olf_25	CA1	Olfactory bulb	3	m	C57BL/6JN	Mus musculus
CA1_olf_26	CA1	Olfactory bulb	15	m	C57BL/6JN	Mus musculus
CA1_olf_27	CA1	Olfactory bulb	18	m	C57BL/6JN	Mus musculus
CA1_olf_28	CA1	Olfactory bulb	21	m	C57BL/6JN	Mus musculus

CA1_olf_29	CA1	Olfactory bulb	3	m	C57BL/6JN	Mus musculus
CA1_olf_30	CA1	Olfactory bulb	15	m	C57BL/6JN	Mus musculus
CA1_olf_31	CA1	Olfactory bulb	18	m	C57BL/6JN	Mus musculus
CA1_olf_32	CA1	Olfactory bulb	21	m	C57BL/6JN	Mus musculus
CA1_cor_14	CA1	Motor cortex	26	m	C57BL/6JN	Mus musculus
CA1_cor_15	CA1	Motor cortex	12	m	C57BL/6JN	Mus musculus
CA1_cor_16	CA1	Motor cortex	21	m	C57BL/6JN	Mus musculus
CA1_cor_17	CA1	Motor cortex	3	m	C57BL/6JN	Mus musculus
CA1_cor_18	CA1	Motor cortex	15	m	C57BL/6JN	Mus musculus
CA1_cor_19	CA1	Motor cortex	18	m	C57BL/6JN	Mus musculus
CA1_cor_20	CA1	Motor cortex	21	m	C57BL/6JN	Mus musculus
CA1_cor_21	CA1	Motor cortex	3	m	C57BL/6JN	Mus musculus
CA1_cor_38	CA1	Motor cortex	15	f	C57BL/6JN	Mus musculus
CA1_cor_39	CA1	Motor cortex	18	f	C57BL/6JN	Mus musculus
CA1_cor_40	CA1	Motor cortex	21	f	C57BL/6JN	Mus musculus
CA1_cor_41	CA1	Motor cortex	3	f	C57BL/6JN	Mus musculus
CA1_cor_42	CA1	Motor cortex	15	f	C57BL/6JN	Mus musculus
CA1_cor_43	CA1	Motor cortex	18	f	C57BL/6JN	Mus musculus
CA1_cor_44	CA1	Motor cortex	21	f	C57BL/6JN	Mus musculus
CA1_cor_45	CA1	Motor cortex	3	f	C57BL/6JN	Mus musculus
CA1_cor_46	CA1	Motor cortex	15	f	C57BL/6JN	Mus musculus
CA1_cor_47	CA1	Motor cortex	18	f	C57BL/6JN	Mus musculus
CA1_cor_48	CA1	Motor cortex	21	f	C57BL/6JN	Mus musculus
CA1_cor_49	CA1	Motor cortex	3	f	C57BL/6JN	Mus musculus
CA1_cor_50	CA1	Motor cortex	15	f	C57BL/6JN	Mus musculus
CA1_cor_51	CA1	Motor cortex	18	f	C57BL/6JN	Mus musculus
CA1_cor_52	CA1	Motor cortex	21	f	C57BL/6JN	Mus musculus
CA1_cor_53	CA1	Motor cortex	3	f	C57BL/6JN	Mus musculus
CA1_cor_54	CA1	Motor cortex	15	f	C57BL/6JN	Mus musculus
CA1_cor_55	CA1	Motor cortex	18	f	C57BL/6JN	Mus musculus
CA1_cor_56	CA1	Motor cortex	21	f	C57BL/6JN	Mus musculus
CA1_cor_57	CA1	Motor cortex	28	m	C57BL/6JN	Mus musculus
CA1_cor_58	CA1	Motor cortex	28	m	C57BL/6JN	Mus musculus
CA1_cor_59	CA1	Motor cortex	28	m	C57BL/6JN	Mus musculus
CA1_cp_1	CA1	Caudate putamen	12	f	C57BL/6JN	Mus musculus
CA1_cp_2	CA1	Caudate putamen	26	m	C57BL/6JN	Mus musculus
CA1_cp_3	CA1	Caudate putamen	12	m	C57BL/6JN	Mus musculus
CA1_cp_4	CA1	Caudate putamen	12	f	C57BL/6JN	Mus musculus
CA1_cp_5	CA1	Caudate putamen	26	m	C57BL/6JN	Mus musculus
CA1_cp_6	CA1	Caudate putamen	12	m	C57BL/6JN	Mus musculus
CA1_cp_7	CA1	Caudate putamen	12	f	C57BL/6JN	Mus musculus
CA1_cp_8	CA1	Caudate putamen	26	m	C57BL/6JN	Mus musculus
CA1_cp_9	CA1	Caudate putamen	12	m	C57BL/6JN	Mus musculus

CA1_cp_10	CA1	Caudate putamen	12	f	C57BL/6JN	Mus musculus
CA1_cp_11	CA1	Caudate putamen	26	m	C57BL/6JN	Mus musculus
CA1_cp_12	CA1	Caudate putamen	12	m	C57BL/6JN	Mus musculus
CA1_cp_13	CA1	Caudate putamen	12	f	C57BL/6JN	Mus musculus
CA1_cp_14	CA1	Caudate putamen	26	m	C57BL/6JN	Mus musculus
CA1_cp_15	CA1	Caudate putamen	12	m	C57BL/6JN	Mus musculus
CA1_cp_16	CA1	Caudate putamen	21	m	C57BL/6JN	Mus musculus
CA1_cp_17	CA1	Caudate putamen	3	m	C57BL/6JN	Mus musculus
CA1_cp_18	CA1	Caudate putamen	15	m	C57BL/6JN	Mus musculus
CA1_cp_19	CA1	Caudate putamen	18	m	C57BL/6JN	Mus musculus
CA1_cp_20	CA1	Caudate putamen	21	m	C57BL/6JN	Mus musculus
CA1_cp_21	CA1	Caudate putamen	3	m	C57BL/6JN	Mus musculus
CA1_cp_22	CA1	Caudate putamen	15	m	C57BL/6JN	Mus musculus
CA1_cp_23	CA1	Caudate putamen	18	m	C57BL/6JN	Mus musculus
CA1_cp_24	CA1	Caudate putamen	21	m	C57BL/6JN	Mus musculus
CA1_cp_26	CA1	Caudate putamen	15	m	C57BL/6JN	Mus musculus
CA1_cp_27	CA1	Caudate putamen	18	m	C57BL/6JN	Mus musculus
CA1_cp_28	CA1	Caudate putamen	21	m	C57BL/6JN	Mus musculus
CA1_cp_29	CA1	Caudate putamen	3	m	C57BL/6JN	Mus musculus
CA1_cp_30	CA1	Caudate putamen	15	m	C57BL/6JN	Mus musculus
CA1_cp_31	CA1	Caudate putamen	18	m	C57BL/6JN	Mus musculus
CA1_cp_32	CA1	Caudate putamen	21	m	C57BL/6JN	Mus musculus
CA1_cp_33	CA1	Caudate putamen	3	m	C57BL/6JN	Mus musculus
CA1_cp_35	CA1	Caudate putamen	18	m	C57BL/6JN	Mus musculus
CA1_cp_36	CA1	Caudate putamen	21	m	C57BL/6JN	Mus musculus
CA1_cp_37	CA1	Caudate putamen	3	f	C57BL/6JN	Mus musculus
CA1_cp_38	CA1	Caudate putamen	15	f	C57BL/6JN	Mus musculus
CA1_cp_39	CA1	Caudate putamen	18	f	C57BL/6JN	Mus musculus
CA1_cp_40	CA1	Caudate putamen	21	f	C57BL/6JN	Mus musculus
CA1_cp_41	CA1	Caudate putamen	3	f	C57BL/6JN	Mus musculus
CA1_cp_42	CA1	Caudate putamen	15	f	C57BL/6JN	Mus musculus
CA1_cp_43	CA1	Caudate putamen	18	f	C57BL/6JN	Mus musculus
CA1_cp_44	CA1	Caudate putamen	21	f	C57BL/6JN	Mus musculus
CA1_cp_45	CA1	Caudate putamen	3	f	C57BL/6JN	Mus musculus
CA1_cp_46	CA1	Caudate putamen	15	f	C57BL/6JN	Mus musculus
CA1_cp_47	CA1	Caudate putamen	18	f	C57BL/6JN	Mus musculus
CA1_cp_48	CA1	Caudate putamen	21	f	C57BL/6JN	Mus musculus
CA1_cp_49	CA1	Caudate putamen	3	f	C57BL/6JN	Mus musculus
CA1_cp_50	CA1	Caudate putamen	15	f	C57BL/6JN	Mus musculus
CA1_cp_51	CA1	Caudate putamen	18	f	C57BL/6JN	Mus musculus
CA1_cp_52	CA1	Caudate putamen	21	f	C57BL/6JN	Mus musculus
CA1_cp_53	CA1	Caudate putamen	3	f	C57BL/6JN	Mus musculus
CA1_cp_54	CA1	Caudate putamen	15	f	C57BL/6JN	Mus musculus

CA1_cp_55	CA1	Caudate putamen	18	f	C57BL/6JN	Mus musculus
CA1_cp_56	CA1	Caudate putamen	21	f	C57BL/6JN	Mus musculus
CA1_cp_57	CA1	Caudate putamen	28	m	C57BL/6JN	Mus musculus
CA1_cp_58	CA1	Caudate putamen	28	m	C57BL/6JN	Mus musculus
CA1_cp_59	CA1	Caudate putamen	28	m	C57BL/6JN	Mus musculus
CA1_svz_1	CA1	Subventricular zone	12	f	C57BL/6JN	Mus musculus
CA1_svz_2	CA1	Subventricular zone	26	m	C57BL/6JN	Mus musculus
CA1_svz_3	CA1	Subventricular zone	12	m	C57BL/6JN	Mus musculus
CA1_svz_4	CA1	Subventricular zone	12	f	C57BL/6JN	Mus musculus
CA1_svz_5	CA1	Subventricular zone	26	m	C57BL/6JN	Mus musculus
CA1_svz_6	CA1	Subventricular zone	12	m	C57BL/6JN	Mus musculus
CA1_svz_7	CA1	Subventricular zone	12	f	C57BL/6JN	Mus musculus
CA1_svz_9	CA1	Subventricular zone	12	m	C57BL/6JN	Mus musculus
CA1_svz_10	CA1	Subventricular zone	12	f	C57BL/6JN	Mus musculus
CA1_svz_11	CA1	Subventricular zone	26	m	C57BL/6JN	Mus musculus
CA1_svz_12	CA1	Subventricular zone	12	m	C57BL/6JN	Mus musculus
CA1_svz_13	CA1	Subventricular zone	12	f	C57BL/6JN	Mus musculus
CA1_svz_14	CA1	Subventricular zone	26	m	C57BL/6JN	Mus musculus
CA1_svz_15	CA1	Subventricular zone	12	m	C57BL/6JN	Mus musculus
CA1_svz_16	CA1	Subventricular zone	21	m	C57BL/6JN	Mus musculus
CA1_svz_17	CA1	Subventricular zone	3	m	C57BL/6JN	Mus musculus
CA1_svz_18	CA1	Subventricular zone	15	m	C57BL/6JN	Mus musculus
CA1_svz_19	CA1	Subventricular zone	18	m	C57BL/6JN	Mus musculus
CA1_svz_20	CA1	Subventricular zone	21	m	C57BL/6JN	Mus musculus
CA1_svz_21	CA1	Subventricular zone	3	m	C57BL/6JN	Mus musculus
CA1_svz_22	CA1	Subventricular zone	15	m	C57BL/6JN	Mus musculus
CA1_svz_23	CA1	Subventricular zone	18	m	C57BL/6JN	Mus musculus
CA1_svz_24	CA1	Subventricular zone	21	m	C57BL/6JN	Mus musculus
CA1_svz_25	CA1	Subventricular zone	3	m	C57BL/6JN	Mus musculus
CA1_svz_26	CA1	Subventricular zone	15	m	C57BL/6JN	Mus musculus
CA1_svz_27	CA1	Subventricular zone	18	m	C57BL/6JN	Mus musculus
CA1_svz_28	CA1	Subventricular zone	21	m	C57BL/6JN	Mus musculus
CA1_svz_29	CA1	Subventricular zone	3	m	C57BL/6JN	Mus musculus
CA1_svz_30	CA1	Subventricular zone	15	m	C57BL/6JN	Mus musculus
CA1_svz_31	CA1	Subventricular zone	18	m	C57BL/6JN	Mus musculus
CA1_svz_32	CA1	Subventricular zone	21	m	C57BL/6JN	Mus musculus
CA1_svz_33	CA1	Subventricular zone	3	m	C57BL/6JN	Mus musculus
CA1_svz_34	CA1	Subventricular zone	15	m	C57BL/6JN	Mus musculus
CA1_svz_35	CA1	Subventricular zone	18	m	C57BL/6JN	Mus musculus
CA1_svz_36	CA1	Subventricular zone	21	m	C57BL/6JN	Mus musculus
CA1_svz_37	CA1	Subventricular zone	3	f	C57BL/6JN	Mus musculus
CA1_svz_38	CA1	Subventricular zone	15	f	C57BL/6JN	Mus musculus
CA1_svz_39	CA1	Subventricular zone	18	f	C57BL/6JN	Mus musculus

CA1 svz 40	CA1	Subventricular zone	21	f	C57BL/6JN	Mus musculus
CA1 svz 41	CA1	Subventricular zone	3	f	C57BL/6JN	Mus musculus
CA1 svz 42	CA1	Subventricular zone	15	f	C57BL/6JN	Mus musculus
CA1 svz 43	CA1	Subventricular zone	18	f	C57BL/6JN	Mus musculus
CA1 svz 44	CA1	Subventricular zone	21	f	C57BL/6JN	Mus musculus
CA1 svz 45	CA1	Subventricular zone	3	f	C57BL/6JN	Mus musculus
CA1 svz 46	CA1	Subventricular zone	15	f	C57BL/6JN	Mus musculus
CA1 svz 47	CA1	Subventricular zone	18	f	C57BL/6JN	Mus musculus
CA1 svz 48	CA1	Subventricular zone	21	f	C57BL/6JN	Mus musculus
CA1 svz 49	CA1	Subventricular zone	3	f	C57BL/6JN	Mus musculus
CA1 svz 50	CA1	Subventricular zone	15	f	C57BL/6JN	Mus musculus
CA1 svz 51	CA1	Subventricular zone	18	f	C57BL/6JN	Mus musculus
CA1 svz 52	CA1	Subventricular zone	21	f	C57BL/6JN	Mus musculus
CA1 svz 53	CA1	Subventricular zone	3	f	C57BL/6JN	Mus musculus
CA1 svz 54	CA1	Subventricular zone	15	f	C57BL/6JN	Mus musculus
CA1 svz 55	CA1	Subventricular zone	18	f	C57BL/6JN	Mus musculus
CA1 svz 56	CA1	Subventricular zone	21	f	C57BL/6JN	Mus musculus
CA1 svz 57	CA1	Subventricular zone	28	m	C57BL/6JN	Mus musculus
CA1 svz 58	CA1	Subventricular zone	28	m	C57BL/6JN	Mus musculus
CA1 svz 59	CA1	Subventricular zone	28	m	C57BL/6JN	Mus musculus
CA1 cc 3	CA1	Corpus callosum	12	m	C57BL/6JN	Mus musculus
CA1 cc 4	CA1	Corpus callosum	12	f	C57BL/6JN	Mus musculus
CA1 cc 5	CA1	Corpus callosum	26	m	C57BL/6JN	Mus musculus
CA1 cc 6	CA1	Corpus callosum	12	m	C57BL/6JN	Mus musculus
CA1 cc 7	CA1	Corpus callosum	12	f	C57BL/6JN	Mus musculus
CA1 cc 8	CA1	Corpus callosum	26	m	C57BL/6JN	Mus musculus
CA1 cc 9	CA1	Corpus callosum	12	m	C57BL/6JN	Mus musculus
CA1 cc 10	CA1	Corpus callosum	12	f	C57BL/6JN	Mus musculus
CA1 cc 11	CA1	Corpus callosum	26	m	C57BL/6JN	Mus musculus
CA1 cc 12	CA1	Corpus callosum	12	m	C57BL/6JN	Mus musculus
CA1 cc 13	CA1	Corpus callosum	12	f	C57BL/6JN	Mus musculus
CA1 cc 14	CA1	Corpus callosum	26	m	C57BL/6JN	Mus musculus
CA1 cc 15	CA1	Corpus callosum	12	m	C57BL/6JN	Mus musculus
CA1 cc 16	CA1	Corpus callosum	21	m	C57BL/6JN	Mus musculus
CA1 cc 17	CA1	Corpus callosum	3	m	C57BL/6JN	Mus musculus
CA1 cc 18	CA1	Corpus callosum	15	m	C57BL/6JN	Mus musculus
CA1 cc 19	CA1	Corpus callosum	18	m	C57BL/6JN	Mus musculus
CA1 cc 20	CA1	Corpus callosum	21	m	C57BL/6JN	Mus musculus
CA1 cc 21	CA1	Corpus callosum	3	m	C57BL/6JN	Mus musculus
CA1 cc 22	CA1	Corpus callosum	15	m	C57BL/6JN	Mus musculus
CA1 cc 23	CA1	Corpus callosum	18	m	C57BL/6JN	Mus musculus
CA1 cc 24	CA1	Corpus callosum	21	m	C57BL/6JN	Mus musculus
CA1 cc 25	CA1	Corpus callosum	3	m	C57BL/6JN	Mus musculus

CA1_cc_26	CA1	Corpus callosum	15	m	C57BL/6JN	Mus musculus
CA1_cc_27	CA1	Corpus callosum	18	m	C57BL/6JN	Mus musculus
CA1_cc_28	CA1	Corpus callosum	21	m	C57BL/6JN	Mus musculus
CA1_cc_29	CA1	Corpus callosum	3	m	C57BL/6JN	Mus musculus
CA1_cc_30	CA1	Corpus callosum	15	m	C57BL/6JN	Mus musculus
CA1_cc_31	CA1	Corpus callosum	18	m	C57BL/6JN	Mus musculus
CA1_cc_32	CA1	Corpus callosum	21	m	C57BL/6JN	Mus musculus
CA1_cc_33	CA1	Corpus callosum	3	m	C57BL/6JN	Mus musculus
CA1_cc_34	CA1	Corpus callosum	15	m	C57BL/6JN	Mus musculus
CA1_cc_35	CA1	Corpus callosum	18	m	C57BL/6JN	Mus musculus
CA1_cc_36	CA1	Corpus callosum	21	m	C57BL/6JN	Mus musculus
CA1_cc_37	CA1	Corpus callosum	3	f	C57BL/6JN	Mus musculus
CA1_cc_38	CA1	Corpus callosum	15	f	C57BL/6JN	Mus musculus
CA1_cc_39	CA1	Corpus callosum	18	f	C57BL/6JN	Mus musculus
CA1_cc_40	CA1	Corpus callosum	21	f	C57BL/6JN	Mus musculus
CA1_cc_41	CA1	Corpus callosum	3	f	C57BL/6JN	Mus musculus
CA1_cc_42	CA1	Corpus callosum	15	f	C57BL/6JN	Mus musculus
CA1_cc_43	CA1	Corpus callosum	18	f	C57BL/6JN	Mus musculus
CA1_cc_44	CA1	Corpus callosum	21	f	C57BL/6JN	Mus musculus
CA1_cc_45	CA1	Corpus callosum	3	f	C57BL/6JN	Mus musculus
CA1_cc_46	CA1	Corpus callosum	15	f	C57BL/6JN	Mus musculus
CA1_cc_47	CA1	Corpus callosum	18	f	C57BL/6JN	Mus musculus
CA1_cc_48	CA1	Corpus callosum	21	f	C57BL/6JN	Mus musculus
CA1_cc_49	CA1	Corpus callosum	3	f	C57BL/6JN	Mus musculus
CA1_cc_50	CA1	Corpus callosum	15	f	C57BL/6JN	Mus musculus
CA1_cc_51	CA1	Corpus callosum	18	f	C57BL/6JN	Mus musculus
CA1_cc_52	CA1	Corpus callosum	21	f	C57BL/6JN	Mus musculus
CA1_cc_53	CA1	Corpus callosum	3	f	C57BL/6JN	Mus musculus
CA1_cc_54	CA1	Corpus callosum	15	f	C57BL/6JN	Mus musculus
CA1_cc_55	CA1	Corpus callosum	18	f	C57BL/6JN	Mus musculus
CA1_cc_56	CA1	Corpus callosum	21	f	C57BL/6JN	Mus musculus
CA1_cc_57	CA1	Corpus callosum	28	m	C57BL/6JN	Mus musculus
CA1_cc_58	CA1	Corpus callosum	28	m	C57BL/6JN	Mus musculus
CA1_cc_59	CA1	Corpus callosum	28	m	C57BL/6JN	Mus musculus
CA1_th_1	CA1	Thalamus	12	f	C57BL/6JN	Mus musculus
CA1_hi_2	CA1	Hippocampus (anterior)	26	m	C57BL/6JN	Mus musculus
CA1_th_3	CA1	Thalamus	12	m	C57BL/6JN	Mus musculus
CA1_th_4	CA1	Thalamus	12	f	C57BL/6JN	Mus musculus
CA1_th_5	CA1	Thalamus	26	m	C57BL/6JN	Mus musculus
CA1_th_6	CA1	Thalamus	12	m	C57BL/6JN	Mus musculus
CA1_th_7	CA1	Thalamus	12	f	C57BL/6JN	Mus musculus
CA1_th_8	CA1	Thalamus	26	m	C57BL/6JN	Mus musculus
CA1_th_9	CA1	Thalamus	12	m	C57BL/6JN	Mus musculus

CA1_th_10	CA1	Thalamus	12	f	C57BL/6JN	Mus musculus
CA1_th_11	CA1	Thalamus	26	m	C57BL/6JN	Mus musculus
CA1_th_12	CA1	Thalamus	12	m	C57BL/6JN	Mus musculus
CA1_th_13	CA1	Thalamus	12	f	C57BL/6JN	Mus musculus
CA1_th_14	CA1	Thalamus	26	m	C57BL/6JN	Mus musculus
CA1_th_15	CA1	Thalamus	12	m	C57BL/6JN	Mus musculus
CA1_th_16	CA1	Thalamus	21	m	C57BL/6JN	Mus musculus
CA1_th_17	CA1	Thalamus	3	m	C57BL/6JN	Mus musculus
CA1_th_58	CA1	Thalamus	28	m	C57BL/6JN	Mus musculus
CA1_th_59	CA1	Thalamus	28	m	C57BL/6JN	Mus musculus
CA1_hy_1	CA1	Hypothalamus	12	f	C57BL/6JN	Mus musculus
CA1_th_2	CA1	Thalamus	26	m	C57BL/6JN	Mus musculus
CA1_hy_3	CA1	Hypothalamus	12	m	C57BL/6JN	Mus musculus
CA1_hy_4	CA1	Hypothalamus	12	f	C57BL/6JN	Mus musculus
CA1_hy_5	CA1	Hypothalamus	26	m	C57BL/6JN	Mus musculus
CA1_hy_6	CA1	Hypothalamus	12	m	C57BL/6JN	Mus musculus
CA1_th_18	CA1	Thalamus	15	m	C57BL/6JN	Mus musculus
CA1_th_19	CA1	Thalamus	18	m	C57BL/6JN	Mus musculus
CA1_th_20	CA1	Thalamus	21	m	C57BL/6JN	Mus musculus
CA1_th_21	CA1	Thalamus	3	m	C57BL/6JN	Mus musculus
CA1_th_22	CA1	Thalamus	15	m	C57BL/6JN	Mus musculus
CA1_th_23	CA1	Thalamus	18	m	C57BL/6JN	Mus musculus
CA1_th_24	CA1	Thalamus	21	m	C57BL/6JN	Mus musculus
CA1_th_25	CA1	Thalamus	3	m	C57BL/6JN	Mus musculus
CA1_th_26	CA1	Thalamus	15	m	C57BL/6JN	Mus musculus
CA1_th_27	CA1	Thalamus	18	m	C57BL/6JN	Mus musculus
CA1_th_28	CA1	Thalamus	21	m	C57BL/6JN	Mus musculus
CA1_th_29	CA1	Thalamus	3	m	C57BL/6JN	Mus musculus
CA1_th_30	CA1	Thalamus	15	m	C57BL/6JN	Mus musculus
CA1_th_31	CA1	Thalamus	18	m	C57BL/6JN	Mus musculus
CA1_th_32	CA1	Thalamus	21	m	C57BL/6JN	Mus musculus
CA1_th_33	CA1	Thalamus	3	m	C57BL/6JN	Mus musculus
CA1_th_34	CA1	Thalamus	15	m	C57BL/6JN	Mus musculus
CA1_th_35	CA1	Thalamus	18	m	C57BL/6JN	Mus musculus
CA1_th_36	CA1	Thalamus	21	m	C57BL/6JN	Mus musculus
CA1_th_37	CA1	Thalamus	3	f	C57BL/6JN	Mus musculus
CA1_th_38	CA1	Thalamus	15	f	C57BL/6JN	Mus musculus
CA1_th_39	CA1	Thalamus	18	f	C57BL/6JN	Mus musculus
CA1_th_40	CA1	Thalamus	21	f	C57BL/6JN	Mus musculus
CA1_th_41	CA1	Thalamus	3	f	C57BL/6JN	Mus musculus
CA1_th_42	CA1	Thalamus	15	f	C57BL/6JN	Mus musculus
CA1_th_43	CA1	Thalamus	18	f	C57BL/6JN	Mus musculus
CA1_th_44	CA1	Thalamus	21	f	C57BL/6JN	Mus musculus

CA1_th_45	CA1	Thalamus	3	f	C57BL/6JN	Mus musculus
CA1_th_46	CA1	Thalamus	15	f	C57BL/6JN	Mus musculus
CA1_th_47	CA1	Thalamus	18	f	C57BL/6JN	Mus musculus
CA1_th_48	CA1	Thalamus	21	f	C57BL/6JN	Mus musculus
CA1_th_49	CA1	Thalamus	3	f	C57BL/6JN	Mus musculus
CA1_th_50	CA1	Thalamus	15	f	C57BL/6JN	Mus musculus
CA1_th_51	CA1	Thalamus	18	f	C57BL/6JN	Mus musculus
CA1_th_52	CA1	Thalamus	21	f	C57BL/6JN	Mus musculus
CA1_th_53	CA1	Thalamus	3	f	C57BL/6JN	Mus musculus
CA1_th_54	CA1	Thalamus	15	f	C57BL/6JN	Mus musculus
CA1_th_55	CA1	Thalamus	18	f	C57BL/6JN	Mus musculus
CA1_th_56	CA1	Thalamus	21	f	C57BL/6JN	Mus musculus
CA1_th_57	CA1	Thalamus	28	m	C57BL/6JN	Mus musculus
CA1_hy_10	CA1	Hypothalamus	12	f	C57BL/6JN	Mus musculus
CA1_hy_11	CA1	Hypothalamus	26	m	C57BL/6JN	Mus musculus
CA1_hy_12	CA1	Hypothalamus	12	m	C57BL/6JN	Mus musculus
CA1_hy_13	CA1	Hypothalamus	12	f	C57BL/6JN	Mus musculus
CA1_hy_14	CA1	Hypothalamus	26	m	C57BL/6JN	Mus musculus
CA1_hy_31	CA1	Hypothalamus	18	m	C57BL/6JN	Mus musculus
CA1_hy_32	CA1	Hypothalamus	21	m	C57BL/6JN	Mus musculus
CA1_hy_33	CA1	Hypothalamus	3	m	C57BL/6JN	Mus musculus
CA1_hy_34	CA1	Hypothalamus	15	m	C57BL/6JN	Mus musculus
CA1_hy_35	CA1	Hypothalamus	18	m	C57BL/6JN	Mus musculus
CA1_hy_36	CA1	Hypothalamus	21	m	C57BL/6JN	Mus musculus
CA1_hy_37	CA1	Hypothalamus	3	f	C57BL/6JN	Mus musculus
CA1_hy_38	CA1	Hypothalamus	15	f	C57BL/6JN	Mus musculus
CA1_hi_4	CA1	Hippocampus (anterior)	12	f	C57BL/6JN	Mus musculus
CA1_hi_5	CA1	Hippocampus (anterior)	26	m	C57BL/6JN	Mus musculus
CA1_hi_6	CA1	Hippocampus (anterior)	12	m	C57BL/6JN	Mus musculus
CA1_hi_7	CA1	Hippocampus (anterior)	12	f	C57BL/6JN	Mus musculus
CA1_hi_8	CA1	Hippocampus (anterior)	26	m	C57BL/6JN	Mus musculus
CA1_hi_9	CA1	Hippocampus (anterior)	12	m	C57BL/6JN	Mus musculus
CA1_hi_10	CA1	Hippocampus (anterior)	12	f	C57BL/6JN	Mus musculus
CA1_hi_11	CA1	Hippocampus (anterior)	26	m	C57BL/6JN	Mus musculus
CA1_hy_39	CA1	Hypothalamus	18	f	C57BL/6JN	Mus musculus
CA1_hy_40	CA1	Hypothalamus	21	f	C57BL/6JN	Mus musculus
CA1_hy_41	CA1	Hypothalamus	3	f	C57BL/6JN	Mus musculus
CA1_hy_42	CA1	Hypothalamus	15	f	C57BL/6JN	Mus musculus
CA1_hy_43	CA1	Hypothalamus	18	f	C57BL/6JN	Mus musculus
CA1_hy_44	CA1	Hypothalamus	21	f	C57BL/6JN	Mus musculus
CA1_hy_45	CA1	Hypothalamus	3	f	C57BL/6JN	Mus musculus

CA1_hy_46	CA1	Hypothalamus	15	f	C57BL/6JN	Mus musculus
CA1_hi_12	CA1	Hippocampus (anterior)	12	m	C57BL/6JN	Mus musculus
CA1_hi_13	CA1	Hippocampus (anterior)	12	f	C57BL/6JN	Mus musculus
CA1_hi_14	CA1	Hippocampus (anterior)	26	m	C57BL/6JN	Mus musculus
CA1_hi_15	CA1	Hippocampus (anterior)	12	m	C57BL/6JN	Mus musculus
CA1_hi_16	CA1	Hippocampus (anterior)	21	m	C57BL/6JN	Mus musculus
CA1_hi_17	CA1	Hippocampus (anterior)	3	m	C57BL/6JN	Mus musculus
CA1_hi_18	CA1	Hippocampus (anterior)	15	m	C57BL/6JN	Mus musculus
CA1_hi_19	CA1	Hippocampus (anterior)	18	m	C57BL/6JN	Mus musculus
CA1_hy_47	CA1	Hypothalamus	18	f	C57BL/6JN	Mus musculus
CA1_hy_48	CA1	Hypothalamus	21	f	C57BL/6JN	Mus musculus
CA1_hy_49	CA1	Hypothalamus	3	f	C57BL/6JN	Mus musculus
CA1_hy_50	CA1	Hypothalamus	15	f	C57BL/6JN	Mus musculus
CA1_hy_51	CA1	Hypothalamus	18	f	C57BL/6JN	Mus musculus
CA1_hy_52	CA1	Hypothalamus	21	f	C57BL/6JN	Mus musculus
CA1_hy_53	CA1	Hypothalamus	3	f	C57BL/6JN	Mus musculus
CA1_hy_54	CA1	Hypothalamus	15	f	C57BL/6JN	Mus musculus
CA1_hi_20	CA1	Hippocampus (anterior)	21	m	C57BL/6JN	Mus musculus
CA1_hi_21	CA1	Hippocampus (anterior)	3	m	C57BL/6JN	Mus musculus
CA1_hi_22	CA1	Hippocampus (anterior)	15	m	C57BL/6JN	Mus musculus
CA1_hi_23	CA1	Hippocampus (anterior)	18	m	C57BL/6JN	Mus musculus
CA1_hi_24	CA1	Hippocampus (anterior)	21	m	C57BL/6JN	Mus musculus
CA1_hi_25	CA1	Hippocampus (anterior)	3	m	C57BL/6JN	Mus musculus
CA1_hi_26	CA1	Hippocampus (anterior)	15	m	C57BL/6JN	Mus musculus
CA1_hi_27	CA1	Hippocampus (anterior)	18	m	C57BL/6JN	Mus musculus
CA1_hy_55	CA1	Hypothalamus	18	f	C57BL/6JN	Mus musculus
CA1_hy_56	CA1	Hypothalamus	21	f	C57BL/6JN	Mus musculus
CA1_hy_57	CA1	Hypothalamus	28	m	C57BL/6JN	Mus musculus
CA1_hy_58	CA1	Hypothalamus	28	m	C57BL/6JN	Mus musculus
CA1_hy_59	CA1	Hypothalamus	28	m	C57BL/6JN	Mus musculus
CA1_hi_1	CA1	Hippocampus (anterior)	12	f	C57BL/6JN	Mus musculus
CA1_hy_2	CA1	Hypothalamus	26	m	C57BL/6JN	Mus musculus
CA1_hi_28	CA1	Hippocampus (anterior)	21	m	C57BL/6JN	Mus musculus
CA1_hi_29	CA1	Hippocampus (anterior)	3	m	C57BL/6JN	Mus musculus
CA1_hi_30	CA1	Hippocampus (anterior)	15	m	C57BL/6JN	Mus musculus
CA1_hi_31	CA1	Hippocampus (anterior)	18	m	C57BL/6JN	Mus musculus
CA1_hi_32	CA1	Hippocampus (anterior)	21	m	C57BL/6JN	Mus musculus

CA1_hi_33	CA1	Hippocampus (anterior)	3	m	C57BL/6JN	Mus musculus
CA1_hi_34	CA1	Hippocampus (anterior)	15	m	C57BL/6JN	Mus musculus
CA1_hi_36	CA1	Hippocampus (anterior)	21	m	C57BL/6JN	Mus musculus
CA1_hi_37	CA1	Hippocampus (anterior)	3	f	C57BL/6JN	Mus musculus
CA1_hi_38	CA1	Hippocampus (anterior)	15	f	C57BL/6JN	Mus musculus
CA1_hi_39	CA1	Hippocampus (anterior)	18	f	C57BL/6JN	Mus musculus
CA1_hi_40	CA1	Hippocampus (anterior)	21	f	C57BL/6JN	Mus musculus
CA1_hi_41	CA1	Hippocampus (anterior)	3	f	C57BL/6JN	Mus musculus
CA1_hi_42	CA1	Hippocampus (anterior)	15	f	C57BL/6JN	Mus musculus
CA1_hi_43	CA1	Hippocampus (anterior)	18	f	C57BL/6JN	Mus musculus
CA1_plx_1	CA1	Choroid Plexus	12	f	C57BL/6JN	Mus musculus
CA1_plx_2	CA1	Choroid Plexus	26	m	C57BL/6JN	Mus musculus
CA1_plx_3	CA1	Choroid Plexus	12	m	C57BL/6JN	Mus musculus
CA1_hi2_4	CA1	Hippocampus (posterior)	12	f	C57BL/6JN	Mus musculus
CA1_plx_5	CA1	Choroid Plexus	26	m	C57BL/6JN	Mus musculus
CA1_plx_6	CA1	Choroid Plexus	12	m	C57BL/6JN	Mus musculus
CA1_plx_7	CA1	Choroid Plexus	12	f	C57BL/6JN	Mus musculus
CA1_plx_8	CA1	Choroid Plexus	26	m	C57BL/6JN	Mus musculus
CA1_hi_45	CA1	Hippocampus (anterior)	3	f	C57BL/6JN	Mus musculus
CA1_hi_46	CA1	Hippocampus (anterior)	15	f	C57BL/6JN	Mus musculus
CA1_hi_47	CA1	Hippocampus (anterior)	18	f	C57BL/6JN	Mus musculus
CA1_hi_48	CA1	Hippocampus (anterior)	21	f	C57BL/6JN	Mus musculus
CA1_hi_49	CA1	Hippocampus (anterior)	3	f	C57BL/6JN	Mus musculus
CA1_hi_50	CA1	Hippocampus (anterior)	15	f	C57BL/6JN	Mus musculus
CA1_hi_51	CA1	Hippocampus (anterior)	18	f	C57BL/6JN	Mus musculus
CA1_hi_52	CA1	Hippocampus (anterior)	21	f	C57BL/6JN	Mus musculus
CA1_hi_53	CA1	Hippocampus (anterior)	3	f	C57BL/6JN	Mus musculus
CA1_hi_54	CA1	Hippocampus (anterior)	15	f	C57BL/6JN	Mus musculus
CA1_hi_55	CA1	Hippocampus (anterior)	18	f	C57BL/6JN	Mus musculus
CA1_hi_56	CA1	Hippocampus (anterior)	21	f	C57BL/6JN	Mus musculus
CA1_hi_57	CA1	Hippocampus (anterior)	28	m	C57BL/6JN	Mus musculus
CA1_hi_59	CA1	Hippocampus (anterior)	28	m	C57BL/6JN	Mus musculus
CA1_plx_9	CA1	Choroid Plexus	12	m	C57BL/6JN	Mus musculus
CA1_plx_10	CA1	Choroid Plexus	12	f	C57BL/6JN	Mus musculus
CA1_plx_11	CA1	Choroid Plexus	26	m	C57BL/6JN	Mus musculus
CA1_plx_12	CA1	Choroid Plexus	12	m	C57BL/6JN	Mus musculus

CA1_plx_13	CA1	Choroid Plexus	12	f	C57BL/6JN	Mus musculus
CA1_plx_14	CA1	Choroid Plexus	26	m	C57BL/6JN	Mus musculus
CA1_plx_15	CA1	Choroid Plexus	12	m	C57BL/6JN	Mus musculus
CA1_plx_16	CA1	Choroid Plexus	21	m	C57BL/6JN	Mus musculus
CA1_plx_57	CA1	Choroid Plexus	28	m	C57BL/6JN	Mus musculus
CA1_plx_58	CA1	Choroid Plexus	28	m	C57BL/6JN	Mus musculus
CA1_plx_59	CA1	Choroid Plexus	28	m	C57BL/6JN	Mus musculus
CA1_hi2_1	CA1	Hippocampus (posterior)	12	f	C57BL/6JN	Mus musculus
CA1_hi2_2	CA1	Hippocampus (posterior)	26	m	C57BL/6JN	Mus musculus
CA1_vis_3	CA1	Visual Cortex	12	m	C57BL/6JN	Mus musculus
CA1_plx_4	CA1	Choroid Plexus	12	f	C57BL/6JN	Mus musculus
CA1_hi2_5	CA1	Hippocampus (posterior)	26	m	C57BL/6JN	Mus musculus
CA1_plx_17	CA1	Choroid Plexus	3	m	C57BL/6JN	Mus musculus
CA1_plx_18	CA1	Choroid Plexus	15	m	C57BL/6JN	Mus musculus
CA1_plx_19	CA1	Choroid Plexus	18	m	C57BL/6JN	Mus musculus
CA1_plx_20	CA1	Choroid Plexus	21	m	C57BL/6JN	Mus musculus
CA1_plx_21	CA1	Choroid Plexus	3	m	C57BL/6JN	Mus musculus
CA1_plx_23	CA1	Choroid Plexus	18	m	C57BL/6JN	Mus musculus
CA1_plx_22	CA1	Choroid Plexus	15	m	C57BL/6JN	Mus musculus
CA1_plx_24	CA1	Choroid Plexus	21	m	C57BL/6JN	Mus musculus
CA1_hi2_6	CA1	Hippocampus (posterior)	12	m	C57BL/6JN	Mus musculus
CA1_hi2_7	CA1	Hippocampus (posterior)	12	f	C57BL/6JN	Mus musculus
CA1_hi2_8	CA1	Hippocampus (posterior)	26	m	C57BL/6JN	Mus musculus
CA1_hi2_9	CA1	Hippocampus (posterior)	12	m	C57BL/6JN	Mus musculus
CA1_hi2_10	CA1	Hippocampus (posterior)	12	f	C57BL/6JN	Mus musculus
CA1_hi2_11	CA1	Hippocampus (posterior)	26	m	C57BL/6JN	Mus musculus
CA1_hi2_12	CA1	Hippocampus (posterior)	12	m	C57BL/6JN	Mus musculus
CA1_hi2_13	CA1	Hippocampus (posterior)	12	f	C57BL/6JN	Mus musculus
CA1_plx_25	CA1	Choroid Plexus	3	m	C57BL/6JN	Mus musculus
CA1_plx_26	CA1	Choroid Plexus	15	m	C57BL/6JN	Mus musculus
CA1_plx_27	CA1	Choroid Plexus	18	m	C57BL/6JN	Mus musculus
CA1_plx_28	CA1	Choroid Plexus	21	m	C57BL/6JN	Mus musculus
CA1_plx_29	CA1	Choroid Plexus	3	m	C57BL/6JN	Mus musculus
CA1_plx_30	CA1	Choroid Plexus	15	m	C57BL/6JN	Mus musculus
CA1_plx_31	CA1	Choroid Plexus	18	m	C57BL/6JN	Mus musculus
CA1_plx_32	CA1	Choroid Plexus	21	m	C57BL/6JN	Mus musculus
CA1_hi2_14	CA1	Hippocampus (posterior)	26	m	C57BL/6JN	Mus musculus
CA1_hi2_15	CA1	Hippocampus (posterior)	12	m	C57BL/6JN	Mus musculus
CA1_hi2_16	CA1	Hippocampus (posterior)	21	m	C57BL/6JN	Mus musculus

CA1_hi2_17	CA1	Hippocampus (posterior)	3	m	C57BL/6JN	Mus musculus
CA1_hi2_18	CA1	Hippocampus (posterior)	15	m	C57BL/6JN	Mus musculus
CA1_hi2_19	CA1	Hippocampus (posterior)	18	m	C57BL/6JN	Mus musculus
CA1_hi2_20	CA1	Hippocampus (posterior)	21	m	C57BL/6JN	Mus musculus
CA1_hi2_21	CA1	Hippocampus (posterior)	3	m	C57BL/6JN	Mus musculus
CA1_plx_33	CA1	Choroid Plexus	3	m	C57BL/6JN	Mus musculus
CA1_plx_34	CA1	Choroid Plexus	15	m	C57BL/6JN	Mus musculus
CA1_plx_35	CA1	Choroid Plexus	18	m	C57BL/6JN	Mus musculus
CA1_plx_36	CA1	Choroid Plexus	21	m	C57BL/6JN	Mus musculus
CA1_plx_37	CA1	Choroid Plexus	3	f	C57BL/6JN	Mus musculus
CA1_plx_38	CA1	Choroid Plexus	15	f	C57BL/6JN	Mus musculus
CA1_plx_39	CA1	Choroid Plexus	18	f	C57BL/6JN	Mus musculus
CA1_plx_40	CA1	Choroid Plexus	21	f	C57BL/6JN	Mus musculus
CA1_hi2_22	CA1	Hippocampus (posterior)	15	m	C57BL/6JN	Mus musculus
CA1_hi2_23	CA1	Hippocampus (posterior)	18	m	C57BL/6JN	Mus musculus
CA1_hi2_24	CA1	Hippocampus (posterior)	21	m	C57BL/6JN	Mus musculus
CA1_hi2_25	CA1	Hippocampus (posterior)	3	m	C57BL/6JN	Mus musculus
CA1_hi2_26	CA1	Hippocampus (posterior)	15	m	C57BL/6JN	Mus musculus
CA1_hi2_27	CA1	Hippocampus (posterior)	18	m	C57BL/6JN	Mus musculus
CA1_hi2_28	CA1	Hippocampus (posterior)	21	m	C57BL/6JN	Mus musculus
CA1_hi2_29	CA1	Hippocampus (posterior)	3	m	C57BL/6JN	Mus musculus
CA1_plx_41	CA1	Choroid Plexus	3	f	C57BL/6JN	Mus musculus
CA1_plx_42	CA1	Choroid Plexus	15	f	C57BL/6JN	Mus musculus
CA1_plx_43	CA1	Choroid Plexus	18	f	C57BL/6JN	Mus musculus
CA1_plx_44	CA1	Choroid Plexus	21	f	C57BL/6JN	Mus musculus
CA1_plx_45	CA1	Choroid Plexus	3	f	C57BL/6JN	Mus musculus
CA1_plx_46	CA1	Choroid Plexus	15	f	C57BL/6JN	Mus musculus
CA1_plx_47	CA1	Choroid Plexus	18	f	C57BL/6JN	Mus musculus
CA1_plx_48	CA1	Choroid Plexus	21	f	C57BL/6JN	Mus musculus
CA1_hi2_30	CA1	Hippocampus (posterior)	15	m	C57BL/6JN	Mus musculus
CA1_hi2_31	CA1	Hippocampus (posterior)	18	m	C57BL/6JN	Mus musculus
CA1_hi2_32	CA1	Hippocampus (posterior)	21	m	C57BL/6JN	Mus musculus
CA1_hi2_33	CA1	Hippocampus (posterior)	3	m	C57BL/6JN	Mus musculus
CA1_hi2_34	CA1	Hippocampus (posterior)	15	m	C57BL/6JN	Mus musculus
CA1_hi2_35	CA1	Hippocampus (posterior)	18	m	C57BL/6JN	Mus musculus
CA1_hi2_36	CA1	Hippocampus (posterior)	21	m	C57BL/6JN	Mus musculus
CA1_hi2_37	CA1	Hippocampus (posterior)	3	f	C57BL/6JN	Mus musculus

CA1_plx_49	CA1	Choroid Plexus	3	f	C57BL/6JN	Mus musculus
CA1_plx_50	CA1	Choroid Plexus	15	f	C57BL/6JN	Mus musculus
CA1_plx_51	CA1	Choroid Plexus	18	f	C57BL/6JN	Mus musculus
CA1_plx_52	CA1	Choroid Plexus	21	f	C57BL/6JN	Mus musculus
CA1_plx_53	CA1	Choroid Plexus	3	f	C57BL/6JN	Mus musculus
CA1_plx_54	CA1	Choroid Plexus	15	f	C57BL/6JN	Mus musculus
CA1_plx_55	CA1	Choroid Plexus	18	f	C57BL/6JN	Mus musculus
CA1_plx_56	CA1	Choroid Plexus	21	f	C57BL/6JN	Mus musculus
CA1_hi2_38	CA1	Hippocampus (posterior)	15	f	C57BL/6JN	Mus musculus
CA1_hi2_39	CA1	Hippocampus (posterior)	18	f	C57BL/6JN	Mus musculus
CA1_hi2_40	CA1	Hippocampus (posterior)	21	f	C57BL/6JN	Mus musculus
CA1_hi2_41	CA1	Hippocampus (posterior)	3	f	C57BL/6JN	Mus musculus
CA1_hi2_42	CA1	Hippocampus (posterior)	15	f	C57BL/6JN	Mus musculus
CA1_hi2_43	CA1	Hippocampus (posterior)	18	f	C57BL/6JN	Mus musculus
CA1_hi2_44	CA1	Hippocampus (posterior)	21	f	C57BL/6JN	Mus musculus
CA1_hi2_45	CA1	Hippocampus (posterior)	3	f	C57BL/6JN	Mus musculus
CA1_hi2_46	CA1	Hippocampus (posterior)	15	f	C57BL/6JN	Mus musculus
CA1_hi2_47	CA1	Hippocampus (posterior)	18	f	C57BL/6JN	Mus musculus
CA1_hi2_48	CA1	Hippocampus (posterior)	21	f	C57BL/6JN	Mus musculus
CA1_hi2_49	CA1	Hippocampus (posterior)	3	f	C57BL/6JN	Mus musculus
CA1_hi2_50	CA1	Hippocampus (posterior)	15	f	C57BL/6JN	Mus musculus
CA1_hi2_51	CA1	Hippocampus (posterior)	18	f	C57BL/6JN	Mus musculus
CA1_hi2_52	CA1	Hippocampus (posterior)	21	f	C57BL/6JN	Mus musculus
CA1_hi2_53	CA1	Hippocampus (posterior)	3	f	C57BL/6JN	Mus musculus
CA1_vis_27	CA1	Visual Cortex	18	m	C57BL/6JN	Mus musculus
CA1_vis_28	CA1	Visual Cortex	21	m	C57BL/6JN	Mus musculus
CA1_vis_29	CA1	Visual Cortex	3	m	C57BL/6JN	Mus musculus
CA1_vis_30	CA1	Visual Cortex	15	m	C57BL/6JN	Mus musculus
CA1_vis_31	CA1	Visual Cortex	18	m	C57BL/6JN	Mus musculus
CA1_vis_32	CA1	Visual Cortex	21	m	C57BL/6JN	Mus musculus
CA1_vis_33	CA1	Visual Cortex	3	m	C57BL/6JN	Mus musculus
CA1_vis_34	CA1	Visual Cortex	15	m	C57BL/6JN	Mus musculus
CA1_hi2_54	CA1	Hippocampus (posterior)	15	f	C57BL/6JN	Mus musculus
CA1_hi2_55	CA1	Hippocampus (posterior)	18	f	C57BL/6JN	Mus musculus
CA1_hi2_56	CA1	Hippocampus (posterior)	21	f	C57BL/6JN	Mus musculus
CA1_hi2_57	CA1	Hippocampus (posterior)	28	m	C57BL/6JN	Mus musculus
CA1_hi2_58	CA1	Hippocampus (posterior)	28	m	C57BL/6JN	Mus musculus

CA1_hi2_59	CA1	Hippocampus (posterior)	28	m	C57BL/6JN	Mus musculus
CA1_vis_1	CA1	Visual Cortex	12	f	C57BL/6JN	Mus musculus
CA1_vis_2	CA1	Visual Cortex	26	m	C57BL/6JN	Mus musculus
CA1_vis_35	CA1	Visual Cortex	18	m	C57BL/6JN	Mus musculus
CA1_vis_36	CA1	Visual Cortex	21	m	C57BL/6JN	Mus musculus
CA1_vis_37	CA1	Visual Cortex	3	f	C57BL/6JN	Mus musculus
CA1_vis_38	CA1	Visual Cortex	15	f	C57BL/6JN	Mus musculus
CA1_vis_39	CA1	Visual Cortex	18	f	C57BL/6JN	Mus musculus
CA1_vis_40	CA1	Visual Cortex	21	f	C57BL/6JN	Mus musculus
CA1_vis_41	CA1	Visual Cortex	3	f	C57BL/6JN	Mus musculus
CA1_vis_42	CA1	Visual Cortex	15	f	C57BL/6JN	Mus musculus
CA1_hi2_3	CA1	Hippocampus (posterior)	12	m	C57BL/6JN	Mus musculus
CA1_vis_5	CA1	Visual Cortex	26	m	C57BL/6JN	Mus musculus
CA1_vis_6	CA1	Visual Cortex	12	m	C57BL/6JN	Mus musculus
CA1_vis_7	CA1	Visual Cortex	12	f	C57BL/6JN	Mus musculus
CA1_vis_8	CA1	Visual Cortex	26	m	C57BL/6JN	Mus musculus
CA1_vis_10	CA1	Visual Cortex	12	f	C57BL/6JN	Mus musculus
CA1_vis_43	CA1	Visual Cortex	18	f	C57BL/6JN	Mus musculus
CA1_vis_44	CA1	Visual Cortex	21	f	C57BL/6JN	Mus musculus
CA1_vis_45	CA1	Visual Cortex	3	f	C57BL/6JN	Mus musculus
CA1_vis_46	CA1	Visual Cortex	15	f	C57BL/6JN	Mus musculus
CA1_vis_47	CA1	Visual Cortex	18	f	C57BL/6JN	Mus musculus
CA1_vis_48	CA1	Visual Cortex	21	f	C57BL/6JN	Mus musculus
CA1_vis_49	CA1	Visual Cortex	3	f	C57BL/6JN	Mus musculus
CA1_vis_50	CA1	Visual Cortex	15	f	C57BL/6JN	Mus musculus
CA1_vis_11	CA1	Visual Cortex	26	m	C57BL/6JN	Mus musculus
CA1_vis_13	CA1	Visual Cortex	12	f	C57BL/6JN	Mus musculus
CA1_vis_14	CA1	Visual Cortex	26	m	C57BL/6JN	Mus musculus
CA1_vis_15	CA1	Visual Cortex	12	m	C57BL/6JN	Mus musculus
CA1_vis_16	CA1	Visual Cortex	21	m	C57BL/6JN	Mus musculus
CA1_vis_17	CA1	Visual Cortex	3	m	C57BL/6JN	Mus musculus
CA1_vis_18	CA1	Visual Cortex	15	m	C57BL/6JN	Mus musculus
CA1_vis_59	CA1	Visual Cortex	28	m	C57BL/6JN	Mus musculus
CA1_ent_1	CA1	Entorhinal cortex	12	f	C57BL/6JN	Mus musculus
CA1_ent_3	CA1	Entorhinal cortex	12	m	C57BL/6JN	Mus musculus
CA1_ent_5	CA1	Entorhinal cortex	26	m	C57BL/6JN	Mus musculus
CA1_ent_6	CA1	Entorhinal cortex	12	m	C57BL/6JN	Mus musculus
CA1_ent_7	CA1	Entorhinal cortex	12	f	C57BL/6JN	Mus musculus
CA1_vis_19	CA1	Visual Cortex	18	m	C57BL/6JN	Mus musculus
CA1_vis_20	CA1	Visual Cortex	21	m	C57BL/6JN	Mus musculus
CA1_vis_21	CA1	Visual Cortex	3	m	C57BL/6JN	Mus musculus
CA1_vis_22	CA1	Visual Cortex	15	m	C57BL/6JN	Mus musculus

CA1_vis_23	CA1	Visual Cortex	18	m	C57BL/6JN	Mus musculus
CA1_vis_24	CA1	Visual Cortex	21	m	C57BL/6JN	Mus musculus
CA1_vis_25	CA1	Visual Cortex	3	m	C57BL/6JN	Mus musculus
CA1_vis_26	CA1	Visual Cortex	15	m	C57BL/6JN	Mus musculus
CA1_ent_8	CA1	Entorhinal cortex	26	m	C57BL/6JN	Mus musculus
CA1_ent_9	CA1	Entorhinal cortex	12	m	C57BL/6JN	Mus musculus
CA1_ent_10	CA1	Entorhinal cortex	12	f	C57BL/6JN	Mus musculus
CA1_ent_11	CA1	Entorhinal cortex	26	m	C57BL/6JN	Mus musculus
CA1_ent_12	CA1	Entorhinal cortex	12	m	C57BL/6JN	Mus musculus
CA1_ent_13	CA1	Entorhinal cortex	12	f	C57BL/6JN	Mus musculus
CA1_ent_14	CA1	Entorhinal cortex	26	m	C57BL/6JN	Mus musculus
CA1_ent_15	CA1	Entorhinal cortex	12	m	C57BL/6JN	Mus musculus
CA1_vis_51	CA1	Visual Cortex	18	f	C57BL/6JN	Mus musculus
CA1_vis_52	CA1	Visual Cortex	21	f	C57BL/6JN	Mus musculus
CA1_vis_53	CA1	Visual Cortex	3	f	C57BL/6JN	Mus musculus
CA1_vis_54	CA1	Visual Cortex	15	f	C57BL/6JN	Mus musculus
CA1_vis_55	CA1	Visual Cortex	18	f	C57BL/6JN	Mus musculus
CA1_vis_56	CA1	Visual Cortex	21	f	C57BL/6JN	Mus musculus
CA1_vis_57	CA1	Visual Cortex	28	m	C57BL/6JN	Mus musculus
CA1_vis_58	CA1	Visual Cortex	28	m	C57BL/6JN	Mus musculus
CA1_ent_16	CA1	Entorhinal cortex	21	m	C57BL/6JN	Mus musculus
CA1_ent_17	CA1	Entorhinal cortex	3	m	C57BL/6JN	Mus musculus
CA1_ent_18	CA1	Entorhinal cortex	15	m	C57BL/6JN	Mus musculus
CA1_ent_19	CA1	Entorhinal cortex	18	m	C57BL/6JN	Mus musculus
CA1_ent_20	CA1	Entorhinal cortex	21	m	C57BL/6JN	Mus musculus
CA1_ent_21	CA1	Entorhinal cortex	3	m	C57BL/6JN	Mus musculus
CA1_ent_22	CA1	Entorhinal cortex	15	m	C57BL/6JN	Mus musculus
CA1_ent_23	CA1	Entorhinal cortex	18	m	C57BL/6JN	Mus musculus
CA1_ent_24	CA1	Entorhinal cortex	21	m	C57BL/6JN	Mus musculus
CA1_ent_25	CA1	Entorhinal cortex	3	m	C57BL/6JN	Mus musculus
CA1_ent_26	CA1	Entorhinal cortex	15	m	C57BL/6JN	Mus musculus
CA1_ent_27	CA1	Entorhinal cortex	18	m	C57BL/6JN	Mus musculus
CA1_ent_28	CA1	Entorhinal cortex	21	m	C57BL/6JN	Mus musculus
CA1_ent_29	CA1	Entorhinal cortex	3	m	C57BL/6JN	Mus musculus
CA1_ent_30	CA1	Entorhinal cortex	15	m	C57BL/6JN	Mus musculus
CA1_ent_32	CA1	Entorhinal cortex	21	m	C57BL/6JN	Mus musculus
CA1_ent_33	CA1	Entorhinal cortex	3	m	C57BL/6JN	Mus musculus
CA1_ent_34	CA1	Entorhinal cortex	15	m	C57BL/6JN	Mus musculus
CA1_ent_35	CA1	Entorhinal cortex	18	m	C57BL/6JN	Mus musculus
CA1_ent_36	CA1	Entorhinal cortex	21	m	C57BL/6JN	Mus musculus
CA1_ent_37	CA1	Entorhinal cortex	3	f	C57BL/6JN	Mus musculus
CA1_ent_38	CA1	Entorhinal cortex	15	f	C57BL/6JN	Mus musculus
CA1_ent_39	CA1	Entorhinal cortex	18	f	C57BL/6JN	Mus musculus

CA1_ent_40	CA1	Entorhinal cortex	21	f	C57BL/6JN	Mus musculus
CA1_ent_41	CA1	Entorhinal cortex	3	f	C57BL/6JN	Mus musculus
CA1_ent_42	CA1	Entorhinal cortex	15	f	C57BL/6JN	Mus musculus
CA1_ent_43	CA1	Entorhinal cortex	18	f	C57BL/6JN	Mus musculus
CA1_ent_44	CA1	Entorhinal cortex	21	f	C57BL/6JN	Mus musculus
CA1_ent_45	CA1	Entorhinal cortex	3	f	C57BL/6JN	Mus musculus
CA1_ent_46	CA1	Entorhinal cortex	15	f	C57BL/6JN	Mus musculus
CA1_ent_47	CA1	Entorhinal cortex	18	f	C57BL/6JN	Mus musculus
CA1_ent_57	CA1	Entorhinal cortex	28	m	C57BL/6JN	Mus musculus
CA1_ent_48	CA1	Entorhinal cortex	21	f	C57BL/6JN	Mus musculus
CA1_ent_49	CA1	Entorhinal cortex	3	f	C57BL/6JN	Mus musculus
CA1_ent_50	CA1	Entorhinal cortex	15	f	C57BL/6JN	Mus musculus
CA1_ent_51	CA1	Entorhinal cortex	18	f	C57BL/6JN	Mus musculus
CA1_ent_52	CA1	Entorhinal cortex	21	f	C57BL/6JN	Mus musculus
CA1_ent_53	CA1	Entorhinal cortex	3	f	C57BL/6JN	Mus musculus
CA1_ent_54	CA1	Entorhinal cortex	15	f	C57BL/6JN	Mus musculus
CA1_ent_55	CA1	Entorhinal cortex	18	f	C57BL/6JN	Mus musculus
CA1_hy_15	CA1	Hypothalamus	12	m	C57BL/6JN	Mus musculus
CA1_hy_16	CA1	Hypothalamus	21	m	C57BL/6JN	Mus musculus
CA1_hy_17	CA1	Hypothalamus	3	m	C57BL/6JN	Mus musculus
CA1_hy_18	CA1	Hypothalamus	15	m	C57BL/6JN	Mus musculus
CA1_hy_19	CA1	Hypothalamus	18	m	C57BL/6JN	Mus musculus
CA1_hy_20	CA1	Hypothalamus	21	m	C57BL/6JN	Mus musculus
CA1_hy_21	CA1	Hypothalamus	3	m	C57BL/6JN	Mus musculus
CA1_hy_22	CA1	Hypothalamus	15	m	C57BL/6JN	Mus musculus
CA1_hy_23	CA1	Hypothalamus	18	m	C57BL/6JN	Mus musculus
CA1_hy_24	CA1	Hypothalamus	21	m	C57BL/6JN	Mus musculus
CA1_hy_25	CA1	Hypothalamus	3	m	C57BL/6JN	Mus musculus
CA1_hy_26	CA1	Hypothalamus	15	m	C57BL/6JN	Mus musculus
CA1_hy_27	CA1	Hypothalamus	18	m	C57BL/6JN	Mus musculus
CA1_hy_28	CA1	Hypothalamus	21	m	C57BL/6JN	Mus musculus
CA1_hy_29	CA1	Hypothalamus	3	m	C57BL/6JN	Mus musculus
CA1_hy_30	CA1	Hypothalamus	15	m	C57BL/6JN	Mus musculus
CA1_pon_1	CA1	Pons	12	f	C57BL/6JN	Mus musculus
CA1_pon_2	CA1	Pons	26	m	C57BL/6JN	Mus musculus
CA1_pon_3	CA1	Pons	12	m	C57BL/6JN	Mus musculus
CA1_pon_5	CA1	Pons	26	m	C57BL/6JN	Mus musculus
CA1_pon_6	CA1	Pons	12	m	C57BL/6JN	Mus musculus
CA1_pon_7	CA1	Pons	12	f	C57BL/6JN	Mus musculus
CA1_pon_8	CA1	Pons	26	m	C57BL/6JN	Mus musculus
CA1_pon_9	CA1	Pons	12	m	C57BL/6JN	Mus musculus
CA1_pon_10	CA1	Pons	12	f	C57BL/6JN	Mus musculus
CA1_pon_12	CA1	Pons	12	m	C57BL/6JN	Mus musculus

CA1_pon_13	CA1	Pons	12	f	C57BL/6JN	Mus musculus
CA1_pon_14	CA1	Pons	26	m	C57BL/6JN	Mus musculus
CA1_pon_15	CA1	Pons	12	m	C57BL/6JN	Mus musculus
CA1_pon_16	CA1	Pons	21	m	C57BL/6JN	Mus musculus
CA1_pon_17	CA1	Pons	3	m	C57BL/6JN	Mus musculus
CA1_pon_58	CA1	Pons	28	m	C57BL/6JN	Mus musculus
CA1_pon_59	CA1	Pons	28	m	C57BL/6JN	Mus musculus
CA1_cer_1	CA1	Cerebellum	12	f	C57BL/6JN	Mus musculus
CA1_cer_2	CA1	Cerebellum	26	m	C57BL/6JN	Mus musculus
CA1_cer_3	CA1	Cerebellum	12	m	C57BL/6JN	Mus musculus
CA1_cer_5	CA1	Cerebellum	26	m	C57BL/6JN	Mus musculus
CA1_cer_6	CA1	Cerebellum	12	m	C57BL/6JN	Mus musculus
CA1_pon_18	CA1	Pons	15	m	C57BL/6JN	Mus musculus
CA1_pon_19	CA1	Pons	18	m	C57BL/6JN	Mus musculus
CA1_pon_20	CA1	Pons	21	m	C57BL/6JN	Mus musculus
CA1_pon_21	CA1	Pons	3	m	C57BL/6JN	Mus musculus
CA1_pon_22	CA1	Pons	15	m	C57BL/6JN	Mus musculus
CA1_pon_23	CA1	Pons	18	m	C57BL/6JN	Mus musculus
CA1_pon_24	CA1	Pons	21	m	C57BL/6JN	Mus musculus
CA1_pon_25	CA1	Pons	3	m	C57BL/6JN	Mus musculus
CA1_cer_7	CA1	Cerebellum	12	f	C57BL/6JN	Mus musculus
CA1_cer_8	CA1	Cerebellum	26	m	C57BL/6JN	Mus musculus
CA1_cer_9	CA1	Cerebellum	12	m	C57BL/6JN	Mus musculus
CA1_cer_10	CA1	Cerebellum	12	f	C57BL/6JN	Mus musculus
CA1_cer_11	CA1	Cerebellum	26	m	C57BL/6JN	Mus musculus
CA1_cer_12	CA1	Cerebellum	12	m	C57BL/6JN	Mus musculus
CA1_cer_13	CA1	Cerebellum	12	f	C57BL/6JN	Mus musculus
CA1_cer_14	CA1	Cerebellum	26	m	C57BL/6JN	Mus musculus
CA1_pon_28	CA1	Pons	21	m	C57BL/6JN	Mus musculus
CA1_pon_29	CA1	Pons	3	m	C57BL/6JN	Mus musculus
CA1_pon_30	CA1	Pons	15	m	C57BL/6JN	Mus musculus
CA1_pon_31	CA1	Pons	18	m	C57BL/6JN	Mus musculus
CA1_pon_32	CA1	Pons	21	m	C57BL/6JN	Mus musculus
CA1_pon_33	CA1	Pons	3	m	C57BL/6JN	Mus musculus
CA1_cer_15	CA1	Cerebellum	12	m	C57BL/6JN	Mus musculus
CA1_cer_16	CA1	Cerebellum	21	m	C57BL/6JN	Mus musculus
CA1_cer_17	CA1	Cerebellum	3	m	C57BL/6JN	Mus musculus
CA1_cer_18	CA1	Cerebellum	15	m	C57BL/6JN	Mus musculus
CA1_cer_19	CA1	Cerebellum	18	m	C57BL/6JN	Mus musculus
CA1_cer_20	CA1	Cerebellum	21	m	C57BL/6JN	Mus musculus
CA1_cer_21	CA1	Cerebellum	3	m	C57BL/6JN	Mus musculus
CA1_pon_36	CA1	Pons	21	m	C57BL/6JN	Mus musculus
CA1_pon_37	CA1	Pons	3	f	C57BL/6JN	Mus musculus

CA1_pon_38	CA1	Pons	15	f	C57BL/6JN	Mus musculus
CA1_pon_39	CA1	Pons	18	f	C57BL/6JN	Mus musculus
CA1_pon_40	CA1	Pons	21	f	C57BL/6JN	Mus musculus
CA1_pon_41	CA1	Pons	3	f	C57BL/6JN	Mus musculus
CA1_cer_23	CA1	Cerebellum	18	m	C57BL/6JN	Mus musculus
CA1_cer_25	CA1	Cerebellum	3	m	C57BL/6JN	Mus musculus
CA1_cer_26	CA1	Cerebellum	15	m	C57BL/6JN	Mus musculus
CA1_cer_27	CA1	Cerebellum	18	m	C57BL/6JN	Mus musculus
CA1_cer_28	CA1	Cerebellum	21	m	C57BL/6JN	Mus musculus
CA1_cer_30	CA1	Cerebellum	15	m	C57BL/6JN	Mus musculus
CA1_cer_39	CA1	Cerebellum	18	f	C57BL/6JN	Mus musculus
CA1_cer_40	CA1	Cerebellum	21	f	C57BL/6JN	Mus musculus
CA1_cer_41	CA1	Cerebellum	3	f	C57BL/6JN	Mus musculus
CA1_cer_42	CA1	Cerebellum	15	f	C57BL/6JN	Mus musculus
CA1_cer_43	CA1	Cerebellum	18	f	C57BL/6JN	Mus musculus
CA1_cer_44	CA1	Cerebellum	21	f	C57BL/6JN	Mus musculus
CA1_cer_45	CA1	Cerebellum	3	f	C57BL/6JN	Mus musculus
CA1_cer_46	CA1	Cerebellum	15	f	C57BL/6JN	Mus musculus
CA1_cer_55	CA1	Cerebellum	18	f	C57BL/6JN	Mus musculus
CA1_cer_56	CA1	Cerebellum	21	f	C57BL/6JN	Mus musculus
CA1_cer_57	CA1	Cerebellum	28	m	C57BL/6JN	Mus musculus
CA1_cer_58	CA1	Cerebellum	28	m	C57BL/6JN	Mus musculus
CA1_cer_59	CA1	Cerebellum	28	m	C57BL/6JN	Mus musculus
CA1_med_1	CA1	Medulla	12	f	C57BL/6JN	Mus musculus
CA1_med_2	CA1	Medulla	26	m	C57BL/6JN	Mus musculus
CA1_med_3	CA1	Medulla	12	m	C57BL/6JN	Mus musculus
CA1_cer_47	CA1	Cerebellum	18	f	C57BL/6JN	Mus musculus
CA1_cer_48	CA1	Cerebellum	21	f	C57BL/6JN	Mus musculus
CA1_cer_49	CA1	Cerebellum	3	f	C57BL/6JN	Mus musculus
CA1_cer_50	CA1	Cerebellum	15	f	C57BL/6JN	Mus musculus
CA1_cer_51	CA1	Cerebellum	18	f	C57BL/6JN	Mus musculus
CA1_cer_52	CA1	Cerebellum	21	f	C57BL/6JN	Mus musculus
CA1_cer_53	CA1	Cerebellum	3	f	C57BL/6JN	Mus musculus
CA1_cer_54	CA1	Cerebellum	15	f	C57BL/6JN	Mus musculus
CA1_med_5	CA1	Medulla	26	m	C57BL/6JN	Mus musculus
CA1_med_6	CA1	Medulla	12	m	C57BL/6JN	Mus musculus
CA1_med_7	CA1	Medulla	12	f	C57BL/6JN	Mus musculus
CA1_med_8	CA1	Medulla	26	m	C57BL/6JN	Mus musculus
CA1_med_9	CA1	Medulla	12	m	C57BL/6JN	Mus musculus
CA1_med_10	CA1	Medulla	12	f	C57BL/6JN	Mus musculus
CA1_med_11	CA1	Medulla	26	m	C57BL/6JN	Mus musculus
CA1_med_12	CA1	Medulla	12	m	C57BL/6JN	Mus musculus
CA1_med_13	CA1	Medulla	12	f	C57BL/6JN	Mus musculus

CA1_med_14	CA1	Medulla	26	m	C57BL/6JN	Mus musculus
CA1_med_15	CA1	Medulla	12	m	C57BL/6JN	Mus musculus
CA1_med_16	CA1	Medulla	21	m	C57BL/6JN	Mus musculus
CA1_med_17	CA1	Medulla	3	m	C57BL/6JN	Mus musculus
CA1_med_18	CA1	Medulla	15	m	C57BL/6JN	Mus musculus
CA1_med_19	CA1	Medulla	18	m	C57BL/6JN	Mus musculus
CA1_med_20	CA1	Medulla	21	m	C57BL/6JN	Mus musculus
CA1_med_21	CA1	Medulla	3	m	C57BL/6JN	Mus musculus
CA1_med_22	CA1	Medulla	15	m	C57BL/6JN	Mus musculus
CA1_med_23	CA1	Medulla	18	m	C57BL/6JN	Mus musculus
CA1_med_24	CA1	Medulla	21	m	C57BL/6JN	Mus musculus
CA1_med_25	CA1	Medulla	3	m	C57BL/6JN	Mus musculus
CA1_med_26	CA1	Medulla	15	m	C57BL/6JN	Mus musculus
CA1_med_27	CA1	Medulla	18	m	C57BL/6JN	Mus musculus
CA1_med_28	CA1	Medulla	21	m	C57BL/6JN	Mus musculus
CA1_med_29	CA1	Medulla	3	m	C57BL/6JN	Mus musculus
CA1_med_30	CA1	Medulla	15	m	C57BL/6JN	Mus musculus
CA1_med_31	CA1	Medulla	18	m	C57BL/6JN	Mus musculus
CA1_med_32	CA1	Medulla	21	m	C57BL/6JN	Mus musculus
CA1_med_33	CA1	Medulla	3	m	C57BL/6JN	Mus musculus
CA1_med_34	CA1	Medulla	15	m	C57BL/6JN	Mus musculus
CA1_med_35	CA1	Medulla	18	m	C57BL/6JN	Mus musculus
CA1_med_36	CA1	Medulla	21	m	C57BL/6JN	Mus musculus
CA1_med_37	CA1	Medulla	3	f	C57BL/6JN	Mus musculus
CA1_med_38	CA1	Medulla	15	f	C57BL/6JN	Mus musculus
CA1_med_39	CA1	Medulla	18	f	C57BL/6JN	Mus musculus
CA1_med_40	CA1	Medulla	21	f	C57BL/6JN	Mus musculus
CA1_med_41	CA1	Medulla	3	f	C57BL/6JN	Mus musculus
CA1_med_42	CA1	Medulla	15	f	C57BL/6JN	Mus musculus
CA1_med_43	CA1	Medulla	18	f	C57BL/6JN	Mus musculus
CA1_med_44	CA1	Medulla	21	f	C57BL/6JN	Mus musculus
CA1_med_45	CA1	Medulla	3	f	C57BL/6JN	Mus musculus
CA1_med_46	CA1	Medulla	15	f	C57BL/6JN	Mus musculus
CA1_med_47	CA1	Medulla	18	f	C57BL/6JN	Mus musculus
CA1_med_49	CA1	Medulla	3	f	C57BL/6JN	Mus musculus
CA1_med_48	CA1	Medulla	21	f	C57BL/6JN	Mus musculus
CA1_med_50	CA1	Medulla	15	f	C57BL/6JN	Mus musculus
CA1_med_51	CA1	Medulla	18	f	C57BL/6JN	Mus musculus
CA1_med_52	CA1	Medulla	21	f	C57BL/6JN	Mus musculus
CA1_med_53	CA1	Medulla	3	f	C57BL/6JN	Mus musculus
CA1_med_54	CA1	Medulla	15	f	C57BL/6JN	Mus musculus
CA1_med_55	CA1	Medulla	18	f	C57BL/6JN	Mus musculus
CA1_med_56	CA1	Medulla	21	f	C57BL/6JN	Mus musculus

CA1_med_57	CA1	Medulla	28	m	C57BL/6JN	Mus musculus
CA1_med_58	CA1	Medulla	28	m	C57BL/6JN	Mus musculus
CA1_med_59	CA1	Medulla	28	m	C57BL/6JN	Mus musculus

Table 3: Alternative paralog identifiers for retained paralog identifiers¹.

Retained paralog identifiers	Alternative paralog identifier
ENSMUST00000151575.7 Drr1	ENSMUST00000133333.1 Drr1
ENSMUST00000190668.6 1700030N03Rik	ENSMUST00000190982.6 1700030N03Rik
ENSMUST00000185226.1 Gm29277	ENSMUST00000186209.1 Gm29089
ENSMUST00000189117.1 Gm29645	ENSMUST00000185976.1 Gm28312
ENSMUST00000177995.1 Gm22109	ENSMUST00000179995.1 n-R5s110
ENSMUST00000179432.1 Gm25212	ENSMUST00000178859.1 n-R5s144
ENSMUST00000179827.1 Gm24759	ENSMUST00000178104.1 Gm24585
ENSMUST00000178442.1 Gm22050	ENSMUST00000180315.1 Gm24654
ENSMUST00000082973.1 Gm25405	ENSMUST00000179017.1 Gm24722
tRNA-Ala-AGC-2-1	tRNA-Ala-AGC-2-2
tRNA-Ala-AGC-4-1	tRNA-Ala-AGC-4-2
tRNA-Ala-AGC-5-1	tRNA-Ala-AGC-5-2
tRNA-Ala-AGC-5-1	tRNA-Ala-AGC-5-3
tRNA-Ala-CGC-1-1	tRNA-Ala-CGC-1-2
tRNA-Ala-CGC-3-1	tRNA-Ala-CGC-3-2
tRNA-Ala-CGC-3-1	tRNA-Ala-CGC-3-3
tRNA-Ala-TGC-2-1	tRNA-Ala-TGC-3-1
tRNA-Ala-TGC-5-1	tRNA-Ala-TGC-5-2
tRNA-Ala-TGC-5-1	tRNA-Ala-TGC-5-3
tRNA-Ala-TGC-7-1	tRNA-Ala-TGC-7-2
tRNA-Arg-ACG-1-1	tRNA-Arg-ACG-1-2
tRNA-Arg-ACG-1-1	tRNA-Arg-ACG-1-3
tRNA-Arg-ACG-3-1	tRNA-Arg-ACG-3-2
tRNA-Arg-CCT-2-1	tRNA-Arg-CCT-2-2
tRNA-Arg-TCG-3-1	tRNA-Arg-TCG-3-2
tRNA-Asn-GTT-3-1	tRNA-Asn-GTT-3-2
tRNA-Asn-GTT-3-1	tRNA-Asn-GTT-3-3
tRNA-Asn-GTT-3-1	tRNA-Asn-GTT-3-4
tRNA-Asn-GTT-3-1	tRNA-Asn-GTT-3-5
tRNA-Asn-GTT-3-1	tRNA-Asn-GTT-3-6
tRNA-Asn-GTT-3-1	tRNA-Asn-GTT-3-7
tRNA-Asn-GTT-3-1	tRNA-Asn-GTT-3-8
tRNA-Asn-GTT-3-1	tRNA-Asn-GTT-3-9
tRNA-Cys-GCA-1-1	tRNA-Cys-GCA-1-2
tRNA-Cys-GCA-3-1	tRNA-Cys-GCA-3-2

tRNA-Cys-GCA-3-1	tRNA-Cys-GCA-3-3
tRNA-Cys-GCA-3-1	tRNA-Cys-GCA-3-3
tRNA-Cys-GCA-4-1	tRNA-Cys-GCA-4-10
tRNA-Cys-GCA-4-1	tRNA-Cys-GCA-4-11
tRNA-Cys-GCA-4-1	tRNA-Cys-GCA-4-12
tRNA-Cys-GCA-4-1	tRNA-Cys-GCA-4-13
tRNA-Cys-GCA-4-1	tRNA-Cys-GCA-4-14
tRNA-Cys-GCA-4-1	tRNA-Cys-GCA-4-15
tRNA-Cys-GCA-4-1	tRNA-Cys-GCA-4-16
tRNA-Cys-GCA-4-1	tRNA-Cys-GCA-4-17
tRNA-Cys-GCA-4-1	tRNA-Cys-GCA-4-18
tRNA-Cys-GCA-4-1	tRNA-Cys-GCA-4-19
tRNA-Cys-GCA-4-1	tRNA-Cys-GCA-4-2
tRNA-Cys-GCA-4-1	tRNA-Cys-GCA-4-20
tRNA-Cys-GCA-4-1	tRNA-Cys-GCA-4-21
tRNA-Cys-GCA-4-1	tRNA-Cys-GCA-4-22
tRNA-Cys-GCA-4-1	tRNA-Cys-GCA-4-23
tRNA-Cys-GCA-4-1	tRNA-Cys-GCA-4-24
tRNA-Cys-GCA-4-1	tRNA-Cys-GCA-4-25
tRNA-Cys-GCA-4-1	tRNA-Cys-GCA-4-26
tRNA-Cys-GCA-4-1	tRNA-Cys-GCA-4-27
tRNA-Cys-GCA-4-1	tRNA-Cys-GCA-4-28
tRNA-Cys-GCA-4-1	tRNA-Cys-GCA-4-29
tRNA-Cys-GCA-4-1	tRNA-Cys-GCA-4-3
tRNA-Cys-GCA-4-1	tRNA-Cys-GCA-4-4
tRNA-Cys-GCA-4-1	tRNA-Cys-GCA-4-5
tRNA-Cys-GCA-4-1	tRNA-Cys-GCA-4-6
tRNA-Cys-GCA-4-1	tRNA-Cys-GCA-4-7
tRNA-Cys-GCA-4-1	tRNA-Cys-GCA-4-8
tRNA-Cys-GCA-4-1	tRNA-Cys-GCA-4-9
tRNA-Gln-CTG-2-1	tRNA-Gln-CTG-2-2
tRNA-Gln-CTG-2-1	tRNA-Gln-CTG-2-3
tRNA-Gln-CTG-2-1	tRNA-Gln-CTG-2-4
tRNA-Gln-CTG-3-1	tRNA-Gln-CTG-3-2
tRNA-Gln-CTG-3-1	tRNA-Gln-CTG-3-3
tRNA-Gln-TTG-3-1	tRNA-Gln-TTG-3-2
tRNA-Glu-CTC-1-1	tRNA-Glu-CTC-1-2
tRNA-Glu-CTC-1-1	tRNA-Glu-CTC-1-3
tRNA-Glu-CTC-1-1	tRNA-Glu-CTC-1-4
tRNA-Glu-CTC-1-1	tRNA-Glu-CTC-1-5
tRNA-Glu-CTC-1-1	tRNA-Glu-CTC-1-6
tRNA-Glu-CTC-1-1	tRNA-Glu-CTC-1-7
tRNA-Glu-CTC-1-1	tRNA-Glu-CTC-1-8

tRNA-Glu-CTC-1-1	tRNA-Glu-CTC-1-9
tRNA-Glu-TTC-1-1	tRNA-Glu-TTC-1-2
tRNA-Glu-TTC-1-1	tRNA-Glu-TTC-1-3
tRNA-Glu-TTC-1-1	tRNA-Glu-TTC-1-4
tRNA-Glu-TTC-2-1	tRNA-Glu-TTC-2-2
tRNA-Glu-TTC-3-1	tRNA-Glu-TTC-3-2
tRNA-Gly-CCC-1-1	tRNA-Gly-CCC-1-2
tRNA-Gly-CCC-2-1	tRNA-Gly-CCC-2-2
tRNA-Gly-GCC-1-1	tRNA-Gly-GCC-1-2
tRNA-Gly-GCC-1-1	tRNA-Gly-GCC-1-3
tRNA-Gly-GCC-2-1	tRNA-Gly-GCC-2-2
tRNA-Gly-GCC-2-1	tRNA-Gly-GCC-2-3
tRNA-Gly-GCC-2-1	tRNA-Gly-GCC-2-4
tRNA-Gly-GCC-2-1	tRNA-Gly-GCC-2-5
tRNA-Gly-GCC-2-1	tRNA-Gly-GCC-2-6
tRNA-Gly-GCC-2-1	tRNA-Gly-GCC-2-7
tRNA-Gly-GCC-2-1	tRNA-Gly-GCC-2-8
tRNA-Gly-TCC-1-1	tRNA-Gly-TCC-1-7
tRNA-Gly-TCC-1-1	tRNA-Gly-TCC-1-6
tRNA-Gly-TCC-1-1	tRNA-Gly-TCC-1-5
tRNA-Gly-TCC-1-1	tRNA-Gly-TCC-1-4
tRNA-Gly-TCC-1-1	tRNA-Gly-TCC-1-3
tRNA-Gly-TCC-1-1	tRNA-Gly-TCC-1-2
tRNA-His-GTG-2-1	tRNA-His-GTG-2-2
tRNA-His-GTG-2-1	tRNA-His-GTG-2-3
tRNA-His-GTG-2-1	tRNA-His-GTG-2-4
tRNA-His-GTG-2-1	tRNA-His-GTG-2-5
tRNA-His-GTG-2-1	tRNA-His-GTG-2-6
tRNA-His-GTG-2-1	tRNA-His-GTG-2-7
tRNA-His-GTG-2-1	tRNA-His-GTG-2-8
tRNA-Ile-AAT-1-1	tRNA-Ile-AAT-1-8
tRNA-Ile-AAT-1-1	tRNA-Ile-AAT-1-7
tRNA-Ile-AAT-1-1	tRNA-Ile-AAT-1-6
tRNA-Ile-AAT-1-1	tRNA-Ile-AAT-1-5
tRNA-Ile-AAT-1-1	tRNA-Ile-AAT-1-4
tRNA-Ile-AAT-1-1	tRNA-Ile-AAT-1-3
tRNA-Ile-AAT-1-1	tRNA-Ile-AAT-1-2
TRNA-Leu-AAG-1-1	tRNA-Leu-AAG-1-2
TRNA-Leu-AAG-1-1	tRNA-Leu-AAG-1-3
tRNA-Leu-CAG-1-1	tRNA-Leu-CAG-1-2
tRNA-Leu-CAG-1-1	tRNA-Leu-CAG-1-3
tRNA-Leu-CAG-1-1	tRNA-Leu-CAG-1-4
tRNA-Leu-CAG-1-1	tRNA-Leu-CAG-1-5

tRNA-Leu-CAG-2-1	tRNA-Leu-CAG-2-2
tRNA-Leu-CAG-2-1	tRNA-Leu-CAG-2-3
tRNA-Lys-CTT-2-1	tRNA-Lys-CTT-2-2
tRNA-Lys-CTT-3-1	tRNA-Lys-CTT-3-2
tRNA-Lys-CTT-3-1	tRNA-Lys-CTT-3-3
tRNA-Lys-CTT-3-1	tRNA-Lys-CTT-3-4
tRNA-Lys-CTT-3-1	tRNA-Lys-CTT-3-5
tRNA-Lys-CTT-3-1	tRNA-Lys-CTT-3-6
tRNA-Lys-CTT-3-1	tRNA-Lys-CTT-3-7
tRNA-Lys-TTT-1-1	tRNA-Lys-TTT-1-2
tRNA-Lys-TTT-1-1	tRNA-Lys-TTT-1-3
tRNA-Lys-TTT-1-1	tRNA-Lys-TTT-1-4
tRNA-Lys-TTT-1-1	tRNA-Lys-TTT-1-5
tRNA-Lys-TTT-1-1	tRNA-Lys-TTT-1-6
tRNA-Lys-TTT-2-1	tRNA-Lys-TTT-2-2
tRNA-Lys-TTT-4-1	tRNA-Lys-TTT-4-2
tRNA-Lys-TTT-4-1	tRNA-Lys-TTT-4-3
tRNA-Met-CAT-1-1	tRNA-Met-CAT-1-2
tRNA-Met-CAT-2-1	tRNA-Met-CAT-2-2
tRNA-Phe-GAA-1-1	tRNA-Phe-GAA-1-2
tRNA-Phe-GAA-1-1	tRNA-Phe-GAA-1-3
tRNA-Phe-GAA-1-1	tRNA-Phe-GAA-1-4
tRNA-Phe-GAA-1-1	tRNA-Phe-GAA-1-5
tRNA-Pro-AGG-1-1	tRNA-Pro-AGG-1-2
tRNA-Pro-AGG-1-1	tRNA-Pro-AGG-1-3
tRNA-Pro-AGG-1-1	tRNA-Pro-AGG-1-4
tRNA-Pro-AGG-1-1	tRNA-Pro-AGG-1-5
tRNA-Pro-AGG-1-1	tRNA-Pro-AGG-1-6
tRNA-Pro-CGG-1-1	tRNA-Pro-CGG-1-2
tRNA-Pro-CGG-1-1	tRNA-Pro-CGG-1-3
tRNA-Pro-TGG-2-1	tRNA-Pro-TGG-2-2
tRNA-Pro-TGG-2-1	tRNA-Pro-TGG-2-3
tRNA-Pro-TGG-2-1	tRNA-Pro-TGG-2-4
tRNA-Ser-AGA-2-1	tRNA-Ser-AGA-2-2
tRNA-Ser-AGA-2-1	tRNA-Ser-AGA-2-3
tRNA-Ser-AGA-2-1	tRNA-Ser-AGA-2-4
tRNA-Ser-AGA-2-1	tRNA-Ser-AGA-2-5
tRNA-Ser-AGA-2-1	tRNA-Ser-AGA-2-6
tRNA-Ser-GCT-4-1	tRNA-Ser-GCT-4-2
tRNA-Ser-GCT-4-1	tRNA-Ser-GCT-4-3
tRNA-Ser-TGA-2-1	tRNA-Ser-TGA-2-2
tRNA-Thr-AGT-1-1	tRNA-Thr-AGT-1-2
tRNA-Thr-AGT-1-1	tRNA-Thr-AGT-1-3

tRNA-Thr-TGT-3-1	tRNA-Thr-TGT-3-2
tRNA-Trp-CCA-3-1	tRNA-Trp-CCA-3-2
tRNA-Trp-CCA-4-1	tRNA-Trp-CCA-4-2
tRNA-Val-AAC-1-1	tRNA-Val-AAC-1-2
tRNA-Val-AAC-2-1	tRNA-Val-AAC-2-2
tRNA-Val-CAC-2-1	tRNA-Val-CAC-2-5
tRNA-Val-CAC-2-1	tRNA-Val-CAC-2-4
tRNA-Val-CAC-2-1	tRNA-Val-CAC-2-3
tRNA-Val-CAC-2-1	tRNA-Val-CAC-2-2
tRNA-Val-TAC-1-1	tRNA-Val-TAC-1-2
tRNA-Val-TAC-1-1	tRNA-Val-TAC-1-3
tRNA-iMet-CAT-1-1	tRNA-iMet-CAT-1-2
tRNA-iMet-CAT-1-1	tRNA-iMet-CAT-1-3
tRNA-iMet-CAT-1-1	tRNA-iMet-CAT-1-4
tRNA-iMet-CAT-1-1	tRNA-iMet-CAT-1-5
tRNA-iMet-CAT-1-1	tRNA-iMet-CAT-1-6
tRNA-iMet-CAT-1-1	tRNA-iMet-CAT-1-7

Table 4: 3'UTR Sequences of tested constructs for miR-29 target validation¹.

3'UTR sequences cloned for respective genes for miRNA-mRNA interaction validation.

gene	NCBI Reference Sequence	reporter plasmid name	sequence	restriction sites
APLNR	NM_00516 1.6	pMIR-APLNR	ACTAGTGGGAAGGCAGCAGGGCTGATGAAT GGATGTA CTCTTGGTTTCATTATGTGAGTGG GGAGTTGGGAAGGGCAACTAGAGAGAGAGGA TGGAGGGGTGTCTGCATTTAGTCCAGACACTG CTTGGCTCGCTCCCCGAGTCCTCCTGTTTCTG ACTTCCTGCATAACTGTGAGCTGAAGGGTTTC CTCATCTCCCCATCTTACCCCATCATACTGATT TCTTTCTTGGGCACTGGTGCTACTTGGTGCCA AGAATCATGTTGTTTGGGATGGAGATGCCTGC CTCTTGCTGTGTGTGTTGTACTTATATGTCTA TATGGATGAGCCTGGCATGAACAGCAGTGTG CCTGGGTCATTTGGACAAACCTCCTCCCACCC CCCAATCCACTGCAACTCTGCTGTTTCACACAT TACCCTTGGCAGGGGGTGGTGGGGGGCAGG GACACACTGAGGCAATGAAAAATGTAGAATAA AAATGAGTCCACCCCGAGCTC	<i>SpeI/SacI</i>
LOX	NM_00231 7.7	pMIR-LOX_1	ACTAGTCTGTAATTACATATTTGACTCTTTCAA AGAAATCCAAATTTCTCATGTTCTTTTGAAAT TG TAGTGCAAAATGGTCAGTATTATCTAAATGA ATGAGCCAAAATGACTTTGAACTGAACTTTTC TAAAGTGCTGGAAC TTTAGTGAAACATAATAAT AATGGGTTTATATATGTCATAGCATAGATGAAT TTAGAAACAATGCCTACTGTTTAAATACATA TGGACACATCTGGTGCTGAGAAAAGAAACAAAC ACATTACCATTGGTGTCAAGAAATATTACTATA TAGCAGAGAAATGGCAATACATGTA CT CAGAT AGTTACATCCCTATATAAAAAGTATGTTTACAT TAAAAAATTAGTAGATAACTTCCTTTCTTTCAA GTGCACAATTTCA TTTTGACTTGAGTCAACTTT TGTTTTGGAACAAATTAAGTAAGGGAGCTGCC CAATCCTGTCTGATATTTCTTGAGGCTGCCCG AGCTC	<i>SpeI/SacI</i>

	NM_00231 7.7	pMIR- LOX_2	ACTAGTCATAGTATTACATACTTGAGGGGTTG GTGAACAAAGGAAAAATATACTTTCTGCAAAA CCAAGGACTGTGCTGCGTAATGAGACAGCTG TGATTTTCAATTTGAAACTGTGAAACCATGTGCCA TAATAGAATTTTGAAGAATTTTGTCTTTTACCTAA ATTCAAGAAAATGAAATTACACTTTTAAAGTTAG TGGTGCTTAAGCATAATTTTTCCTATATTAACC AGTATTAATAATCTCAAGTAAGATTTTCCAGTGC CAGAACATGTTAGGTGGAATTTTAAAAGTGCC TCGGCATCCTGTATTACATGTCATAGAATTGTA AAGTCAACATCAATTACAAGTAATCATTCTGCA CTCACTGGGTGCATAGCATGGTTAGAGGGGC TAGAGATGGACAGTCATCAACTGGCGGATATA GCGGTACATATGATCCTTAGCCACCAGGGCA CAAGCTTACCAGTAGACAATACAGACAGAGCT TTTGTTGAGGAGCTC	SpeI/SacI
	NM_00231 7.7	pMIR- LOX_3	ACTAGTGATTCTAGAAGAAATGCAATTCATTA AATTTTCTGGCACTGAGAGTTAATCTTTAGCA GATTGCATGAAAATACTGAATTCCTGGTAAGG AGATATTTTGTTTTAAAAATAATGTGTTTTGATA CGAATCAGTGTATTAAGTATAACTAAAAAGTA CTCTTTTTCTATATATACATATTTTTTGA ACTCATATTCACAATCAACATATTCAATCAGTGAGT TAAGTCTCATTCTAGCTACCAAAATTCCTGG GCCACTTTAAACACTAAACATTTTCAATTTATCC TCTAAGCTAAAATGGTGTGCTGAGTTATTTAAATC TGAATGTAAAATGCATTAATCTTAGCTTGTGG TATATAAACATTTAATTAATATAAAACTGCTTGC TATAAACTAAGTAACATGTCATTTGGTGTAGG TTTTTAGTGAAGTTTTAGCTTCTCCCAAATTTTT CAGGAATGTTATTTGTAAGACGTGTAACGAGC TC	SpeI/SacI
VASH1	NM_01490 9.5	pMIR- VASH1_1	ACTAGTGAATGACAGGGTTTGAGGGGAGTAG ATATGAGAGGGAGCCGCTCCTGGTTCTGGAG TCTTAGGAGGTTCCAACCTTGCAAGATCCTTTC CCAGAGCCCTCCATGGAGAAAACAGCAAAAT GAAGCCCTTACCTGCTTGCTGTCTGCAAGGGA GGGAGCCGAGCCCCAGCTGATAATCCCCCAG CACTCACCTTCTGAGCTGAGACTTCGGGG CTGTGGAGACCAGCACAGGACATAGTGGTGC TTTTTAAATTTATTTTTAACTGTTTCTCATATGT AGCAACCCCTCCTCCCCTCCTGGGCATGTTTA CACAGGCTCTGCTCTGGGGGCTGGCCTGGCT GTGAGGTTTCTGGGGAGGCAGAGAGGCAGG GACTTTGGGGCCTTAGTCACCATCCATGGTAT CACCTCATCTCACTTCTGTGAGGGACAGGG CCTGGCTGATGTGATCCCAGCTCCCCCAGTT CAGGACTGTCTTTCAGCTCCGAGCTC	SpeI/SacI
	NM_01490 9.5	pMIR- VASH1_2	ACTAGTGTGAATGTGTGCAACTGCTTTTTCTG CCTGGAATGTTTTCTGGCTCAGCTGCAGCAAC ATCTGTGAGCCCAGTGTCTGCCCTGTGTCCCT GGGCTCGCTCCAAGTGCAGGAACATACATGC AGGGCCCAACATGATGATGGTGTGAAGGGCA GGAAACAGTCTCTGAAGGAGTGGGGAGGTG GGCAGTCTGCCCCCGCCAGGTACCATCGCCT CCTGCCAGCTTCTTAGACCAGGCAGGGCTG CCATGGTGCTAGCTGCAAGTCCATCAGTATTG ACCGTCTCGCTCCATCTTGGTCTCCGGAGTC CCAAGTTTCTTTTTCATCAAATCTGACAAGAGA GAAGAAACATGGGTGTGCTTGGCCCACAGGG CCTGGTGGTGTGATGGACCTCCCCGCTCCCTCA AGCTCTGGATGGCTGCAGTGTGACTAGACT TTGTTTCAAGGCTGTTCTCATCTCAGTATTGCC CTTCTTTCACTTTTACACAGGAGCTC	SpeI/SacI

ADAM12	NM_00347 4.6	pMIR-ADAM12 _1	ACTAGTGAAGCCGACACCTTTTTTCAACAGTG AAGACAGAAGTTTGCAGTATCTTTTCAGCTCCA GTTGGAGTTTTTGTACCAACTTTTAGGATTTT TTTTAATGTTTTAAAACATCATTACTATAAGA AATTTGAGCTACTGCCGTCAGTGCTGTGCTGTGCT ATGGTGCTCTGTCTACTTGCTCAGGTACTTGT AAATTATTAATTTATGCAGAATGTTGATTACAG TGCAGTGCCTGTAGTAGGCATTTTTACCATC ACTGAGTTTTCCATGGCAGGAAGGCTTGTTGT GCTTTTAGTATTTTAGTGAACCTGAAATATCCT GCTTGATGGGATTCTGGACAGGATGTGTTTGC TTTCTGATCAAGGCCTTATTGGAAAGCAGTCC CCCAACTACCCCGAGCTGTGCTTATGGTACCA GATGCAGCTCAAGAGATCCCAAGTAGAATCTC AGTTGATTTTCTGGATTCCCATCTCAGGCCA GAGCCAAGGAGCTC	SpeI/SacI
	NM_00347 4.6	pMIR-ADAM12 _2	ACTAGTCTGTAGGAGAGTCAATACTCCTGACG AGTCTCGGGGGGGGGGCATTTTTATGCCTTCT TAACTTTATGAGAATTCTCAGGCTGAACATAG GCCATTGTTCCCAGGCAAATCAATACATCAAT GCATCCTCAAAAAAAAAAAAAAAAAAAAAAAC CGGCTAAAACGTGTCAAATGTTCTTAAGGA GCCTATGGTCTCCACGGTGTAAAAAGAGCCT GGTGTGGGCGGACTGGCAGGGCTGAGCATC CTCCTGCCCCCTCGCCACTGATGTTTACTAAG CACTCTGAGCCAATGAGACCCCGAGCAGCAG AAAGGGCACAAGGTGGCGCCAGGGCAGCAG GGCCAGATCTTTCTCATGCACCTCGACCTCTT GCAGACTTTCTTCGTGAGATGTACTACTCATT CAAACTGCTTTCAGGGCTCCCCTATGTATT CGGGGGGCCACGGCACACTCAGGCTGGAG ATCCTTCTCACTGCGGAGCTC	SpeI/SacI
ADAMTS 17	NM_13905 7.4	pMIR-ADAMTS 17_1	ACTAGTCACCCTACCTGCAAGGAGGCCGGGC AGGGACCCTAGATGCCAGGAGGCCTGTTTTG CTCACCAACTTGGTGGGCATTTTATGGGTGCT TATGTTCTAGGACTTTACCGTAAATAACACCTC CTCCCTGATTTTACAGACGGAAGGTCTCACTTGG ACTTCCATGGGATCATCTCCCTGTGCTTCTTG ATTTATTGGTGCTGTGTTTCTGTGTTTTGTTTT GTTACATGTCACAACCGTAGAGTTAGCTTAAA TCAGAAAGAAGCCTCTCTGCCTTCTCCACCCT GTCTTACGAGCTGTGTTTTTGTGTTTTACTACCC TAGAGGCAGAGAAGCGGTAGGGATGTCAGGG AATTTACTCACTTCCACTTGAATCAACGAGAAG TGTTGAGAACTTCCGTGGGTGCTCTGTGGAA AGAACCGAGGGTGTGAGGATGGAGCGGCCCA CCCTCGCCCCGCGGCCTGCGCAGACTGCTGT CCTCCCCTCAGGGCAGCTC	SpeI/SacI
	NM_13905 7.4	pMIR-ADAMTS 17_2	ACTAGTCGAGCAGTGATTTTCAAGTAAAACCATC ATAAACATTCTTGTCCACTAGATGCTGATCAC AGCAGTGATGTTTCTGTGTTAATACCCTGACT GTCCCTCGAGTACTGTACCTTTGTGCTTGCAC ACGTGTCACTAACGCACGTGTTACCAGAGTCT CACGACCCTACGGTGTATTTTTATTGGTGCA AAATTAACCCCTCAGCTGACCGTTGCTGGA TAGGATCAGAATGCAGGAAAAGAGCCTCTATG GCAATACGATTGCTTTTTTTCGTTTCAGAGTC AAATGTATCTATTTTCCATTGTTAACTTGCAT TACATACTGTACCCATGGAATTTTTGTTTTACT TTTTGGGCTGGTTTTGAAAGGAAAAAAAAACG GAAGACAAACATTGGACGCCATTATACATGAA AATTATATAGAAAAATTAATCATTTTATTGGAA GCAAGTTGAATATGTGTAATAAAATGTTTTTCC ATAACGAGCTC	SpeI/SacI

COL1A2 (positive control, PC)	NM_00008 9.4	pMIR- COL1A2	ACTAGTCCATAAACATTTGCACCACTTGTGGC TTTTGAATATCTTCCACAGAGGGAAGTTAAAA CCCAAACCTTCCAAAGGTTTAAACTACCTCAAAA CACTTTCCCATGAGTGTGATCCACATTGTTAG GTGCTGACCTAGACAGAGATGAACTGAGGTC CTTGTTTTGTTTTGTTTCATAATACAAAGGTGCT AATTAATAGTATTTTCAGATACTTGAAGAATGTT GATGGTGCTAGAAGAATTTGAGAAGAAATACT CCTGTATTGAGTTGTATCGTGTGGTGTATTTTT TAAAAAATTTGATTTAGCATTTCATATTTCCATC TTATTCCCAATTAAGTATGCAGATTATTTGC CCAAATCTTCTTCAGATTCAGCATTGTTCTTT GCCAGTCTCATTTTCATCTTCTTCCATGGTTCC ACAGAAGCTTTGTTTCTTGGGCAAGCAGAAAA ATTAATTGTACCTATTTTGTATATGGAGCTC	<i>SpeI/SacI</i>
--	-----------------	-----------------	---	------------------

Acknowledgement

Mein Dank gilt allen meinen Kooperationspartnern, ohne die diese Arbeit nicht möglich gewesen wäre. Im Speziellen möchte ich mich bei Nicole Ludwig und Martin Hart für ihre Unterstützung mit der experimentellen Arbeit bedanken. Oliver Hahn sowie Tony Wyss-Coray und dem gesamten Team in Stanford möchte ich danken, dass sie uns diese wertvollen Proben zur Verfügung gestellt haben und den Transport trotz aller Widrigkeiten organisiert haben. Annika Engel möchte ich danken, dass sie mit mir zusammen das non-coding Brain Aging Projekt durchführt. Eckart Meese möchte ich danken, dass ich in seinem Labor den Großteil der experimentellen Arbeiten durchführen durfte. Insgesamt möchte ich mich bei allen Kollegen sowohl in der Arbeitsgruppe der Humangenetik in Homburg wie auch in der Gruppe der klinischen Bioinformatik in Saarbrücken bedanken.

Außerdem gilt mein Dank meinen Studenten und Hiwis, die mit ihrer Arbeit wertvolle Beiträge zu dieser Arbeit geleistet haben.

Vor allem möchte ich meinem Doktorvater, Prof. Andreas Keller danken, dass er mir diese Arbeit ermöglicht hat. Vielen Dank für das interessante Forschungsprojekt, an dem ich die letzten Jahre arbeiten konnte und dafür, dass ich in Labor Experimente durchführen konnte und gleichzeitig auch meine Fähigkeiten in der Datenanalyse vertiefen konnte. Danke für die Unterstützung und das immer schnelle und produktive Feedback.

Zuletzt möchte ich meiner Familie, Freunden und meinem Partner meinen Dank aussprechen, dass sie mich alle während der gesamten Zeit meiner Doktorarbeit immer unterstützt haben.

Lebenslauf

Aus datenschutzrechtlichen Gründen wird der Lebenslauf in der elektronischen Fassung der Dissertation nicht veröffentlicht.